IMPACT OF SEASONAL RHYTHMS EFFECTS ON GUT MICROBIOTA: INFLUENCE ON PROANTHOCYANIDINS FUNCTIONALITY IN OBESITY

Verónica Arreaza Gil

Impact of seasonal rhythms effects on gut microbiota: influence on proanthocyanidins functionality in obesity

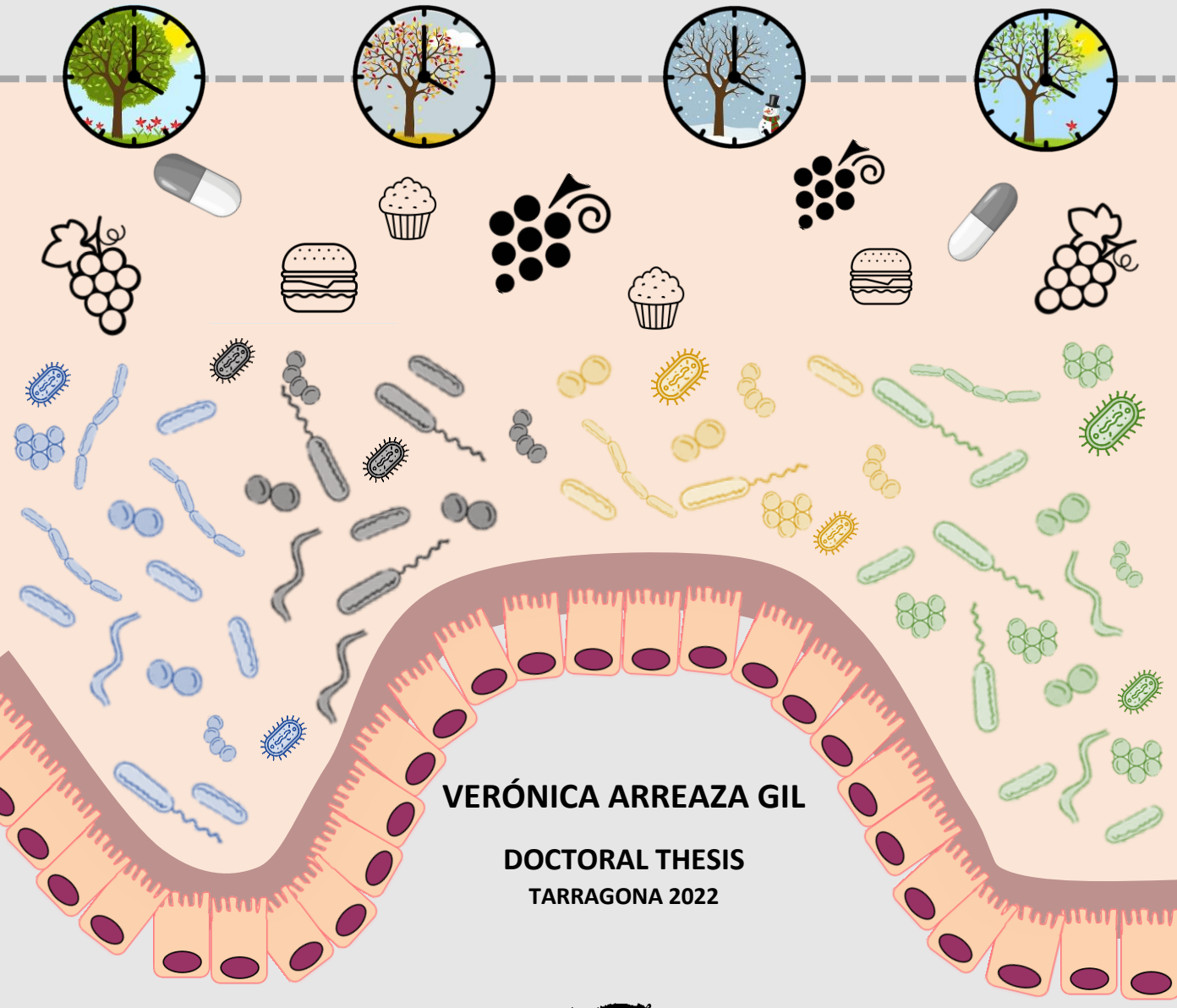

VERÓNICA ARREAZA GIL

DOCTORAL THESIS

TARRAGONA 2022

UNIVERSITAT ROVIRA i VIRGILI

Verónica Arreaza Gil

Impact of seasonal rhythms effects on gut microbiota: influence on proanthocyanidins functionality in obesity

DOCTORAL THESIS

Supervised by

Dr. Anna Arola Arnal

Dr. Cristina Torres Fuentes

Department of Biochemistry and Biotechnology

Nutrigenomics Research Group

UNIVERSITAT
ROVIRA i VIRGILI

Tarragona 2022

UNIVERSITAT ROVIRA i VIRGILI
DEPARTAMENT DE BIOQUÍMICA I BIOTECNOLOGIA
Campus Sescelades
C/Marcel·lí Domingo, 1
43007 Tarragona
Tel. +34 977 55 95 21
Fax +34 977 55 82 32

FAIG CONSTAR que aquest treball, titulat "**Impacte dels ritmes estacionals a la microbiota intestinal: influència en la funcionalitat de proantocianidines en obesitat**", que presenta **Verónica Arreaza Gil** per a l'obtenció del títol de Doctor, ha estat realitzat sota la meva direcció al Departament de Bioquímica i Biotecnologia de la universitat Rovira i Virgili i que compleix els requisits per a l'obtenció de la Menció Internacional de Doctoral.

HAGO CONSTAR que el presente trabajo, titulado "Impacto **de los ritmos estacionales en la microbiota intestinal: influencia en la funcionalidad de proantocianidinas en obesidad**", que presenta **Verónica Arreaza Gil** para la obtención del título de Doctor, ha sido realizado bajo mi dirección en el Departamento de Bioquímica y Biotecnología de la universidad Rovira i Virgili y cumple con los requisitos para la obtención de la mención Internacional de Doctorado.

I STATE that the present study, entitled "**Impact of seasonal rhythms effects on gut microbiota: influence on proanthocyanidins functionality in obesity**", presented by **Verónica Arreaza Gil** for the award of the degree of Doctor, has been carried out under my supervision at the Department de Bioquímica i Biotecnologia from the University Rovira i Virgili and that is eligible to apply for the International Doctoral Mention.

Tarragona, 29 junio 2022

El/s director/s de la tesi doctoralEl/los director/es de la tesis doctoral
Doctoral Thesis Supervisor/s

Dr. Anna Arola Arnal

Dr. Cristina Torres Fuentes

Esta tesis fue enmarcada en el proyecto PLAN NACIONAL: *Estudio de la interacción de los ritmos circadianos y estacionales con la efectividad de los ingredientes funcionales* [MCIN/AEI/10.13039/501100011033/ FEDER "Una manera de hacer Europa" (AGL2016-77105-R)], cuyo objetivo es estudiar si los efectos beneficiosos de compuestos funcionales observados en obesidad y otras patologías asociadas al síndrome metabólico pueden verse modificados según el momento del año en el que son administrados. Además, se enmarca en el proyecto DIPTA: *desarrollo de un prototipo para establecer disbiosis en la microbiota intestinal* [co-financiado por la Diputació de Tarragona (2021PGR-DIPTA-URV09)], cuyo objetivo es establecer un modelo de disbiosis intestinal para estudiar el impacto de la microbiota intestinal en la biodisponibilidad y actividad de compuestos funcionales, así como el impacto de la estacionalidad. Verónica Arreaza Gil es beneficiaria de una ayuda a la contratación de personal investigador predoctoral (Martí i Franquès; PMF-PIPF-35) de la Universitat Rovira i Virgili. Durante la tesis (del 9 de abril al 29 de septiembre de 2021) se realizó una estancia de investigación en el grupo *Missing Microbes In Infants Born By C-Section (MIMIC) en el APC microbiome (University College Cork) en* Cork (Irlanda), bajo la supervisión de los profesores Catherine Stanton y Paul Ross. Además, durante esta estancia se realizó una colaboración con la Dr. Harriët Schellekens del departamento de anatomía y neurociencias del *APC microbiome*, la cual forma parte de esta tesis. En esta etapa Verónica Arreaza Gil fue beneficiaria de una beca de movilidad internacional financiada por la Unión Europea (Programa Erasmus+ y MOU 20/21) y de una bolsa de viaja concedida por la Sociedad Española de Genética.

This thesis is framed within the NATIONAL CALL: *Study of the interaction of circadian and seasonal rhythms with the effectiveness of functional ingredients* [MCIN/AEI/10.13039/501100011033/ FEDER "Una manera de hacer Europa" (AGL2016-77105-R)], which aims to evaluate whether the beneficial effects of functional compounds observed in obesity and other pathologies associated

with the metabolic syndrome can be modified depending on the time of year in which they are administered. This thesis is also part of the DIPTA project: *Development of a prototype for the establishment of a dysbiosis (alteration) in the intestinal microbiota* [co-financed by Diputació de Tarragona (2021PGR-DIPTA-URV09)], whose objective is to establish a model of microbiota dysbiosis and study the impact of the gut microbiota on the bioavailability and activity of the functional compounds, as well as the impact of the seasonality. Verónica Arreaza Gil is a beneficiary of a grant for the hiring of predoctoral research staff for training of PhDs (Martí i Franquès; PMF-PIPF-35) from the Universitat Rovira i Virgili. An international internship was carried from 9th April to 29th September 2021, at Missing Microbes In Infants Born By C-Section (MIMIC) group from APC microbiome in the University College Cork (Cork, Ireland) under the supervision of Professor Catherine Stanton and Professor Paul Ross. In addition, during the internship a collaboration with Dr. Harriët Schellekens of the Department of Anatomy and Neuroscience from APC microbiome was performed, which contributed a one part of this thesis. The internship was supported by an Erasmus+ and MOU grant from the European Union and by a travel grant from the Genetic Spanish Society.

ACKNOWLEDGMENTS

Parecía que no iba a llegar nunca… pero, ¡aquí está! Acaba una etapa que no hubiera sido posible sin las personas que me han acompañado y apoyado durante este camino, esta tesis tiene un pedacito de cada uno de vosotros.

En primer lugar, quiero agradecer a mis directoras, la Dra. Anna Arola y la Dra. Cristina Torres, por su trabajo, dedicación y apoyo. Muchas gracias por vuestra confianza, y por guiarme durante estos años. También quiero agradecer al grupo de nutrigenómica por darme la oportunidad de realizar esta tesis y por el apoyo recibido a lo largo de este tiempo. Agradecer también al departamento de Bioquímica y Biotecnología en el cual he podido realizar la tesis. Muchas gracias también a los técnicos de laboratorio, Niurka y Rosa, sois una parte fundamental del grupo. Gracias por estar siempre disponible, por vuestros consejos, ayuda en todo lo que necesitamos y por hacer más llevadero los largos ratos de estabulario.

I would also like to thank the Professor Catherine Stanton and the Professor Paul Ross for accepting and welcoming me in their research group at the APC microbiome during my internship. Many thanks for involving me in your research projects and for your support. I would also like to thank the rest of the group, especially Emilene, with whom I spent the first weeks in the lab, Iwona, for her time and help at all times and Elena, for her kindness and help. I have learned a lot from all of you! Finally, I would also like to thank to Dr. Härriet Schellekens for collaborating with a part of my thesis, and for making me feel part of her group. Thank you, Natasha, Tim and Cristina for making me feel very comfortable. Thank you all for this great experience despite the COVID pandemic situation.

Agradecer también a las personas que han compartido conmigo este camino día a día. A los nutris: Álvaro, Romi, Marina, Raúl, Pauli, Jorge, Iván, Néstor, Francesca, Josefina y Èlia. Juntos hemos pasado por todos los colores, las rojas, las verdes, las rosas… A las nuevas incorporaciones: Rafa y Marc, con quién he

compartido estos últimos meses, y a los mobiofood: Marta, Alba, Carme, Esther y Florijan. Muchas gracias a todos por las risas, por los muchos momentos compartidos, el apoyo y por el buen ambiente en el despacho, que sin duda ha hecho que todo este trabajo sea mucho más fácil. Entre todos habéis hecho que me sintiera como en casa.

No puedo evitar hacer también alguna mención especial. A Pauli, la alegría en persona, muchas gracias por tu apoyo, no solo a nivel profesional sino a nivel personal, en este tiempo te has convertido en un gran amigo. A Néstor, gracias por tu apoyo durante este tiempo, y por ser un gran compañero. A Iván, mi pareja científica. Y a Jorge, gracias por todo, has sido un gran apoyo durante la tesis y la estancia, convirtiéndote en un amigo y en una persona muy importante, qué bien haberte conocido.

Quiero agradecer también a Javi, por todos los momentos de risa, los paseos por Tarragona, y por todo el apoyo, consejos y ánimos que siempre me ha dado, incluso a pesar de la distancia. ¡Muchas gracias!

A mis amigos, a los de siempre, y los que han ido llegando. No es necesario que os nombre, ya sabéis quienes sois. Gracias por vuestro apoyo y cariño a pesar de la distancia.

Por último y principalmente, agradecer a mi familia. Especialmente a mis padres, ya que gracias a ellos he llegado hasta aquí, y junto con mi hermano, siempre me han apoyado incondicionalmente en todo. La distancia impide abrazos, no sentimientos. También a mi abuelo, que se sentiría muy contento, y al que me hubiera gustado poder enseñarle este libro. ¡Gracias familia!

¡Muchísimas gracias a todos!

A mis padres y hermano,

A mi familia

y amigos,

"Caminante, no hay camino, se hace camino al andar"

Antonio Machado

LIST OF PUBLICATIONS

A) Published papers included in this thesis:

Arreaza-Gil V, Escobar-Martínez I, Suárez M, Bravo FI, Muguerza B, Arola-Arnal A*, Torres-Fuentes C. Gut Seasons: Photoperiod Effects on Fecal Microbiota in Healthy and Cafeteria-Induced Obese Fischer 344 Rats. *Nutrients*. 2022 Feb, 14(3):722. DOI: 10.3390/nu14030722. Impact Factor (2021): 6.706. SI Journal Citation Reports © Ranking 15/90 (Q1) in Nutrition & Dietetics.

Ávila-Román J*, **Arreaza-Gil V**, Cortés-Espinar AJ, Soliz-Rueda JR, Mulero M, Muguerza B, Arola-Arnal A, Arola L, Torres-Fuentes C*. Impact of gut microbiota on plasma oxylipins profile under healthy and obesogenic conditions. *Clinical Nutrition*. 2021 Apr, 40(4):1475-1486. DOI: 10.1016/j.clnu.2021.02.035. Impact Factor (2021): 7.643. SI Journal Citation Reports © Ranking 13/90 (Q1) in Nutrition & Dietetics.

Arreaza-Gil V, Escobar-Martínez I, Muguerza B, Aragonès G, Suárez M, Torres-Fuentes C*, Arola-Arnal A. The effects of Grape Seed Proanthocyanidins in cafeteria diet-induced obese Fischer 344 rats are influenced by fecal microbiota in a photoperiod dependent manner. [Article in Press in Food & Function. Impact Factor (2021): 6.317. SI Journal Citation Reports © Ranking 67/296 (Q1) in Biochemistry & molecular biology and 24/143 in Food science & Technology].

B) Submitted papers included in this thesis:

Arreaza-Gil V, Ávila-Román J, Escobar-Martínez I, Muguerza B, Suárez M, Arola-Arnal A*, Torres-Fuentes C. Photoperiod conditions modulate serum oxylipins levels in healthy and obese rats: impact of proanthocyanidins and gut microbiota. [Submitted to Journal of Photochemistry & Photobiology, B: Biology].

Arreaza-Gil V, Escobar-Martínez I, Soliz-Rueda JR, Suárez M, Schellekens H*, Torres-Fuentes C*, Arola-Arnal, A. Photoperiod effects on corticosterone and seasonal clocks in obese Fischer 344 rats are influenced by gut microbiota. [Submitted to The FASEB journal].

C) Papers in preparation included in this thesis:

Arreaza-Gil V, Escobar-Martínez I, Suárez M, Mulero M, Muguerza B, Arola-Arnal A*, Torres-Fuentes C. Gut microbiota influences the photoperiod effects on proanthocyanidins bioavailability.

D) Other published papers:

Escobar-Martínez I, **Arreaza-Gil V**, Muguerza B, Arola-Arnal A, Bravo FI, Torres-Fuentes C*, Suárez M. Administration Time Significantly Affects Plasma Bioavailability of Grape Seed Proanthocyanidins Extract in Healthy and Obese Fischer 344 Rats. *Molecular Nutrition & Food Research*. 2022 Feb, 66(3):e2100552. DOI: 10.1002/mnfr.202100552. Impact Factor (2021): 6.575. SI Journal Citation Reports © Ranking 21/143 (Q1) in Food Science & Technology.

LIST OF CONFERENCE PAPERS

A) Poster communications:

Torres-Fuentes C, **Arreaza-Gil V**, Gracia-Antón P, Arola-Arnal A, Arola L, Ávila-Román J. Impact of the gut microbiota on plasma oxylipins profile in cafeteria fed Wistar rats. *XI Seminario sobre Alimentación y Estilos de Vida Saludables* – Barcelona, Cataluña, **España 2019**.

Soliz-Rueda JR, **Arreaza-Gil V**, Torres-Fuentes C, Arola-Arnal A and Muguerza B. Grape seed proanthocyanidins attenuate the activity changes trigged by the disruption of photoperiod rhythms in cafeteria diet fed rats. *XI Seminario sobre Alimentación y Estilos de Vida Saludables* – Barcelona, Cataluña, **España 2019**.

Soliz-Rueda JR, **Arreaza-Gil V**, Torres-Fuentes C, Arola-Arnal A and Muguerza B. Grape seed proanthocyanidins-mediated adaptation of seasonal rhythms after an abrupt disruption of the photoperiod in obese rats. *NuGOweek, 16th edition* – Agroscope, Bern, **Switzerland 2019**.

Arreaza-Gil V, Soliz-Rueda JR, Muguerza B, Arola-Arnal A and Torres-Fuentes C. Impact of the gut microbiota on the effects of a grape seed proanthocyanin extract (GSPE) in cafeteria-fed diet Fischer 344 rats under different photoperiods. *Nutrition Winter School 2020, 6th edition. Diet and Microbes: Gut health for the brain and body* – Levi, Lapland, **Finland 2020**.

Ávila-Román J, **Arreaza-Gil V**, Gracia-Antón P, Arola-Arnal A, Arola L, Torres-Fuentes C. Gut microbiota and cafeteria diet effects on PUFA-derived mediators of inflammation. *Nutrition Winter School 2020, 6th edition. Diet and Microbes: Gut health for the brain and body* – Levi, Lapland, **Finland 2020**.

Arreaza-Gil V, Escobar-Martínez I, Suárez M, Arola-Arnal A, Torres-Fuentes C. Gut microbiota dysbiosis in cafeteria-fed rats under different photoperiods. *International Human Microbiome Consortium (IHMC), 8th congress* – Barcelona, Cataluña, **Spain, 2021**.

Arreaza-Gil V, Escobar-Martínez I, Suárez M, Torres-Fuentes C, Arola-Arnal A. Effects of a grape seed proanthocyanidin extract (GSPE) on cafeteria diet-induced obese rats: role of seasonal rhythms and gut microbiota. *I Jornadas Nutracéutica: Compuestos Bioactivos y Nutracéuticos* – Tarragona, Cataluña, **España 2022**.

B) Oral communications:

Arreaza Gil, V. Gut Seasons: Photoperiod Effects on Fecal Microbiota in Healthy and Cafeteria-Induced Obese Rats. *Jornadas de la sociedad Catalana de Biología. Cataluya Sud – Reus, Cataluña,* **España 2022**.

Index

SUMMARY

Biological rhythms are crucial to adjust the physiological and metabolic processes of the organism to the time of day (circadian rhythms) or year (seasonal rhythms). This synchronization is orchestrated by external signals (*Zeitgeber*), being the light the most important one. In this context, the gut microbiota, which plays an important role in maintaining the homeostasis of the organism, can be influenced by changes in the light length of the day (photoperiod). This fact is of great relevance as the gut microbiota is involved in the metabolism of bioactive compounds, such as proanthocyanidins (PAs), which are the most abundant polyphenols in western diet. In fact, these compounds have shown beneficial effects on metabolic disorders such as obesity. Therefore, the functionality of these PAs could be influenced by the time of the year or even the day in which they are administered. Hence, this thesis aims to study the relationship between seasonal rhythms, which have been less studied than circadian rhythms, gut microbiota, and their impact on the functionality of PAs in obesity. To do this, we studied the influence of seasonal rhythms on gut microbiota composition and other physiological parameters in healthy and cafeteria-induced obese Fischer 344 rats, and evaluated the effect of PAs administration in different conditions of gut microbiota dysbiosis. The results showed that seasonal rhythms alter the composition of the gut microbiota, which was associated with changes in weight, glucose tolerance, and levels of oxylipins (inflammatory mediators). Likewise, this interaction between seasonal rhythms and the gut microbiota affected the functionality and bioavailability of PAs, which showed a differently effect depending on the photoperiod conditions in which they were administered. Therefore, these results contribute to expand the knowledge in the field of chrononutrition, establishing the importance of taking into account seasonal rhythms and gut microbiota when evaluating the beneficial effects of bioactive compounds.

RESUMEN

Los ritmos biológicos son cruciales para adaptar los procesos fisiológicos y metabólicos del organismo al momento del día (ritmos circadianos) o del año (ritmos estacionales). Esta sincronización es llevada a cabo por señales externas (*Zeitgeber*), siendo la luz una de las más importante. En este contexto, la microbiota intestinal, la cual desempeña un papel muy importante en el mantenimiento de la homeostasis del organismo, puede verse afectada por los cambios en la duración de luz del día (fotoperiodo). Este hecho es de gran relevancia, ya que la microbiota intestinal está implicada en el metabolismo de compuestos bioactivos, como las proantocianididas (PAs), uno de los polifenoles más abundantes de la dieta occidental, los cuales han demostrado efectos beneficiosos en trastornos metabólicos como la obesidad. Por tanto, la funcionalidad de las PAs podría variar según el momento del año o incluso del día en el que son administradas. Por ello, esta tesis tiene como objetivo estudiar la relación entre los ritmos estacionales, los cuales han sido menos estudiados que los circadianos, y la microbiota intestinal, así como su impacto en la funcionalidad de las PAs en un contexto de obesidad. Para ello, se estudió la influencia de los ritmos estacionales en la composición microbiana intestinal y otros parámetros fisiológicos en ratas Fischer 344 sanas y obesas (alimentadas con dieta de cafetería), y se evaluó el efecto de la administración de PAs en diferentes condiciones de disbiosis intestinal. Los resultados mostraron que los ritmos estacionales alteran la composición de la microbiota intestinal, lo cual fue asociado con cambios en el peso, tolerancia a la glucosa, y niveles de oxilipinas (mediadores inflamatorios). Asimismo, esta interacción entre ritmos estacionales y microbiota intestinal afectó a la funcionalidad y biodisponibilidad de las PAs, las cuales mostraron un efecto diferencial según el fotoperiodo en el que fueron administradas. Así, los resultados de esta tesis contribuyen a ampliar el conocimiento en el campo de la crononutrición, estableciendo la importancia de tener en cuenta los ritmos estacionales a la hora de evaluar los efectos beneficiosos de los compuestos bioactivos.

RESUM

Els ritmes biològics són crucials per adaptar els processos fisiològics i metabòlics de l'organisme al moment del dia (ritmes circadians) o de l'any (ritmes estacionals). Aquesta sincronització és duta a terme per senyals externs (Zeitgeber), sent la llum més important. En aquest context, la microbiota intestinal, que exerceix un paper molt important en el manteniment de l'homeòstasi de l'organisme, es pot veure modulada pels canvis en la durada de llum del dia (fotoperíode). Aquest fet és de gran rellevància, ja que la microbiota intestinal està implicada en el metabolisme de compostos bioactius, com les proantocinidides (PAs), un dels polifenols més abundants de la dieta occidental, els quals han demostrat efectes beneficiosos en trastorns metabòlics com la obesitat. Per tant, la funcionalitat d'aquestes PAs podria variar segons el moment de l'any o fins i tot del dia en què són administrades. Per això, aquesta tesi té com a objectiu estudiar la relació entre els ritmes estacionals, els quals han estat menys estudiats que els circadians, i la microbiota intestinal, i el seu impacte a la funcionalitat de les PAs en un context d'obesitat. Per això, es va estudiar la influència dels ritmes estacionals a la composició microbiana intestinal i altres paràmetres fisiològics en rates Fischer 344 sanes i obeses (alimentades amb dieta de cafeteria), i es va avaluar l'efecte de l'administració de PAs en diferents condicions de disbiosi intestinal. Els resultats van mostrar que els ritmes estacionals alteren la composició de la microbiota intestinal, la qual cosa es va associar amb canvis en el pes, tolerància a la glucosa i nivells d'oxilipines (mediadors inflamatoris). Així mateix, aquesta interacció entre ritmes estacionals i microbiota intestinal va afectar la funcionalitat i biodisponibilitat de les PAs, les quals van mostrar un efecte diferencial segons el fotoperíode en què van ser administrades. Per tant, aquests resultats contribueixen a ampliar el coneixement al camp de la crononutrició, establint la importància de tenir en compte els ritmes estacionals a l'hora d'avaluar els efectes beneficiosos dels compostos bioactius.

LIST OF ABBREVIATION

15-epi Lipoxin A4	15-epi LXA4
6-keto PGF1α	6-keto Prostaglandin F1α
ABX	Antibiotic cocktail
ANOVA	Analysis of variance
ARA	Arachidonic acid
AUC	Area under the curve
BMAL1	Brain and muscle Arnt-like 1
BMAL2	Brain and muscle Arnt-like 2
BW	Body weight
CAF	Cafeteria diet
CG-QTOF	Gas chromatography-quadrupole time-of-flight
CHGA	Chromogranin-A
Clock	Circadian locomotor output cycles kaput
COX	Cyclooxygenase
Cry1	Cryptochrome 1
Cry2	Cryptochrome 2
CYP	Cythochrome P450
DEC1	Deleted in esophageal cancer 1
DHA	Docosahexaenoic acid
DIO2	Type II iodothyronine deiodinase
E-box	Enhancer box
EPA	Eicosapentanoic acid
eWAT	Epididymal white adipose tissue
EYA3	Eyes-absent-3
F/B	Firmicutes-to-Bacteroidetes
F344	Fischer 344

FAs	Fatty acids
FDR	False discovery rate
FSH	Follicle stimulating hormone
GnRH	Hypothalamic gonadotropin-releasing hormone
GR	Glucocorticoid receptor
GSPE	Grape seed proanthocyanidin extract
HFD	High fat diet
HPA	Hypothalamic-pituitary-adrenal
HPG	Hypothalamic-pituitary-gonadal
HPLC-MS/MS	Liquid chromatography tandem mass spectrometry
HPT	Hypothalamic-pituitary-thyroid
iWAT	Inguinal white adipose tissue
L12	Photoperiod 12 h light/12 h darkness
L18	Photoperiod 18 h light/6 h darkness
L6	Photoperiod 6 h light/18 h darkness
LA	Linoleic acid
LC-QqQ	Liquid chromatography coupled to a triple quadrupole mass spectrometer
LD	Long summer-like day length conditions
Leukotriene B4	LTB4
LH	Luteinizing hormone
LA	Linoleic acid
LOX	Lipoxygenase
LP	Long photoperiod
LPS	Lipopolysaccharide
MetS	Metabolic syndrome
mWAT	Mesenteric white adipose tissue
NAD	Nicotinamida adenina dinucleótido

NAMPT	Nicotinamide phosphoribosyltransferase
NEFAs	Non-esterified free fatty acid
OGTT	Oral glucose tolerance test
OA	Oleic acid
OXLs	Oxylipins
PAs	Proanthocyanidins
PCA	Principal component analysist
PCoA	Principal coordinates analysis
PD	Pars distalis
PER1	Period 1
PER2	Period 2
PERMANOVA	Permutational multivariate analysis of variance
Prostaglandin E2	PGE2
PT	Pars tuberalis
PUFAs	Polyunsaturated fatty acids
RvD2	Resolvin D2
REV-ERBα	Nuclear Receptor Subfamily 1 Group D Member 1
rho	Spearman's rank correlation coefficient
RHT	Retinohypothalamic tract
RORα and –γ	Retinoic acid orphan receptor α and –γ
RWAT	Retroperitoneal white adipose tissue
SAD	Seasonal Affective Disorder
SCFAs	Short chain fatty acids
SCN	Suprachiasmatic nucleus
SD	Short winter-like day length
SD	Standard derivation
SEM	Standard error mean

SP	Short photoperiod
STD	Standard chow diet
T3	Tri-iodothyronine
T4	Inactive thyroxine
TH	Thyroid hormone
TRH	Thyrotropin-releasing hormone
TSH	Thyroid-stimulating hormone
TSHβ	α and β sub-units of thyroid-stimulating hormone
VH	Vehicle
WAT	White adipose tissue

INTRODUCTION

1. Biological rhythms

All organisms are constantly exposed to predictable variations in the geophysical environment. These periodic changes are consequences of Earth's rotation around its axis (photoperiod), its tilt (day length variations) and its simultaneous translation around the sun (seasonal changes) [1]. Adaptation to these environmental changes is essential for survival. Thus, all organisms evolved in order to anticipate environmental variations through the development of time-measuring system, driven by internal clocks, allowing them to adjust their physiology and metabolism to daily (circadian rhythms) and annual (seasonal or circannual rhythms) changes [2,3].

Circadian rhythms, whose mechanisms are widely known and studied, play a crucial role in regulating most of the processes of the human body such as the endocrine system, blood pressure, body temperature, gastrointestinal tract, liver metabolism and sleep-wake cycle in a period of 24 hours [4]. On the other hand, seasonal rhythms, which are not currently as well studied as circadian rhythms, include annual cycles of growth, metabolism, food intake, body weight (BW), thermogenesis, migration and sexual behavior, all of which provide an adaptive seasonal program [5]. This synchronization between biological rhythms and the physiological and metabolic activities is mainly orchestrated by changes in the light-dark cycles, being the light one of the most important external cues (*Zeitgeber*) in that interaction [6]. In addition to light, others external cues such as food and dietary patterns have been linked to influence on biological rhythms [7]. In this context, disturbance of biological rhythms caused by modern lifestyles (shiftwork, artificial light exposure, diet type or eating time) have been associated with metabolism disorders development, including type 2 diabetes mellitus [8], obesity and metabolic syndrome (MetS) [9], as well as, with neurological disorders such as cognitive dysfunction, depression and anxiety [10].

1.1. Seasonal rhythms

Animals living in seasonal environments are faced with predictable environmental challenges of cycles of food availability and climatic variability, which require that they adjust their physiology throughout the year in order to survive. Mammals exhibit a remarkably wide spectrum of seasonal physiological adaptations, which includes annual cycles of growth, metabolism, thermogenesis, weight management, hibernation, migration, shedding and pelage growth, and sexual behavior. All of these processes are synchronized by external cues, which regulate the internal timing mechanism that, in turn, provides an adaptive seasonal response in the organisms [5].

Seasonal changes in food availability and temperature are considered crucial and predictable cues to activate the synchronization of physiological processes in mammals and birds. However, there are evidences that seasonal changes in day length (photoperiod) provide the primary environmental cue [11]. Thus, animals are capable of registering changes in photoperiods and translating them into a neuroendocrine response, adjusting the physiological and metabolic processes for optimal function and efficiency to the specific season of the year.

In this context, seasonal rhythms have been associated with the human health, and their alteration by current lifestyle (shift work, artificial light or disturbance in the sleep-wake cycle) promotes the development of different diseases. The most known and firstly described disorder (1984) linked to seasonal rhythms is the Seasonal Affective Disorder (SAD), which causes a recurrent depression that occurs annually at the same time each year (winter) and disappears spontaneously in spring or summer [10,12]. More recently, other many diseases have been related to seasonal rhythms. Thus, altered diurnal and seasonal behavioral have been linked to Alzheimer's disease and related dementias [13]. Cardiovascular diseases have been described to follow a seasonal pattern, showing broadly defined peaks of all subtypes of cardiovascular diseases in

winter [14]. Moreover, seasonality have also been associated with development of MetS [9] and inflammatory diseases [15]. Therefore, seasonal rhythms are currently recognized as a critical feature in the physiology and metabolism of animals.

1.1.1. Seasonal rhythms machinery

The mechanism of seasonal rhythms is still not well elucidated. However, the number of studies has increased in the last years due to the growing interest in knowing the role of seasonal rhythms in the organism, allowing us to present a comprehensive view of the pathways and mechanism for seasonal rhythms generation.

In mammals, it is extensively described that changes in day length are the main cue to detect change of season and regulate the physiological processes. The suprachiasmatic nucleus (SCN) mediates these responses by generating an endogenous neural signal of day length. Thus, the SCN adjusts the duration of this signal in response to seasonal changes in the light length of the day, which it is detected via the retinohypothalamic tract (RHT) [16]. Through efferent connections from the SCN to the pineal gland, the day-length signal is encoded in the duration of nocturnal melatonin secretion, which becomes longer in winter and shorter in summer. Sites that respond to the melatonin signal are capable of inducing changes in behavior and physiology that are programmed to occur during the season [11]. Therefore, melatonin is the hormone of darkness, which provides the major internal endocrine representation of the external photoperiod cue, accurately tracking seasonal changes in night length and in turn regulating seasonal physiology [17].

Among the sites of melatonin action, the pars tuberalis (PT) of the pituitary gland plays a critical role as mediator of photoperiodic neuroendocrine responses in seasonal animals [18]. Thus, the PT has been described as the key seasonal central clock. This structure is located close to the median eminence, the portal system, the pars distalis (PD) and also connected with the third

ventricle via glial cells known as tanacytes, constituting these elements the main anatomical structures of the seasonal pacemaker in animals (Figure 1) [17].

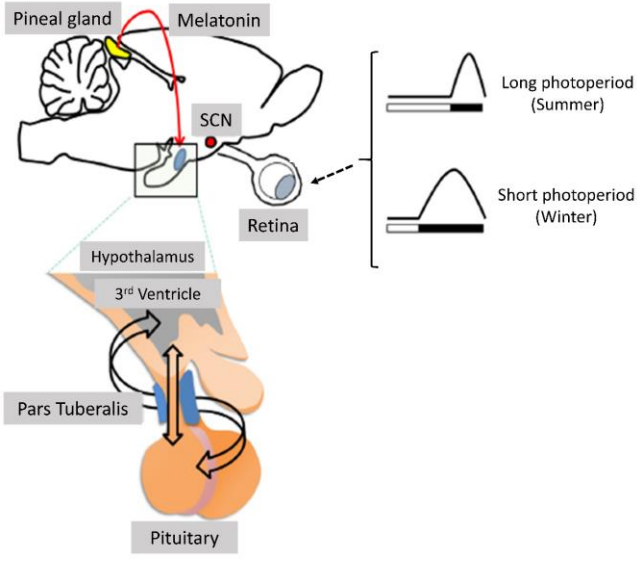

Figure 1. Anatomical structure of the seasonal central clock in animals. *The photic input pathway from the retina to the SCN drives rhythmic melatonin production by the pineal gland, becoming shorter in summer and longer in winter and providing the internal seasonal signal. Figure adapted from Wood, SH, et al., 2017* [11].

Moreover, the PT is constituted by a mixture of endocrine cells, being the most abundant the melatonin-responsive thyrotrophs cells, known as calendar cells. These cells present a higher expression of melatonin receptors MT1 to register the systemic signal, and to discriminate between short and long daily exposure to melatonin. Additionally, the calendar cells also express both α and β sub-units of thyroid-stimulating hormone (TSH), but lack of receptors for the hypothalamic thyrotropin-releasing hormone (TRH), and thus do not respond to conventional hypothalamic outputs [19]. In this context, it has been reported that TSH acts via a retrograde pathway into the brain, driving long-term seasonal responses. This pathway regulates the type II iodothyronine deiodinase (DIO2) gene expression in the hypothalamus in response to long photoperiod (LP) exposure, rising the THSβ receptors within calendar cells. That photoperiodic induction of TSHβ receptors operates as an essential molecular

switch, governing the changes in seasonal metabolism and reproductive biology [20].

Importantly, the rise of TSHβ expression in the calendar cells is closely linked to the transcription activation of co-activator eyes-absent-3 (EYA3), which has been considered a key regulator of summer photoperiodic response [21]. On short photoperiods (SP), the peak phase of EYA3 is 12 h after dark onset, coincident with nocturnal melatonin signal, which suppresses EYA3 expression and activate chromogranin-A (CHGA), which is considered a winter-seasonal mark. On LP, the phase of expression is now coincident with light, and the gene is de-inhibited, which leads to co-activation of the TSHβ and the subsequently stimulation of DIO2. Moreover, the activation of EYA3 suppresses CHGA in the calendar cells, promoting a neuroendocrine cascade triggered in this case by the summer [22,23]. This support the concept that calendar cells operate as a binary switch mechanism, being found only in two states: 'summer-like' or 'winter-like'.

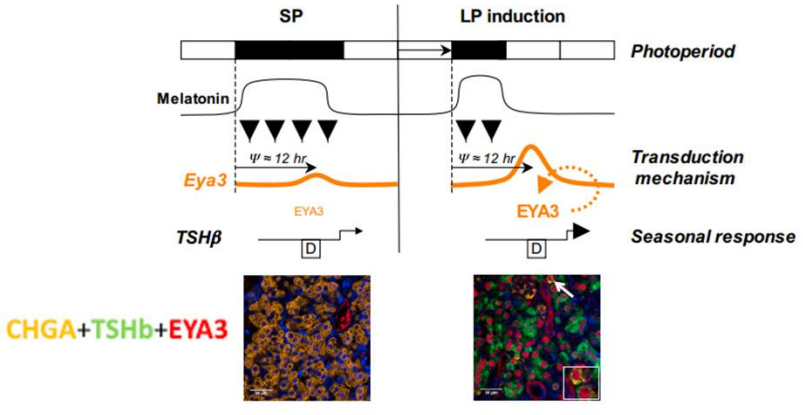

Figure 2. Model for Photoperiodic induction of EYA3 expression and their winter or summer phenotype in the Pars Tuberalis*. SP: short photoperiod; LP: long photoperiod; EYA3: eyes-absent 3; TSHβ: beta-subunit of thyroid-stimulating hormone; CHGA: chromogranin-A. Figure adapted from Dardente et al., 2010 and Shona HW, et al., 2015 [22,23].*

Therefore, the pituitary gland plays an important role as a pacemaker of the seasonal rhythms, regulating EYA3 and CHGA expression via the melatonin

signal, which are key marks of summer and winter states respectively. The regulation of these genes together with the control of the TSHβ, generate the photoperiodic responses in the whole organism, adjusting their physiological and metabolic activity throughout the year [5,24].

1.2. Crosstalk between seasonal rhythms and circadian rhythms

Seasonal rhythms are closely interrelated with the circadian rhythms since both of them are driven by light-dark cycles, which entrain the SCN. Thus, the variations of the light-dark cycles among seasons are the external driver of the central pacemaker of the circadian rhythms [19]. Moreover, several studies have confirmed that PT is a melatonin-dependent circadian oscillator, which follows a circadian rhythmicity, expressing the molecular component of the circadian rhythms [25].

Circadian rhythms are endogenous and self-sustained timing systems that modulate the oscillation of several physiological and metabolic processes in a 24-hour timescale in order to maintain the homeostasis. Thus, sleep/wake and feeding/fasting cycles, as well as other physiological parameters such as body temperature, blood pressure and hormone secretion follow 24-hour rhythmicity [26]. The mammalian circadian clock system is classified hierarchically in the central or pacemaker clock in the SCN of the hypothalamus and the peripheral clocks in peripheral tissues such as liver, muscle, pancreas, intestine and adipose tissue [2]. Although the central clock is capable of working autonomously without any external input, it is also modulated by different external cues, being the light-dark cycles the most important one, as it was previously mentioned [6]. In this context, light influences the central clock, providing via the autonomic nervous system or circulating humoral factors such as melatonin and corticosterone, a signal to maintain rhythmicity and ensure a temporally coordinated physiology in the peripheral tissues. However, although the central clock is the master clock regulator, peripheral tissues are capable of

local and autonomous clock regulation [2]. Thus, they can be modulated by behavioral signals such as physical activity, type of diet and fasting-feeding cycles, suggesting that central and peripheral clocks are bidirectional regulated [26,27].

The molecular circadian machinery is therefore found in all cells of the organism, consisting in multiple sets of transcription factors, which result in autoregulatory transcription-translation feedback loops with a periodicity of 24 h. The main transcription-translation feedback loop is regulated by the transcription factors BMAL1 (brain and muscle aryl hydrocarbon receptor nuclear translocator-like 1) and CLOCK (circadian locomotor output cycles kaput). In particular, transcription of *Bmal1* and *Clock* genes, lead to the heterodimerization in the cytoplasm of the BMAL1:CLOCK complex, which translocates into the nucleus where it binds to canonical Enhancer Box(E-box)-sequences. Among the different target genes, BMAL1:CLOCK promotes the expression of the components of the negative arm of the molecular clock, such as period (*Per1* and *Per2*) and cryptochrome (*Cry1* and *Cry2*). PER and CRY form a complex in the cytoplasm, and after reaching an appropriate concentration, this complex translocates into the nucleus, inhibiting the transcriptional activity of BMAL1:CLOCK complex. PER and CRY in turn, are regulated by ubiquitin proteins for degradations. Decrease in PER and CRY proteins levels relieves the suppression of BMAL1:CLOCK activity, thereby permitting to establish a new oscillatory cycle [28–30]. In addition to the main loop, further key regulators of the circadian clock, such as the nuclear receptors REV-ERB α and β (Nuclear Receptor Subfamily 1 Group D Member 1 α and β), as well as the retinoic acid orphan receptor (RORα and –γ) establish another important feedback loop. Concretely, while REV-ERBs act as transcriptional repressors of *Bmal1* expression, RORs positively regulate the expression of *Bmal1* by binding to sites Retinoic acid receptor-related Orphan Receptor Element elements in the *Bmal1* gene promoter [6,31,32].

In the PT, increased nocturnal melatonin concentrations promote the up-regulation of CRY mRNA levels, whereas PER expression are down-regulated. Because the activation of *Cry* genes occurs in the dark phase, and the activation of *Per* genes occur in the early light phase, the PER/CRY interval phase varies directly with photoperiod, being shorter in SP compared to LP. Thus, the photoperiod modulates these clock genes expression, providing a potential mechanism for decoding the melatonin signal and generating a season-specific photoperiodic change [25]. Moreover, EYA3 can also be regulated by the circadian system. *Dardente et al*. identified conserved E-boxes in the *Eya3* gene promoter, which might be regulated by BMAL1 and CLOCK [22]. In this context, the increase of CRY transcription during the dark phase promoted by melatonin signal represses the BMAL1:CLOCK complex until dawn, which it is the time when occurs the activation of *Eya3* transcription (Figure 3) [11,22]. Furthermore, TSHβ receptor regulation by BMAL1:CLOCK has also been reported through E-box elements [33,34].

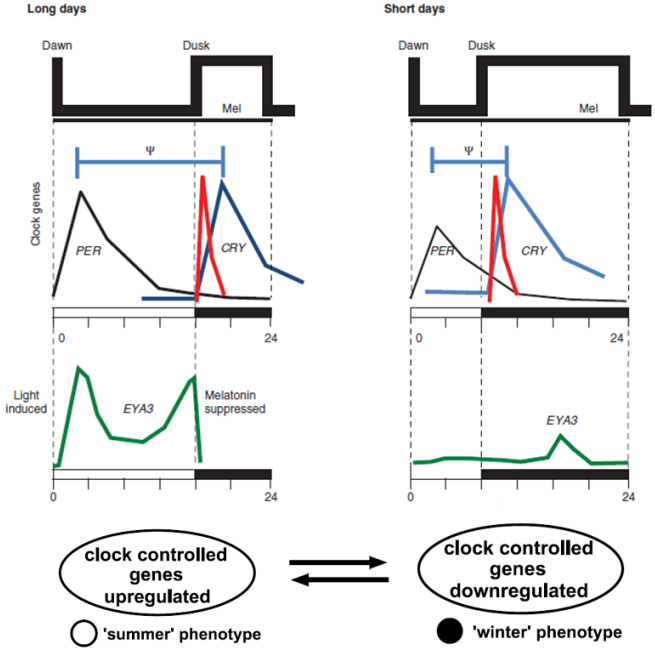

Figure 3. Decoding the melatonin signal in calendar cells involves changes in the temporal expression of circadian clock elements. *Mel: melatonin; PER: period; CRY: cryptochrome; EYA3: eyes-absent 3; ψ: phase. Figure adapted form Wood SH et al., 2014* [5].

Additionally, BMAL2 transcription factor (a paralogue of the circadian regulator BMAL1) has been recently reported as another important co-activator of *Eya3*. Wood et al., reported that LP induce the circadian transcription factor BMAL2, in the PT triggers summer phenotype through the EYA3/THS pathway. Conversely, long-duration melatonin signals on SP induce circadian repressors of deleted in esophageal cancer 1 (DEC1), suppressing EYA3 transcription by repressing BMAL2 activation and EYA3/TSH pathway, triggering winter phenotype. These actions are also associated with progressive genome-wide changes in chromatin state, elaborating the synchronization between circadian and seasonal rhythms (**Figure 4**) [35].

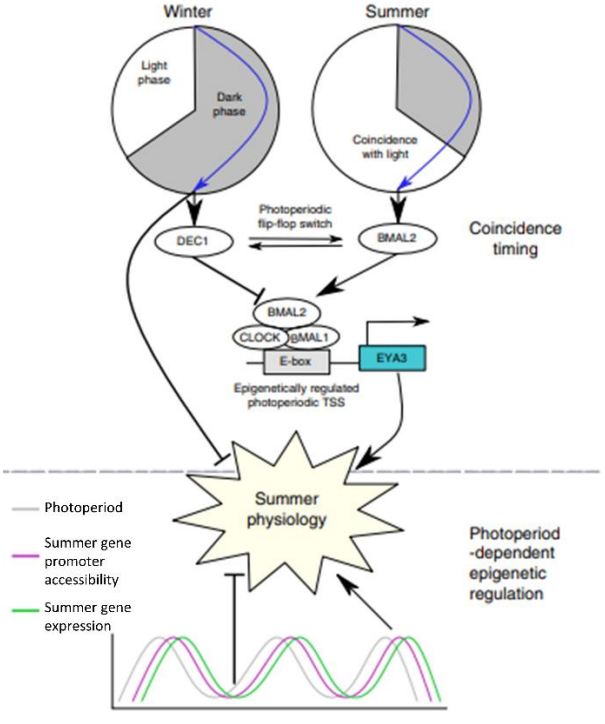

Figure 4. Seasonal phenotype regulation by circadian transcription factors and epigenetic mechanism*. BMAL1: brain and muscle Arnt-like protein-1; CLOCK: circadian locomotor output cycles kaput; BMAL2: brain and muscle Arnt-like protein 2; DEC1: deleted in esophageal cancer 1; EYA3: eyes-absent 3; Figure adapted from Wood SH, et al., 2020* [35].

1.3. Seasonal rhythms and their influence on physiology and metabolism

Adaptive changes in behavior and physiology are the most important aspects for the organism's survival in seasonal environment. For this reason, investigating the changes in physiology and metabolic processes promoted by seasonal rhythms throughout the year have emerged as an interesting field of study within chronobiology in order to develop strategies to improve health status.

In this context, Shoemaker *et al.* reported that Fischer 344 (F344) rats showed reduced body mass, food intake, and testicle size in response to SP [36]. Furthermore, normoweight rats exposed to different photoperiods have been reported to show metabolic changes, suggesting that glucose- and lipid-related pathologies such as obesity and MetS could be influenced by light variations, showing seasonal rhythms an important control on physiological responses of the body [37]. More recently, alterations in biomarkers of oxidative stress and biochemical pathways in rats of different ages have been reported to be influenced by seasonality. Thus, melatonin-related mechanisms of antioxidative protection against lipid peroxidation and oxidative modification of proteins in hepatic tissue, depended on metabolic processes modulated by photoperiod [38].

Although little is known about specific mechanisms by which photoperiods affect the organism, it has been reported that the environmental adjustments of the organism involve both hormonal and neural signals in order to ensure a properly physiology and metabolism functionality [5]. Thus, accumulated evidence suggest that seasonal rhythms control the neuroendocrine functions via PT, which is highly regulated by seasonal rhythms. In this context, seasonal rhythms are key controller of neuroendocrine responses, modulating different axis such as hypothalamic-pituitary-thyroid (HPT), hypothalamic-pituitary-

adrenal (HPA) and hypothalamic-pituitary-gonadal (HPG), and generating physiological and metabolic changes [5,39].

The most studied axis is the HPT since it is known that seasonal rhythms change thyroid hormone (TH) availability within the brain. This is mediated by local control of TH-metabolizing enzymes within tanacytes in the third ventricle of the hypothalamus. In these cells, DIO2 is activated in response to summer day lengths, converting metabolically inactive thyroxine (T4) to triiodothyronine (T3). Thus, TH is a key element in the control of seasonal responses in mammals, being modulated by melatonin signals from pituitary gland [39]. These changes in TH levels due to the seasonal changes are crucial control of metabolic processes in the organism since the HPT axis is involved in a high number of functions such as body heat, metabolic processes that generate energy, tissue growth and nervous, cardiovascular and gastrointestinal system maintenance [40,41].

The HPA axis is also important since cortisol, a glucocorticoid effector of this axis secreted by the adrenal gland, is responsible for the control of stress stimulus and the regulation of the main physiological processes such as metabolism, immune function, and cardiovascular activity [42,43]. Furthermore, increased levels of cortisol have been linked to higher risk of obesity and MetS development [44,45]. Thus, given its influential effects, homeostatic regulation of the levels and rhythm of endogenous circulating cortisol is critical for the maintenance of a healthy state. Accordingly, HPA-axis physiology is modulated by photoperiod as reflected in altered mineralocorticoid receptor, glucocorticoid receptor (GR) gene expression, circulating glucocorticoid concentrations, negative feedback mechanism, and behavioral response to glucocorticoid administration [46]. In this context, glucocorticoid can interact with melatonin, which may underlie differential photoperiodic responses to environmental stress in a tissue specific manner. Several species increase circulating glucocorticoids levels and GR expression in short days [47,48]. Indeed, GR expression was also increased in the Siberian

hamster hippocampus and in the house sparrow spleen following short day exposure [49,50]. Hence, it is known that cortisol levels exhibit substantial seasonal rhythmicity, with peak levels occurring during the short-photoperiod winter and reduced levels occurring in long-photoperiod summer, allowing the synchronization of peripheral biological processes to the environment [51,52].

Finally, seasonality impacts on the HPG axis allow for regulating reproductive processes, also playing an important role in the metabolism of carbohydrates and lipids, in the cardiovascular system and in osteogenesis processes [53]. Hypothalamic gonadotropin-releasing hormone (GnRH) induces the release of both luteinizing hormone (LH) and follicle stimulating hormone (FSH) by the PD of pituitary. These hormones reach sexual organs and activate the synthesis of testosterone in males and estrogen and progesterone in females. In turn, these sexual hormones act as a modulator of the HPG through its inhibitory activity in the hypothalamus and pituitary [54]. The seasonal changes in GnRH hormone have long been recognized in mammals as being regulated by the melatonin signal. Thus, the transition from the breeding to non-breeding season is associated with a dramatic reduction in the frequency of GnRH pulses in sheep, suppressing the gonadotropins reach to the gonads, resulting in gonadal regression [55]. This fact is relevant to animals, which adjust their sexual behavior and the birth to the moment of the year in which the possibility of survival is higher. In addition, in humans it has been reported that the modern lifestyle such as shiftwork or artificial light exposure, can alter the seasonal rhythms, promoting reproductive disorders [56].

Therefore, seasonal rhythms act on the different neuroendocrine pathways to maintain the functionality of the organism and further investigations are needed to elucidate the potential mechanisms involved.

2. The Gut Microbiota and health

The gut microbiota is one of the largest components of our body, which is defined as crucial to maintain homeostasis and metabolic health of the host [57]. It is believed that there are approximately 1-2 kg of microorganisms in the human gut which contain over 100 times more genes than the human genome itself [58], being the ration between somatic and microbial cells close to 1:1 [59,60]. The gut microbiota contains a high diversity distributed in more than 50 different phyla. However, *Bacteroidetes*, *Firmicutes*, *Actinobacteria*, *Proteobacteria* and *Verrucomicrobia* phyla make up to 90% of the total microbial population in humans [61]. Furthermore, density and composition of microbiota widely varies along the gastrointestinal tract, being the colon the most colonized organ with approximately 70% of all bacteria in the human body [62]. Gut bacteria have a crucial symbiotic relationship with the human body throughout its evolution, protecting and supporting the structure of intestinal mucosa [63]. Thus, gut bacteria play an important role in a high number of functions in the organism including: fermentation of non-digestible polysaccharides from diet in short chain fatty acids (SCFAs), which are energy sources for microbial and host's cells, as well as controller of several physiological processes such as energy expenditure and satiety [64]; regulation of fat storage and harvest energy from the diet [65]; metabolization of dietary phenolic compound such as flavonoids, which exert beneficial effects on the host [66]; production of essential vitamins such as vitamin K and folic acid [67,68] and participation in bile acid metabolism [69]; Furthermore, gut microbiota also affect immune system, insulin, and glucose metabolism [70], as well as endocrine signaling pathways via the microbiota–gut–brain axis [71]. Hence, gut microbiota is becoming increasingly recognized as a key regulator of host physiology, and undeniably has a role in health.

Alterations in the composition of gut microbiota promote metabolic disorders development such as obesity and diabetes [63]. Thus, a healthy gut microbiota

is crucial for proper metabolic function and homoeostasis of the host [63,72]. Therefore, knowing the factors that alter the gut microbiota composition and how it could be modulated, might provide potential therapy strategies to avoid metabolic disorders development, which are serious and widespread health concerns worldwide [73].

2.1. Gut microbiota: role of diet and its impact on obesity development

Gut microbiota composition can be altered by many intrinsic factors including age, sex, genetic or birth delivery, but also by external factors such as diet, antibiotics, stress and life style [74]. Among these factors, the diet plays a dominant contribution to gut microbial composition. Indeed, dietary patterns have been associated with distinct combination of bacteria in the intestine, also called enterotypes [75]. Thus, considering that the role of the gut microbiota is to ferment dietary substrates, complex diets can provide a range of growth-promoting and growth-inhibiting factors for specific group of bacteria [76]. In this context, diets rich in fiber and low in both sugar and fat, such as the Mediterranean diet, have long been associated with an increase of gut microbiota diversity and with a higher health status [77]. By contrast, Western-style diets, high in sugar and fat, have profound effects on gut microbiota composition, decreasing its diversity and often correlating with deleterious metabolic health effects (**Figure 5**) [78]. For instance, Wistar rats fed a cafeteria diet (CAF), which consists of high palatable and energy-dense foods regularly consumed by humans, showed a lower bacterial diversity and an increase of *Bacteroidetes* and *Proteobacteria* phyla relative abundance compared to standard chow diet-fed rats. These effects were linked to decreased beneficial microbial-derived metabolites and higher visceral adiposity, demonstrating the strong effect of the diet on gut microbiota composition and its relationship with obesity development [79].

In this context, diets high in fat and sugar can promote the alteration of gut microbiota composition, known as dysbiosis [80]. Dysbiosis of gut microbiota leads to altered functionality and integrity of the gut barrier, increasing its permeability and allowing the translocation of bacterial pro-inflammatory toxins such as lipopolysaccharides (LPS). This increase of systemic LPS levels contribute to low-grade inflammation and to fat storage in adipose tissue, a characteristic trait of obesity and the MetS [81].

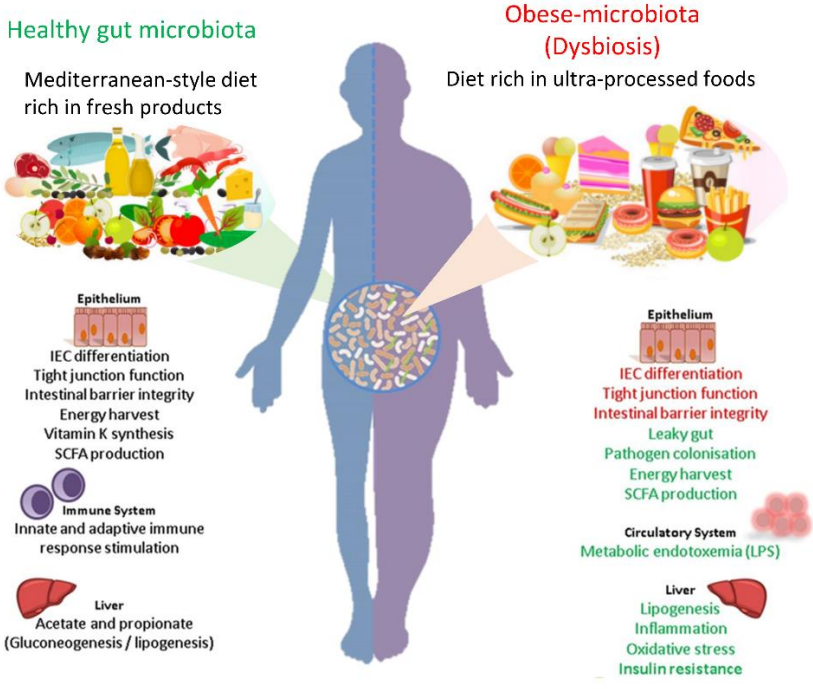

Figure 5. Functions in the healthy gut microbiota versus the obese microbiota caused by high fat and high sugar diet*. The metabolic processes in peripheral organs leading to increased adiposity, inflammation, oxidative stress and insulin resistance are associated with the altered microbiota profile associated with the obese phenotype. IEC, intestinal epithelial cell; LPS, lipopolysaccharide; SCFA, short chain fatty acid. Figure adapted from Patterson et al., 2016* [63].

In this regard, several studies have reported the role of the gut microbiota in obesity development. Turnbaugh *et al*., performed one of the first studies that definitively linked the gut microbiota with weight gain, caused by an increase in the energy-harvesting capabilities of the microbiota from obese mice [82]. Furthermore, germfree mice colonized with an 'obese-microbiota' isolated

from genetically obese *ob/ob* mice had a greater increase in body fat than those colonized with a 'lean-microbiota', despite no significant differences in energy consumption or initial body fat/weight between the groups [82]. Additionally, alteration in the production of SCFAs have been reported in obese human [83]. The gut microbiome possesses glycoside hydrolase enzymes, not found in the human genome and that are crucially involved in hydrolysing and fermenting a wide variety of dietary polysaccharides that enhance host energy status [84]. The microbial derived energy from these otherwise indigestible complex polysaccharides is in the form of SCFAs (acetate, butyrate, and propionate, predominantly). SCFAs are the principal energy source for colonocytes as well as playing a key role in the prevention and treatment of metabolic disorders [85–87].

At the compositional level, obesity is associated with changes in the abundance ratio of two of the most dominant phyla: *Firmicutes* and *Bacteroidetes*. However, while some studies have described an increased proportion of Firmicutes-to-Bacteroidetes (F/B) in obesity [88] and weight loss has been reported to reduce the F/B ratio in human subjects [89], these findings are not universal [90]. Hence, the usefulness of the F/B ratio as a compositional biomarker for obesity remains unclear [91]. Additionally, several compositional and richness differences have been reported at genera taxonomic level in obesity. Thus, higher adiposity and insulin resistance in obese subjects have been associated with lower richness and higher prevalence of proinflammatory genera such as *Bacteroides*, *Parabacteroides*, *Ruminococcus*, *Campylobacter*, *Porphyromonas*, *Staphylococcus* and *Anaerostipes*, while in lean subjects, higher bacterial richness was observed together with an increase of genera associated with health properties such as *Faecalibacterium*, *Bifidobacterium*, *Lactobacillus*, *Butyrivibrio*, *Alistipes*, *Akkermansia*, and *Coprococcus* [91]. Moreover, it was concluded that subjects with low bacterial richness and an obese phenotype had a reduction in butyrate-producing bacteria, an increase in mucus degradation and an increase in the potential to manage oxidative

stress [91]. Thus, it appears that obese individuals have lower bacterial richness and harbor a microbiota that predisposes them to an inflammatory status.

Additionally, it is worth highlighting that antibiotics have shown to alter the gut microbiota composition, causing dysbiosis and ultimately affecting host physiology and metabolism [92,93]. Thus, overuse of antibiotics and exposure to them during early life has been related to reduction in the population size of specific bacteria, which subsequently disrupt gut barrier function, resulting in a low-grade chronic inflammation and metabolic endotoxemia [94,95]. In this context, epidemiological studies show that exposure to antibiotics early in life is associated with increased risk of obesity and related metabolic disorders [95,96]. Moreover, studies in mice and rats have shown that the administration of different antibiotics is associated with specific changes in microbial community composition, which can modify BW gain and glycemic phenotypes [97]. These findings support the relationship between gut microbiota and metabolic diseases.

Hence, gut microbiota dysbiosis actively contributes to the onset of obesity and related chronic low-grade inflammation, playing the diet a key on the modulation of its composition. These findings have important implications since modulation of intestinal microbiota by dietary interventions might provide potential novel anti-obesity strategies.

2.2. Gut microbiota and oxylipins metabolism: possible obesity biomarkers

Gut microbiota plays a crucial role in the maintenance of the homeostasis in the host and mediates the effects of diet, thereby modifying host metabolism and the incidence of metabolic disorders, as it has been previously mentioned [57]. This fact is highly relevant for the society since obesity and its comorbidities (ie, type 2 diabetes, cardiovascular disease, and increased pro-inflammatory status) continue increasing worldwide affecting more than two billion people [98–100].

In this context, it has been reported that gut microbiota mediates saturation of polyunsaturated fatty acids (PUFAs) derived from dietary fat as a detoxifying mechanism in the gastrointestinal tract [101]. The total fat and saturated-fat intake as percentage of total calories continued to decrease in Western diets [102]. However, the intake of omega-6 fat that includes primarily the essential fatty acid linoleic acid (LA) has increased, whereas intake of omega-3 fat that includes other essential fatty acids has decreased. This change in the composition of PUFAs substantially increases the incidence and prevalence of overweight and obesity [103]. Furthermore, Miyamoto *et al.* showed that gut microbiota conferred resistance to high fat diet (HFD)-induced obesity by modulating dietary PUFAs metabolism [104]. Therefore, this impact of gut microbiota on PUFA-derived metabolites may have potential as therapeutic target for the prevention of the pathophysiology of obesity. Thus, gut microbiota has been recently described as a pivotal factor in the modulation of oxylipins (OXLs) metabolism. OXLs are potent bioactive lipid mediators that are involved in the activation and resolution of inflammatory processes [105]. These metabolites are produced as a result of the oxygenation of dietary polyunsaturated fatty acids (PUFAs) by cyclooxygenase (COX), lipoxygenase (LOX) and cythochrome P450 (CYP) enzymes [106]. Most oxylipins are generated from arachidonic acid (ARA, 20:4n-6), which is produced in the initial phase of inflammation [103]. ARA-derived OXLs can be both proinflammatory, such as prostaglandins, leukotrienes and thromboxanes, or anti-inflammatory, such as lipoxins, [107]. Moreover, OXLs can also be synthetized from both dietary eicosapentanoic acid (EPA, 20:5n-3) and docosahexaenoic acid (DHA, 22:6n-3), generating mostly anti-inflammatory OXLs such as resolvins, protectins and maresins [108,109]. Hence, OXLs play a key role in the maintenance of inflammatory homeostasis, being of significant relevance in several disorders associated to chronic inflammation such as obesity [110]. In fact, altered OXLs profile has been linked to obesity in both animals and human subjects, suggesting that these metabolites can be used as obesity biomarkers

and as a target for the prevention of this disorder [111,112], being gut microbiota a possible target for their modulation.

2.3. Gut microbiota and seasonal rhythms: impacts on health

Biological rhythms have been established in recent years as key factors in the control of the gut microbiota composition and functionality [113,114]. In this regard, although the interaction between gut microbiota and seasonal rhythms has not been sufficiently investigated so far, it has been demonstrated that gut microbiota composition changes according to photoperiod exposure conditions, following a seasonal rhythmicity. Thus, Bailey *et al.* reported that male Siberian hamster housed under summer-like day length showed a significant increase of *Proteobacteria* phyla. This effect was primarily due to a significant increase in the abundance of the genus *Citrobacter*, which significantly correlated with body mass and with inguinal fat mass [114]. Liu *et al.* also demonstrated that Sprague–Dawley male rats under the same feeding conditions and housed under summer- or winter-like day length showed significant differences in gut microbiota composition [115]. These changes may contribute to a better environmental adaptation by promoting a more efficient pattern of energy harvesting from diet. In the same way, a study with human fecal samples obtained in different seasons revealed higher *Actinobacteria* and lower *Bacteroidetes* relative abundance in summer compared to other seasons. Furthermore, the F/B ratio was significantly higher in summer-derived samples than in winter-derived ones [116], which suggest that gut microbiota composition is strongly influenced by seasonal rhythms. Additionally, it has been reported that implanting Siberian hamster with fecal microbiota from long-day hamsters resulted in a reversal of seasonal aggression, whereby short-day hamsters displayed aggression levels typical of long-day hamster, correlating the aggressive behavior with several bacterial taxa [117]. Therefore, this result suggests that gut microbiota takes part in the photoperiodic mechanism regulating seasonal host behavior and contribute toward a more

comprehensive understanding of the relationship between the microbiota, host and environment.

It is worth highlighting that the relationship between circadian rhythms and gut microbiota is better known compared to that with seasonal rhythms. Thus, gut microbiota is subject to diurnal variation and is entrained by host circadian rhythms [113]. Accordingly, the bacteria fluctuations along the day, several metabolites derived from gut microbiota display diurnal rhythmicity in both intestinal lumen and serum [118]. For instance, SCFAs level were diurnally expressed in faces and cecum content, and associated with peripheral clock entrainment [119]. Therefore, growing body of evidence has demonstrated that the host circadian cycle governs the structure of the gut microbiota and its diurnal rhythmicity, whereas the microbes contribute to maintenance of the clock function. The alteration of the cyclical nature of this microbe-host interaction profoundly influences disease pathology such as MetS and obesity [113]. In this context, due to the close relationship between circadian and seasonal rhythms, it could be hypothesized that seasonal variations of the gut microbiota could influence on host peripheral circadian rhythms. In fact, a recent study carried out in giant pandas, showed that seasonal shift of the gut microbiota synchronized liver peripheral circadian rhythms via butyrate for physiological adaptations [120].

Therefore, the relationship between gut microbiota, biological rhythms, and its impact on the physiology of the host is profoundly complex, and further investigation is needed to elucidate the causative link of these factors. The final goal of the future studies will be to promote time-of-year or –day interventions to treat various disorders and provide health benefits. Furthermore, better understanding of the interactions between biological rhythms and gut microbiota-host physiology may help to improve chronotherapies.

3. Polyphenols

The association between diet, health and the presence of bioactive compounds in food has received great attention in recent years. Thus, the interest in food products that promote well-being and reduce the risk of developing diseases is increasing.

Polyphenols are secondary metabolites of plants, which have attracted great attention from the scientific community due to their beneficial effect on health [121,122]. In plants, they are involved in the defense against ultraviolet radiation, attraction of pollinators, aggression by pathogens and herbivores, reproduction, nutrition and growth. Their synthesis is increased under abiotic stress conditions such as drought, salinity, high/low temperature, ultraviolet radiations or heavy metal presence [123]. Polyphenols are naturally present in fruits, vegetables, whole grains, leaves and roots, but also in other types of foods and beverages such as tea, chocolate and wine. The diversity and wide distribution of polyphenols in plants have led to different ways of categorizing these natural compounds, by their source, origin, biological function, and chemical structure [121]. Thus, focusing on their chemical classification, polyphenols are characterized by the presence of phenolic structural features and can be classified in flavonoids and non-flavonoids. More than 8000 phenolic structures are currently known [124,125].

3.1. Chemical classification of polyphenols

Polyphenols are classified in two main groups: flavonoids and non-flavonoids, based on the number of phenol rings that they contain, the number and disposition of their carbon atoms and the structural elements bonded to these rings, such as sugars or organic acids [124,125].

3.1.1. Flavonoids

Flavonoids are the largest group of polyphenols, consisting generally of 15 carbons with two aromatic rings (Ring A and Ring B) connected by a heterocyclic

ring (Ring C). They can be separated into different sub-groups due to the hydroxylation pattern or variations in the three carbon bridge (**Figure 6**) [116].

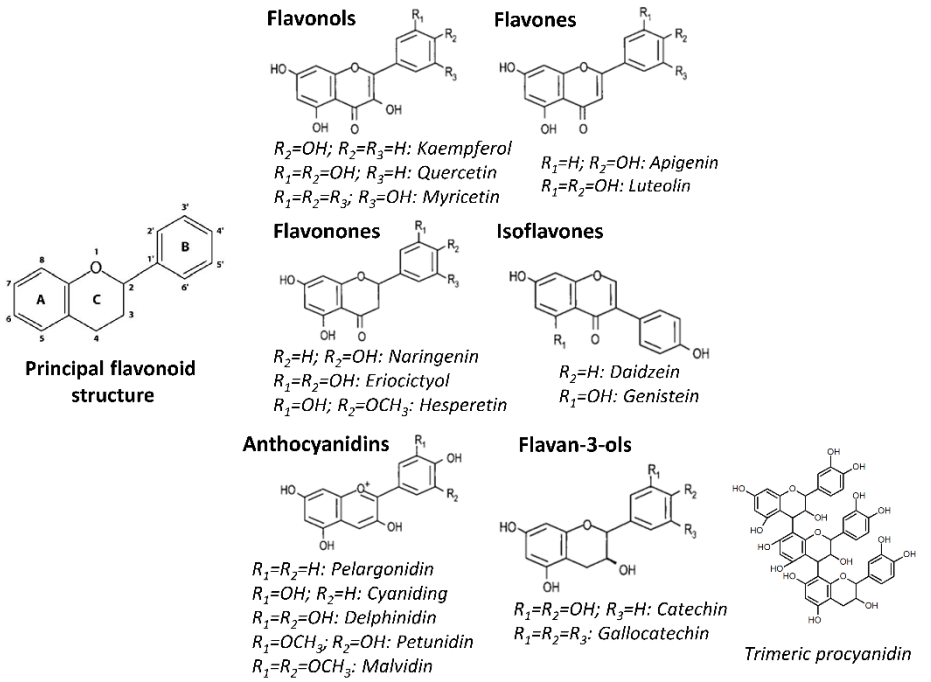

Figure 6. Flavonoids structures. *The principal flavonoid structure consist in two aromatic rings (Ring A and Ring B) of 6C connected by a heterocyclic ring (Ring C), which can undergo modifications, resulting in the different sub-classes of flavonoids (flavonols, flavones, flavonones, isoflavones, anthocyanidins and flavan-3-ols). Figure adapted from Manach et al. 2004*[126].

The principal subgroups are:

- Flavonols

Flavonols are present in glycosylated forms in nature, often binding glucose or rhamnose, but other sugars might be involved. These compounds are widely present at relatively low concentrations in fruits and vegetables. Some examples are quercetin and kaempferol [126].

- Flavones

Flavones are much less common than flavonols in fruits and vegetables, but their structures are similar, containing mainly glycosides. Luteolin and apigenin

are two representative examples of flavones found in chamomile and parsley, which are the main food sources of these compounds [126].

- Flavanones

This group is structurally similar to flavones. They are generally glycosylated by a disaccharide at position 7, having being identified about 87 flavanove glycosides to date. The principal food resources of these compounds are citrus fruits, but they can also be found in tomatoes and certain aromatic plants such as mint [126].

- Isoflavones

Isoflavones present a similar structure to estrogens, which confer pseudohormonal properties such as the ability to bind to estrogen receptors. They are found exclusively in leguminous plants, being soy and its processed products the main source in the human diet. The most representative molecules are genistein, daidzein and glycitein [126].

- Anthocyanidins

Anthocyanidins are found in plant tissue in their glycosidic forms, known as anthocyanins. More than 500 anthocyanins are known and differ depending on the hydroxylation, methoxylation or glycosylation pattern. However, the most commonly and widely distributed in foods are pelargonidin, cyaniding, peonidin, delphinidin, petunidin and malvidin. These flavonoids are the principal components of the red, blue and purple pigments of the majority of flowers' petals, fruits and vegetables, as well as certain special varieties of grains. Thus, they are consumed in the diet of berries, red grapes, apples, red wine, and various vegetables such as aubergines, red/purple cabbage, beans, onions or radishes [126].

- Flavan-3-ols

Flavan-3-ols are commonly called catechins and are the most structurally complex subclass of flavonoids. The hydroxylation at C3, allows flavan-3-ols to have two chiral centers on the molecule (on C2 and C3), resulting in four possible diastereoisomers. Moreover, catechin and epicatechin (the principal monomeric flavan-3-ols) can be hydroxylated to form gallocatechins and also undergo esterification with gallic acid to complex structures including oligomeric and polymeric proanthocyanidins (PAs), which are also known as condensed tannins. In contrast to other classes of flavonoids, flavan-3-ols are not glycosylated in foods. The main food sources of these compounds are many fruits, particularly skins of grapes, apples, blueberries, tea leaves and cacao bean [126,127].

3.1.2. Non-flavonoids

The main subclasses of phenolic compounds that are not flavonoids, are the following (**Figure 7**) [126]:

- Phenolic acids

Phenolic acids are one of the most widely distributed non-flavonoid phenolic compounds present in free, conjugated-soluble and insoluble-bound forms. Phenolic acids are characterized by having one or more hydroxyl groups and a carboxylic acid function at the benzene ring. They are derived from two main phenolic compounds, benzoic acid (such as syringic acid, vanillic acid, gentisic acid…) and cinnamic acids (such as caffeic acid, ferulic acid, *p*-coumaric acid…) [125].

- Stilbenes

Stilbenes are found in low concentrations in the human diet, being resveratrol the most studied and well-known. It is found in red wine and peanuts and in lower amounts in berries, red cabbage, spinach and certain herbs [128].

- Lignans

Lignans are diphenolic compounds derived from the combination of two phenylpropanoid units. The richest dietary source are oilseeds (flax, soy, rapeseed, and sesame), whole-grain cereals (wheat, oats, rye, and barley), legumes, various vegetables, and fruit (particularly berries) [129].

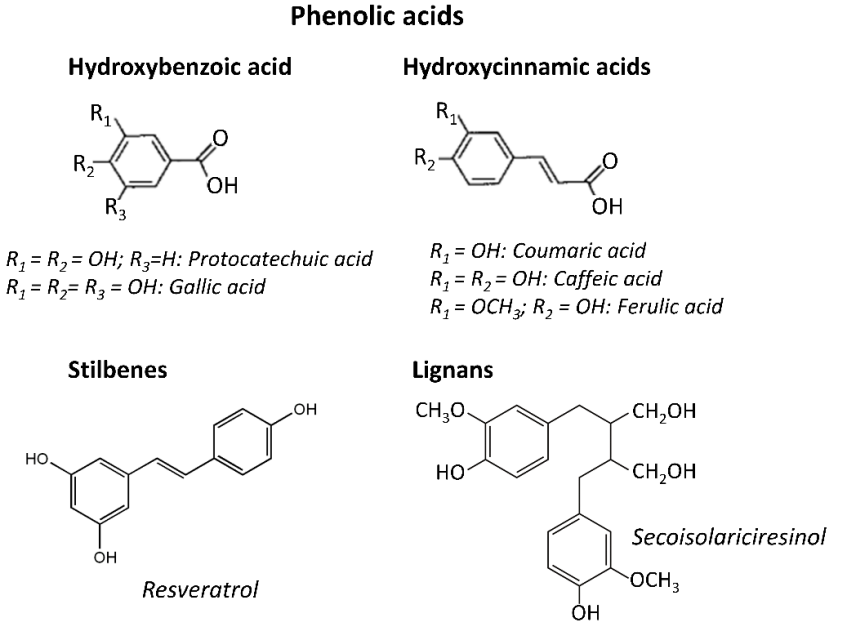

Figure 7. Non-flavonoids chemical structure*. Figure adapted from Manach et al. 2004* [126].

3.2. Beneficial effects of Proanthocyanidins on obesity: role of gut microbiota and biological rhythms.

PAs are the most abundant flavonoids in the human diet [130]. They are present in many edible plants sources including barley, hops, maize, apples, grapes, strawberries, cocoa, almond, cinnamon, peanuts, and tea. Grape seeds in particular provide a diverse great amount of PAs [131].

As previously mentioned, PAs are one of the most structurally complex flavonoid, comprising the elementary monomeric subunit of flavan-3-ols (catechin and epicatechin), which in turn, can be gallated, to form oligomers

(degree of polymerization, DP = 2-5) and polymers (DP > 5) [146]. Grape seed proanthocyanidin extract (GSPE), mainly composed of dimers, trimerics and oligomers of PAs [147], used in this thesis, has been studied previously *in vitro* and *in vivo* by our group, demonstrating several beneficial effects on health. Thus, GSPE significantly improves insulin resistance [148], hypertension [149–151], oxidative stress [152] and mitochondrial dysfunctionality [153] and lipid metabolism [154–156], showing the potential role of PAs in the prevention of obesity and MetS [157,158].

Thus, focusing on GSPE and its beneficial properties in obesity development, it was found that GSPE can improve lipid metabolism by reducing fat depots [159]. This effect is due to GSPE is able to reduce lipid accumulation through inhibiting preadipocyte differentiation, reducing the formation of new adipocytes and regulating white adipose tissue (WAT) hypertrophy and proliferation, improving therefore WAT function [160–162]. Furthermore, GSPE administration improves insulin resistance [148], prevents the increase in blood of glucose, triglycerides, and insulin levels by increasing adipokine secretion and decreasing oxidative stress pathways [163]. Hence, GSPE can effectively prevent obesity through different mechanisms [164].

In this regard, it was also reported that the administration of GSPE improved the structural diversity of gut microbiota in HFD-fed mice, increasing the relative abundance of *Faecalibaculum*, *Bacteroides* and *Akkermansia* as well as, the levels of butyric and propionic acids, changes that correlated with reduced final BW, decreased insulin resistance and elevated levels of adiponectin and leptin [165]. Moreover, GSPE ameliorated plasma levels of inflammatory factors such as interleukin-6 or tumor necrosis factor-alpha, reduced epididymal fat mass and improved insulin sensitivity by modulating bacterial content such as *Clostridium*, *Roseburia* and *Prevotella* in HFD mice [166]. Moreover, gut microbiota plays an important role in the polyphenols metabolism [66,167–169]. Therefore, GSPE can act as a prebiotic, and at the same time, intestinal bacteria can modulate the metabolism of phenolic compounds, being this

bidirectional interaction another possible mechanism by which GSPE affects metabolism processes and prevent obesity development. Therefore, evidence suggests that polyphenols can modulate gut microbiota composition and, at the same time, intestinal bacteria can modulate the metabolism of phenolic compounds, showing a bidirectional interaction that may have a significant impact on phenolic compounds bioactivity.

On the other hand, polyphenols can also influence biological rhythms, which may be another important pathway by which these bioactive compounds regulate and exert their beneficial effects on the organism. Thus, it is known that GSPE is able to modulate the clock genes in liver, modulating nicotinamide phosphoribosyltransferase (NAMPT) and nicotinamida adenina dinucleótido (NAD) in opposite ways depending on its administration time (decreasing their levels when it was administered in the morning and increasing their levels at the night administration). Consequently, GSPE may improve the energetic profile via increase mitochondrial functional oxidation. Finally, it was reported that BMAL1 acetylation pattern was depending on GSPE administration time, explaining the NAMPT overexpression and the following NAD peak in the liver at night in both healthy and obese rats [144,145]. Moreover, GSPE was able to restore the mitochondrial dynamic and function through clock-genes modulation in liver from CAF-induced obese rats [170]. In turn, GSPE effects can be influenced by biological rhythms. In this context, GSPE administration in the morning was associated with a potential antidiabetic effect without affecting adiposity and energy intake. In contrast, GSPE administration at night improved adipose tissue expansion decreasing adipocyte size in the inguinal WAT. In turn, GSPE only when it was administered at night, repressed the expression of the clock gene CRY1 in the inguinal WAT, suggesting that GSPE may influence the metabolic response of WAT through its interaction with the circadian rhythms [171].

In addition to circadian rhythms, seasonal rhythms may alter the effects of polyphenols. In this context, our group showed that hypothalamic leptin

sensitivity was influenced by polyphenol-rich seasonal fruits (cherry and grape), in a photoperiod-dependent manner in F344 rats [172]. Thus, a significant increased hypothalamic gene expression of leptin receptor isoform B was observed only when cherries were consumed in short-day photoperiod. Furthermore, hypothalamic pro-opiomelanocortin expression, which is under leptin regulation, was significantly increased by both grapes and cherries intake only in the short day photoperiod, indicating a clear photoperiod effect [37].

According all these studies, polyphenols are able to interact with mammalian physiology in a photoperiod-dependent manner, which may be explained by the Xenohormesis theory. In this context, polyphenols have been considered chemical cues, also called phytochemicals, which are synthetized by plants under adverse conditions such as extreme temperatures, predation and water or nutrient availability, providing a chemical signature of the state of the environment [173,174]. The Xenohormesis theory stablishes that the heterotroph organism (i.e. humans) are able to sense signaling stress-induced molecules from other species (i.e. plants) [175]. By this adaptation capacity, heterotrophs use these phytochemicals cues from other species, through the diet, to get information on the environmental status, adjusting their metabolism in anticipation of adverse conditions to increase their chances of survival [176]. Thus, according to the Xenohormesis theory, the consumption of fruits out of their natural conditions season, from far distant geographical regions or the cultivated under conditions that modulate their phytochemical profile in a non-natural way, would provide chemical cues that do not correspond to the current environment situation to the consuming organism, and thus result in a non-efficient adaptation of their physiology [175]. Indeed, our group has shown that the consumption of fruits in- or out-season has different effects in F344 rats. Concretely, Cruz-Carrion et al. reported that consumption of cherries in-season, independently of their origin, may promote health by preventing oxidative stress [177]. Furthermore, the consumption of cherries out of their traditional consumption season has shown to influence the

regulation of key clock genes in adipose tissue [172]. Additionally, tomatoes from two different geographical origins (local or non-local tomato) with a specific phenolic signature had a specific-photoperiod response, showing high protective effects against oxidative stress when they were consumed in-season [178]. In the same way, consumption of orange from the northern or southern hemispheres modulated fat accumulation, morphology and gene expression in the adipose tissue of F344 rats when they were consumed out-season [179]. Thus, polyphenols may provide physiological and metabolic signals facilitating the adaptation to the environment, interacting with the biological clock system.

2.1. Bioavailability and metabolism of proanthocyanidins: role of gut microbiota and biological rhythms.

In general terms, bioavailability can be defined as the fraction of a nutrient or non-nutrient (compounds such as drugs) that is available for the host for physiological functions and/or storage. In the specific case of phenolic compounds bioavailability involves chemical modifications during digestion, absorption by enterocytes, microbial metabolism of non-absorbed compound and those compounds undergoing enterohepatic recirculation, phase-II metabolism, transport through the blood and body distribution of the generated bioactive compounds, as well as their excretion via the kidney or the faces [180]. In this context, PAs bioavailability and metabolism are the main limiting factors for PAs bioactivity [180]. Therefore, the study of PAs bioavailability and metabolism is of key relevance to understand the biological functions associated with PAs consumption.

The metabolism of PAs is complex, and a simplification of these processes to GSPE can be found in **Figure 8**. In this regard, in the first step of the digestion process, low molecular weight PAs can be hydrolyzed to flavan-3-ol monomers (cathechin and epicathechin), whereas high molecular weight PAs are transported into the large intestine in their original form. Therefore, the stomach is the minor location of absorption of polyphenols [181]. In the small

intestine, monomeric epicathechin and catechin are partly absorbed in their original form and is then subjected to glucoronidation, sulphatation and/or O-methylation [182]. On the other hand, oligemeric PAs are not directly absorbed from the small intestine, although dimers and trimers can be detected in plasma [182,183]. The absorbed phenolic compounds and their metabolites are transported to the liver by the portal circulation, where are transformed into phase-II metabolism. Several phase-II metabolites can co-exist in the plasma, including singly-conjugated metabolites like catechin glucuronide, and multiply-conjugated metabolites, such as methyl-catechin glucuronide [184]. Generally, maximum concentrations of phase-II metabolites in plasma are reached in between 1 and 4 hours after the ingestion of PAs [183]. Thus, the administration of 1g/kg of GSPE resulted in a maximum peak concentration of several metabolites in plasma, such as catechin and epicathechin glucuronide and methyl-glucuronidated, two hours after GSPE ingestion [185].

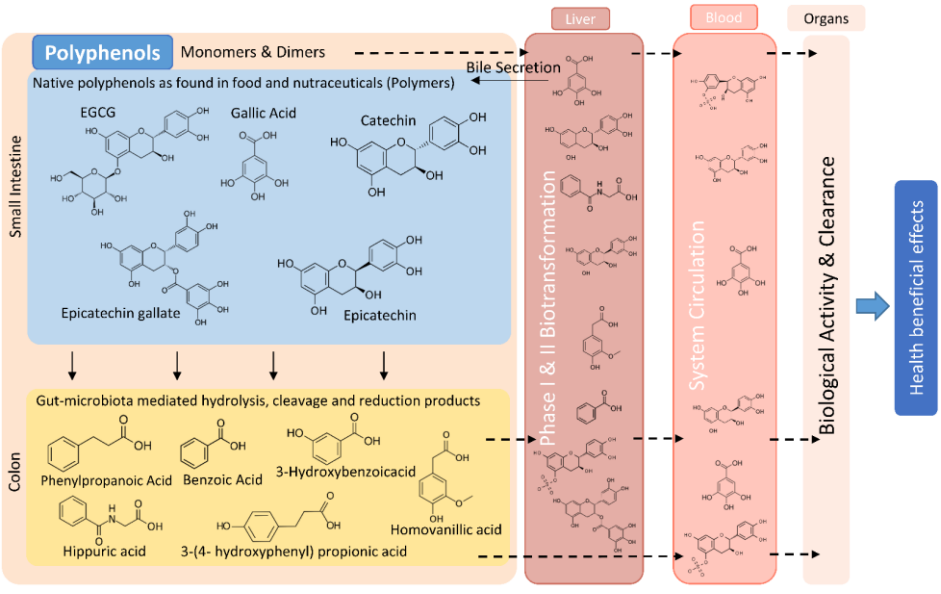

Figure 8. Metabolism of a grape seed proanthocyanidin extract (GSPE). *Tissue and systemic distribution of the main polyphenol identified in Wistar rats after oral administration of GSPE (1 g/kg). Part of the polyphenols found in the extract were absorbed in the small intestine and distributed to different tissues. Other polyphenols reach the colon where they were metabolized by gut microbiota, and absorbed by the colonocites for their distribution. Liver undergo further the metabolites. Figure adapted from Ávila-Roman et al. 2021.* [186]

Additionally, these metabolites may be transferred back into the intestine through the enterohepatic cycle. Finally, the absorbed metabolites are transported through the systemic circulation to the different tissues [183]. For instance, catechin, epicathechin, and dimeric procyanidin B2, and glucuronidated form of catechin and epicathechin, and methyl-epicatechin glucuronide were quantified in brain and liver, between 1 and 2 hours after GSPE dose (1 g/kg) administration in rats [187].

However, intestinal and hepatic absorption and metabolism of phenolic compounds is not the only way by which these compounds are bioavailable. In the colon, phenolic compounds are metabolized by the gut microbiota (via deglycosilation, dihydroxylation and demethylation reactions) and absorbed by the colonocytes [188]. In fact, it is considered that only a small part of the ingested polyphenols is absorbed by the small intestine (5-10%) while the rest (90-95%) reach the colon [188]. Therefore, the gut microbiota plays a crucial role in the bioavailability and metabolism of PAs [192]. Thus, once in the colon, flavanol-3-ols can be transformed by three different metabolic pathways (**Figure 9**). The first pathway is meta-substitution of the flavanol A ring producing 5-(2, 4-dihydroxy) phenyl-2-ene-valeric acid [167]. The second pathway is biotransformation to valerolactone compounds, by the microbial cleavage of flavanol C- and A- rings [189]. The final pathway is microbial cleavage of the flavanol interflavanic bond C4-C8 to be undergo in monomeric forms. In turn, these monomeric flavan-3-ols can undergo a microbial cleavage of the C-ring to produce propan-2-ol metabolites with different degrees of hydroxylation by a microbial dihydroxylation of the B-ring [190]. Propan-2-ol metabolites may become valerolactones by microbial A-ring cleavage, which further undergo in valeric acids. Valeric acids may suffer a β-oxidation of the branched chain to form phenyl propionic acids and their derivatives, which are the main compounds form the microbial metabolism [189]. Thus, the main microbial-derived metabolites from GSPE in plasma of healthy rats were phenyl-propionic acids at 24 h after administration [169]. Then, microbial-

derived metabolites reach the liver though the portal vein and reach different organs and tissues such as plasma, brain and aorta [169,191,192]. In this context, the gut microbiota diversity is also crucial on the type and amount of microbial-derived metabolites generated [193]. Thus, different microbial-derived metabolites profiles have been reported after administering of GSPE in healthy and obese animals [194]. For instance, the methylated metabolites of gallic acid (3-O-methyl gallic acid) and homovanillic acid were the only conjugated microbial metabolites that were found a higher concentration in CAF-induced obese rats administered with GSPE (1 g/kg). In fact, the microbial derivate 3-O-methyl gallic acid was higher in CAF-fed rats compared to healthy rats, and homovanillic acid was only found in CAF-fed rats with maximum values at 4 and 24 h after GSPE ingestion [194].

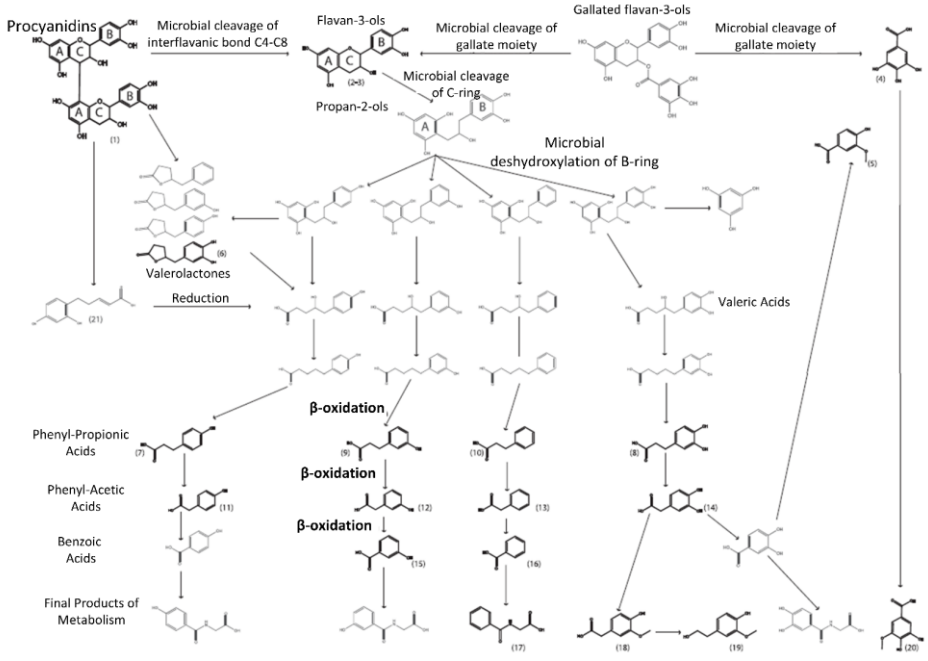

***Figure 9**. Microbial colonic biotransformation pathways of GSPE (1 g/kg) administration in rat plasma after 0, 2, 7, 24 and 48 hours. Adapted from Margalef et al. 2015 [169].*

It is worth highlighting, that bioavailability can be affected by different external and internal factors such as dose, length of the treatment, sex and age [195].

More recently, biological rhythms have emerged as a very important factor affecting the bioavailability of polyphenols [174].

In this context, a study carried out by our group, showed that the bioavailability of GSPE (dose of 25 mg/kg) was affected by the administration time in an animal model of MetS. Thus, the phase-II and gut microbiota-derived phenolic metabolites were different depending on the time administration of GSPE (8:00 am or 8:00 pm) [196]. Moreover, seasonal rhythms have also shown to impact on the bioavailability of polyphenols. Iglesias-Carres et al. showed that bioavailability from red grapes, rich in polyphenols, in serum F344 rats was different according to the photoperiod exposure. Those rats exposed to winter-like length day presented higher bioavailability of grape phenolics, suggesting that seasonality affect to bioavailability [197]. However, specific study using GSPE has not been reported to date.

Hence, the bioavailability of the polyphenols can change according to the photoperiod exposure [197], because of this it is plausible to speculate that the bioactive activity of polyphenols could be affected by the time-of-season in which they are consumed, altering their beneficial properties on obesity and MetS development. Therefore, gut microbiota and biological rhythms are key factors to take into account to establish more accurate dietary polyphenols intake due to the inter-relationship between them that can affect the beneficial effects exert by polyphenols on human health.

References

[1] Apte C V. Biological clocks: The coming of age. Int J Appl Basic Med Res 2012;2:1. https://doi.org/10.4103/2229-516X.96788.

[2] Dibner C, Schibler U, Albrecht U. The Mammalian Circadian Timing System: Organization and Coordination of Central and Peripheral Clocks. Http://DxDoiOrg/101146/Annurev-Physiol-021909-135821 2010;72:517–49. https://doi.org/10.1146/ANNUREV-PHYSIOL-021909-135821.

[3] Helm B, Ben-Shlomo R, Sheriff MJ, Hut RA, Foster R, Barnes BM, et al. Annual rhythms that underlie phenology: biological time-keeping meets environmental change. Proc R Soc B Biol Sci 2013;280. https://doi.org/10.1098/RSPB.2013.0016.

[4] Panda S. The arrival of circadian medicine. Nat Rev Endocrinol 2019;15:67–9. https://doi.org/10.1038/S41574-018-0142-X.

[5] Wood S, Loudon A. Clocks for all seasons: Unwinding the roles and mechanisms of circadian and interval timers in the hypothalamus and pituitary. J Endocrinol 2014;222. https://doi.org/10.1530/JOE-14-0141.

[6] Reppert SM, Weaver DR. Coordination of circadian timing in mammals. Nat 2002 4186901 2002;418:935–41. https://doi.org/10.1038/nature00965.

[7] Kohsaka A, Laposky AD, Ramsey KM, Estrada C, Joshu C, Kobayashi Y, et al. High-Fat Diet Disrupts Behavioral and Molecular Circadian Rhythms in Mice. Cell Metab 2007;6:414–21. https://doi.org/10.1016/J.CMET.2007.09.006/ATTACHMENT/B1B506A6-A0E7-41A3-8740-7BD6B88664DF/MMC1.PDF.

[8] Kalsbeek A, La Fleur S, Fliers E. Circadian control of glucose metabolism. Mol Metab 2014;3:372–83. https://doi.org/10.1016/J.MOLMET.2014.03.002.

[9] Reiter RJ, Tan DX, Korkmaz A, Ma S. Obesity and metabolic syndrome: Association with chronodisruption, sleep deprivation, and melatonin suppression. Ann Med 2012;44:564–77. https://doi.org/10.3109/07853890.2011.586365.

[10] Wirz-Justice A. Seasonality in affective disorders. Gen Comp Endocrinol 2018;258:244–9. https://doi.org/10.1016/j.ygcen.2017.07.010.

[11] Wood S, Loudon A. The pars tuberalis: The site of the circannual clock in mammals? Gen Comp Endocrinol 2018;258:222–35. https://doi.org/10.1016/j.ygcen.2017.06.029.

[12] Rosenthal NE, Sack DA, Gillin JC, Lewy AJ, Goodwin FK, Davenport Y, et al. Seasonal Affective Disorder: A Description of the Syndrome and Preliminary Findings With Light Therapy. Arch Gen Psychiatry 1984;41:72–80. https://doi.org/10.1001/archpsyc.1984.01790120076010.

[13] Lim ASP. Diurnal and seasonal molecular rhythms in the human brain and their relation to Alzheimer disease. Handb Clin Neurol 2021;179:271–84. https://doi.org/10.1016/B978-0-12-819975-6.00017-0.

[14] Stewart S, Keates AK, Redfern A, McMurray JJV. Seasonal variations in cardiovascular disease. Nat Rev Cardiol 2017;14:654–64. https://doi.org/10.1038/NRCARDIO.2017.76.

[15] Onishi KG, Maneval AC, Cable EC, Tuohy MC, Scasny AJ, Sterina E, et al. Circadian and circannual timescales interact to generate seasonal changes in immune function. Brain Behav Immun 2020;83:33–43. https://doi.org/10.1016/j.bbi.2019.07.024.

[16] Korf HW. Signaling pathways to and from the hypophysial pars tuberalis, an important center for the control of seasonal rhythms. Gen Comp Endocrinol 2018;258:236–43. https://doi.org/10.1016/j.ygcen.2017.05.011.

[17] Fitzgerald KT. The structure and function of the pars tuberalis of the vertebrate adenohypophysis. Gen Comp Endocrinol 1979;37:383–99. https://doi.org/10.1016/0016-6480(79)90012-1.

[18] Malpaux B, Migaud M, Tricoire H, Chemineau P. Biology of mammalian photoperiodism and the critical role of the pineal gland and melatonin. J Biol Rhythms 2001;16:336–47. https://doi.org/10.1177/074873001129002051.

[19] Johnston JD. Measuring seasonal time within the circadian system: Regulation of the suprachiasmatic nuclei by photoperiod. J Neuroendocrinol 2005;17:459–65. https://doi.org/10.1111/j.1365-2826.2005.01326.x.

[20] Nakao N, Ono H, Yamamura T, Anraku T, Takagi T, Higashi K, et al. Thyrotrophin in the pars tuberalis triggers photoperiodic response. Nature 2008;452:317–22. https://doi.org/10.1038/NATURE06738.

[21] Dupré SM, Miedzinska K, Duval C V., Yu L, Goodman RL, Lincoln GA, et al. The identification of a conserved Eya3 signal and prolactin-releasing factors in the long day response of a seasonal mammal. Curr Biol 2010;20:829. https://doi.org/10.1016/J.CUB.2010.02.066.

[22] Dardente H, Wyse CA, Birnie MJ, Dupré SM, Loudon ASI, Lincoln GA, et al. A molecular switch for photoperiod responsiveness in mammals. Curr Biol 2010;20:2193–8. https://doi.org/10.1016/J.CUB.2010.10.048/ATTACHMENT/25AEE83E-6383-4714-ABB1-95D107956508/MMC1.PDF.

[23] Wood SH, Christian HC, Miedzinska K, Saer BRC, Johnson M, Paton B, et al. Binary Switching of Calendar Cells in the Pituitary Defines the Phase of the Circannual Cycle in Mammals. Curr Biol 2015;25:2651–62. https://doi.org/10.1016/j.cub.2015.09.014.

[24] Lincoln G. A brief history of circannual time. J Neuroendocrinol 2019;31:1–12. https://doi.org/10.1111/jne.12694.

[25] Lincoln GA, Anderson H, Loudon A. Clock genes in calendar cells as the basis of annual timekeeping in mammals - A unifying hypothesis. J Endocrinol 2003;179:1–13. https://doi.org/10.1677/joe.0.1790001.

[26] Aoyama S, Shibata S. Time-of-Day-Dependent Physiological Responses to Meal and Exercise. Front Nutr 2020;7:18. https://doi.org/10.3389/FNUT.2020.00018.

[27] Schibler U, Ripperger J, Brown SA. Peripheral circadian oscillators in mammals: time and food. J Biol Rhythms 2003;18:250–60. https://doi.org/10.1177/0748730403018003007.

[28] Dunlap JC. Molecular bases for circadian clocks. Cell 1999;96:271–90. https://doi.org/10.1016/S0092-8674(00)80566-8.

[29] Young MW, Kay SA. Time zones: a comparative genetics of circadian clocks. Nat Rev Genet 2001;2:702–15. https://doi.org/10.1038/35088576.

[30] Takahashi JS. Transcriptional architecture of the mammalian circadian clock. Nat Rev Genet 2016 183 2016;18:164–79. https://doi.org/10.1038/nrg.2016.150.

[31] Preitner N, Damiola F, Luis-Lopez-Molina, Zakany J, Duboule D, Albrecht U, et al. The orphan nuclear receptor REV-ERBalpha controls circadian transcription within the positive limb of the mammalian circadian oscillator. Cell 2002;110:251–60. https://doi.org/10.1016/S0092-8674(02)00825-5.

[32] Guillaumond F, Dardente H, Giguère V, Cermakian N. Differential control of Bmal1 circadian transcription by REV-ERB and ROR nuclear receptors. J Biol Rhythms 2005;20:391–403. https://doi.org/10.1177/0748730405277232.

[33] Dardente H, Hazlerigg DG, Ebling FJP. Thyroid hormone and seasonal rhythmicity. Front Endocrinol (Lausanne) 2014;5:19. https://doi.org/10.3389/FENDO.2014.00019/BIBTEX.

[34] Unfried C, Ansari N, Yasuo S, Korf HW, Von Gall C. Impact of melatonin and molecular clockwork components on the expression of thyrotropin beta-chain (Tshb) and the Tsh receptor in the mouse pars tuberalis. Endocrinology 2009;150:4653–62. https://doi.org/10.1210/EN.2009-0609.

[35] Wood SH, Hindle MM, Mizoro Y, Cheng Y, Saer BRC, Miedzinska K, et al. Circadian clock mechanism driving mammalian photoperiodism. Nat Commun 2020 111 2020;11:1–15. https://doi.org/10.1038/s41467-020-18061-z.

[36] Shoemaker MB, Heideman P. Reduced body mass, food intake, and testis size in response to short photoperiod in adult F344 rats. BMC Physiol 2002;2:11. https://doi.org/10.1186/1472-6793-2-11.

[37] Mariné-Casadó R, Domenech-Coca C, del Bas JM, Bladé C, Arola L, Caimari A. The exposure to different photoperiods strongly modulates the glucose and lipid metabolisms of normoweight fischer 344 rats. Front Physiol 2018;9:1–17. https://doi.org/10.3389/fphys.2018.00416.

[38] Kurhaluk N, Tkachenko H, Lukash O. Photoperiod-induced alterations in biomarkers of oxidative stress and biochemical pathways in rats of different ages: Focus on individual physiological reactivity. Chronobiol Int 2021;38:1673–91. https://doi.org/10.1080/07420528.2021.1939364.

[39] Lewis JE, Ebling FJP. Tanycytes As Regulators of Seasonal Cycles in Neuroendocrine Function. Front Neurol 2017;8. https://doi.org/10.3389/FNEUR.2017.00079.

[40] Haus E. Chronobiology in the endocrine system. Adv Drug Deliv Rev 2007;59:985–1014. https://doi.org/10.1016/j.addr.2007.01.001.

[41] Mullur R, Liu YY, Brent GA. Thyroid Hormone Regulation of Metabolism. Physiol Rev 2014;94:355. https://doi.org/10.1152/PHYSREV.00030.2013.

[42] Lightman SL, Birnie MT, Conway-Campbell BL. Dynamics of ACTH and Cortisol Secretion and Implications for Disease. Endocr Rev 2020;41:470–90. https://doi.org/10.1210/ENDREV/BNAA002.

[43] Pierre K, Rao RT, Hartmanshenn C, Androulakis IP. Modeling the Influence of Seasonal Differences in the HPA Axis on Synchronization of the Circadian Clock and Cell Cycle. Endocrinology 2018;159:1808–26. https://doi.org/10.1210/en.2017-03226.

[44] Kawai H, Inabe J, Ishibashi T, Kudo N, Kawashima Y, Mitsumoto A. Short and long photoperiods differentially exacerbate corticosterone-induced physical and psychological symptoms in mice. Biomed Res 2018;39:47–55. https://doi.org/10.2220/biomedres.39.47.

[45] Gathercole LL, Morgan SA, Bujalska IJ, Hauton D, Stewart PM, Tomlinson JW. Regulation of Lipogenesis by Glucocorticoids and Insulin in Human Adipose Tissue. PLoS One 2011;6:e26223. https://doi.org/10.1371/JOURNAL.PONE.0026223.

[46] Weil ZM, Borniger JC, Cisse YM, Salloum BAA, Nelson RJ. function 2016:108–18. https://doi.org/10.1016/j.yfrne.2014.10.001.Neuroendocrine.

[47] Bilbo SD, Dhabhar FS, Viswanathan K, Saul A, Yellon SM, Nelson RJ. Short day lengths augment stress-induced leukocyte trafficking and stress-induced enhancement of skin immune function. Proc Natl Acad Sci U S A 2002;99:4067–72. https://doi.org/10.1073/PNAS.062001899.

[48] Pyter LM, Adelson JD, Nelson RJ. Short days increase hypothalamic-pituitary-adrenal axis responsiveness. Endocrinology 2007;148:3402–9. https://doi.org/10.1210/EN.2006-1432.

[49] Lattin CR, Waldron-Francis K, Romero LM. Intracellular glucocorticoid receptors in spleen, but not skin, vary seasonally in wild house sparrows (Passer domesticus). Proc R Soc B Biol Sci 2013;280. https://doi.org/10.1098/RSPB.2012.3033.

[50] Walton JC, Grier AJ, Weil ZM, Nelson RJ. Photoperiod and stress regulation of corticosteroid receptor, brain-derived neurotrophic factor, and glucose transporter GLUT3 mRNA in the hippocampus of male Siberian hamsters (Phodopus sungorus). Neuroscience 2012;213:106–11. https://doi.org/10.1016/J.NEUROSCIENCE.2012.03.043.

[51] Otsuka T, Goto M, Kawai M, Togo Y, Sato K, Katoh K, et al. Photoperiod Regulates Corticosterone Rhythms by Altered Adrenal Sensitivity via Melatonin-Independent Mechanisms in Fischer 344 Rats and C57BL/6J Mice. PLoS One 2012;7:e39090. https://doi.org/10.1371/JOURNAL.PONE.0039090.

[52] Bauman BM, Buban KN, Russell AL, Handa RJ, Wu TJ. regulating seasonal shi.

Neuroscience 2019;406:268–77. https://doi.org/10.1016/j.neuroscience.2019.03.013.

[53] Ashwell E. The endocrine system and associated disorders. Https://DoiOrg/1012968/Bjon2022316316 2022;31:316–20. https://doi.org/10.12968/BJON.2022.31.6.316.

[54] Reiter RJ. The pineal and its hormones in the control of reproduction in mammals. Endocr Rev 1980;1:109–31. https://doi.org/10.1210/EDRV-1-2-109.

[55] Goldman BD. Mammalian photoperiodic system: Formal properties and neuroendocrine mechanisms of photoperiodic time measurement. J Biol Rhythms 2001;16:283–301. https://doi.org/10.1177/074873001129001980.

[56] Sciarra F, Franceschini E, Campolo F, Gianfrilli D, Pallotti F, Paoli D, et al. Disruption of Circadian Rhythms: A Crucial Factor in the Etiology of Infertility. Int J Mol Sci 2020;21. https://doi.org/10.3390/IJMS21113943.

[57] Torres-Fuentes C, Schellekens H, Dinan TG, Cryan JF. The microbiota–gut–brain axis in obesity. Lancet Gastroenterol Hepatol 2017;2:747–56. https://doi.org/10.1016/S2468-1253(17)30147-4.

[58] Eckburg PB, Bik EM, Bernstein CN, Purdom E, Dethlefsen L, Sargent M, et al. Diversity of the Human Intestinal Microbial Flora n.d.

[59] Sender R, Fuchs S, Milo R. Revised Estimates for the Number of Human and Bacteria Cells in the Body. PLOS Biol 2016;14:e1002533. https://doi.org/10.1371/JOURNAL.PBIO.1002533.

[60] Sender R, Fuchs S, Milo R. Are We Really Vastly Outnumbered? Revisiting the Ratio of Bacterial to Host Cells in Humans. Cell 2016;164:337–40. https://doi.org/10.1016/J.CELL.2016.01.013.

[61] Gomaa EZ. Human gut microbiota/microbiome in health and diseases: a review n.d. https://doi.org/10.1007/s10482-020-01474-7.

[62] Hillman ET, Lu H, Yao T, Nakatsu CH. Microbial Ecology along the Gastrointestinal Tract. Microbes Environ 2017;32:300–13. https://doi.org/10.1264/JSME2.ME17017.

[63] Patterson EE, Ryan PM, Cryan JF, Dinan TG, Paul Ross R, Fitzgerald GF, et al. Gut microbiota, obesity and diabetes. Postgrad Med J 2016;92:286–300. https://doi.org/10.1136/postgradmedj-2015-133285.

[64] Samuel BS, Shaito A, Motoike T, Rey FE, Backhed F, Manchester JK, et al. Effects of the gut microbiota on host adiposity are modulated by the short-chain fatty-acid binding G protein-coupled receptor, Gpr41. Proc Natl Acad Sci U S A 2008;105:16767–72. https://doi.org/10.1073/pnas.0808567105.

[65] Bäckhed F, Ding H, Wang T, Hooper L V., Gou YK, Nagy A, et al. The gut microbiota as an environmental factor that regulates fat storage. Proc Natl Acad Sci U S A 2004;101:15718–23. https://doi.org/10.1073/pnas.0407076101.

[66] Monagas M, Urpi-Sarda M, Sánchez-Patán F, Llorach R, Garrido I, Gómez-Cordovés C, et al. Insights into the metabolism and microbial biotransformation

of dietary flavan-3-ols and the bioactivity of their metabolites. Food Funct 2010;1:233–53. https://doi.org/10.1039/C0FO00132E.

[67] Engevik MA, Morra CN, Röth D, Engevik K, Spinler JK, Devaraj S, et al. Microbial Metabolic Capacity for Intestinal Folate Production and Modulation of Host Folate Receptors. Front Microbiol 2019;10. https://doi.org/10.3389/FMICB.2019.02305/FULL.

[68] Ellis JL, Karl JP, Oliverio AM, Fu X, Soares JW, Wolfe BE, et al. Dietary vitamin K is remodeled by gut microbiota and influences community composition. Gut Microbes 2021;13:1–16. https://doi.org/10.1080/19490976.2021.1887721.

[69] Yang M, Gu Y, Li L, Liu T, Song X, Sun Y, et al. Bile Acid–Gut Microbiota Axis in Inflammatory Bowel Disease: From Bench to Bedside. Nutr 2021, Vol 13, Page 3143 2021;13:3143. https://doi.org/10.3390/NU13093143.

[70] Khan MJ, Gerasimidis K, Edwards CA, Shaikh MG. Role of Gut Microbiota in the Aetiology of Obesity: Proposed Mechanisms and Review of the Literature. J Obes 2016;2016:7353642–7353642. https://doi.org/10.1155/2016/7353642.

[71] Sandhu K V., Sherwin E, Schellekens H, Stanton C, Dinan TG, Cryan JF. Feeding the microbiota-gut-brain axis: diet, microbiome, and neuropsychiatry. Transl Res 2017;179:223–44. https://doi.org/10.1016/j.trsl.2016.10.002.

[72] Ottman N, Smidt H, de Vos WM, Belzer C. The function of our microbiota: who is out there and what do they do? Front Cell Infect Microbiol 2012;2:104. https://doi.org/10.3389/fcimb.2012.00104.

[73] O'Neill S, O'Driscoll L. Metabolic syndrome: a closer look at the growing epidemic and its associated pathologies. Obes Rev 2015;16:1–12. https://doi.org/10.1111/OBR.12229.

[74] Martel J, Chang SH, Ko YF, Hwang TL, Young JD, Ojcius DM. Gut barrier disruption and chronic disease. Trends Endocrinol Metab 2022;33:247–65. https://doi.org/10.1016/J.TEM.2022.01.002.

[75] Graf D, Di Cagno R, Fåk F, Flint HJ, Nyman M, Saarela M, et al. Contribution of diet to the composition of the human gut microbiota. Microb Ecol Heal Dis 2015;26. https://doi.org/10.3402/MEHD.V26.26164/SUPPL_FILE/ZMEH_A_11835063_SM0001.PDF.

[76] Flint HJ, Scott KP, Louis P, Duncan SH. The role of the gut microbiota in nutrition and health. Nat Rev Gastroenterol Hepatol 2012 910 2012;9:577–89. https://doi.org/10.1038/nrgastro.2012.156.

[77] Del Chierico F, Vernocchi P, Dallapiccola B, Putignani L. Mediterranean diet and health: Food effects on gut microbiota and disease control. Int J Mol Sci 2014;15:11678–99. https://doi.org/10.3390/ijms150711678.

[78] Shi Z. Gut microbiota: An important link between western diet and chronic diseases. Nutrients 2019;11:10–2. https://doi.org/10.3390/nu11102287.

[79] Gual-Grau A, Guirro M, Mayneris-Perxachs J, Arola L, Boqué N. Impact of

different hypercaloric diets on obesity features in rats: a metagenomics and metabolomics integrative approach. J Nutr Biochem 2019;71:122–31. https://doi.org/10.1016/j.jnutbio.2019.06.005.

[80] Cani PD, Delzenne NM, Amar J, Burcelin R. Role of gut microflora in the development of obesity and insulin resistance following high-fat diet feeding. Pathol Biol (Paris) 2008;56:305–9. https://doi.org/10.1016/J.PATBIO.2007.09.008.

[81] Hersoug LG, Møller P, Loft S. Gut microbiota-derived lipopolysaccharide uptake and trafficking to adipose tissue: implications for inflammation and obesity. Obes Rev 2016;17:297–312. https://doi.org/10.1111/OBR.12370.

[82] Turnbaugh PJ, Ley RE, Mahowald MA, Magrini V, Mardis ER, Gordon JI. An obesity-associated gut microbiome with increased capacity for energy harvest. Nature 2006;444:1027–31. https://doi.org/10.1038/nature05414.

[83] Kim KN, Yao Y, Ju SY. Short Chain Fatty Acids and Fecal Microbiota Abundance in Humans with Obesity: A Systematic Review and Meta-Analysis. Nutrients 2019;11. https://doi.org/10.3390/NU11102512.

[84] Sonnenburg JL, Xu J, Leip DD, Chen CH, Westover BP, Weatherford J, et al. Glycan foraging in vivo by an intestine-adapted bacterial symbiont. Science 2005;307:1955–9. https://doi.org/10.1126/SCIENCE.1109051/SUPPL_FILE/SONNENBURG.SOM.PDF.

[85] Lu Y, Fan C, Li P, Lu Y, Chang X, Qi K. Short Chain Fatty Acids Prevent High-fat-diet-induced Obesity in Mice by Regulating G Protein-coupled Receptors and Gut Microbiota. Sci Reports 2016 61 2016;6:1–13. https://doi.org/10.1038/srep37589.

[86] Hu GX, Chen GR, Xu H, Ge RS, Lin J. Activation of the AMP activated protein kinase by short-chain fatty acids is the main mechanism underlying the beneficial effect of a high fiber diet on the metabolic syndrome. Med Hypotheses 2010;74:123–6. https://doi.org/10.1016/J.MEHY.2009.07.022.

[87] Gao Z, Yin J, Zhang J, Ward RE, Martin RJ, Lefevre M, et al. Butyrate improves insulin sensitivity and increases energy expenditure in mice. Diabetes 2009;58:1509–17. https://doi.org/10.2337/db08-1637.

[88] Turnbaugh PJ, Hamady M, Yatsunenko T, Cantarel BL, Duncan A, Ley RE, et al. A core gut microbiome in obese and lean twins. Nat 2008 4577228 2008;457:480–4. https://doi.org/10.1038/nature07540.

[89] Ley RE, Turnbaugh PJ, Klein S, Gordon JI. Microbial ecology: human gut microbes associated with obesity. Nature 2006;444:1022–3. https://doi.org/10.1038/4441022A.

[90] Magne F, Gotteland M, Gauthier L, Zazueta A, Pesoa S, Navarrete P, et al. The firmicutes/bacteroidetes ratio: A relevant marker of gut dysbiosis in obese patients? Nutrients 2020;12. https://doi.org/10.3390/nu12051474.

[91] Le Chatelier, E., Nielsen, T., Qin, J. et al. Richness of human gut microbiome

correlates with metabolic markers. Nature 2013;500. https://doi.org/10.1038/NATURE12506.

[92] Leong KSW, Derraik JGB, Hofman PL, Cutfield WS. Antibiotics, gut microbiome and obesity. Clin Endocrinol (Oxf) 2018;88:185–200. https://doi.org/10.1111/cen.13495.

[93] Rodrigues RR, Greer RL, Dong X, DSouza KN, Gurung M, Wu JY, et al. Antibiotic-induced alterations in gut microbiota are associated with changes in glucose metabolism in healthy mice. Front Microbiol 2017;8:2306. https://doi.org/10.3389/FMICB.2017.02306/BIBTEX.

[94] Cho I, Yamanishi S, Cox L, Methé BA, Zavadil J, Li K, et al. Antibiotics in early life alter the murine colonic microbiome and adiposity. Nature 2012;488:621–6. https://doi.org/10.1038/nature11400.

[95] Cox LM, Blaser MJ. Antibiotics in early life and obesity. Nat Rev Endocrinol 2014 113 2014;11:182–90. https://doi.org/10.1038/nrendo.2014.210.

[96] Vallianou N, Dalamaga M, Stratigou T, Karampela I, Tsigalou C. Do Antibiotics Cause Obesity Through Long-term Alterations in the Gut Microbiome? A Review of Current Evidence. Curr Obes Rep 2021;10:244–62. https://doi.org/10.1007/S13679-021-00438-W/TABLES/3.

[97] Rajpal DK, Klein JL, Mayhew D, Boucheron J, Spivak AT, Kumar V, et al. Selective Spectrum Antibiotic Modulation of the Gut Microbiome in Obesity and Diabetes Rodent Models. PLoS One 2015;10:e0145499. https://doi.org/10.1371/JOURNAL.PONE.0145499.

[98] Blüher M. Obesity: global epidemiology and pathogenesis. Nat Rev Endocrinol 2019;15:288–98. https://doi.org/10.1038/S41574-019-0176-8.

[99] Gadde KM, Martin CK, Berthoud HR, Heymsfield SB. Obesity: Pathophysiology and Management. J Am Coll Cardiol 2018;71:69–84. https://doi.org/10.1016/J.JACC.2017.11.011.

[100] Gjermeni E, Kirstein AS, Kolbig F, Kirchhof M, Bundalian L, Katzmann JL, et al. Obesity-An Update on the Basic Pathophysiology and Review of Recent Therapeutic Advances. Biomolecules 2021;11. https://doi.org/10.3390/BIOM11101426.

[101] POLAN CE, MCNEILL JJ, TOVE SB. BIOHYDROGENATION OF UNSATURATED FATTY ACIDS BY RUMEN BACTERIA. J Bacteriol 1964;88:1056–64. https://doi.org/10.1128/JB.88.4.1056-1064.1964.

[102] Galgani JE, Uauy RD, Aguirre CA, Díaz EO. Effect of the dietary fat quality on insulin sensitivity. Br J Nutr 2008;100:471–9. https://doi.org/10.1017/S0007114508894408.

[103] Melissa Gabbs, Leng S, Devassy JG, Monirujjaman M, Aukema HM. Advances in Our Understanding of Oxylipins Derived from Dietary PUFAs. Adv Nutr 2015;6:513–40. https://doi.org/10.3945/AN.114.007732.

[104] Miyamoto J, Igarashi M, Watanabe K, Karaki S ichiro, Mukouyama H, Kishino S,

et al. Gut microbiota confers host resistance to obesity by metabolizing dietary polyunsaturated fatty acids. Nat Commun 2019;10. https://doi.org/10.1038/S41467-019-11978-0.

[105] Colas RA, Shinohara M, Dalli J, Chiang N, Serhan CN. Identification and signature profiles for pro-resolving and inflammatory lipid mediators in human tissue. Am J Physiol - Cell Physiol 2014;307:C39. https://doi.org/10.1152/AJPCELL.00024.2014.

[106] Hajeyah AA, Griffiths WJ, Wang Y, Finch AJ, O'Donnell VB. The Biosynthesis of Enzymatically Oxidized Lipids. Front Endocrinol (Lausanne) 2020;11. https://doi.org/10.3389/FENDO.2020.591819.

[107] Liakh I, Janczy A, Pakiet A, Korczynska J, Proczko-Stepaniak M, Kaska L, et al. One-anastomosis gastric bypass modulates the serum levels of pro- and anti-inflammatory oxylipins, which may contribute to the resolution of inflammation. Int J Obes 2021 462 2021;46:408–16. https://doi.org/10.1038/s41366-021-01013-y.

[108] Kutzner L, Rund KM, Ostermann AI, Hartung NM, Galano JM, Balas L, et al. Development of an Optimized LC-MS Method for the Detection of Specialized Pro-Resolving Mediators in Biological Samples. Front Pharmacol 2019;10:169. https://doi.org/10.3389/FPHAR.2019.00169/BIBTEX.

[109] Pal A, Al-Shaer AE, Guesdon W, Torres MJ, Armstrong M, Quinn K, et al. Resolvin E1 derived from eicosapentaenoic acid prevents hyperinsulinemia and hyperglycemia in a host genetic manner. FASEB J 2020;34:10640–56. https://doi.org/10.1096/FJ.202000830R.

[110] Barden A, Shinde S, Tsai IJ, Croft KD, Beilin LJ, Puddey IB, et al. Effect of weight loss on neutrophil resolvins in the metabolic syndrome. Prostaglandins Leukot Essent Fatty Acids 2019;148:25–9. https://doi.org/10.1016/J.PLEFA.2019.07.001.

[111] Möller K, Ostermann AI, Rund K, Thoms S, Blume C, Stahl F, et al. Influence of weight reduction on blood levels of C-reactive protein, tumor necrosis factor-α, interleukin-6, and oxylipins in obese subjects. Prostaglandins, Leukot Essent Fat Acids 2016;106:39–49. https://doi.org/10.1016/J.PLEFA.2015.12.001.

[112] Tans R, Bande R, van Rooij A, Molloy BJ, Stienstra R, Tack CJ, et al. Evaluation of cyclooxygenase oxylipins as potential biomarker for obesity-associated adipose tissue inflammation and type 2 diabetes using targeted multiple reaction monitoring mass spectrometry. Prostaglandins, Leukot Essent Fat Acids 2020;160:102157. https://doi.org/10.1016/J.PLEFA.2020.102157.

[113] Teichman EM, O'Riordan KJ, Gahan CGM, Dinan TG, Cryan JF. When Rhythms Meet the Blues: Circadian Interactions with the Microbiota-Gut-Brain Axis. Cell Metab 2020;31:448–71. https://doi.org/10.1016/j.cmet.2020.02.008.

[114] Bailey MT, Walton JC, Dowd SE, Weil ZM, Nelson RJ. Photoperiod modulates gut bacteria composition in male Siberian hamsters (Phodopus sungorus). Brain Behav Immun 2010;24:577–84. https://doi.org/10.1016/j.bbi.2009.12.010.

[115] Liu J, Song Y, Lu X, Chen T, Guo W, Fan Z, et al. Seasonal Variation Influences on

Intestinal Microbiota in Rats. Curr Microbiol 2018;75:1006–10. https://doi.org/10.1007/S00284-018-1480-6.

[116] Koliada A, Moseiko V, Romanenko M, Piven L, Lushchak O, Kryzhanovska N, et al. Seasonal variation in gut microbiota composition: Cross-sectional evidence from Ukrainian population. BMC Microbiol 2020;20:1–9. https://doi.org/10.1186/S12866-020-01786-8/TABLES/3.

[117] Shor EK, Brown SP, Freeman DA. Bacteria and Bellicosity: Photoperiodic Shifts in Gut Microbiota Drive Seasonal Aggressive Behavior in Male Siberian Hamsters. J Biol Rhythms 2022;37:296–309. https://doi.org/10.1177/07487304221092105.

[118] Thaiss CA, Levy M, Amit I, Segal E, Elinav E, Korem T, et al. Microbiota Diurnal Rhythmicity Programs Host Transcriptome Oscillations. Cell 2016;167:1495–510. https://doi.org/10.1016/j.cell.2016.11.003.

[119] Tahara Y, Yamazaki M, Sukigara H, Motohashi H, Sasaki H, Miyakawa H, et al. Gut Microbiota-Derived Short Chain Fatty Acids Induce Circadian Clock Entrainment in Mouse Peripheral Tissue. Nat Sci Reports 2018;8. https://doi.org/10.1038/s41598-018-19836-7.

[120] Huang G, Wang L, Li J, Hou R, Wang M, Wang Z, et al. Seasonal shift of the gut microbiome synchronizes host peripheral circadian rhythm for physiological adaptation to a low-fat diet in the giant panda. Cell Rep 2022;38:110203. https://doi.org/10.1016/J.CELREP.2021.110203.

[121] Del Rio D, Rodriguez-Mateos A, Spencer JPE, Tognolini M, Borges G, Crozier A. Dietary (poly)phenolics in human health: Structures, bioavailability, and evidence of protective effects against chronic diseases. Antioxidants Redox Signal 2013;18:1818–92. https://doi.org/10.1089/ARS.2012.4581/ASSET/IMAGES/LARGE/FIGURE41.JPEG.

[122] Pérez-Jiménez J, Neveu V, Vos F, Scalbert A. Identification of the 100 richest dietary sources of polyphenols: an application of the Phenol-Explorer database. Eur J Clin Nutr 2010 643 2010;64:S112–20. https://doi.org/10.1038/ejcn.2010.221.

[123] Sharma A, Shahzad B, Rehman A, Bhardwaj R, Landi M, Zheng B. Response of Phenylpropanoid Pathway and the Role of Polyphenols in Plants under Abiotic Stress. Mol 2019, Vol 24, Page 2452 2019;24:2452. https://doi.org/10.3390/MOLECULES24132452.

[124] Lind CM, Moore IT, Vernasco BJ, Farrell TM. Seasonal testosterone and corticosterone patterns in relation to body condition and reproduction in a subtropical pitviper, Sistrurus miliarius. Gen Comp Endocrinol 2018;267:51–8. https://doi.org/10.1016/j.ygcen.2018.05.027.

[125] de Araújo FF, de Paulo Farias D, Neri-Numa IA, Pastore GM. Polyphenols and their applications: An approach in food chemistry and innovation potential. Food Chem 2021;338:127535. https://doi.org/10.1016/J.FOODCHEM.2020.127535.

[126] Manach C, Scalbert A, Morand C, Rémésy C, Jiménez L. Polyphenols: food sources and bioavailability 1,2. vol. 79. 2004.

[127] Márquez Campos E, Jakobs L, Simon MC. Antidiabetic Effects of Flavan-3-ols and Their Microbial Metabolites. Nutrients 2020;12. https://doi.org/10.3390/NU12061592.

[128] Benbouguerra N, Hornedo-Ortega R, Garcia F, El Khawand T, Richard T. Stilbenes in grape berries and wine and their potential role as anti-obesity agents: a 1 review 2 2021.

[129] Adlercreutz H. Lignans and Human Health. Http://DxDoiOrg/101080/10408360701612942 2008;44:483–525. https://doi.org/10.1080/10408360701612942.

[130] Bladé C, Aragonès G, Arola-Arnal A, Muguerza B, Bravo FI, Salvadó MJ, et al. Proanthocyanidins in health and disease. BioFactors 2016;42:5–12. https://doi.org/10.1002/BIOF.1249.

[131] Mannino G, Chinigò G, Serio G, Genova T, Gentile C, Munaron L, et al. Proanthocyanidins and Where to Find Them: A Meta-Analytic Approach to Investigate Their Chemistry, Biosynthesis, Distribution, and Effect on Human Health. Antioxidants 2021, Vol 10, Page 1229 2021;10:1229. https://doi.org/10.3390/ANTIOX10081229.

[132] Zhou K, Raffoul JJ. Potential Anticancer Properties of Grape Antioxidants. J Oncol 2012;2012. https://doi.org/10.1155/2012/803294.

[133] Terra X, Montagut G, Bustos M, Llopiz N, Ardèvol A, Bladé C, et al. Grape-seed procyanidins prevent low-grade inflammation by modulating cytokine expression in rats fed a high-fat diet. J Nutr Biochem 2009;20:210–8. https://doi.org/10.1016/J.JNUTBIO.2008.02.005.

[134] Koudoufio M, Feldman F, Ahmarani L, Delvin E, Spahis S, Desjardins Y, et al. Intestinal protection by proanthocyanidins involves anti-oxidative and anti-inflammatory actions in association with an improvement of insulin sensitivity, lipid and glucose homeostasis. Sci Rep 2021;11. https://doi.org/10.1038/S41598-020-80587-5.

[135] Terra X, Valls J, Vitrac X, Mérrillon JM, Arola L, Ardèvol A, et al. Grape-seed procyanidins act as antiinflammatory agents in endotoxin-stimulated RAW 264.7 macrophages by inhibiting NFkB signaling pathway. J Agric Food Chem 2007;55:4357–65. https://doi.org/10.1021/JF0633185.

[136] Cos P, Bruyne T, Hermans N, Apers S, Berghe D, Vlietinck A. Proanthocyanidins in health care: current and new trends. Curr Med Chem 2004;11:1345–59. https://doi.org/10.2174/0929867043365288.

[137] Rasmussen SE, Frederiksen H, Krogholm KS, Poulsen L. Dietary proanthocyanidins: occurrence, dietary intake, bioavailability, and protection against cardiovascular disease. Mol Nutr Food Res 2005;49:159–74. https://doi.org/10.1002/MNFR.200400082.

[138] de las Heras N, Galiana A, Ballesteros S, Olivares-álvaro E, Fuller PJ, Lahera V, et

al. Proanthocyanidins Maintain Cardiac Ionic Homeostasis in Aldosterone-Induced Hypertension and Heart Failure. Int J Mol Sci 2021;22. https://doi.org/10.3390/IJMS22179602.

[139] Liu J, He Z, Ma N, Chen Z-Y. Beneficial Effects of Dietary Polyphenols on High-Fat Diet-Induced Obesity Linking with Modulation of Gut Microbiota 2019. https://doi.org/10.1021/acs.jafc.9b06817.

[140] Chen Y, Wang J, Zou L, Cao H, Ni X, Xiao J. Dietary proanthocyanidins on gastrointestinal health and the interactions with gut microbiota. Crit Rev Food Sci Nutr 2022. https://doi.org/10.1080/10408398.2022.2030296.

[141] Shao D, Di Y, Lian Z, Zhu B, Xu X, Guo D, et al. Grape seed proanthocyanidins suppressed macrophage foam cell formation by miRNA-9 via targeting ACAT1 in THP-1 cells. Food Funct 2020;11:1258–69. https://doi.org/10.1039/C9FO02352F.

[142] Choi KC, Myung GJ, Lee YH, Joo CY, Seung HK, Kang HB, et al. Epigallocatechin-3-gallate, a histone acetyltransferase inhibitor, inhibits EBV-induced B lymphocyte transformation via suppression of RelA acetylation. Cancer Res 2009;69:583–92. https://doi.org/10.1158/0008-5472.CAN-08-2442.

[143] Joven J, Espinel E, Rull A, Aragonès G, Rodríguez-Gallego E, Camps J, et al. Plant-derived polyphenols regulate expression of miRNA paralogs miR-103/107 and miR-122 and prevent diet-induced fatty liver disease in hyperlipidemic mice. Biochim Biophys Acta 2012;1820:894–9. https://doi.org/10.1016/J.BBAGEN.2012.03.020.

[144] Ribas-Latre A, Baselga-Escudero L, Casanova E, Arola-Arnal A, Salvadó MJ, Arola L, et al. Chronic consumption of dietary proanthocyanidins modulates peripheral clocks in healthy and obese rats. J Nutr Biochem 2015;26:112–9. https://doi.org/10.1016/J.JNUTBIO.2014.09.006.

[145] Ribas-Latre A, Baselga-Escudero L, Casanova E, Arola-Arnal A, Salvadó MJ, Bladé C, et al. Dietary proanthocyanidins modulate BMAL1 acetylation, Nampt expression and NAD levels in rat liver. Sci Reports 2015 51 2015;5:1–13. https://doi.org/10.1038/srep10954.

[146] Tsang C, Auger C, Mullen W, Bornet A, Rouanet J-M, Crozier A, et al. The absorption, metabolism and excretion of flavan-3-ols and procyanidins following the ingestion of a grape seed extract by rats. Br J Nutr 2005;94:170–81. https://doi.org/10.1079/BJN20051480.

[147] Margalef M, Pons Z, Iglesias-Carres L, Arola L, Muguerza B, Arola-Arnal A. Gender-related similarities and differences in the body distribution of grape seed flavanols in rats. Mol Nutr Food Res 2016;60:760–72. https://doi.org/10.1002/MNFR.201500717.

[148] Montagut G, Bladé C, Blay M, Fernández-Larrea J, Pujadas G, Salvadó MJ, et al. Effects of a grapeseed procyanidin extract (GSPE) on insulin resistance. J Nutr Biochem 2010;21:961–7. https://doi.org/10.1016/J.JNUTBIO.2009.08.001.

[149] Mas-Capdevila A, Iglesias-Carres L, Arola-Arnal A, Suárez M, Bravo FI, Muguerza B. Changes in arterial blood pressure caused by long-term administration of

grape seed proanthocyanidins in rats with established hypertension. Food Funct 2020;11:8735–42. https://doi.org/10.1039/D0FO00981D.

[150] Pons Z, Margalef M, Bravo FI, Arola-Arnal A, Begoña Muguerza ·. Acute administration of single oral dose of grape seed polyphenols restores blood pressure in a rat model of metabolic syndrome: role of nitric oxide and prostacyclin. Eur J Nutr 2016;55:749–58. https://doi.org/10.1007/s00394-015-0895-0.

[151] Pons Z, Margalef M, Bravo FI, Arola-Arnal A, Muguerza B. Chronic administration of grape-seed polyphenols attenuates the development of hypertension and improves other cardiometabolic risk factors associated with the metabolic syndrome in cafeteria diet-fed rats. Br J Nutr 2017;117:200–8. https://doi.org/10.1017/S0007114516004426.

[152] Puiggròs F, Sala E, Vaque M, Ardevol A, Blay M, Fernández-Larrea J, et al. In vivo, in vitro, and in silico studies of Cu/Zn-superoxide dismutase regulation by molecules in grape seed procyanidin extract. J Agric Food Chem 2009;57:3934–42. https://doi.org/10.1021/JF8034868.

[153] Pajuelo D, Quesada H, Díaz S, Fernández-Iglesias A, Arola-Arnal A, Bladé C, et al. Chronic dietary supplementation of proanthocyanidins corrects the mitochondrial dysfunction of brown adipose tissue caused by diet-induced obesity in Wistar rats. Br J Nutr 2012;107:170–8. https://doi.org/10.1017/S0007114511002728.

[154] Bladé C, Arola L, Salvadó MJ. Hypolipidemic effects of proanthocyanidins and their underlying biochemical and molecular mechanisms. Mol Nutr Food Res 2010;54:37–59. https://doi.org/10.1002/MNFR.200900476.

[155] Quesada H, Del Bas JM, Pajuelo D, Díaz S, Fernandez-Larrea J, Pinent M, et al. Grape seed proanthocyanidins correct dyslipidemia associated with a high-fat diet in rats and repress genes controlling lipogenesis and VLDL assembling in liver. Int J Obes (Lond) 2009;33:1007–12. https://doi.org/10.1038/IJO.2009.136.

[156] Baiges I, Palmfeldt J, Bladé C, Gregersen N, Arola L. Lipogenesis Is Decreased by Grape Seed Proanthocyanidins According to Liver Proteomics of Rats Fed a High Fat Diet. Mol Cell Proteomics 2010;9:1499. https://doi.org/10.1074/MCP.M000055-MCP201.

[157] Liu M, Yun P, Hu Y, Yang J, Khadka RB, Peng X. Effects of Grape Seed Proanthocyanidin Extract on Obesity. Obes Facts 2020;13:279–91. https://doi.org/10.1159/000502235.

[158] Salvadó MJ, Casanova E, Fernández-Iglesias A, Arola L, Bladé C. Roles of proanthocyanidin rich extracts in obesity. Food Funct 2015;6:1053. https://doi.org/10.1039/c4fo01035c.

[159] Pascual-Serrano A, Arola-Arnal A, Suárez-García S, Bravo FI, Suárez M, Arola L, et al. Grape seed proanthocyanidin supplementation reduces adipocyte size and increases adipocyte number in obese rats. Int J Obes 2017;41:1246–55. https://doi.org/10.1038/IJO.2017.90.

[160] Guerrero L, Margalef M, Pons Z, Quiñones M, Arola L, Arola-Arnal A, et al. Serum metabolites of proanthocyanidin-administered rats decrease lipid synthesis in HepG2 cells. J Nutr Biochem 2013;24:2092–9. https://doi.org/10.1016/J.JNUTBIO.2013.08.001.

[161] Pascual-Serrano A, Bladé C, Suárez M, Arola-Arnal A. Grape Seed Proanthocyanidins Improve White Adipose Tissue Expansion during Diet-Induced Obesity Development in Rats. Int J Mol Sci 2018, Vol 19, Page 2632 2018;19:2632. https://doi.org/10.3390/IJMS19092632.

[162] Pinent M, Bladé MC, Salvadó MJ, Arola L, Hackl H, Quackenbush J, et al. Grape-seed derived procyanidins interfere with adipogenesis of 3T3-L1 cells at the onset of differentiation. Int J Obes 2005 298 2005;29:934–41. https://doi.org/10.1038/sj.ijo.0802988.

[163] Caimari A, Del Bas JM, Crescenti A, Arola L. Low doses of grape seed procyanidins reduce adiposity and improve the plasma lipid profile in hamsters. Int J Obes 2013 374 2012;37:576–83. https://doi.org/10.1038/ijo.2012.75.

[164] Rodríguez-Pérez C, García-Villanova B, Guerra-Hernández E, Verardo V. Grape Seeds Proanthocyanidins: An Overview of In Vivo Bioactivity in Animal Models. Nutrients 2019;11. https://doi.org/10.3390/NU11102435.

[165] Du H, Wang Q, Li T, Ren D, Yang X. Grape seed proanthocyanidins reduced the overweight of C57BL/6J mice through modulating adipose thermogenesis and gut microbiota. Food Funct 2021;12:8467–77. https://doi.org/10.1039/D1FO01361K.

[166] Liu W, Zhao S, Wang J, Shi J, Sun Y, Wang W, et al. Grape seed proanthocyanidin extract ameliorates inflammation and adiposity by modulating gut microbiota in high-fat diet mice. Mol Nutr Food Res 2017;61:1601082. https://doi.org/10.1002/MNFR.201601082.

[167] Clifford MN. Diet-derived phenols in plasma and tissues and their implications for health. Planta Med 2004;70:1103–14. https://doi.org/10.1055/S-2004-835835/ID/2.

[168] Cardona F, Andrés-Lacueva C, Tulipani S, Tinahones FJ, Queipo-Ortuño MI. Benefits of polyphenols on gut microbiota and implications in human health. J Nutr Biochem 2013;24:1415–22. https://doi.org/10.1016/j.jnutbio.2013.05.001.

[169] Margalef M, Pons Z, Bravo FI, Muguerza B, Arola-Arnal A. Plasma kinetics and microbial biotransformation of grape seed flavanols in rats. J Funct Foods 2015;Complete:478–88. https://doi.org/10.1016/J.JFF.2014.12.007.

[170] Rodríguez RM, Cortés-Espinar AJ, Soliz-Rueda JR, Feillet-Coudray C, Casas F, Colom-Pellicer M, et al. Time-of-Day Circadian Modulation of Grape-Seed Procyanidin Extract (GSPE) in Hepatic Mitochondrial Dynamics in Cafeteria-Diet-Induced Obese Rats. Nutrients 2022;14. https://doi.org/10.3390/NU14040774.

[171] Colom-Pellicer M, Rodríguez RM, Navarro-Masip È, Bravo FI, Mulero M, Arola L, et al. Time-of-day dependent effect of proanthocyanidins on adipose tissue metabolism in rats with diet-induced obesity. Int J Obes (Lond) 2022.

https://doi.org/10.1038/S41366-022-01132-0.

[172] Ibars M, Aragonès G, Ardid-Ruiz A, Gibert-Ramos A, Arola-Arnal A, Suárez M, et al. Seasonal consumption of polyphenol-rich fruits affects the hypothalamic leptin signaling system in a photoperiod-dependent mode. Sci Rep 2018;8. https://doi.org/10.1038/S41598-018-31855-Y.

[173] Hooper PL, Hooper PL, Tytell M, Vígh L. Xenohormesis: health benefits from an eon of plant stress response evolution. Cell Stress Chaperones 2010;15:761. https://doi.org/10.1007/S12192-010-0206-X.

[174] Arola-Arnal A, Cruz-Carrión Á, Torres-Fuentes C, Ávila-Román J, Aragonès G, Mulero M, et al. Chrononutrition and polyphenols: Roles and diseases. Nutrients 2019;11:1–18. https://doi.org/10.3390/nu11112602.

[175] Howitz KT, Sinclair DA. Xenohormesis: Sensing the Chemical Cues of Other Species. Cell 2008;133:387–91. https://doi.org/10.1016/J.CELL.2008.04.019.

[176] Baur JA, Sinclair DA. What is Xenohormesis? Am J Pharmacol Toxicol 2008;3:149–56. https://doi.org/10.3844/AJPTSP.2008.152.159.

[177] Cruz-Carrión Á, de Azua MJR, Mulero M, Arola-Arnal A, Suárez M. Oxidative Stress in Rats is Modulated by Seasonal Consumption of Sweet Cherries from Different Geographical Origins: Local vs. Non-Local. Nutrients 2020;12:1–15. https://doi.org/10.3390/NU12092854.

[178] Cruz-Carrión Á, Ruiz De Azua MJ, Bravo FI, Aragonès G, Muguerza B, Suárez M, et al. Tomatoes consumed in-season prevent oxidative stress in Fischer 344 rats: impact of geographical origin. Food Funct 2021;12:8340–50. https://doi.org/10.1039/D1FO00955A.

[179] Gibert-Ramos A, Palacios-Jordan H, Salvadó MJ, Crescenti A. Consumption of out-of-season orange modulates fat accumulation, morphology and gene expression in the adipose tissue of Fischer 344 rats. Eur J Nutr 2020;59:621–31. https://doi.org/10.1007/S00394-019-01930-9.

[180] Bohn T. Dietary factors affecting polyphenol bioavailability. Nutr Rev 2014;72:429–52. https://doi.org/10.1111/NURE.12114.

[181] Spencer JPE, Chaudry F, Pannala AS, Srai SK, Debnam E, Rice-Evans C. Decomposition of cocoa procyanidins in the gastric milieu. Biochem Biophys Res Commun 2000;272:236–41. https://doi.org/10.1006/BBRC.2000.2749.

[182] Natsume M, Osakabe N, Oyama M, Sasaki M, Baba S, Nakamura Y, et al. Structures of (-)-epicatechin glucuronide identified from plasma and urine after oral ingestion of (-)-epicatechin: differences between human and rat. Free Radic Biol Med 2003;34:840–9. https://doi.org/10.1016/S0891-5849(02)01434-X.

[183] Zhang L, Wang Y, Li D, Ho CT, Li J, Wan X. The absorption, distribution, metabolism and excretion of procyanidins. Food Funct 2016;7:1273–81. https://doi.org/10.1039/C5FO01244A.

[184] Van Duynhoven J, Vaughan EE, Jacobs DM, Kemperman RA, Van Velzen EJJ, Gross G, et al. Metabolic fate of polyphenols in the human superorganism. Proc

Natl Acad Sci U S A 2011;108:4531–8. https://doi.org/10.1073/PNAS.1000098107/ASSET/88261615-2862-4C93-953C-FA302313D49A/ASSETS/GRAPHIC/PNAS.1000098107FIG03.JPEG.

[185] Serra A, Macià A, Romero MP, Valls J, Bladé C, Arola L, et al. Bioavailability of procyanidin dimers and trimers and matrix food effects in in vitro and in vivo models. Br J Nutr 2010;103:944–52. https://doi.org/10.1017/S0007114509992741.

[186] Ávila-Román J, Soliz-Rueda JR, Bravo FI, Aragonès G, Suárez M, Arola-Arnal A, et al. Phenolic compounds and biological rhythms: Who takes the lead? Trends Food Sci Technol 2021;113:77–85. https://doi.org/10.1016/J.TIFS.2021.04.050.

[187] Arola-Arnal A, Oms-Oliu G, Crescenti A, del Bas JM, Ras MR, Arola L, et al. Distribution of grape seed flavanols and their metabolites in pregnant rats and their fetuses. Mol Nutr Food Res 2013;57:1741–52. https://doi.org/10.1002/MNFR.201300032.

[188] Ozdal T, Sela DA, Xiao J, Boyacioglu D, Chen F, Capanoglu E. The Reciprocal Interactions between Polyphenols and Gut Microbiota and Effects on Bioaccessibility. Nutr 2016, Vol 8, Page 78 2016;8:78. https://doi.org/10.3390/NU8020078.

[189] Appeldoorn MM, Vincken JP, Aura AM, Hollman PCH, Gruppen H. Procyanidin dimers are metabolized by human microbiota with 2-(3,4-dihydroxyphenyl)acetic acid and 5-(3,4-dihydroxyphenyl)-γ- valerolactone as the major metabolites. J Agric Food Chem 2009;57:1084–92. https://doi.org/10.1021/JF803059Z/SUPPL_FILE/JF803059Z_SI_001.PDF.

[190] Selma M V., Espín JC, Tomás-Barberán FA. Interaction between phenolics and gut microbiota: Role in human health. J Agric Food Chem 2009;57:6485–501. https://doi.org/10.1021/JF902107D/ASSET/IMAGES/LARGE/JF-2009-02107D_0003.JPEG.

[191] Margalef M, Pons Z, Iglesias-Carres L, Quiñones M, Bravo FI, Arola-Arnal A, et al. Rat health status affects bioavailability, target tissue levels, and bioactivity of grape seed flavanols. Mol Nutr Food Res 2017;61. https://doi.org/10.1002/MNFR.201600342.

[192] Gasperotti M, Passamonti S, Tramer F, Masuero D, Guella G, Mattivi F, et al. Fate of microbial metabolites of dietary polyphenols in rats: is the brain their target destination? ACS Chem Neurosci 2015;6:1341–52. https://doi.org/10.1021/ACSCHEMNEURO.5B00051.

[193] Espín JC, González-Sarrías A, Tomás-Barberán FA. The gut microbiota: A key factor in the therapeutic effects of (poly)phenols. Biochem Pharmacol 2017;139:82–93. https://doi.org/10.1016/J.BCP.2017.04.033.

[194] Margalef M, Pons Z, Iglesias-Carres L, Bravo FI, Muguerza B, Arola-Arnal A. Flavanol plasma bioavailability is affected by metabolic syndrome in rats. Food Chem 2017;231:287–94. https://doi.org/10.1016/J.FOODCHEM.2017.03.141.

[195] D'Archivio M, Filesi C, Varì R, Scazzocchio B, Masella R. Bioavailability of the Polyphenols: Status and Controversies. Int J Mol Sci 2010, Vol 11, Pages 1321-

1342 2010;11:1321–42. https://doi.org/10.3390/IJMS11041321.

[196] Escobar-Martínez I, Arreaza-Gil V, Muguerza B, Arola-Arnal A, Bravo FI, Torres-Fuentes C, et al. Administration Time Significantly Affects Plasma Bioavailability of Grape Seed Proanthocyanidins Extract in Healthy and Obese Fischer 344 Rats. Mol Nutr Food Res 2022;66. https://doi.org/10.1002/MNFR.202100552.

[197] Iglesias-Carres L, Mas-Capdevila A, Bravo FI, Arola L, Muguerza B, Arola-Arnal A. Exposure of Fischer 344 rats to distinct photoperiods influences the bioavailability of red grape polyphenols. J Photochem Photobiol B Biol 2019;199:111623. https://doi.org/10.1016/j.jphotobiol.2019.111623.

HYPOTHESIS AND OBJECTIVES

Biological rhythms play a crucial role in adjusting the physiological and metabolic processes of the organism to external and predicable environmental variations such as the light/darkness cycles. This adaptation to environmental changes is essential for survival, allowing the optimization of the metabolism and energy expenditure to the time of day (circadian rhythms) and year (seasonal rhythms). Thus, physiological and metabolic processes are influenced by both circadian and seasonal rhythms. In fact, disturbances of circadian rhythms caused by modern lifestyles (shift work, artificial light exposition, diet type or eating time) have been associated with metabolism disorders development, including type 2 diabetes mellitus, obesity and metabolic MetS. Moreover, obesity development lead to rhythms disruption in several metabolic and physiological processes. Thus, there is a bidirectional interaction between metabolism and rhythms. This is relevant because of these metabolic disorders are reaching epidemic proportions worldwide. However, the impact of season rhythms on obesity is less understood. In this regard, gut microbiota, which plays a crucial role in obesity development, has shown seasonal oscillations in healthy animals. In addition, according to the xenohormesis theory, phenolic compounds, which are plant secondary metabolites, act as external cues allowing animals to adapt to environmental changes to the heterotrophs that consume them. These compounds have been reported to have several health effects depending on photoperiod conditions and also to interact with microbiota. In addition, the gut microbiota is a fundamental feature in the metabolism of dietary polyphenols. .

Therefore, we hypothesized that seasonal rhythms can modulate gut microbiota in obesity, also impacting the functionality of PAs in this disorder via these bacteria.

Hence, the aim of this thesis was to evaluate the relationship between seasonal rhythms and gut microbiota, and its impact on the functionality of PAs in an obesity context. As a strategy to address this general objective, a grape seed proanthocyanidin-rich extract (GSPE) was used, given that its beneficial effects

on different key aspects of MetS and obesity disorder have been extensively investigated by our group.

To achieve this general goal, the following specific objectives were proposed:

1. **To evaluate the relationship between seasonal rhythms and gut microbiota in healthy and CAF-induced obese Fischer 344 (F344) rats (*Chapter 1*).**

Seasonal rhythms influence on gut microbiota under an obesogenic context has not been sufficiently investigated yet. Moreover, potential mechanisms involved are still poorly understood. In this regard, it is known that corticosterone, one of the main hormones involved in gut microbiota-mediated effects, is modulated by seasonal rhythms through the HPA. At the same time, corticosterone is also involved in the regulation of clock genes. However, little is known about the influence of gut microbiota in corticosterone seasonal oscillations and seasonal clock genes expression. Hence, the following goals were proposed:

1.1. To investigate the effects of photoperiods, which mimics seasonal changes, on fecal microbiota composition and its impact on BW gain and fat parameters [**Manuscript 1**].

1.2. To elucidate if the effects of seasonal rhythms on corticosterone, as well as on circadian and seasonal clock genes are influenced by gut microbiota [**Manuscript 2**].

2. **To investigate the influence of seasonal rhythms and gut microbiota in the functionality and bioavailability of PAs in CAF-induced obese F344 rats *(Chapter 2)*.**

PAs can modulate gut microbiota composition and, at the same time, intestinal bacteria can modulate the metabolism of phenolic compounds, showing a bidirectional interaction. Moreover, the beneficial effects of PAs have been

attributed to phenolic compounds generated by their metabolism, in which gut microbiota composition plays a crucial role. Thus, for this objective, two main goals were proposed:

2.1. To elucidate if GSPE anti-obesity effects can be modulated by gut microbiota in a photoperiod dependent manner [**Manuscript 3**].

2.2. To evaluate if GSPE bioavailability is influenced by different photoperiod exposure via gut microbiota modulation in an obesogenic context **[Manuscript 4**].

3. To elucidate the photoperiod influence on serum oxylipins levels in healthy and obese rats, as well as the impact of PAs and gut microbiota on these lipid metabolites (*Chapter 3*).

OXLs are lipid mediators of inflammatory processes, which have been reported as potential obesity biomarkers. Gut microbiota seems to play an important role in their metabolism. Furthermore, polyphenols and diet can also modulate their biosynthesis. As it was previously mentioned, seasonal rhythms influence many physiological processes, including inflammation. Consequently, OXLs metabolism could be affected by seasonal rhythms and modulated by both gut microbiota and PAs. However, the impact of these factors on OXLs metabolism has not been investigated yet. To this purpose, two main goals were proposed:

3.1. To investigate the role of gut microbiota on OXLs metabolism in healthy and CAF-diet induced obese Wistar rats [**Manuscript 5**].

3.2. To investigate the effects of seasonal rhythms on OXLs metabolites in healthy and CAF-diet induced obese F344 rats, and the impact of PAs and gut microbiota [**Manuscript 6**].

WORK PLAN:
Experimental procedures used

To assess the main hypothesis and objectives previously described in this thesis (with the exception of the specific objective 3.1), one hundred twenty 13-week-old male F344 rats were housed by pairs in specific light-dark cycles to simulate three specific photoperiods: short photoperiod [L6, 6 h light/18 h darkness], standard photoperiod [L12, 12 h light/12 h darkness], or long photoperiod [L18, 18 h light/6 h darkness]. In each photoperiod, rats were fed either a standard chow diet (STD) (72% carbohydrate, 8% lipid, and 19% protein; Safe-A04c, Germany) or a CAF composed of highly palatable and energy-dense human foods (58% CH, 31% lipid, and 11% protein) for 9 weeks. Furthermore, CAF-fed animals were further divided into five groups depending on the treatment administered during the last four weeks of the experiment. Thus, this experimental design consisted in five experimental groups per photoperiod (15 groups in total; n=8/group): 1) rats fed a STD and receiving vehicle (VH, condensed milk diluted with water in 1:5 proportion), 2) rats fed a CAF and receiving VH, 3) rats fed a CAF and receiving an antibiotic cocktail (ABX) in drinking water, 4) rats fed a CAF and administered a daily oral dose of a GSPE (25mg/kg BW dissolved in VH), and 5) rats fed a CAF and receiving both a daily oral dose of GSPE and ABX in drinking water. CAF was freshly prepared every day and included the following (grams per rat and per day): biscuits with pâté and cheese (15-17 g), bacon (7-10 g), ensaimada (pastry) (10-15 g), carrot (11-12 g), standard chow (20-25 g) and milk containing 22% sucrose (w/v). The antibiotic cocktail (0.5 g/l ampicillin, 0.250 g/l vancomycin and 0.125 g/l imipenem; Discovery fine chemicals, UK) was freshly prepared every day and the animals were given free access to it. VH and GSPE dose was administered one hour after the light was turned on by allowing rats to drink it from the tip of a syringe. Animals were sacrificed by decapitation. Fecal samples from the colon, pituitary gland and colon tissue were freshly collected and immediately frozen in liquid nitrogen until further analysis. WAT depots including mesenteric (mWAT), retroperitoneal (RWAT), inguinal (iWAT), epididymal (eWAT) and subcutaneous, were precisely removed via dissection and weighed. The blood

was collected from the neck, in non-heparinized tubes, incubated for 1 h at room temperature and immediately centrifuged at 1200x g for 15 min to collect the serum.

To achieve the mentioned specific objectives the following specific design and analysis were carried out:

Objective 1.1. To investigate the effects of photoperiods, which mimics seasonal changes, on fecal microbiota composition and its impact on BW gain and fat parameters in healthy and cafeteria-induced obese male F344 rats [Manuscript 1].

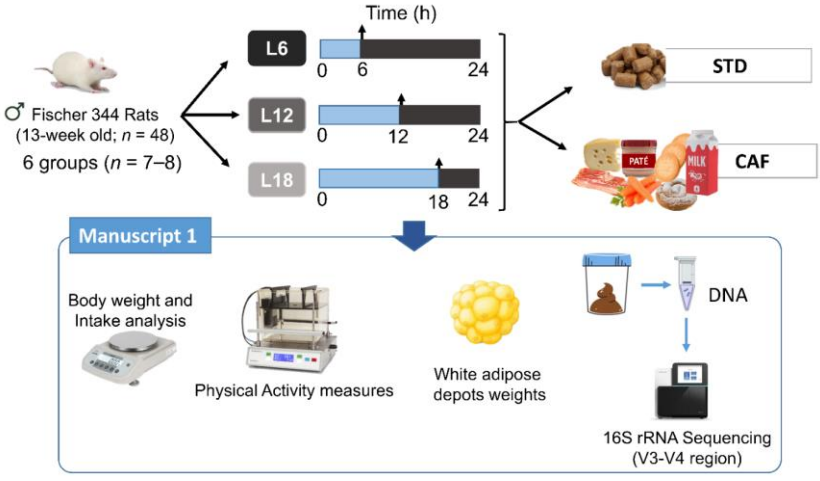

Figure 10. Experimental design for the objective 1.1. *L6: short photoperiod (6h light/18h dark); L12: standard photoperiod (12h light/12h dark); L18: long photoperiod (18h light/6h dark); STD: standard chow diet; CAF: cafeteria diet.*

For this specific objective, the experimental treatments groups 1 and 2 described above were included for each photoperiod condition (**Figure 10**). Fecal samples were used to isolate total DNA and perform 16S rRNA sequencing (Ion S5 system). Then, visceral mass was calculated as the sum of visceral adipose tissue depots (mWAT, RWAT and eWAT). Total body fat mass was measured as the sum of the visceral fat and subcutaneous fat (iWAT and subcutaneous). Finally, the Adiposity Index was expressed as total body fat mass/final BW. BW and food intake recorded weekly during the whole

experimental procedure were analyzed. Physical activity was evaluated using OxyletProTM system at weeks 8th and -9th of the study.

Objective 2.2. To elucidate if seasonal rhythms are influenced by gut microbiota at hormonal and molecular levels: impact on corticosterone and seasonal clock genes expression [Manuscript 2].

To accomplish this objective, the experimental groups 1, 2 and 3 described above were included for each photoperiod conditions (**Figure 11**). BW gain and fecal microbiota composition were analyzed as explained for objective 1.1. Moreover, oral glucose tolerance test (OGTT) was carried out at the last week of the experiment. Glucose was orally administered after 6 h fasting (2 g/kg BW, 50% w/v) and blood glucose levels were measured with a glucometer (Glucocard SM, Menarini Diagnostics, Italy) at 0, 15, 30, 60 and 120 min after glucose administration. In addition, serum corticosterone hormone was measured by liquid chromatography coupled to a triple quadrupole mass spectrometer (LC-QqQ). Seasonal (EYA3 and CHGA) and circadian clock (*Bmal1*, *Clock*, *Per1*, *Cry1*, *Rorα* and *Rev-erbα* genes expressions were also evaluated in pituitary gland and colon tissue by quantitative polymerase chain reaction.

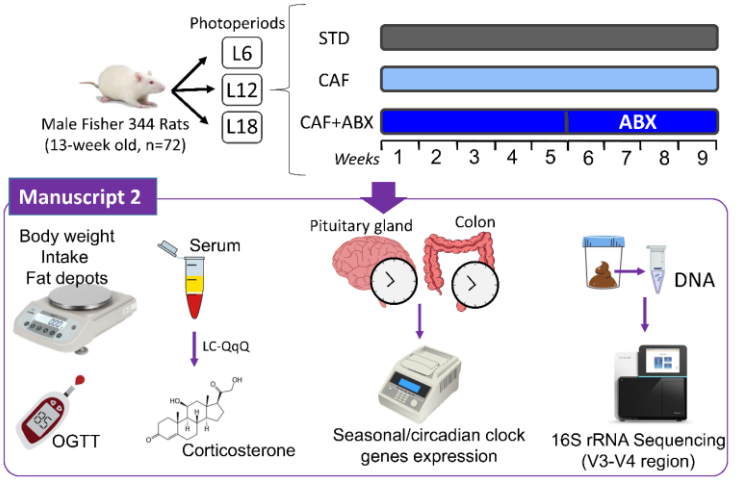

Figure 11. Experimental design for the objective 1.2*. OGTT: oral glucose tolerance test; L6: 6h light/18h darkness; L12: 12h light/12h darkness; L18: 18h light/6h darkness; STD: standard chow diet; CAF: cafeteria diet; VH: vehicle; ABX: antibiotic cocktail.*

Objective 2.1. To elucidate if GSPE anti-obesity effects can be modulated by gut microbiota in a photoperiod dependent manner [Manuscript 3].

To achieve this objective, the experimental groups 2, 3, 4 and 5 described above were used in each photoperiod condition (**Figure 11**). Body composition, OGTT and fecal microbiota composition were analyzed as described for the previous objectives. Moreover, biochemical parameters were analyzed in serum by enzymatic colorimetric assays (glucose, cholesterol, triglycerides and non-esterified fatty acids (NEFAs)) and by ELISA kit (insulin) according to the manufacturers' instructions.

Objective 2.2. To evaluate if GSPE bioavailability is influenced by different photoperiod exposure via gut microbiota modulation in an obesogenic context. [Manuscript 4].

In this case, same experimental groups as for the specific objective 2.1 were used (**Figure 12**). Serum bioavailability of phenolic compounds from GSPE was determined by liquid chromatography-tandem mass spectrometry (HPLC-MS/MS).

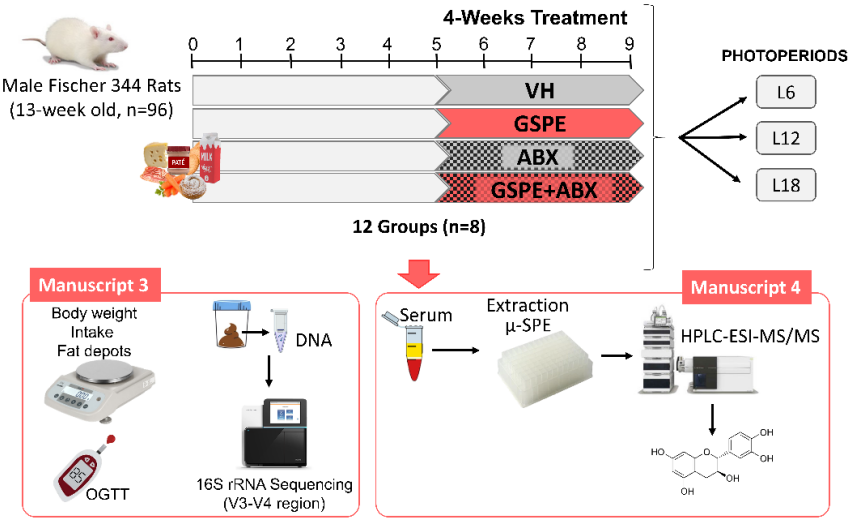

Figure 12. Experimental design for the objectives 2.1 and 2.2. *GSPE: grape seed proanthocyanidin; Vehicle and ABX-treated animals were included as controls. L6: 6h light/18h darkness; L12: 12h light/12h darkness; L18: 18h light/6h darkness; CAF: cafeteria diet; VH: vehicle.*

Objective 3.1. To investigate the role of gut microbiota on OXLs metabolism in healthy and CAF-diet induced obese Wistar rats [Manuscript 5].

In this case, a different experimental design was used (**Figure 13**). Hence, we firstly investigated how alterations in gut microbiota composition induced by ABX treatment may impact on plasmatic oxylipins (OXLs) profile in Wistar rats under healthy and obesogenic conditions. To this aim, male Wistar rats were fed either a STD or CAF diet and treated for the last two weeks with ABX in drinking water. No treated animals were included as controls (VH). Blood samples were collected in EDTA-tubes from the saphenous vein using capillary action. Plasma was obtained by centrifugation (5000 g, 5 min, and 4^{o}C) and OXLs profiles were analyzed by LC-MS/MS. Fecal samples were freshly collected and immediately frozen in liquid nitrogen. Fecal DNA was isolated and 16S rRNA sequencing was performed to obtain the gut microbiota relative abundance (Ion S5 system).

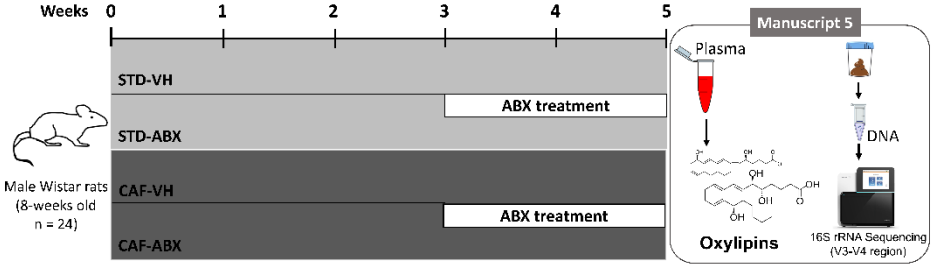

Figure 13. Experimental design for the objective 3.1*. STD: standard chow diet; CAF: cafeteria diet; VH: vehicle (control animals); ABX: antibiotic cocktail (g/l ampicillin, 0.5 g/l vancomycin and 0.25 g/l imipenem).*

Objective 3.2. To investigate the effects of seasonal rhythms on OXLs metabolites in healthy and obesogenic conditions, and the impact of PAs and gut microbiota [Manuscript 6].

To accomplish this specific objective, the five experimental groups described above were included for each photoperiod condition (**Figure 14**). Serum levels of OXLs were measured using ELISA kits. The analyzed OXLs were the following: 6-keto Prostaglandin F1α, 15-epi Lipoxin A4, Leukotriene B4, Prostaglandin E2

and Resolvin D2. Furthermore, the levels of oleic acid (OA) and linoleic acid (LA) was analyzed from serum samples by gas chromatography-quadrupole time-of-flight (CG-qTOF).

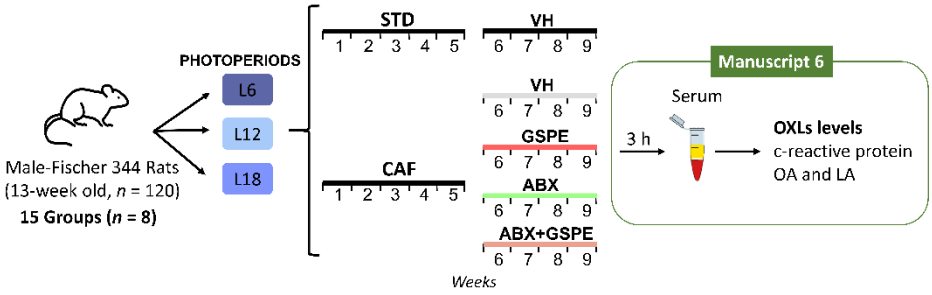

Figure 14. Experimental procedure for specific objective 3.2. *OXLs: oxylipins; OA: oleic acid; LA: linoleic acid.*

RESULTS

RESULTS

CHAPTER 1

To evaluate the seasonal rhythms effects on gut microbiota in healthy and CAF-induced obese Fischer 344 (F344) rats

RESULTS

Manuscript 1

Objective: To investigate the effects of photoperiods, which mimics seasonal changes, on fecal microbiota composition and its impact on body weight gain and fat parameters

Gut Seasons: Photoperiod Effects on Fecal Microbiota in Healthy and Cafeteria-Induced Obese Fischer 344 Rats

Arreaza-Gil V, Escobar-Martínez I, Suárez M, Bravo FI, Muguerza B, Arola-Arnal A*, Torres-Fuentes C.

Universitat Rovira i Virgili, Department de Biochemistry and Biotechnology, Nutrigenomics Research Group, Tarragona, 43007, Spain

*Corresponding author

Published in *Nutrients*. 2022 Feb, 14(3):722. DOI: 10.3390/nu14030722. Impact Factor (2021): 6.706. SI Journal Citation Reports © Ranking 15/90 (Q1) in Nutrition & Dietetics.

RESULTS

nutrients

MDPI

Article

Gut Seasons: Photoperiod Effects on Fecal Microbiota in Healthy and Cafeteria-Induced Obese Fisher 344 Rats

Verónica Arreaza-Gil, Iván Escobar-Martínez, Manuel Suárez, Francisca Isabel Bravo, Begoña Muguerza, Anna Arola-Arnal * and Cristina Torres-Fuentes

Nutrigenomics Research Group, Departament de Bioquímica i Biotecnologia, Universitat Rovira i Virgili, 43007 Tarragona, Spain; veronica.arreaza@urv.cat (V.A.-G.); ivan.escobar@urv.cat (I.E.-M.); manuel.suarez@urv.cat (M.S.); franciscaisabel.bravo@urv.cat (F.I.B.); begona.muguerza@urv.cat (B.M.); cristina.torres@urv.cat (C.T.-F.)

* Correspondence: anna.arola@urv.cat

Abstract: Gut microbiota and biological rhythms are emerging as key factors in the modulation of several physiological and metabolic processes. However, little is known about their interaction and how this may affect host physiology and metabolism. Several studies have shown oscillations of gut microbiota that follows a circadian rhythmicity, but, in contrast, variations due to seasonal rhythms have not been sufficiently investigated yet. Thus, the goal of this study was to investigate the impact of different photoperiods, which mimic seasonal changes, on fecal microbiota composition and how this interaction affects diet-induced obesity development. To this aim, Fisher 344 male rats were housed under three photoperiods (L6, L12 and L18) and fed with standard chow diet or cafeteria diet (CAF) for 9 weeks. The 16S ribosomal sequencing of collected fecal samples was performed. The photoperiod exposure significantly altered the fecal microbiota composition under L18, especially in CAF-fed rats. Moreover, these alterations were associated with changes in body weight gain and different fat parameters. These findings suggest a clear impact of seasonal rhythms on gut microbiota, which ultimately translates into different susceptibilities to diet-induced obesity development. This is the first time to our knowledge that the photoperiod impact on gut microbiota composition has been described in an obesity context although further studies are needed in order to elucidate the mechanisms involved.

Keywords: gut microbiota; photoperiods; seasonal rhythms; obesity; cafeteria diet

Citation: Arreaza-Gil, V.; Escobar-Martínez, I.; Suárez, M.; Bravo, F.I.; Muguerza, B.; Arola-Arnal, A.; Torres-Fuentes, C. Gut Seasons: Photoperiod Effects on Fecal Microbiota in Healthy and Cafeteria-Induced Obese Fisher 344 Rats. *Nutrients* **2022**, *14*, 722. https://doi.org/10.3390/nu14030722

Academic Editor: Lindsay Brown

Received: 13 January 2022
Accepted: 6 February 2022
Published: 8 February 2022

1. Introduction

Gut microbiota composition has been described as critical for the maintenance of homeostasis and metabolic function in the host [1]. Alterations in gut microbiota, also known as dysbiosis, may interfere with this balance, contributing to the development of metabolic diseases such as obesity and metabolic syndrome (MetS) [2]. Changes in dietary patterns are one of the most critical, modifiable factors that significantly alter the gut microbiota composition [3]. Thus, traditional diets such as the Mediterranean diet, which consists of high consumption of fiber and low consumption of sugar and fat, have long been associated with an increase in gut microbiota diversity and with a higher health status [4]. By contrast, Western-style diets have been shown to have strong effects on gut microbiota diversity and composition, often correlated with deleterious metabolic health effects [5]. For instance, the chronic consumption of a cafeteria diet significantly decreased gut bacterial diversity, reducing Firmicutes and increasing Bacteroidetes and Proteobacteria abundances, which were correlated with altered levels of plasma leptin and glycerol, as well as adipose tissue and liver inflammation, leading to the development of obesity and MetS [6].

In addition to diet, biological rhythms are emerging as a key factor to take into consideration when investigating gut microbiota changes. Indeed, several studies have shown

oscillations of gut microbiota during 24 h cycles [7,8]. In the latest years, a growing body of evidence has shown that circadian rhythms can interact with nutrients, influencing several metabolic and physiological functions [9,10]. This relatively new field is described as "chrononutrition". Hence, the food-intake pattern during the day has a significant influence on postprandial glucose, consequently affecting metabolism. The presence of these rhythms allows the organism to adjust to environmental factors such as changes in food availability or climatic variability, ensuring reproductive success and survival [11]. The effects of circadian rhythms on metabolism and physiology have been the most studied but those related to circannual rhythms are recently receiving increasing interest due to their important role in the regulation of physiological responses [12,13]. The synchronization between seasonal rhythms and physiological processes is driven by changes in the length of the daylight phase duration (photoperiods) [14,15]. The response to changes in photoperiods is encoded by the suprachiasmatic nucleus in the hypothalamus through the control of pineal melatonin production [15,16]. The melatonin signal communicates photoperiod information to a variety of targets throughout the body and brain, being therefore the hypothalamic–pituitary axis indispensable for the interaction between seasonal changes and both metabolic and physiological processes [17]. Thus, seasonal rhythms have been related to psychiatric disorders [18] and reproductive alterations in humans [19]. Furthermore, recent studies have shown that exposure of normal-weight rats to different photoperiods led to different metabolic changes suggesting that glucose- and lipid-related pathologies, such as obesity and MetS, could be influenced by light variations such as those observed in the different seasons [20]. However, little is known about the specific mechanisms involved. In fact, the effects of seasonal rhythms on gut microbiota which, as mentioned above, is one of the main links between diet and host metabolism, have not been sufficiently investigated yet.

In this regard, it has been shown that gut microbiota composition changes in both winter and summer due to seasonal variations in both the length of the daylight phase [21] and in dietary patterns [22]. Previous studies indicated that the relative abundance of certain bacteria differed for Siberian hamsters housed in long- versus short-day lengths [21,23]. In addition, seasonal variations in gut bacteria related to dietary changes were found in plateau pikas [24]. In another study in giant pandas, seasonal oscillations of gut microbiota and higher short chain fatty acid (SCFA) production in the shoot-eating season were observed [25]. In addition, seasonal changes including an increase in the breeding season of the relative abundance of gut bacteria related to lipid metabolism, carbohydrate metabolism, and nucleotide metabolism were observed in wild ground squirrels [26]. Significant seasonal oscillations in structure and function of gut bacteria were also found in forest and alpine musk deer [27]. In particular, a decrease in both the relative abundance of Firmicutes and the ratio of Firmicutes to Bacteroidetes, as well as an increase in Bacteroidetes, was observed in summer compared to winter. Authors concluded that these changes may contribute to a better environmental adaptation by promoting the digestion and metabolism of food. In another study carried out in frogs, seasonal food and body mass oscillations were significantly correlated with gut microbiota composition suggesting that gut bacteria may change due to dietary pattern variations associated with seasonal environmental changes [28]. Furthermore, a recent study in mice also demonstrated that exposure to regular light/dark cycles or the constant darkness exposure promoted a different gut microbiota profile [29]. In another recently published study with mice housed under different photoperiod conditions, although no significant differences were observed in the overall composition of the gut microbiota, authors were able to extract amplicon sequence variants that were predictive of photoperiod conditions with >91% accuracy [30]. Hence, these studies identify the photoperiod as an important factor which can modulate the gut microbiota composition. However, all of them were done in healthy animals and, therefore, further studies are needed to elucidate the relationship between photoperiod, gut microbiota and diet and its impact on metabolic diseases such as obesity.

Therefore, the aim of the current study was to investigate the effects of photoperiods on fecal microbiota and its impact on body weight gain and different fat depots in healthy and cafeteria-induced obese Fisher 344 rats.

2. Materials and Methods

2.1. Animals

Forty-eight 13-week-old male Fisher 344 rats from Janvier Laboratories (Le Genest-Saint-Isle, France) were housed in pairs at standard conditions (22 °C, 65% relative humidity and 12:12 h light/dark cycle). After one week of adaptation to the facility with free access to food and water, animals were weighed and randomly distributed under specific light-dark cycles to simulate three specific photoperiods: short photoperiod (L6, 6 h light/18 h darkness), standard photoperiod (L12, 12 h light/12 h darkness), or long photoperiod (L18, 18 h light/6 h darkness). In each photoperiod, rats were fed either a standard chow diet (STD) (72% carbohydrate, 8% lipid, and 19% protein; Safe-A04c, Scientific Animal Food and Engineering, Barcelona, Spain) or a cafeteria diet (CAF) composed of highly palatable and energy-dense human foods (58% CH, 31% lipid, and 11% protein) for 9 weeks (6 groups, n = 7–8 per group) (Figure 1). CAF diet was freshly prepared every day as previously described [31]. Body weight and food intake were recorded weekly during the whole experimental procedure.

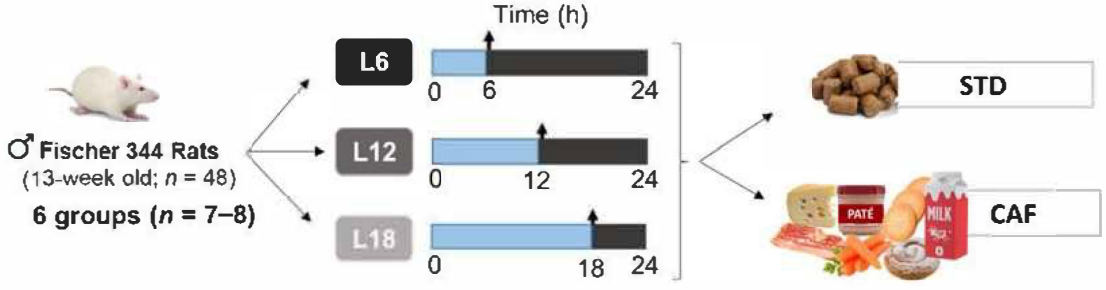

Figure 1. Animal experimental design. 13-week-old male STD- or CAF-fed Fischer 344 rats were pair-housed under three different photoperiods (6, 12 or 18 h of light per day) for 9 weeks. (n = 7–8). ♂: represents male sex; L6: short photoperiod (6 h light/18 h dark); L12: standard photoperiod (12 h light/12 h dark); L18: long photoperiod (18 h light/6 h dark); STD: standard chow diet; CAF: cafeteria diet.

Animals were sacrificed by decapitation. Fecal samples were freshly collected from the colon and immediately snap-frozen until further microbiota analysis. The cecum as well as white adipose tissue depots, including mesenteric (mWAT), retroperitoneal (RWAT), inguinal (iWAT), epididymal (eWAT) and subcutaneous, were collected, weighed and immediately frozen in liquid nitrogen. The visceral mass was calculated as the sum of visceral adipose tissue depots (mWAT, RWAT and eWAT). Total body fat mass was measured as the sum of the visceral fat and subcutaneous fat (iWAT and subcutaneous). The adiposity index was expressed as total body fat mass/final body weight. All the samples were stored at −80 °C until further analyses. The Animal Ethics Committee of the Rovira i Virgili University (Tarragona, Spain) and the Generalitat de Catalunya approved all the procedures (number reference 9495) in accordance with the EU Directive 2010/63/EU for animal experiments.

2.2. Physical Activity Measurements

Physical activity was evaluated using OxyletProTM system (Panlab, Barcelona, Spain). The measurements were performed at weeks 8 and 9 of the study. Animals were transferred to a standard rodent home cage (Oxylet LE 405 gas analyzer, Panlab) to ensure a contained sample environment. Rats were maintained at 22 °C under the different light/dark cycle conditions, according to the photoperiod, with free access to food and water. The cages

were placed on a platform with strain weight transducers to register movements. Data were collected and analyzed.

2.3. 16S rRNA Analysis

DNA from fecal samples was isolated using QiAamp Fast DNA Stool mini kit (Qiagen Inc., Hilden, Germany) and stored at −20 °C until further analysis. The 16S ribosomal RNA sequencing was carried out using an Ion S5 system (Life Technologies, Carlsbad, CA, USA) as described previously [32]. Briefly, V3 and V4 regions were amplified using the following primer pairs: 341F-532R (5′-CCTACGGGRSGCAGCAG-3′; 5′-ATTACCGCGGCTGCT-3′) and 15F-806R (5′-GTGCCAGCMGCCGCGGTAA-3′; 5′-GGACTACHVGGGTWTCTAAT-3′). Specific Ion Torrent compatible adapters and a barcode sequence were added in order to sequence several samples simultaneously. Amplicons were visualized by electrophoresis (2% agarose) and DNA purification was performed with NucleoSpin (Macherey-Nagel, Berlin, Germany). Quality, length, and concentration of the libraries were analyzed using an Agilent 2100 Bioanalyzer (Agilent Technologies, CA, USA). Individual libraries (40 pM) were combined in equimolar amounts in groups of 38 samples. Template preparation and analysis was carried out in an Ion 510 & 520 & Ion 530 Kit-Chef (A34019, Life Technologies, Carlsbad, CA, USA) according to the manufacturer's instructions. Samples were loaded on a 530 chip (Ion 530TM Chip Kit–4 Reactions) and sequenced using the Ion S5 system (Life Technologies, Carlsbad, CA, USA). Low-quality reads (phred quality score <17) and polyclonal sequences were removed by filtering with the PGM software resulting in a total of 63,212,452 reads. Final sequences were further analyzed by QIIME (quantitative insights into microbial ecology) and GreenGenes database.

2.4. Statistical Analysis

Statistical analysis was performed using SPSS software (IBM SPSS statistics 25, Armonk, NY, USA). In the case of body weight gain, food intake, activity and fats depots data, normality as well as homogeneity of variance were tested by Shapiro–Wilk and Levene test, respectively. Body weight gain over time was analyzed using repeated-measured ANOVA followed by LSD post hoc test at each individual time point. AUC of body weight gain, food intake, activity and fat parameters were analyzed by two-way ANOVA followed by LSD post hoc test. Data were represented as mean ± standard deviation (SD) using Graphpad Prism (v.8.0; Graphapad software Inc., San Diego, CA, USA).

MicrobiomeAnalyst web-based tool [32,33] was used for fecal microbiota analysis. Relative abundance data was filtered (minimum count: 2; prevalence in sample: 10%) in order to exclude low abundance data or those appearing in only one sample. After data filtering, the number of features left was 35,759. Chao1 index and Kruskal–Wallis test were used to calculate and to elucidate alpha diversity differences between groups. Beta diversity was calculated based on Bray–Curtis distances and analyzed by permutational multivariate analysis of variance (PERMANOVA). Differences in relative abundance of specific bacteria taxa were analyzed using either Mann–Whitney (if comparing two groups) or Kruskal–Wallis test followed by Dunn's multiple comparison with Bonferroni adjustment of p values.

Spearman's rank-order correlation analysis between fecal microbiota at different taxonomic levels with body weight gain and fat parameters was carried out using Python script as previously described [31]. The FDR (false discovery rate) control for p-value correction in multiple comparisons was applied. The script was developed using PyCharm software (v.2018.2.4, JetBrains s.r.o., Prague, Czech Republic) and Python version 3.7.7.

Statistical significances were depicted as follows: *indicating diet effect $p < 0.05$, and ab letters indicating photoperiod effect $p < 0.05$.

3. Results

3.1. Photoperiod Effect on Body Weight

CAF-fed rats showed a significant increased body weight gain ($p < 0.001$) and corresponding AUC compared to STD-fed rats under the three different photoperiod conditions across the 9 weeks of the experiment (Figure 2a,b).

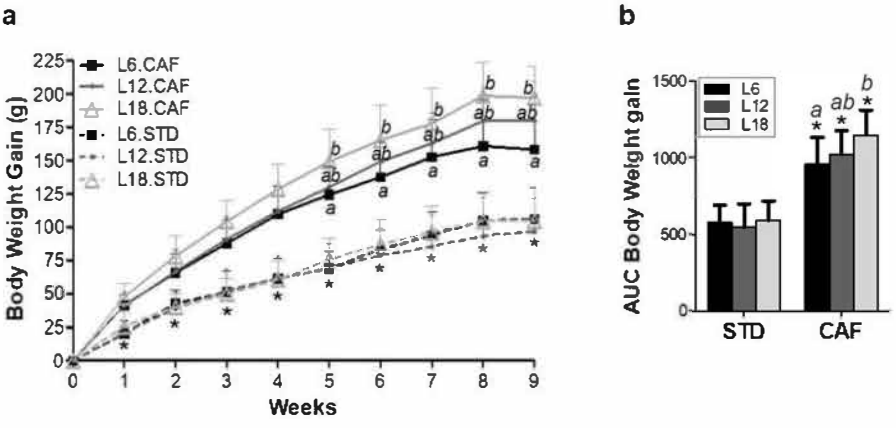

Figure 2. Effects of photoperiods on body weight gain in STD- and CAF-fed rats. (**a**) Body weight gain under short (L6), standard (L12) and long (L18) photoperiods across the 9 weeks of the experiment. * indicates significant CAF effect and *a,b* letters indicate significant CAF and photoperiod effects respectively, analyzed by repeated measures ANOVA followed by LSD post hoc test ($p < 0.05$). (**b**) Area under the curve (AUC) of body weight gain. * indicates significant CAF effect and *a,b* letters indicate photoperiod effect, analyzed by 2-way ANOVA followed by LSD post hoc test ($p < 0.05$). Data are plotted as the mean ± SD ($n = 7–8$). L6: short photoperiod (6 h light/18 h dark); L12: standard photoperiod (12 h light/12 h dark); L18: long photoperiod (18 h light/6 h dark); STD: standard chow diet; CAF: cafeteria diet.

Exposure to different photoperiods did not affect body weight gain in STD-fed rats (Figure 2). In contrast, CAF-fed rats exposed to the long photoperiod (L18) showed higher body weight gain during the last 5 weeks of the experiment (weeks 5–9) and a significantly higher corresponding area under the curve (AUC) when compared to rats exposed to the short photoperiod (L6) ($p < 0.05$) (Figure 2). These changes in body weight gain were not associated either with higher food intake (Figure S1a–f) or with lower activity in rats housed under L18 conditions (Figure S1g,h).

3.2. Photoperiods Affect Fecal Microbiota Composition: Higher Impact on Cafeteria Diet-Fed Rats

PERMANOVA analysis of fecal microbiota beta diversity revealed a significant CAF effect under each photoperiod condition (Figure S2). In addition, a significant photoperiod effect in both STD- ($p < 0.001$) and CAF-fed ($p < 0.001$) rats under L18 conditions was found (Figure 3a,b). Interestingly, the CAF effect on rats housed under L18 conditions was stronger than in both L6 and L12. Thus, samples were grouped according to diet type along the PC1 axis. (Figure S2c).

CAF feeding significantly reduced fecal microbiota diversity independently of photoperiod exposure ($p < 0.01$) (Figure 3c). Remarkably, fecal microbiota alpha diversity also showed an interesting photoperiod effect. Both STD- and CAF-fed rats under L12 showed a significant higher alpha diversity than rats under L6 and L18 ($p < 0.05$) (Figure 3c).

The relative abundance at phylum level was analyzed to evaluate photoperiod and CAF effects on fecal microbiota composition. A significant effect of CAF feeding on phyla relative abundance was observed independently of photoperiod exposure (Figure 3d, Table S1). Thus, CAF feeding led to a significant increase in Bacteroidetes, Proteobacteria, Verrucromicrobia and Cyanobacteria and a decrease in Firmicutes and Tenericutes ($p < 0.05$).

Moreover, the Firmicutes and Bacteroidetes alteration by CAF feeding caused a significant decrease in the Firmicutes to Bacteroidetes ratio ($p < 0.016$) (Table S1).

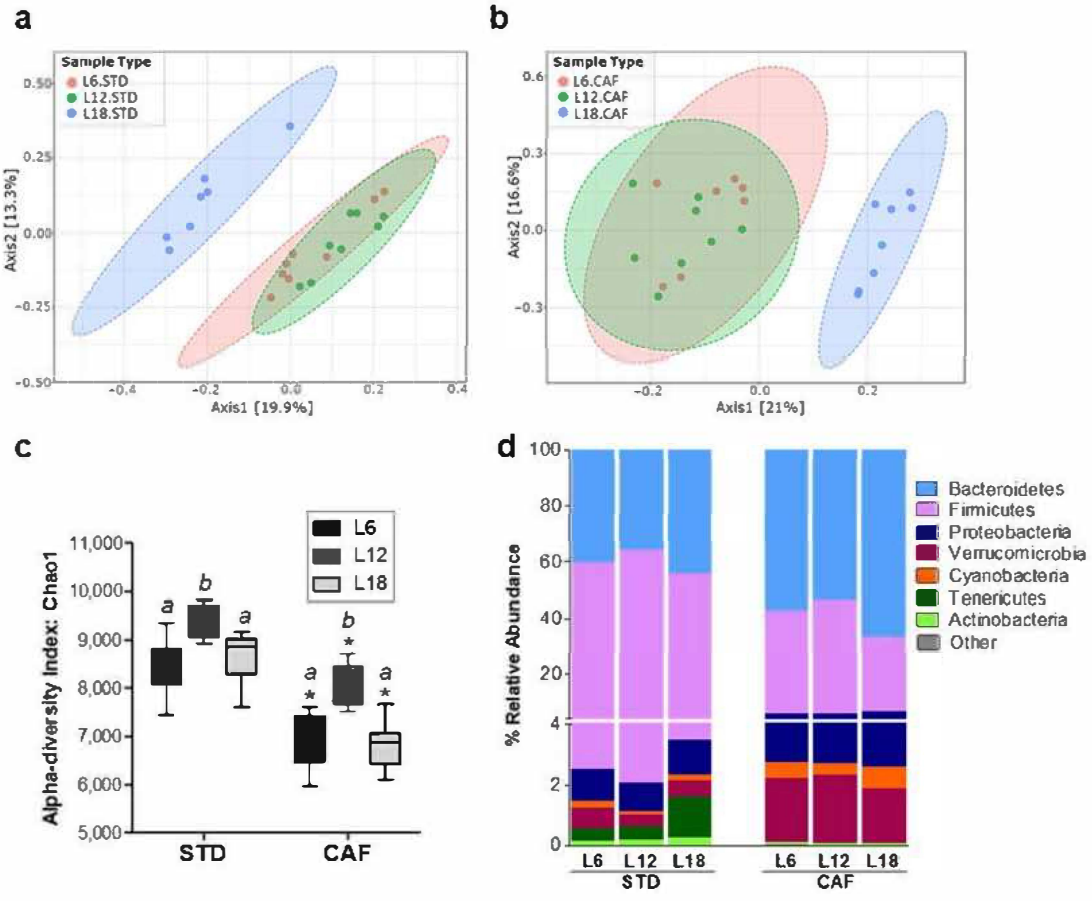

Figure 3. Effect of photoperiods (Ph) on both fecal microbial diversity and bacteria phyla relative abundance. Principal coordinates analysis (PCoA) 2D plot (PERMANOVA, $p < 0.001$) of fecal microbiota beta diversity based on Bray–Curtis distances in (**a**) STD- and in (**b**) CAF-fed rats; (**c**) alpha diversity calculated by chao-1 index in STD- and CAF-fed rats under the three different Ph conditions. Data are plotted as box and whiskers (median with interquartile ranges). * Indicates significant diet effect between STD and CAF-fed rats under same photoperiod conditions, analyzed by U-Mann–Whitney ($p < 0.05$); *a,b* letters indicate significant photoperiod effect analyzed by Kruskal–Wallis test followed by Bonferroni correction for multiple comparisons ($p < 0.016$); (**d**) relative abundance of different bacteria taxa at phylum level. (n = 7–8). L6: short photoperiod (6 h light/18 h dark); L12: standard photoperiod (12 h light/12 h dark); L18: long photoperiod (18 h light/6 h dark); STD: standard chow diet; CAF: cafeteria diet.

Regarding the photoperiod effect, STD-fed rats did not show a photoperiod effect on fecal bacteria relative abundance at phylum level, whereas CAF-fed rats showed a trend towards decreased Firmicutes ($p = 0.07$) and increased Bacteroidetes ($p = 0.08$) relative abundance levels under L18 compared to both L6 and L12 (Figure 3d). Besides this trend effect under L18, no photoperiod effects were observed on the Firmicutes to Bacteroidetes ratio (F/B ratio) (Table S1).

When looking at genera level, several of the bacteria genera relative abundances were affected by CAF feeding (Figure 4; Table S2). Thus, changes in genera belonging to Firmicutes and Bacteroidetes phyla were observed in CAF-fed rats while changes in less

abundant genera (relative abundance <0.1%) belonging to Actinobacteria, Bacteroidetes, Firmicutes and Proteobacteria phyla were observed in STD-fed rats.

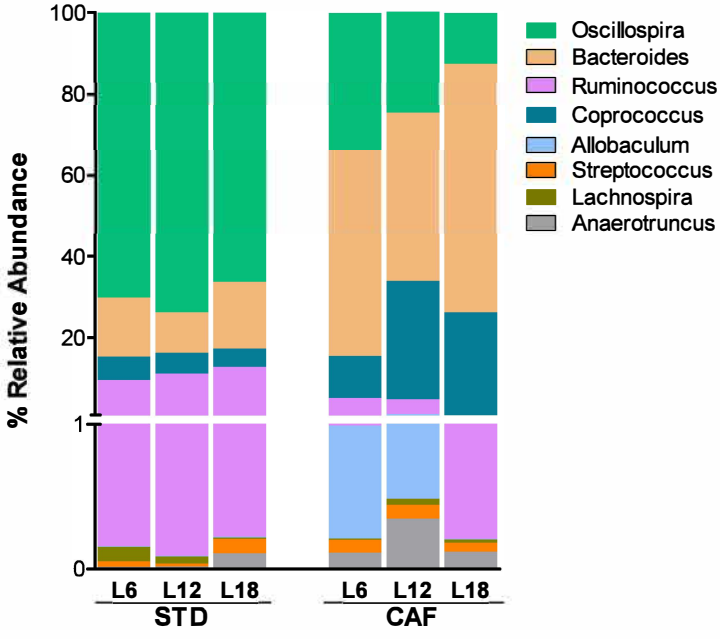

Figure 4. Relative abundance at genus level of the most abundant genera significantly altered by photoperiods. Stacked bar plots showing the relative abundance of each taxa at genus level. (n = 7–8). L6: short photoperiod (6 h light/18 h dark); L12: standard photoperiod (12 h light/12 h dark); L18: long photoperiod (18 h light/6 h dark); STD: standard chow diet; CAF: cafeteria diet.

Furthermore, photoperiod housing conditions also affected gut microbiota composition at this taxonomical level, mainly in CAF-fed rats (Figure 4; Table S2). Thus, it is worth highlighting some of the most abundant genera which altered significantly among photoperiods. Bacteroides, one of the most abundant genera that was increased by CAF feeding, increased in rats housed under L18 conditions. Oscillospira and Ruminococcus, which were significantly decreased by CAF feeding, showed significantly lower levels in rats housed under L18 conditions compared to those housed under L6. Other bacteria genera such as Coprococcus and Allobaculum, which were increased by CAF feeding, were also altered by photoperiod (Figure 4).

3.3. Correlations between Fecal Microbiota Taxa, Body Weight Gain and Fat Parameters

Bacteria taxa significantly altered by CAF or photoperiod conditions were selected in order to investigate if they correlated with body weight and fat parameters (fat depots accumulation, fat mass, visceral mass and adiposity index; Figure S3). Several correlations were observed (Table S3) and two main clusters were identified at phylum level. The first cluster involved Proteobacteria, Bacteroidetes, Cyanobacteria and Verrucromicrobia phyla showing positive correlations with the different fat parameters. The second cluster included Actinobacteria, Firmicutes and Tenericutes phyla showing negative correlations with these parameters (Figure 5). Proteobacteria and Firmicutes, two of the most abundance phyla, showed the highest number of strong to moderate significant correlations with iWAT, RWAT, visceral fat, fat mass and adiposity index (rho < 0.5/rho < −0.5, p < 0.05, FDR < 0.05) (Table S3). The analysis at family level showed strong and moderate positive correlations of *Lachnospiraceae*, *Bacteroidaceae*, *Streptococcaceae* and *Verrucomicrobiaceae* with the different analyzed parameters (rho = 0.7–0.5, p < 0.05, FDR < 0.05), while, *Clostridiaceae*

and *Ruminococcaceae* presented strong negative correlations (rho = −0.7–−0.5, $p < 0.05$, FDR < 0.05) (Table S3).

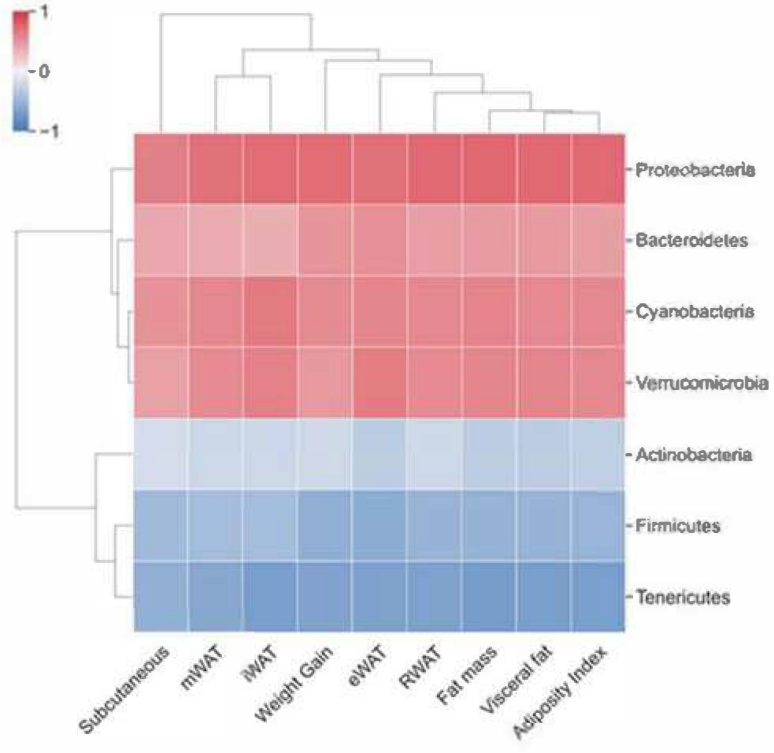

Figure 5. Correlations between fecal microbiota and body weight gain and fat parameters analyzed by Spearman's rank correlation coefficient (rho) at phylum level. Heat map with hierarchical clustering based on correlation coefficient between bacteria and biometric parameters at phylum level. Positive and negative correlations are represented in red and blue respectively. The higher the color intensity the higher the degree of correlation.

Since the assessment of these results revealed significant correlations between the relative abundance of different bacteria taxa and the different fat parameters, we further investigated these associations at genera level, focusing only on bacteria significantly altered by photoperiod conditions. Two clear clusters were identified: a first remarkable cluster positively correlated with the fat parameters, involving principally bacteria belonging to the Firmicutes, Bacteroidetes and Proteobacteria phyla, and a second cluster negatively correlated with the different fat parameters, involving mostly bacteria belonging to the Firmicutes phyla (Figure 6a). It is worth highlighting the strongest correlations observed in both clusters. Thus, *Bacteroides* and *Coprococcus* genera (belonging to Bacteroidetes and Firmicutes phyla respectively) showed a higher positive correlation with mWAT, RWAT, fat mass, visceral fat, adiposity index and body weight gain (rho = 0.67–0.6, $p < 0.001$, FDR < 0.05) (Figure 6b). On the other hand, in the second cluster, strong negative correlations with the different fat depots and body weight gain were observed for *Oscillospira* and *Ruminococcus* genera (rho = 0.6–0.7, $p < 0.001$, FDR < 0.05) (Figure 6b).

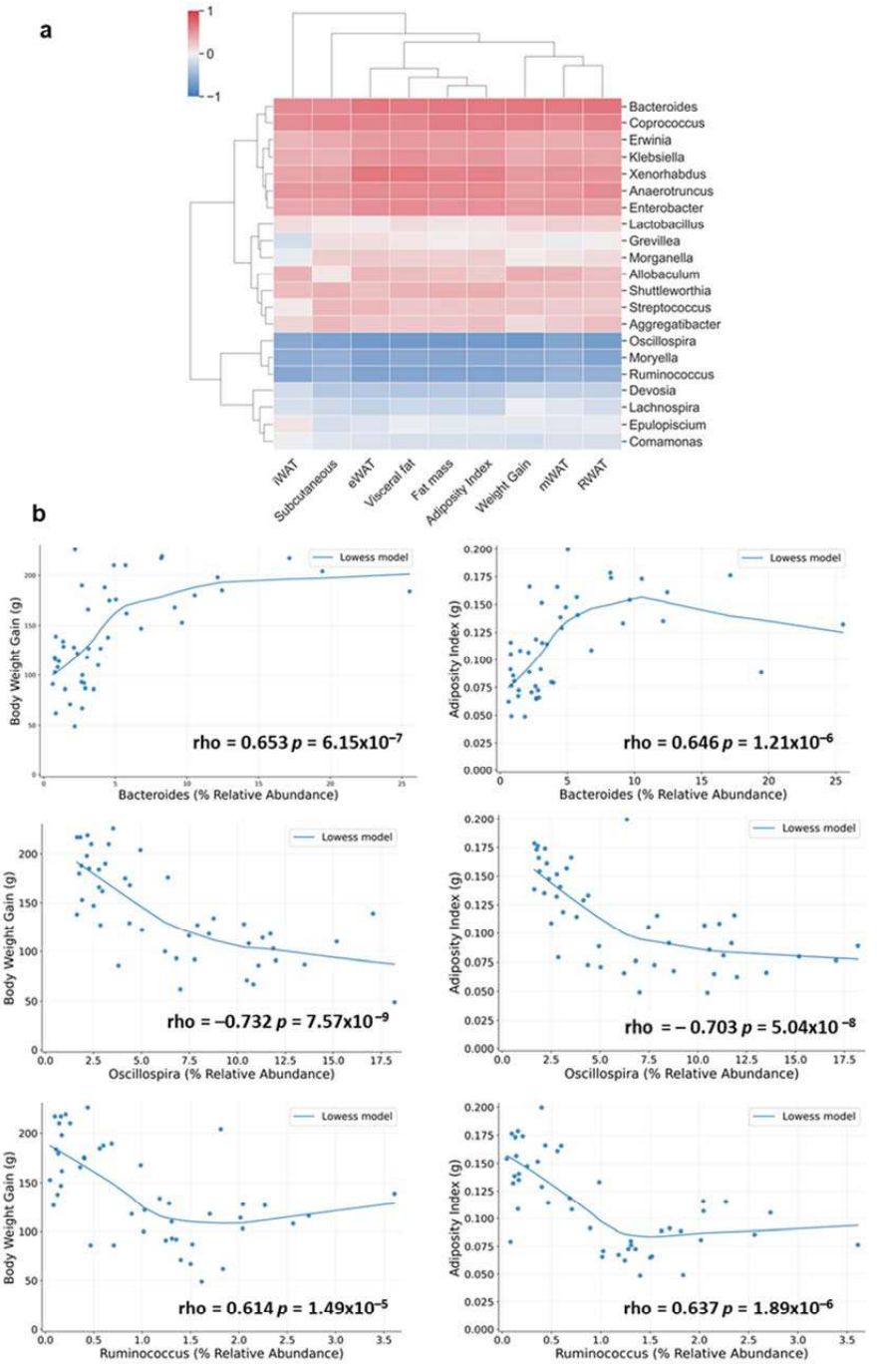

Figure 6. Correlations between fecal microbiota and fat parameters analyzed by Spearman's rank correlation coefficient (rho) at genus level. (**a**) Heat map with hierarchical clustering based on correlation coefficient between bacteria and fat parameters at genus level. Positive and negative correlations are represented in red and blue, respectively. The higher the color intensity the higher the degree of correlation. (**b**) Locally weighted linear regression (Lowess model) analysis of the strongest observed correlation in several bacteria genera affected by photoperiod.

4. Discussion

In the latest years, several studies have demonstrated that gut bacteria significantly affect host metabolism and physiology [1]. This has led to an increasing interest in understanding how gut microbiota composition is modulated. Dietary pattern is among the main factors that shape these gut microbes [34], but other environmental and intrinsic factors such as antibiotic intake [35], age [36], gender [37], physical activity [38] or stress [39] may be also involved. In addition to these factors, the exposure to different light cycles has recently been demonstrated to impact gut microbiota composition [21,29]. This is important as changes in gut microbiota composition may lead to different metabolic and physiologic responses, contributing to the adaptation to changes in environmental conditions associated to the different seasons. However, the relationship between seasonal rhythms and gut microbiota and its impact on the host physiology is still poorly understood. Hence, as mentioned earlier, only a few studies have focused on investigating seasonal variations of gut bacteria. Moreover, these studies have used non-obese animals and therefore the effects of seasonal variations under an obesogenic context has not been sufficiently investigated yet [24,25,27,40]. Therefore, we investigated the effect of different photoperiods on gut microbiota composition in both healthy and obese rats and how those changes correlated with parameters related to obesity development such as body weight gain and fat depots accumulation.

Obesity was induced by cafeteria diet feeding. This diet is a well-established model to induce obesity and other pathologies related to the metabolic syndrome and consists of highly palatable foods that lead to high caloric intake with poor nutritional value contributing to the development of different disorders such as insulin resistance, metabolic disruption and alterations of the gut microbiota composition [41,42]. Indeed, CAF-fed rats showed higher body weight gain, higher adiposity accumulation and gut microbiota dysbiosis compared to STD-fed rats. Additionally, obesity has been widely related with a reduction of alpha microbial diversity [43] and an increase of the Firmicutes to Bacteroidetes ratio in obese humans and animals [44]. In this context, CAF-fed rats showed lower alpha diversity but the Firmicutes/Bacteroidetes ratio was decreased due to the increase of Bacteroidetes and the reduction of Firmicutes relative abundance. However, this is in accordance with other studies using this type of cafeteria diet [4,45]. This discrepancy regarding Firmicutes/Bacteroidetes ratio with other high fat diets induced obesity models may be promoted by differences in the type of fat present in the diets, mainly lard and milk-derived fat-based diets [46]. Thus, the conflicting effects of CAF and other high fat diets on the Firmicutes/Bacteroidetes ratio may be explained by higher consumption of milk fat in CAF and higher intake of lard in other high fat diets. Indeed, clinical studies have also demonstrated that increased Firmicutes/Bacteroidetes ratio is not always related to obesity [47]. Hence, the association of this ratio with obesity should be considered carefully. Moreover, it is worth highlighting that CAF feeding did also significantly alter other phyla such as Proteobacteria and Verrucromicrobia, and other bacteria relative abundances at different taxonomic levels such as *Clostridiaceae*, *Lachnospiraceae* and *Prevotellaceae* at family level and *Bacteroides*, *Oscillospira*, *Ruminococcus* and *Akkermansia* at genus level, which have been related with obesity and metabolic disorders [48].

Different photoperiod conditions were used to simulate seasonal rhythms. Thus, the short photoperiod conditions emulated the hours of light in short days typical of the winter season while the long photoperiod conditions simulated the long days typical of the summer season. Interestingly, the photoperiod conditions significantly affected the overall fecal microbiota profile, and these changes were associated with differences in body weight gain and fat content. These results are in accordance with previous studies in Siberian hamsters, which showed variations in gut microbiota composition caused by different photoperiod conditions [21,23]. In particular, we observed a decreased alpha microbial diversity under L6 and L18 compared to L12 in both STD- and CAF-fed rats. This is in accordance with a previous studies that found that alpha diversity of fecal microbiota was significantly decreased in mice under 24 h light conditions compared to those under

normal 12-h LD cycles, suggesting that light cycles help to maintain a higher variety of gut microbiota [49]. In addition, rats housed under L18 conditions showed a significant different overall gut microbiota composition as elucidated by beta diversity analysis in both the STD- and CAF-fed diet. Interestingly, CAF-fed rats housed under this photoperiod condition also showed higher body weight gain and fat content. Remarkably, the increase in these parameters was not due to a change either in diet or in activity. This is common in mammals which are able to adapt to changes in the environment driven by changes in the light and dark cycle during the different seasons [50]. Hence, one specific trait of seasonal manifestation in mammals is a more efficient pattern of energy harvesting, expenditure and storage during the reproductive part of the year, which usually happens under the long photoperiod. In contrast, energy exploitation is scarce during the short photoperiod, which usually corresponds to the unproductive season [51,52]. Thus, it seems that the enhanced masses may be due to differences in the ability of the rats to harvest energy from the consumed food, being more efficient under L18 conditions. In addition, the gut microbiota profile from obese animals has been shown to have a higher capacity to harvest energy from the diet due to an increased glucose absorption and fatty acid absorption and production [53,54]. CAF-fed rats housed under L18 showed higher abundance of *Bacteroidetes* and lower abundance of *Firmicutes*. Indeed, *Bacteroidetes* was positively correlated with the body composition while *Firmicutes* was negatively correlated with these parameters. Interestingly, both phyla are often involved in carbohydrate metabolism [55,56]. The products of carbohydrate fermentation provide the host with energy, supporting the idea that these phyla are associated with an obesity susceptibility in the host [57]. In CAF-fed rats, most of the bacteria genera altered by photoperiod belonged to Firmicutes and Bacteroidetes phyla. Interestingly, two of the most abundant genera, *Oscillospira* and *Ruminococcus* were decreased in CAF rats under L18 and correlated negatively with the biometric parameters. These genera have been shown to be decreased in obese subjects and are known as potential butyrate producers [58,59]. This short chain fatty acid has been demonstrated to exert beneficial effects against obesity by increasing energy expenditure and lipid oxidation [60]. In addition, *Bacteroides* genera, prominent among obese individuals, was increased in this group and correlated positively with body composition. Therefore, these results revealed a relationship between gut microbiota and body weight gain and fat depots that might be driven by photoperiod conditions.

Finally, it is remarkable that STD-fed rats also showed a photoperiod effect on the fecal microbiota composition. However, these changes were observed in genera with a low relative abundance (<0.1%). In addition, these changes were not associated with differences in the body weight gain and fat depots, which were not affected by photoperiod in STD-fed rats. These findings were in agreement with previous work by our laboratory [20,61], but in contrast with other studies that showed significant changes in body weight gain and fat depot accumulation after a chronic exposure to different photoperiods in STD-fed rats [62,63]. This absence of variation in these parameters may be due to a potential adaptative response to chronic short photoperiod exposition, ensuring survival and avoiding reproductive suppression [64]. Thus, these results could mean that there is an interaction between photoperiod, diet and gut microbiota, obese-induced diet rats being more susceptible to photoperiod.

5. Conclusions

In conclusion, the current study suggests an interaction between photoperiod and gut microbiota being linked to metabolic disorders such as obesity. This interaction, which affects the body composition, may also affect physiological responses. Therefore, our research can set the basis to understand the potential benefits of microbiota-targeted therapies and to continue the study of the mechanisms regulating seasonal shifts associated with the development of metabolic diseases such as obesity.

Supplementary Materials: The following supporting information can be downloaded at: https://www.mdpi.com/article/10.3390/nu14030722/s1, Figure S1: Food intake and physical activity, Figure S2: Effect of diet on the beta-diversity in STD and CAF groups, Figure S3: Effects of photoperiod on white adipose tissue depots and cecum weight, Table S1: Relative abundance at phylum level of STD- and CAF-fed rats under the three different photoperiod conditions (L6, L12 and L18), Table S2: Significant photoperiod and diet effect at genus level, Table S3: Significant Spearman's correlations between body weight gain and fat parameters with the relative abundance bacteria at different taxonomic levels.

Author Contributions: Conceptualization, V.A.-G., A.A.-A. and C.T.-F.; methodology, V.A.-G., A.A.-A. and C.T.-F.; validation, V.A.-G., A.A.-A. and C.T.-F.; formal analysis, V.A.-G. and I.E.-M.; investigation, V.A.-G., I.E.-M., M.S., F.I.B., B.M., A.A.-A. and C.T.-F.; resources, M.S., F.I.B., B.M., A.A.-A. and C.T.-F.; data curation, V.A.-G.; writing—original draft preparation, V.A.-G.; writing—review and editing, A.A.-A. and C.T.-F.; visualization, V.A.-G.; supervision, A.A.-A. and C.T.-F.; project administration, V.A.-G., M.S., F.I.B., B.M., A.A.-A. and C.T.-F.; funding acquisition, M.S., F.I.B., B.M., A.A.-A. and C.T.-F. All authors have read and agreed to the published version of the manuscript.

Funding: Project AGL2016-77105-R funded by MCIN/AEI/10.13039/501100011033/ FEDER "Una manera de hacer Europa". V.A.-G. has a predoctoral Fellowship supported by Universitat Rovira i Virgili (PMF-PIPF-35 Martí i Franquès). I.E.-M. is supported by Youth Employment Initiative from the European Social Fund, Minesterio de Ciencia e Innovación, Agencia Estatal de Investigación and Universitat Rovira i Virgili (PEJ2018-002778-A). A.A.-A. and F.I.B. are Serra Húnter Fellows. C.T.-F. is supported by Beatriu de Pinós postdoctoral programme of the Government of Catalonia's Secretariat for Universities and Research of the Ministry of Economy and Knowledge.

Institutional Review Board Statement: The animal study protocol was approved by the Institutional Review Board (or Ethics Committee) of University Rovira i Virgili (Tarragona, Spain) (Project identification code 9495; File number: FUE-2017-00499873).

Informed Consent Statement: Not applicable.

Data Availability Statement: The data presented in this study are available, on request from authors, in Zenodo repository at doi:10.5281/zenodo.5785702.

Acknowledgments: The authors would like to thank Niurka Dariela Llópiz and Rosa Pastor for their assistance and technical support and Jorge Ricardo Soliz Rueda for developing python correlation script and bioinformatics support.

Conflicts of Interest: The authors declare no conflict of interest.

References

1. Patterson, E.; Ryan, P.M.; Cryan, J.F.; Dinan, T.G.; Ross, R.P.; Fitzgerald, G.F.; Stanton, C. Gut microbiota, obesity and diabetes. *Postgrad. Med. J.* **2016**, *92*, 286–300. [CrossRef] [PubMed]
2. Torres-Fuentes, C.; Schellekens, H.; Dinan, T.G.; Cryan, J.F. The microbiota–gut–brain axis in obesity. *Lancet Gastroenterol. Hepatol.* **2017**, *2*, 747–756. [CrossRef]
3. Sandhu, K.V.; Sherwin, E.; Schellekens, H.; Stanton, C.; Dinan, T.; Cryan, J.F. Feeding the microbiota-gut-brain axis: Diet, microbiome, and neuropsychiatry. *Transl. Res.* **2017**, *179*, 223–244. [CrossRef]
4. Del Chierico, F.; Vernocchi, P.; Dallapiccola, B.; Putignani, L. Mediterranean diet and health: Food effects on gut microbiota and disease control. *Int. J. Mol. Sci.* **2014**, *15*, 11678–11699. [CrossRef]
5. Shi, Z. Gut microbiota: An important link between western diet and chronic diseases. *Nutrients* **2019**, *11*, 2287. [CrossRef] [PubMed]
6. Del Bas, J.M.; Guirro, M.; Boqué, N.; Cereto, A.; Ras, R.; Crescenti, A.; Caimari, A.; Canela, N.; Arola, L. Alterations in gut microbiota associated with a cafeteria diet and the physiological consequences in the host. *Int. J. Obes.* **2018**, *42*, 746–754. [CrossRef]
7. Nobs, S.P.; Tuganbaev, T.; Elinav, E. Microbiome diurnal rhythmicity and its impact on host physiology and disease risk. *EMBO Rep.* **2019**, *20*, e47129. [CrossRef]
8. Thaiss, C.A.; Levy, M.; Korem, T.; Dohnalová, L.; Shapiro, H.; Jaitin, D.A.; David, E.; Winter, D.; Gury-BenAri, M.; Tatirovsky, E.; et al. Microbiota Diurnal Rhythmicity Programs Host Transcriptome Oscillations. *Cell* **2016**, *167*, 1495–1510.e12. [CrossRef]
9. Claustrat, B.; Leston, J. Melatonin: Physiological effects in humans. *Neurochirurgie* **2015**, *61*, 77–84. [CrossRef]

10. Johnston, J.D.; Ordovás, J.M.; Scheer, F.A.; Turek, F.W. Circadian rhythms, metabolism, and chrononutrition in rodents and humans. *Adv. Nutr.* **2016**, *7*, 399–406. [CrossRef]
11. Refinetti, R. Integration of biological clocks and rhythms. *Compr. Physiol.* **2012**, *2*, 1213–1239. [CrossRef] [PubMed]
12. Rácz, B.; Dušková, M.; Stárka, L.; Hainer, V.; Kunešová, M. Links between the circadian rhythm, obesity and the microbiome. *Physiol. Res.* **2018**, *67*, S409–S420. [CrossRef] [PubMed]
13. Onishi, K.G.; Maneval, A.C.; Cable, E.C.; Tuohy, M.C.; Scasny, A.J.; Sterina, E.; Love, J.A.; Riggle, J.P.; Malamut, L.K.; Mukerji, A.; et al. Circadian and circannual timescales interact to generate seasonal changes in immune function. *Brain Behav. Immun.* **2019**, *83*, 33–43. [CrossRef] [PubMed]
14. Murphy, B.A. Circadian and Circannual Regulation in the Horse: Internal Timing in an Elite Athlete. *J. Equine Veter. Sci.* **2019**, *76*, 14–24. [CrossRef]
15. Tackenberg, M.C.; McMahon, D.G. Photoperiodic Programming of the SCN and Its Role in Photoperiodic Output. *Neural Plast.* **2018**, *2018*, 1–9. [CrossRef]
16. Coomans, C.; Ramkisoensing, A.; Meijer, J.H. The suprachiasmatic nuclei as a seasonal clock. *Front. Neuroendocr.* **2015**, *37*, 29–42. [CrossRef]
17. Haus, E. Chronobiology in the endocrine system. *Adv. Drug Deliv. Rev.* **2007**, *59*, 985–1014. [CrossRef]
18. Vitale, J.A.; Briguglio, M.; Galentino, R.; Dell'Osso, B.; Malgaroli, A.; Banfi, G.; Porta, M. Exploring circannual rhythms and chronotype effect in patients with Obsessive-Compulsive Tic Disorder (OCTD): A pilot study. *J. Affect. Disord.* **2020**, *262*, 286–292. [CrossRef]
19. Jin, J.; Yaegashi, T.; Hashizume, T. Effects of photoperiod on the secretion of growth hormone and prolactin during nighttime in female goats. *Anim. Sci. J.* **2013**, *84*, 130–135. [CrossRef]
20. Mariné-Casadó, R.; Coca, C.D.; Del Bas, J.M.; Bladé, C.; Arola, L.; Caimari, A. The exposure to different photoperiods strongly modulates the glucose and lipid metabolisms of normoweight fischer 344 rats. *Front. Physiol.* **2018**, *9*, 416. [CrossRef]
21. Bailey, M.T.; Walton, J.C.; Dowd, S.; Weil, Z.; Nelson, R.J. Photoperiod modulates gut bacteria composition in male Siberian hamsters (Phodopus sungorus). *Brain Behav. Immun.* **2010**, *24*, 577–584. [CrossRef]
22. Davenport, E.; Mizrahi-Man, O.; Michelini, K.; Barreiro, L.; Ober, C.; Gilad, Y. Seasonal variation in human gut microbiome composition. *PLoS ONE* **2014**, *9*, e90731. [CrossRef]
23. Shor, E.K.; Brown, S.P.; Freeman, D.A. A novel role for the pineal gland: Regulating seasonal shifts in the gut microbiota of Siberian hamsters. *J. Pineal Res.* **2020**, *69*, e12696. [CrossRef] [PubMed]
24. Fan, C.; Zhang, L.; Jia, S.; Tang, X.; Fu, H.; Li, W.; Liu, C.; Zhang, H.; Cheng, Q.; Zhang, Y. Seasonal variations in the composition and functional profiles of gut microbiota reflect dietary changes in plateau pikas. *Integr. Zool.* **2022**. [CrossRef] [PubMed]
25. Huang, G.; Wang, L.; Li, J.; Hou, R.; Wang, M.; Wang, Z.; Qu, Q.; Zhou, W.; Nie, Y.; Hu, Y.; et al. Seasonal shift of the gut microbiome synchronizes host peripheral circadian rhythm for physiological adaptation to a low-fat diet in the giant panda. *Cell Rep.* **2022**, *38*, 110203. [CrossRef]
26. Yang, X.; Yao, Y.; Zhang, X.; Zhong, J.; Gao, F.; Zhang, H.; Han, Y.; Weng, Q.; Yuan, Z. Seasonal Changes in the Distinct Taxonomy and Function of the Gut Microbiota in the Wild Ground Squirrel (*Spermophilus dauricus*). *Animals* **2021**, *11*, 2685. [CrossRef]
27. Jiang, F.; Gao, H.; Qin, W.; Song, P.; Wang, H.; Zhang, J.; Liu, D.; Wang, D.; Zhang, T. Marked Seasonal Variation in Structure and Function of Gut Microbiota in Forest and Alpine Musk Deer. *Front. Microbiol.* **2021**, *12*, 2460. [CrossRef] [PubMed]
28. Huang, C.; Liao, W. Seasonal variation in gut microbiota related to diet in *Fejervarya limnocharis*. *Animals* **2021**, *11*, 1393. [CrossRef] [PubMed]
29. Wu, G.; Tang, W.; He, Y.; Hu, J.; Gong, S.; He, Z.; Wei, G.; Lv, L.; Jiang, Y.; Zhou, H.; et al. Light exposure influences the diurnal oscillation of gut microbiota in mice. *Biochem. Biophys. Res. Commun.* **2018**, *501*, 16–23. [CrossRef]
30. Oyola, M.G.; Johnson, R.C.; Bauman, B.M.; Frey, K.G.; Russell, A.L.; Cho-Clark, M.; Buban, K.N.; Bishop-Lilly, K.A.; Merrell, D.S.; Handa, R.J.; et al. Gut microbiota and metabolic marker alteration following dietary isoflavone-photoperiod interaction. *Endocrinol. Diabetes Metab.* **2021**, *4*, e00190. [CrossRef]
31. Ávila-Román, J.; Arreaza-Gil, V.; Cortés-Espinar, A.J.; Soliz-Rueda, J.R.; Mulero, M.; Muguerza, B.; Arola-Arnal, A.; Arola, L.; Torres-Fuentes, C. Impact of gut microbiota on plasma oxylipins profile under healthy and obesogenic conditions. *Clin. Nutr.* **2021**, *40*, 1475–1486. [CrossRef] [PubMed]
32. Dhariwal, A.; Chong, J.; Habib, S.; King, I.L.; Agellon, L.B.; Xia, J. MicrobiomeAnalyst: A web-based tool for comprehensive statistical, visual and meta-analysis of microbiome data. *Nucleic Acids Res.* **2017**, *45*, W180–W188. [CrossRef] [PubMed]
33. Chong, J.; Liu, P.; Zhou, G.; Xia, J. Using MicrobiomeAnalyst for comprehensive statistical, functional, and meta-analysis of microbiome data. *Nat. Protoc.* **2020**, *15*, 799–821. [CrossRef]
34. Voreades, N.; Kozil, A.; Weir, T.L. Diet and the development of the human intestinal microbiome. *Front. Microbiol.* **2014**, *5*, 494. [CrossRef]
35. Gibson, M.K.; Crofts, T.S.; Dantas, G. Antibiotics and the developing infant gut microbiota and resistome. *Curr. Opin. Microbiol.* **2015**, *27*, 51–56. [CrossRef] [PubMed]
36. Coman, V.; Vodnar, D.C. Gut microbiota and old age: Modulating factors and interventions for healthy longevity. *Exp. Gerontol.* **2020**, *141*, 111095. [CrossRef]
37. Kim, Y.S.; Unno, T.; Kim, B.-Y.; Park, M.-S. Sex Differences in Gut Microbiota. *World J. Mens Health* **2020**, *38*, 48–60. [CrossRef]

38. O'Sullivan, O.; Cronin, O.; Clarke, S.F.; Murphy, E.F.; Molloy, M.G.; Shanahan, F.; Cotter, P. Exercise and the microbiota. *Gut Microbes* **2015**, *6*, 131–136. [CrossRef]
39. Rea, K.; Dinan, T.; Cryan, J.F. The microbiome: A key regulator of stress and neuroinflammation. *Neurobiol. Stress* **2016**, *4*, 23–33. [CrossRef]
40. Ren, C.C.; Sylvia, K.E.; Munley, K.M.; Deyoe, J.E.; Henderson, S.G.; Vu, M.P.; Demas, G.E. Photoperiod modulates the gut microbiome and aggressive behavior in Siberian hamsters. *J. Exp. Biol.* **2020**, *223*, jeb212548. [CrossRef]
41. Macedo, I.C.; de Freitas, J.S.; Torres, I.L.D.S. The influence of palatable diets in reward system activation: A mini review. *Adv. Pharmacol. Sci.* **2016**, *2016*, 1–7. [CrossRef] [PubMed]
42. Guirro, M.; Costa, A.; Gual-Grau, A.; Herrero, P.; Torrell, H.; Canela, N.; Arola, L. Effects from diet-induced gut microbiota dysbiosis and obesity can be ameliorated by fecal microbiota transplantation: A multiomics approach. *PLoS ONE* **2019**, *14*, e0218143. [CrossRef] [PubMed]
43. Le Chatelier, E.; Nielsen, T.; Qin, J.; Prifti, E.; Hildebrand, F.; Falony, G.; Almeida, M.; Arumugam, M.; Batto, J.-M.; Kennedy, S.; et al. Richness of human gut microbiome correlates with metabolic markers. *Nature* **2013**, *500*, 541–546. [CrossRef]
44. Zhang, C.; Zhang, M.; Pang, X.; Zhao, Y.; Wang, L.; Zhao, L. Structural resilience of the gut microbiota in adult mice under high-fat dietary perturbations. *ISME J.* **2012**, *6*, 1848–1857. [CrossRef]
45. Gual-Grau, A.; Guirro, M.; Mayneris-Perxachs, J.; Arola, L.; Boqué, N. Impact of different hypercaloric diets on obesity features in rats: A metagenomics and metabolomics integrative approach. *J. Nutr. Biochem.* **2019**, *71*, 122–131. [CrossRef] [PubMed]
46. Devkota, S.; Wang, Y.; Musch, M.W.; Leone, V.; Fehlner-Peach, H.; Nadimpalli, A.; Antonopoulos, D.A.; Jabri, B.; Chang, E.B. Dietary-fat-induced taurocholic acid promotes pathobiont expansion and colitis in Il10-/- mice. *Nature* **2012**, *487*, 104–108. [CrossRef]
47. Magne, F.; Gotteland, M.; Gauthier, L.; Zazueta, A.; Pesoa, S.; Navarrete, P.; Balamurugan, R. The firmicutes/bacteroidetes ratio: A relevant marker of gut dysbiosis in obese patients? *Nutrients* **2020**, *12*, 1474. [CrossRef] [PubMed]
48. Crovesy, L.; Masterson, D.; Rosado, E.L. Profile of the gut microbiota of adults with obesity: A systematic review. *Eur. J. Clin. Nutr.* **2020**, *74*, 1251–1262. [CrossRef]
49. Deaver, J.A.; Eum, S.Y.; Toborek, M. Circadian disruption changes gut microbiome taxa and functional gene composition. *Front. Microbiol.* **2018**, *9*, 737. [CrossRef]
50. Goldman, B.D. Mammalian photoperiodic system: Formal properties and neuroendocrine mechanisms of photoperiodic time measurement. *J. Biol. Rhythm.* **2001**, *16*, 283–301. [CrossRef]
51. Varpe, O.H. Life History Adaptations to Seasonality. In *Integrative and Comparative Biology*; Oxford University Press: Oxford, UK, 2017; Volume 57, pp. 943–960. [CrossRef]
52. Hut, R.A.; Beersma, D.G.M. Evolution of time-keeping mechanisms: Early emergence and adaptation to photoperiod. *Philos. Trans. R. Soc. B Biol. Sci.* **2011**, *366*, 2141–2154. [CrossRef] [PubMed]
53. Jumpertz, R.; Le, D.S.; Turnbaugh, P.J.; Trinidad, C.; Bogardus, C.; Gordon, J.I.; Krakoff, J. Energy-balance studies reveal associations between gut microbes, caloric load, and nutrient absorption in humans. *Am. J. Clin. Nutr.* **2011**, *94*, 58–65. [CrossRef] [PubMed]
54. Bäckhed, F.; Ding, H.; Wang, T.; Hooper, L.V.; Koh, G.Y.; Nagy, A.; Semenkovich, C.F.; Gordon, J.I. The gut microbiota as an environmental factor that regulates fat storage. *Proc. Natl. Acad. Sci. USA* **2004**, *101*, 15718–15723. [CrossRef]
55. Ramakrishna, B. Role of the gut microbiota in human nutrition and metabolism. *J. Gastroenterol. Hepatol.* **2013**, *28*, 9–17. [CrossRef]
56. Samuel, B.S.; Shaito, A.; Motoike, T.; Rey, F.E.; Backhed, F.; Manchester, J.K.; Hammer, R.E.; Williams, S.C.; Crowley, J.; Yanagisawa, M.; et al. Effects of the gut microbiota on host adiposity are modulated by the short-chain fatty-acid binding G protein-coupled receptor, Gpr41. *Proc. Natl. Acad. Sci. USA* **2008**, *105*, 16767–16772. [CrossRef]
57. Ottman, N.; Smidt, H.; De Vos, W.M.; Belzer, C. The function of our microbiota: Who is out there and what do they do? *Front. Cell. Infect. Microbiol.* **2012**, *2*, 104. [CrossRef] [PubMed]
58. Raman, M.; Ahmed, I.; Gillevet, P.M.; Probert, C.S.; Ratcliffe, N.M.; Smith, S.; Greenwood, R.; Sikaroodi, M.; Lam, V.; Crotty, P.; et al. Fecal microbiome and volatile organic compound metabolome in obese humans with nonalcoholic fatty liver disease. *Clin. Gastroenterol. Hepatol.* **2013**, *11*, 868–875.e3. [CrossRef] [PubMed]
59. Zarrinpar, A.; Chaix, A.; Yooseph, S.; Panda, S. Diet and feeding pattern affect the diurnal dynamics of the gut microbiome. *Cell Metab.* **2014**, *20*, 1006–1017. [CrossRef] [PubMed]
60. Gao, Z.; Yin, J.; Zhang, J.; Ward, R.E.; Martin, R.J.; Lefevre, M.; Cefalu, W.T.; Ye, J. Butyrate improves insulin sensitivity and increases energy expenditure in mice. *Diabetes* **2009**, *58*, 1509–1517. [CrossRef]
61. Mariné-Casadó, R.; Domenech-Coca, C.; Del Bas, J.M.; Bladé, C.; Arola, L.; Caimari, A. Intake of an Obesogenic Cafeteria Diet Affects Body Weight, Feeding Behavior, and Glucose and Lipid Metabolism in a Photoperiod-Dependent Manner in F344 Rats. *Front. Physiol.* **2018**, *9*, 1–16. [CrossRef]
62. Shoemaker, M.B.; Heideman, P.D. Reduced body mass, food intake, and testis size in response to short photoperiod in adult F344 rats. *BMC Physiol.* **2002**, *2*, 11. [CrossRef] [PubMed]
63. Tavolaro, F.M.; Thomson, L.M.; Ross, A.; Morgan, P.; Helfer, G. Photoperiodic Effects on Seasonal Physiology, Reproductive Status and Hypothalamic Gene Expression in Young Male F344 Rats. *J. Neuroendocr.* **2015**, *27*, 79–87. [CrossRef] [PubMed]
64. Heideman, P.D.; Sylvester, C.J. Reproductive Photoresponsiveness in Unmanipulated Male Fischer 344 Laboratory Rats1. *Biol. Reprod.* **1997**, *57*, 134–138. [CrossRef] [PubMed]

SUPPLEMENTARY MATERIAL

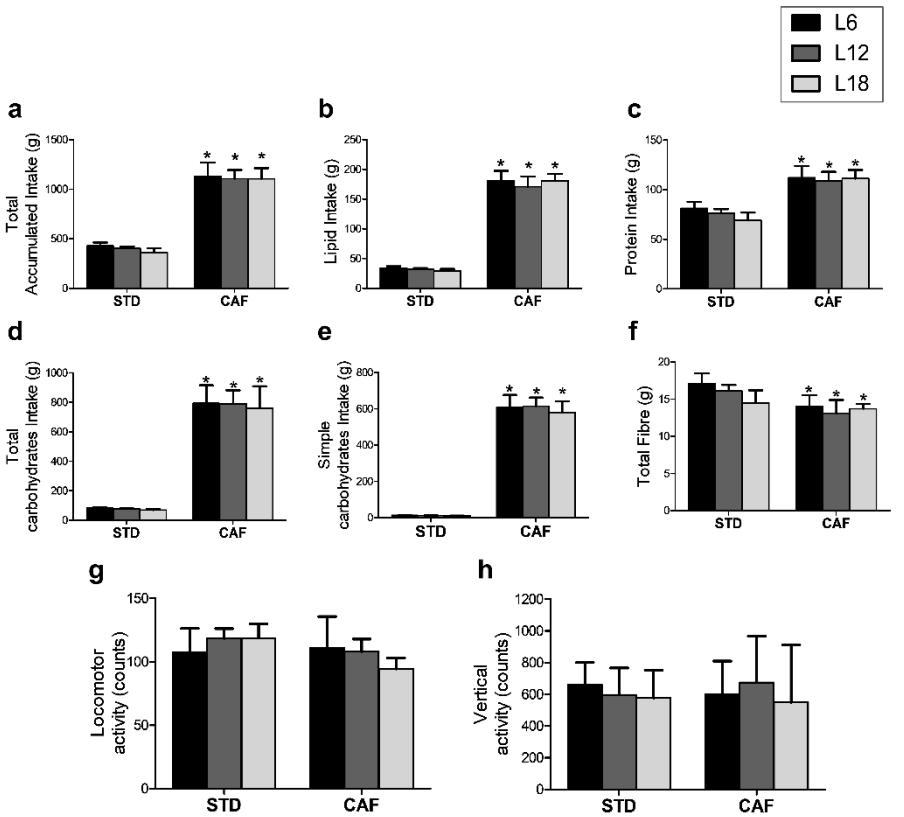

Figure S1. Food intake and Physical activity. *(**a** to **f**): Accumulate food intake (**a**) and total intake derived from each macronutrient within each dietary groups, showing lipid (**b**), protein (**c**), complex carbohydrates (**d**), simple carbohydrates (**e**) and fibre (**f**) consumed by animals during the whole experiment. (g to h): Locomotor and vertical activity. Diet and Photoperiod effects were analysed by 2-way ANOVA followed by LSD post hoc test (p<0.05). * indicates diet effect comparing STD and CAF-fed rats into each photoperiod conditions. Not significant photoperiod effects were found. Data are plotted as the mean ± SD (n=7-8). L6: 6h light/18h darkness; L12: 12h light/12h darkness; L18: 18h light/6h darkness; STD: standard diet; CAF: cafeteria diet.*

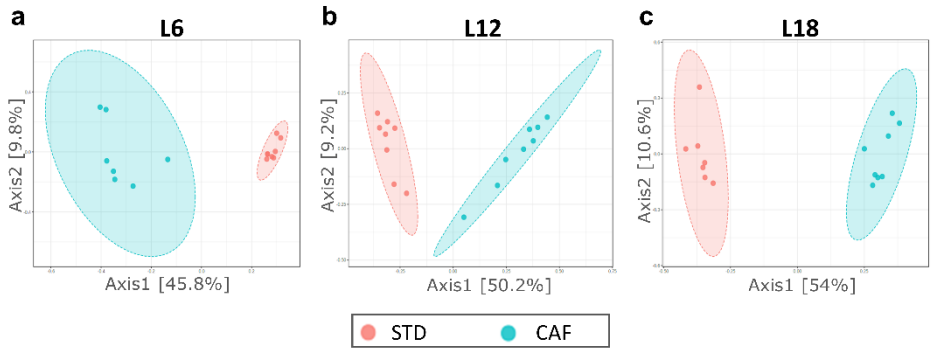

Figure S2. Effect of diet on the β-diversity in STD and CAF groups. *β-diversity based on Bray-Curtis distances and visualized by a principle coordinates analysis (PCoA) 2D plot of Diet effect. (PERMANOVA test, p<0.001). (n=7-8). L6: 6h light/18h darkness; L12: 12h light/12h darkness; L18: 18h light/6h darkness; STD: standard diet; CAF: cafeteria diet.*

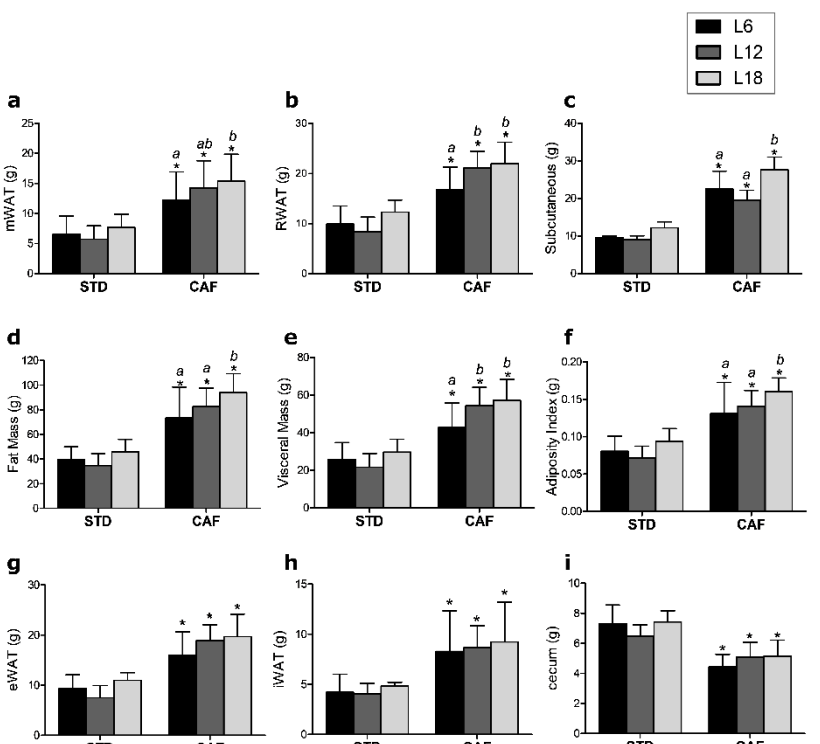

Figure S3. Effects of photoperiod on white adipose tissue depots and cecum weight. *(**a** to **f**): White adipose tissue depots affected by photoperiods: mesenteric white adipose tissue (mWAT), retroperitoneal (RWAT), Subcutaneous, fat mass, visceral mass and adiposity index. (**g** to **i**): White adipose tissue depots and Cecum affected only by diet: epididymal white adipose tissue (eWAT), inguinal white adipose tissue (iWAT) and cecum; Diet and Photoperiod effects were analysed by 2-way ANOVA followed by LSD post hoc test (p<0.05). * and ab indicate diet and photoperiod effect respectively. Data are plotted as the mean±SD (n=7-8). L6: 6h light/18h darkness; L12: 12h light/12h darkness; L18: 18h light/6h darkness; STD: standard diet; CAF: cafeteria diet.*

Table S1. Relative abundance at phylum level of STD- and CAF-fed rats under the three different photoperiods conditions (L6, L12 and L18)

Bacteria at Phylum level	Photoperiod	STD	P-value Ph STD[b]	CAF	P-value Ph CAF[b]	P-value DIET[c]
		Median (Q1-Q3)[a]		Median (Q1-Q3)[a]		
Other	L6	0.002(0.001-0.003)	0.109	0.02(0.0054-0.03)**	0.292	0.008
	L12	8.71e-04(4.83e-04-0.002)		0.01(0.004-0.01)**		0.001
	L18	0.002(0.002-0.006)		0.006(0.005-0.008)*		0.049
Actinobacteria	L6	0.07(0.05-0.13)	0.408	0.08(0.04-0.18)	0.321	1.000
	L12	0.08(0.04-0.36)		0.05(0.05-0.06)		0.294
	L18	0.10(0.07-0.49)		0.06(0.03-0.06)*		0.021
Bacteroidetes	L6	43.71(25.91-50.17)	0.383	52.24(44.61-70.78)*	0.084	0.064
	L12	34.34(26.74-45.67)		53.86(46.92-61.94)**		0.006
	L18	46.78(31.68-56.16)		69.27(54.76-76.93)**		0.005
Cyanobacteria	L6	0.19(0.11-0.23)	0.075	0.51(0.17-0.97)	0.538	0.105
	L12	0.10(0.07-0.17)		0.30(0.23-0.42)**		0.002
	L18	0.18(0.14-0.28)		0.41(0.30-0.57)**		0.004
Firmicutes	L6	53.26(46.50-71.98)	0.383	42.02(23.69-49.75)*	0.072	0.021
	L12	63.49(52.40-71.10)		40.02(32.87-48.83)**		0.003
	L18	50.65(39.90-61.40)		24.51(18.53-37.85)**		0.005
Proteobacteria	L6	1.10(0.69-1.33)	0.553	3.02(2.22-3.71)**	0.418	0.001
	L12	0.96(0.53-1.28)		3.26(1.89-3.98)**		0.002
	L18	1.07(0.86-1.21)		4.23(2.06-5.26)**		0.004
Tenericutes	L6	0.44(0.12-0.69)	0.092	7.66e-04(2.64e-04-0.009)**	0.846	0.001
	L12	0.53(0.30-0.60)		0.001(6.53e-05-0.003)**		0.001
	L18	1.21(0.35-1.66)		7.92e-04(3.27e-04-0.002)**		0.001
Verrucomicrobia	L6	0.54(0.39-0.83)	0.167	1.92(1.23-2.26)*	0.722	0.011
	L12	0.30(0.14-0.47)		1.63(0.71-3.76)**		0.002
	L18	0.54(0.36-0.65)		1.13(0.92-1.83)**		0.002
Ratio Firmicutes to Bacteroidetes	L6	1.22(0.93-2.98)	0.383	0.80(0.33-1.12)*	0.099	0.037
	L12	1.90(1.16-2.66)		0.75(0.52-1.04)**		0.006
	L18	1.08(0.71-1.94)		0.35(0.24-0.70)**		0.005

*[a]Data shown as median (first and third quartile) in percentage of relative abundance (n=7-8); [b]P-value by Kruskal-Wallis test comparing photoperiods in STD- or in CAF-fed rats. No photoperiod effect was found at phylum level (P>0.05); [c]P-value by U-Mann Whitney to evaluate diet effect: * indicates diet effect when comparing STD and CAF-fed rats by U-Mann Whitney test into each photoperiod. *P<0.05; **P<0.01; L6: 6h light/18h darkness; L12: 12h light/12h darkness; L18: 18h light/6h darkness; STD: standard diet; CAF: cafeteria diet.*

RESULTS

Table S2 Significant Photoperiod and Diet effect at Genus level

Bacteria at Genus level	Photoperiod	STD	P-value	CAF	P-value	P-value
		Median (Q1-Q3)[a]	Ph STD[b]	Median (Q1-Q3)[a]	Ph CAF[b]	DIET[c]
Oscillospira	L6	9.94(7.81-12.9)	0.674	3.80(2.86-4.95)**a	0.015	0.001
	L12	10.7(7.89-11.6)		2.65(2.00-3.42)**ab		0.001
	L18	8.52(6.23-11.9)		2.03(1.77-2.63)**b		0.001
Bacteroides	L6	2.06(0.96-2.87)	0.856	5.77(3.97-12.4)***a*	0.004	0.001
	L12	1.45(0.87-2.60)		4.37(2.77-4.82)***a*		0.006
	L18	2.11(0.79-2.70)		10.1(8.22-15.9)***b*		0.001
Ruminococcus	L6	1.33(1.20-2.11)	0.820	0.47(0.17-0.98)**a*	0.014	0.015
	L12	1.60(1.33-1.97)		0.38(0.18-0.56)***a*		0.001
	L18	1.62(1.01-2.04)		0.14(0.10-0.17)***b*		0.001
Coprococcus	L6	0.82(0.46-1.04)	0.807	1.17(0.57-3.53)*a*	0.040	0.247
	L12	0.74(0.67-0.85)		3.06(1.91-4.57)***ab*		0.001
	L18	0.57(0.51-0.97)		4.12(2.23-5.57)***b*		0.001
Lactobacillus	L6	1.10(0.41-1.91)	0.642	0.69(0.53-1.53)*a*	0.025	0.908
	L12	1.39(0.59-2.72)		2.38(1.19-3.94)*b*		0.345
	L18	1.40(1.01-2.43)		0.64(0.17-2.16)*a*		0.298
Akkermansia	L6	0.54(0.39-0.86)	0.167	1.92(1.23-2.26)*	0.722	0.011
	L12	0.30(0.14-0.47)		1.63(0.71-3.76)**		0.002
	L18	0.54(0.36-0.65)		1.13(0.92-1.83)**		0.002
Parabacteroides	L6	0.63(0.26-0.79)	0.875	12.45(12.01-17.97)**	0.774	0.001
	L12	0.43(0.23-0.74)		16.87(5.55-19.77)**		0.002
	L18	0.47(0.32-0.87)		16.29(11.20-23.30)**		0.001
SMB53	L6	0.12(0.01-0.31)	0.940	7.99e-04(0-2.36e-03)**	0.625	0.004
	L12	0.09(0.06-0.17)		3.34e-04(5.31e-05-1.01e-03)**		0.001
	L18	0.07(0-0.42)		2.45e-04(5.91e-05-7.09e-04)**		0.001
Anaeroplasma	L6	0.09(0.03-0.29)	0.964	2.64e-04(0-5.11e-04)**	0.151	0.005
	L12	0.16(0.01-0.41)		1.21e-04(0-7.75e-04)**		0.003
	L18	0.04(0-1.13)		5.75e-04(3.17e-04-1.70e-03)*		0.024
Blautia	L6	0.08(0.07-0.13)	0.215	8.68(5.19-17.1)**	0.610	0.001
	L12	0.13(0.09-0.19)		8.00(6.86-10.2)**		0.001
	L18	0.19(0.09-0.20)		7.48(3.27-11.6)**		0.001
Lactococcus	L6	0.12(0.05-0.16)	0.431	4.64e-03(1.24e-03-7.91e-03)**	0.483	0.001
	L12	0.06(0.04-0.11)		6.39e-03(2.39e-03-1.78e-02)**		0.002
	L18	0.09(0.07-0.30)		1.27e-02(2.96e-03-2.74e-02)**		0.001

	L6	0.02(0-0.09)		4.42e-03(5.27e-04-5.25e-02)		0.728
Bifidobacterium	L12	0.04(0.01-0.30)	0.543	2.87e-03(1.18e-03-6.38e-03)*	0.528	0.021
	L18	0.06(0.01-0.43)		1.59e-03(5.97e-04-1.00e-02)**		0.005
	L6	0.06(0.04-0.08)		5.90e-04(0-2.51e-02)**		0.005
Anaerostipes	L12	0.09(0.05-0.12)	0.343	6.58e-04(5.68e-05-4.10e-02)*	0.589	0.021
	L18	0.11(0.06-0.16)		3.43e-04(0-7.47e-04)**		0.001
	L6	0.05(0.03-0.07)		0.27(5.96e-02-0.46)*		0.021
Dehalobacterium	L12	0.07(0.05-0.09)	0.774	0.13(1.48e-02-0.20)	0.162	0.401
	L18	0.06(0.03-0.08)		9.50e-02(1.58e-03-0.15)		0.643
	L6	0.06(0.05-0.07)		0.12(3.32e-02-0.17)		0.355
Dorea	L12	0.06(0.05-0.10)	0.589	0.19(0.11-0.39)*	0.270	0.027
	L18	0.07(0.06-0.08)		0.28(0.10-0.39)*		0.021
	L6	0.06(0.03-0.08)		1.05(0.89-1.59)**		0.001
Sutterella	L12	0.04(0.02-0.13)	0.190	1.10(0.74-2.39)**	0.976	0.001
	L18	0.09(0.05-0.15)		1.24(0.50-2.55)**		0.001
	L6	0.04(0.01-0.06)		0.30(0.02-0.84)*		0.049
Roseburia	L12	0.08(0.03-0.10)	0.278	0.12(0.06-0.24)	0.475	0.141
	L18	0.06(0.03-0.11)		0.21(0.07-0.27)		0.083
	L6	0.01(0.01-0.03)		5.60e-03(1.53e-03-1.50e-02)		0.083
Clostridium	L12	0.01(0.01-0.03)	0.564	2.14e-03(4.80e-04-8.64e-03)*	0.059	0.012
	L18	0.01(0.01-0.02)		8.93e-04(2.43e-04-1.53e-03)**		0.001
	L6	0.01(0-0.04)*a*		1.02e-03(2.64e-04-6.29e-03)*		0.015
Lachnospira	L12	0.01(0.01-0.02)*a*	0.002	4.43e-03(1.47e-03-8.48e-03)	0.344	0.115
	L18	1.10e-03(7.80e-04-2.03e-03)*b*		3.81e-03(1.36e-03-6.98e-03)*		0.037
	L6	7.85e-03(4.31e-03-1.04e-02)		3.20e-03(7.66e-04-8.28e-03)		0.064
Bilophila	L12	6.50e-03(2.53e-03-1.04e-02)	0.653	1.29e-03(2.21e-04-2.77e-03)*	0.201	0.015
	L18	4.62e-03(3.05e-03-9.62e-03)		9.70e-04(2.41e-04-2.04e-03)**		0.003
	L6	5.49e-03(3.43e-03-1.19e-02)*ab*		1.02e-02(5.80e-03-1.66e-02)		0.298
Streptococcus	L12	3.00e-03(1.36e-03-5.00e-03)*a*	0.010	1.00e-02(7.10e-03-1.29e-02)**	0.834	0.003
	L18	1.30e-02(7.51e-03-1.74e-02)*b*		1.03e-02(5.91e-03-1.46e-02)		0.298
	L6	3.59e-03(1.99e-03-6.70e-03)*a*		8.28e-04(6.00e-04-1.32e-03)**		0.008
Moryella	L12	9.51e-03(7.90e-03-1.27e-02)*ab*	0.033	1.01e-03(9.23e-04-1.11e-03)**	0.092	0.001
	L18	8.04e-03(4.19e-03-1.20e-02)*b*		1.89e-03(1.19e-03-2.08e-03)**		0.001
	L6	3.91e-03(8.89e-04-4.87e-03)*ab*		6.21e-03(3.40e-03-1.33e-02)		0.132
Aggregatibacter	L12	1.81e-03(5.51e-05-2.97e-03)*a*	0.034	5.00e-03(1.89e-03-1.09e-02)	0.739	0.074
	L18	7.39e-03(3.90e-03-2.16e-02)*b*		1.25e-02(2.96e-03-2.02e-02)		0.643

	L6	2.40e-03(1.40e-03-2.99e-03)*a*		1.28e-02(5.00e-03-8.49e-02)**		0.005
Anaerotruncus	L12	2.62e-03(1.69e-03-4.13e-03)*a*	0.006	3.68e-02(1.82e-02-6.35e-02)**	0.431	0.003
	L18	1.41e-02(1.12e-02-3.99e-02)*b*		1.98e-02(1.32e-02-4.27e-02)		0.643
	L6	8.24e-04(2.79e-04-4.74e-03)		8.86e-02(7.66e-04-0.18)*a*		0.064
Allobaculum	L12	6.53e-04(2.00e-04-3.45e-03)	0.492	3.16e-03(5.99e-04-6.75e-02)*ab*	0.044	0.093
	L18	5.78e-04(0-1.61e-03)		4.53e-04(2.39e-04-1.70e-03)*b*		0.816
	L6	1.89e-03(6.90e-04-3.64e-03)*ab*		6.63e-04(4.49e-04-8.28e-04)*a*		0.132
Epulopiscium	L12	2.29e-03(1.04e-03-4.44e-03)*a*	0.021	2.60e-03(1.22e-03-4.22e-03)*b*	0.027	0.916
	L18	2.20e-04(0-7.62e-04)*b*		7.85e-04(5.32e-05-1.66e-03)*ab*		0.346
	L6	1.18e-03(9.56e-04-2.46e-03)		1.24e-03(4.49e-04-1.47e-03)		0.954
Rothia	L12	8.92e-04(2.81e-04-2.18e-03)	0.156	8.67e-04(5.15e-04-1.24e-03)	0.050	0.916
	L18	2.87e-03(1.16e-03-4.26e-03)		3.72e-04(6.33e-05-6.66e-04)**		0.001
	L6	2.11e-04(4.48e-05-1.24e-03)*a*		9.99e-04(2.64e-04-1.53e-03)**a*		0.034
Enterobacter	L12	2.10e-04(0-4.30e-04)*a*	0.037	7.51e-04(2.47e-04-4.37e-03)**a*	0.009	0.035
	L18	3.21e-03(2.89e-04-7.06e-03)*b*		5.85e-03(3.36e-03-9.10e-03)*b*		0.105
	L6	5.37e-04(2.06e-04-9.26e-04)*a*		1.53e-03(4.49e-04-7.66e-03)		0.165
Shuttleworthia	L12	6.36e-04(2.26e-04-1.74e-03)*a*	0.008	1.22e-03(5.83e-04-2.21e-03)	0.875	0.270
	L18	0(0-0)*b*		1.30e-03(2.41e-04-5.48e-03)**		0.004
	L6	7.18e-04(4.17e-04-9.33e-04)*a*		1.39e-02(4.74e-03-2.04e-02)*		0.011
Xenorhabdus	L12	6.30e-04(4.47e-04-1.85e-03)*a*	0.018	1.32e-02(1.34e-03-0.15)*	0.884	0.012
	L18	1.75e-03(1.16e-03-5.15e-03)*b*		1.32e-02(3.54e-03-4.84e-02)		0.064
	L6	4.72e-04(2.73e-04-1.25e-03)*a*		4.00e-04(0-5.11e-04)		0.267
Comamonas	L12	0(0-0)*b*	0.009	0(0-0)	0.112	0.927
	L18	4.48e-04(2.54e-04-1.75e-03)*a*		2.16e-04(0-7.24e-04)		0.239
	L6	2.99e-04(2.05e-04-6.84e-04)		8.25e-03(0-1.38e-02)		0.245
Escherichia	L12	3.84e-04(5.09e-05-4.58e-04)	0.382	4.61e-03(5.74e-04-6.38e-02)*	0.328	0.012
	L18	8.75e-04(2.54e-04-2.69e-03)		1.24e-02(1.56e-03-3.15e-02)*		0.028
	L6	8.96e-05(0-8.23e-04)		1.02e-03(8.28e-04-1.66e-03)*		0.045
Anaerofustis	L12	3.01e-04(3.87e-05-4.32e-04)	0.955	1.66e-03(9.29e-04-2.66e-03)**	0.219	0.003
	L18	2.89e-04(0-7.62e-04)		8.84e-04(3.45e-04-1.47e-03)		0.063
	L6	8.96e-05(0-2.20e-04)		5.27e-04(3.32e-04-8.84e-04)**		0.007
Butyrivibrio	L12	2.04e-04(0-3.55e-04)	0.205	5.94e-04(2.95e-04-1.80e-03)*	0.761	0.030
	L18	0(0-0)		1.03e-03(3.20e-04-1.50e-03)**		0.005
	L6	0(0-1.89e-04)*a*		4.49e-04(2.64e-04-1.79e-03)**		0.005
Klebsiella	L12	1.77e-04(0-2.16e-04)*b*	0.013	1.26e-03(0-1.14e-02)	0.751	0.178
	L18	5.20e-04(2.20e-04-8.75e-04)*ab*		1.23e-03(4.87e-04-3.82e-03)		0.247

	L6	0(0-2.24e-05)a		2.64e-04(0-1.33e-03)*		0.046
Morganella	L12	9.94e-05(0-3.82e-04)b	0.024	0(0-6.63e-04)	0.340	0.469
	L18	2.60e-04(2.20e-04-4.48e-04)ab		2.50e-04(5.41e-05-1.19e-03)		1.000

[a]Data shown as median (first and third quartile) in percentage of relative abundance (n=7-8).

[b]P-value by Kruskal-Wallis test comparing photoperiods in STD- or in CAF-fed rats. ab letters indicate Photoperiod effect analyzed by Kruskal-Wallis test followed by Bonferroni p-values adjustment: p<0.016.

*[c]P-value by U-Mann Whitney to evaluate diet effect. * indicates diet effect when comparing STD- and CAF-fed rats into each photoperiod by U-Mann Whitney test: *P<0.05. **P<0.01.*

L6: 6h light/18h darkness; L12: 12h light/12h darkness; L18: 18h light/6h darkness; STD: standard diet; CAF: cafeteria diet.

Table S3. Significant Spearman's correlations between Body weight gain and fat parameters with the relative abundance bacteria at different taxonomic levels.

Body weight gain and Fat parameters (g)	Bacteria	rho[a]	P-value[b]	FDR[b]
	PHYLUM			
Fat mass	Proteobacteria	0.743	3.25E-09	0.001
RWAT	Proteobacteria	0.740	4.16E-09	0.002
Visceral fat	Proteobacteria	0.734	6.55E-09	0.002
Adiposity Index	Proteobacteria	0.731	8.14E-09	0.003
Gain weight	Proteobacteria	0.723	1.38E-08	0.004
iWAT	Proteobacteria	0.719	1.76E-08	0.005
eWAT	Proteobacteria	0.700	6.06E-08	0.006
Fat mass	Tenericutes	-0.697	7.45E-08	0.006
mWAT	Proteobacteria	0.689	1.21E-07	0.007
iWAT	Tenericutes	-0.677	2.34E-07	0.008
Adiposity Index	Tenericutes	-0.676	2.60E-07	0.009
Visceral fat	Tenericutes	-0.672	3.16E-07	0.010
RWAT	Tenericutes	-0.663	5.13E-07	0.010
eWAT	Tenericutes	-0.663	5.19E-07	0.011
iWAT	Cyanobacteria	0.648	1.10E-06	0.012
Gain weight	Tenericutes	-0.643	1.45E-06	0.013
eWAT	Verrucomicrobia	0.629	2.85E-06	0.013
Subcutaneous	Proteobacteria	0.621	4.11E-06	0.014
mWAT	Tenericutes	-0.609	7.21E-06	0.015
iWAT	Verrucomicrobia	0.607	7.60E-06	0.016
Fat mass	Cyanobacteria	0.591	1.52E-05	0.017
Visceral fat	Verrucomicrobia	0.586	1.90E-05	0.017
Fat mass	Verrucomicrobia	0.585	1.94E-05	0.018
eWAT	Cyanobacteria	0.579	2.46E-05	0.019
eWAT	Firmicutes	-0.572	3.22E-05	0.020
mWAT	Cyanobacteria	0.570	3.52E-05	0.021
Adiposity Index	Verrucomicrobia	0.567	4.03E-05	0.021
Adiposity Index	Cyanobacteria	0.564	4.45E-05	0.022
RWAT	Cyanobacteria	0.564	4.48E-05	0.023
RWAT	Verrucomicrobia	0.562	4.82E-05	0.024
mWAT	Verrucomicrobia	0.559	5.49E-05	0.025
Visceral fat	Cyanobacteria	0.558	5.51E-05	0.025
Gain weight	Firmicutes	-0.550	7.53E-05	0.026
Gain weight	Cyanobacteria	0.547	8.39E-05	0.027
Subcutaneous	Tenericutes	-0.542	9.92E-05	0.028
eWAT	Bacteroidetes	0.528	1.64E-04	0.029
Subcutaneous	Cyanobacteria	0.521	2.04E-04	0.029
Fat mass	Firmicutes	-0.519	2.18E-04	0.030
Visceral fat	Firmicutes	-0.514	2.55E-04	0.031
RWAT	Firmicutes	-0.509	3.05E-04	0.032
Gain weight	Bacteroidetes	0.504	3.55E-04	0.033
Adiposity Index	Firmicutes	-0.500	4.00E-04	0.033
Gain weight	Verrucomicrobia	0.477	8.11E-04	0.034
Visceral fat	Bacteroidetes	0.469	1.00E-03	0.035
Fat mass	Bacteroidetes	0.465	1.12E-03	0.036
Subcutaneous	Firmicutes	-0.457	1.42E-03	0.037
RWAT	Bacteroidetes	0.450	1.72E-03	0.037
Adiposity Index	Bacteroidetes	0.448	1.81E-03	0.038

Subcutaneous	Verrucomicrobia	0.445	1.95E-03	0.039
iWAT	Firmicutes	-0.443	2.06E-03	0.040
mWAT	Firmicutes	-0.438	2.31E-03	0.040
Subcutaneous	Bacteroidetes	0.406	5.15E-03	0.041
mWAT	Bacteroidetes	0.388	7.63E-03	0.042
iWAT	Bacteroidetes	0.364	1.28E-02	0.043
Visceral fat	Actinobacteria	-0.312	3.45E-02	0.044
eWAT	Actinobacteria	-0.311	3.57E-02	0.044
Fat mass	Actinobacteria	-0.302	4.11E-02	0.045
Adiposity Index	Actinobacteria	-0.284	5.57E-02	0.046
mWAT	Actinobacteria	-0.222	1.39E-01	0.047
RWAT	Actinobacteria	-0.221	1.40E-01	0.048
iWAT	Actinobacteria	-0.220	1.42E-01	0.048
Gain weight	Actinobacteria	-0.210	1.61E-01	0.049
Subcutaneous	Actinobacteria	-0.167	2.67E-01	0.050
	CLASS			
Fat mass	Betaproteobacteria	0.774	2.93E-10	0.000
Adiposity Index	Betaproteobacteria	0.769	4.37E-10	0.001
Gain weight	Betaproteobacteria	0.762	7.54E-10	0.001
RWAT	Betaproteobacteria	0.759	9.72E-10	0.002
Visceral fat	Betaproteobacteria	0.753	1.58E-09	0.002
eWAT	Betaproteobacteria	0.744	3.02E-09	0.003
iWAT	Betaproteobacteria	0.740	4.28E-09	0.003
eWAT	Erysipelotrichi	0.737	5.30E-09	0.003
Gain weight	Erysipelotrichi	0.734	6.50E-09	0.004
mWAT	Betaproteobacteria	0.725	1.21E-08	0.004
Visceral fat	Erysipelotrichi	0.716	2.16E-08	0.005
Fat mass	Erysipelotrichi	0.712	2.82E-08	0.005
RWAT	Erysipelotrichi	0.704	4.67E-08	0.006
Subcutaneous	Betaproteobacteria	0.699	6.54E-08	0.006
Adiposity Index	Erysipelotrichi	0.697	7.32E-08	0.006
iWAT	Erysipelotrichi	0.692	9.89E-08	0.007
Fat mass	Mollicutes	-0.688	1.28E-07	0.007
Visceral fat	Mollicutes	-0.673	2.95E-07	0.008
eWAT	Mollicutes	-0.670	3.60E-07	0.008
mWAT	Erysipelotrichi	0.669	3.70E-07	0.009
Adiposity Index	Mollicutes	-0.669	3.81E-07	0.009
RWAT	Mollicutes	-0.666	4.45E-07	0.009
iWAT	Mollicutes	-0.655	7.86E-07	0.010
iWAT	4C0d_2	0.650	9.92E-07	0.010
Gain weight	Mollicutes	-0.629	2.83E-06	0.011
eWAT	Verrucomicrobiae	0.629	2.85E-06	0.011
iWAT	Verrucomicrobiae	0.607	7.60E-06	0.012
eWAT	Clostridia	-0.604	8.88E-06	0.012
mWAT	Mollicutes	-0.604	8.89E-06	0.012
Gain weight	Clostridia	-0.594	1.33E-05	0.013
Fat mass	4C0d_2	0.591	1.51E-05	0.013
Subcutaneous	Erysipelotrichi	0.590	1.60E-05	0.014
Visceral fat	Verrucomicrobiae	0.586	1.90E-05	0.014
Fat mass	Verrucomicrobiae	0.585	1.94E-05	0.015
eWAT	4C0d_2	0.581	2.35E-05	0.015

mWAT	4C0d_2	0.570	3.57E-05	0.015
Adiposity Index	Verrucomicrobiae	0.567	4.03E-05	0.016
RWAT	4C0d_2	0.565	4.36E-05	0.016
Adiposity Index	4C0d_2	0.564	4.51E-05	0.017
RWAT	Verrucomicrobiae	0.562	4.82E-05	0.017
Visceral fat	4C0d_2	0.559	5.41E-05	0.018
mWAT	Verrucomicrobiae	0.559	5.49E-05	0.018
Fat mass	Clostridia	-0.555	6.18E-05	0.018
Visceral fat	Clostridia	-0.553	6.61E-05	0.019
Gain weight	4C0d_2	0.548	7.99E-05	0.019
Subcutaneous	Mollicutes	-0.542	9.88E-05	0.020
RWAT	Clostridia	-0.538	1.17E-04	0.020
Adiposity Index	Clostridia	-0.535	1.29E-04	0.021
eWAT	Bacteroidia	0.528	1.64E-04	0.021
Fat mass	Actinobacteria	-0.524	1.86E-04	0.021
Subcutaneous	4C0d_2	0.520	2.13E-04	0.022
eWAT	Actinobacteria	-0.518	2.27E-04	0.022
Visceral fat	Actinobacteria	-0.509	3.03E-04	0.023
Gain weight	Bacteroidia	0.504	3.55E-04	0.023
Adiposity Index	Actinobacteria	-0.501	3.88E-04	0.024
Subcutaneous	Clostridia	-0.489	5.62E-04	0.024
mWAT	Clostridia	-0.482	6.90E-04	0.024
iWAT	Clostridia	-0.481	7.10E-04	0.025
Gain weight	Verrucomicrobiae	0.477	8.11E-04	0.025
Visceral fat	Bacteroidia	0.469	1.00E-03	0.026
Fat mass	Bacteroidia	0.465	1.12E-03	0.026
RWAT	Bacteroidia	0.450	1.72E-03	0.026
Adiposity Index	Bacteroidia	0.448	1.81E-03	0.027
Subcutaneous	Verrucomicrobiae	0.445	1.95E-03	0.027
iWAT	Deltaproteobacteria	0.438	2.33E-03	0.028
RWAT	Actinobacteria	-0.428	2.98E-03	0.028
iWAT	Actinobacteria	-0.425	3.21E-03	0.029
Gain weight	Actinobacteria	-0.419	3.79E-03	0.029
mWAT	Actinobacteria	-0.407	5.05E-03	0.029
Subcutaneous	Bacteroidia	0.406	5.15E-03	0.030
Subcutaneous	Actinobacteria	-0.405	5.22E-03	0.030
mWAT	Bacteroidia	0.388	7.63E-03	0.031
iWAT	Bacteroidia	0.364	1.28E-02	0.031
Visceral fat	Gammaproteobacteria	0.352	1.63E-02	0.032
eWAT	Alphaproteobacteria	0.350	1.70E-02	0.032
Subcutaneous	Alphaproteobacteria	0.341	2.02E-02	0.032
RWAT	Alphaproteobacteria	0.334	2.33E-02	0.033
RWAT	Deltaproteobacteria	0.321	2.94E-02	0.033
mWAT	Gammaproteobacteria	0.318	3.12E-02	0.034
	ORDER			
Fat mass	Burkholderiales	0.773	3.00E-10	3.70E-04
Adiposity Index	Burkholderiales	0.768	4.51E-10	0.001
Gain weight	Burkholderiales	0.764	6.68E-10	0.001
RWAT	Burkholderiales	0.760	9.25E-10	0.001
Visceral fat	Burkholderiales	0.753	1.55E-09	0.002

eWAT	Burkholderiales	0.745	2.99E-09	0.002
iWAT	Burkholderiales	0.737	5.08E-09	0.003
eWAT	Erysipelotrichales	0.737	5.30E-09	0.003
Gain weight	Erysipelotrichales	0.734	6.50E-09	0.003
mWAT	Burkholderiales	0.725	1.20E-08	0.004
Visceral fat	Erysipelotrichales	0.716	2.16E-08	0.004
Fat mass	Erysipelotrichales	0.712	2.82E-08	0.004
RWAT	Erysipelotrichales	0.704	4.67E-08	0.005
Subcutaneous	Burkholderiales	0.698	7.10E-08	0.005
Adiposity Index	Erysipelotrichales	0.697	7.32E-08	0.006
iWAT	Erysipelotrichales	0.692	9.89E-08	0.006
RWAT	Turicibacterales	-0.685	1.48E-07	0.006
eWAT	Pseudomonadales	0.679	2.19E-07	0.007
eWAT	Turicibacterales	-0.674	2.89E-07	0.007
mWAT	Erysipelotrichales	0.669	3.70E-07	0.007
Visceral fat	Turicibacterales	-0.668	3.90E-07	0.008
Fat mass	Turicibacterales	-0.668	3.96E-07	0.008
mWAT	Turicibacterales	-0.657	7.02E-07	0.009
Adiposity Index	Turicibacterales	-0.652	9.38E-07	0.009
iWAT	YS2	0.650	9.92E-07	0.009
Visceral fat	Pseudomonadales	0.644	1.39E-06	0.010
eWAT	Verrucomicrobiales	0.629	2.85E-06	0.010
Fat mass	Pseudomonadales	0.618	4.66E-06	0.010
iWAT	Turicibacterales	-0.615	5.51E-06	0.011
iWAT	Verrucomicrobiales	0.607	7.60E-06	0.011
eWAT	Clostridiales	-0.604	8.88E-06	0.011
Gain weight	Turicibacterales	-0.597	1.21E-05	0.012
Adiposity Index	Pseudomonadales	0.596	1.25E-05	0.012
Gain weight	Clostridiales	-0.594	1.33E-05	0.013
Fat mass	YS2	0.591	1.51E-05	0.013
Subcutaneous	Erysipelotrichales	0.590	1.60E-05	0.013
Visceral fat	Verrucomicrobiales	0.586	1.90E-05	0.014
Fat mass	Verrucomicrobiales	0.585	1.94E-05	0.014
eWAT	YS2	0.581	2.35E-05	0.014
RWAT	Anaeroplasmatales	-0.579	2.50E-05	0.015
RWAT	Pseudomonadales	0.575	2.96E-05	0.015
mWAT	YS2	0.570	3.57E-05	0.016
Adiposity Index	Verrucomicrobiales	0.567	4.03E-05	0.016
RWAT	YS2	0.565	4.36E-05	0.016
mWAT	Pseudomonadales	0.564	4.50E-05	0.017
Adiposity Index	YS2	0.564	4.51E-05	0.017
Gain weight	Pseudomonadales	0.563	4.66E-05	0.017
RWAT	Verrucomicrobiales	0.562	4.82E-05	0.018
Visceral fat	YS2	0.559	5.41E-05	0.018
mWAT	Verrucomicrobiales	0.559	5.49E-05	0.019
Fat mass	Clostridiales	-0.555	6.18E-05	0.019
Visceral fat	Clostridiales	-0.553	6.61E-05	0.019
Gain weight	YS2	0.548	7.99E-05	0.020
RWAT	Clostridiales	-0.538	1.17E-04	0.020
Adiposity Index	Clostridiales	-0.535	1.29E-04	0.020

mWAT	Anaeroplasmatales	-0.530	1.53E-04	0.021
iWAT	Anaeroplasmatales	-0.529	1.57E-04	0.021
eWAT	Bacteroidales	0.528	1.64E-04	0.021
iWAT	Pseudomonadales	0.526	1.76E-04	0.022
Subcutaneous	YS2	0.520	2.13E-04	0.022
Fat mass	Anaeroplasmatales	-0.519	2.22E-04	0.023
Visceral fat	Anaeroplasmatales	-0.513	2.64E-04	0.023
Adiposity Index	Anaeroplasmatales	-0.510	2.97E-04	0.023
Gain weight	Bacteroidales	0.504	3.55E-04	0.024
Subcutaneous	Pseudomonadales	0.502	3.78E-04	0.024
eWAT	Anaeroplasmatales	-0.499	4.17E-04	0.024
Subcutaneous	Clostridiales	-0.489	5.62E-04	0.025
Subcutaneous	Turicibacterales	-0.486	6.12E-04	0.025
mWAT	Clostridiales	-0.482	6.90E-04	0.026
iWAT	Clostridiales	-0.481	7.10E-04	0.026
Gain weight	Verrucomicrobiales	0.477	8.11E-04	0.026
eWAT	Bifidobacteriales	-0.475	8.44E-04	0.027
Fat mass	Bifidobacteriales	-0.471	9.55E-04	0.027
Visceral fat	Bacteroidales	0.469	1.00E-03	0.027
Gain weight	Anaeroplasmatales	-0.466	1.10E-03	0.028
Fat mass	Bacteroidales	0.465	1.12E-03	0.028
Visceral fat	Bifidobacteriales	-0.455	1.51E-03	0.029
RWAT	Bacteroidales	0.450	1.72E-03	0.029
Adiposity Index	Bacteroidales	0.448	1.81E-03	0.029
Adiposity Index	Bifidobacteriales	-0.445	1.92E-03	0.030
Subcutaneous	Verrucomicrobiales	0.445	1.95E-03	0.030
Fat mass	Actinomycetales	-0.424	3.31E-03	0.030
Subcutaneous	Bacteroidales	0.406	5.15E-03	0.031
Visceral fat	Actinomycetales	-0.399	6.04E-03	0.031
RWAT	Actinomycetales	-0.397	6.37E-03	0.031
Adiposity Index	Actinomycetales	-0.393	6.84E-03	0.032
iWAT	Bifidobacteriales	-0.389	7.58E-03	0.032
mWAT	Bacteroidales	0.388	7.63E-03	0.033
Gain weight	Bifidobacteriales	-0.388	7.63E-03	0.033
RWAT	Bifidobacteriales	-0.375	1.03E-02	0.033
iWAT	Bacteroidales	0.364	1.28E-02	0.034
mWAT	Bifidobacteriales	-0.363	1.33E-02	0.034
Subcutaneous	Actinomycetales	-0.356	1.51E-02	0.034
Subcutaneous	Anaeroplasmatales	-0.355	1.54E-02	0.035
Subcutaneous	Bifidobacteriales	-0.355	1.55E-02	0.035
eWAT	Actinomycetales	-0.347	1.81E-02	0.036
mWAT	Actinomycetales	-0.345	1.89E-02	0.036
iWAT	Actinomycetales	-0.335	2.28E-02	0.036
Subcutaneous	Pasteurellales	0.321	2.95E-02	0.037
Visceral fat	Rhizobiales	-0.315	3.30E-02	0.037
	FAMILY			
jjFat mass	Clostridiaceae	-0.807	1.28E-11	3.27E-04
Adiposity Index	Clostridiaceae	-0.791	5.93E-11	0.001
Visceral fat	Clostridiaceae	-0.786	9.38E-11	0.001
eWAT	Clostridiaceae	-0.786	9.82E-11	0.001

RWAT	Clostridiaceae	-0.755	1.38E-09	0.002
eWAT	Erysipelotrichaceae	0.737	5.30E-09	0.002
Fat mass	Ruminococcaceae	-0.735	6.05E-09	0.002
Gain weight	Erysipelotrichaceae	0.734	6.50E-09	0.003
Visceral fat	Ruminococcaceae	-0.726	1.16E-08	0.003
Adiposity Index	Ruminococcaceae	-0.725	1.18E-08	0.003
Gain weight	Lachnospiraceae	0.723	1.41E-08	0.004
Gain weight	Clostridiaceae	-0.722	1.45E-08	0.004
mWAT	Clostridiaceae	-0.721	1.62E-08	0.004
Visceral fat	Erysipelotrichaceae	0.716	2.16E-08	0.005
Fat mass	Erysipelotrichaceae	0.712	2.82E-08	0.005
Gain weight	Ruminococcaceae	-0.711	3.01E-08	0.005
iWAT	Ruminococcaceae	-0.711	3.08E-08	0.006
iWAT	Lachnospiraceae	0.711	3.13E-08	0.006
Visceral fat	Lachnospiraceae	0.709	3.60E-08	0.006
mWAT	Lachnospiraceae	0.709	3.61E-08	0.007
Fat mass	Lachnospiraceae	0.707	3.93E-08	0.007
RWAT	Ruminococcaceae	-0.706	4.11E-08	0.007
RWAT	Erysipelotrichaceae	0.704	4.67E-08	0.008
Visceral fat	Porphyromonadaceae	0.703	5.24E-08	0.008
RWAT	Lachnospiraceae	0.702	5.33E-08	0.008
eWAT	Ruminococcaceae	-0.697	7.32E-08	0.008
Adiposity Index	Erysipelotrichaceae	0.697	7.32E-08	0.009
iWAT	Clostridiaceae	-0.696	8.03E-08	0.009
iWAT	Erysipelotrichaceae	0.692	9.89E-08	0.009
Adiposity Index	Porphyromonadaceae	0.692	1.02E-07	0.010
Adiposity Index	Lachnospiraceae	0.691	1.07E-07	0.010
Fat mass	Porphyromonadaceae	0.690	1.16E-07	0.010
eWAT	Porphyromonadaceae	0.681	1.89E-07	0.011
eWAT	Lachnospiraceae	0.679	2.10E-07	0.011
RWAT	Bacteroidaceae	0.678	2.25E-07	0.011
Fat mass	Mogibacteriaceae	-0.674	2.83E-07	0.012
Gain weight	Porphyromonadaceae	0.670	3.46E-07	0.012
mWAT	Erysipelotrichaceae	0.669	3.70E-07	0.012
RWAT	Porphyromonadaceae	0.667	4.17E-07	0.013
iWAT	Streptococcaceae	-0.666	4.46E-07	0.013
mWAT	Ruminococcaceae	-0.660	6.02E-07	0.013
Gain weight	Bacteroidaceae	0.660	6.15E-07	0.014
eWAT	Bacteroidaceae	0.658	6.64E-07	0.014
eWAT	Moraxellaceae	0.657	7.26E-07	0.014
Fat mass	Bacteroidaceae	0.656	7.46E-07	0.015
Subcutaneous	Clostridiaceae	-0.647	1.20E-06	0.015
Adiposity Index	Bacteroidaceae	0.647	1.21E-06	0.015
mWAT	Bacteroidaceae	0.646	1.22E-06	0.016
Adiposity Index	Mogibacteriaceae	-0.641	1.60E-06	0.016
Gain weight	Mogibacteriaceae	-0.641	1.62E-06	0.016
Visceral fat	Mogibacteriaceae	-0.640	1.64E-06	0.017
Visceral fat	Bacteroidaceae	0.640	1.67E-06	0.017
iWAT	Porphyromonadaceae	0.635	2.09E-06	0.017
Subcutaneous	Ruminococcaceae	-0.634	2.24E-06	0.018

eWAT	Verrucomicrobiaceae	0.629	2.85E-06	0.018
mWAT	Porphyromonadaceae	0.629	2.91E-06	0.018
eWAT	Mogibacteriaceae	-0.628	3.00E-06	0.019
Visceral fat	Moraxellaceae	0.627	3.10E-06	0.019
RWAT	Mogibacteriaceae	-0.622	3.95E-06	0.019
iWAT	Mogibacteriaceae	-0.619	4.46E-06	0.020
Gain weight	Streptococcaceae	-0.616	5.07E-06	0.020
RWAT	Streptococcaceae	-0.614	5.63E-06	0.020
iWAT	Verrucomicrobiaceae	0.607	7.60E-06	0.021
Fat mass	Moraxellaceae	0.605	8.30E-06	0.021
Fat mass	Streptococcaceae	-0.604	8.88E-06	0.021
Subcutaneous	Erysipelotrichaceae	0.590	1.60E-05	0.022
Visceral fat	Verrucomicrobiaceae	0.586	1.90E-05	0.022
Fat mass	Verrucomicrobiaceae	0.585	1.94E-05	0.022
Adiposity Index	Moraxellaceae	0.585	1.95E-05	0.023
RWAT	Anaeroplasmataceae	-0.579	2.50E-05	0.023
Subcutaneous	Mogibacteriaceae	-0.579	2.53E-05	0.023
Subcutaneous	Porphyromonadaceae	0.578	2.55E-05	0.024
mWAT	Mogibacteriaceae	-0.574	3.02E-05	0.024
Visceral fat	Streptococcaceae	-0.574	3.03E-05	0.024
Adiposity Index	Streptococcaceae	-0.570	3.58E-05	0.025
Visceral fat	Rikenellaceae	-0.569	3.70E-05	0.025
Adiposity Index	Verrucomicrobiaceae	0.567	4.03E-05	0.025
eWAT	Streptococcaceae	-0.564	4.51E-05	0.025
RWAT	Verrucomicrobiaceae	0.562	4.82E-05	0.026
mWAT	Verrucomicrobiaceae	0.559	5.49E-05	0.026
RWAT	Moraxellaceae	0.558	5.52E-05	0.026
eWAT	Rikenellaceae	-0.555	6.18E-05	0.027
mWAT	Moraxellaceae	0.552	7.10E-05	0.027
iWAT	Bacteroidaceae	0.549	7.91E-05	0.027
Subcutaneous	Lachnospiraceae	0.548	8.02E-05	0.028
Subcutaneous	Bacteroidaceae	0.546	8.68E-05	0.028
mWAT	Streptococcaceae	-0.546	8.81E-05	0.028
Gain weight	Moraxellaceae	0.542	1.01E-04	0.029
mWAT	Anaeroplasmataceae	-0.530	1.53E-04	0.029
iWAT	Anaeroplasmataceae	-0.529	1.57E-04	0.029
Fat mass	Rikenellaceae	-0.527	1.66E-04	0.030
iWAT	Moraxellaceae	0.523	1.90E-04	0.030
Gain weight	Rikenellaceae	-0.521	2.02E-04	0.030
Fat mass	Anaeroplasmataceae	-0.519	2.22E-04	0.031
RWAT	Rikenellaceae	-0.514	2.60E-04	0.031
Visceral fat	Anaeroplasmataceae	-0.513	2.64E-04	0.031
Adiposity Index	Anaeroplasmataceae	-0.510	2.97E-04	0.032
Adiposity Index	Rikenellaceae	-0.501	3.93E-04	0.032
eWAT	Anaeroplasmataceae	-0.499	4.17E-04	0.032
Subcutaneous	Moraxellaceae	0.493	5.07E-04	0.033
mWAT	Rikenellaceae	-0.491	5.34E-04	0.033
Gain weight	Verrucomicrobiaceae	0.477	8.11E-04	0.033
eWAT	Bifidobacteriaceae	-0.475	8.44E-04	0.034
Subcutaneous	Streptococcaceae	-0.473	8.99E-04	0.034

Fat mass	Bifidobacteriaceae	-0.471	9.55E-04	0.034
Gain weight	Anaeroplasmataceae	-0.466	1.10E-03	0.035
iWAT	Rikenellaceae	-0.459	1.35E-03	0.035
Visceral fat	Bifidobacteriaceae	-0.455	1.51E-03	0.035
Adiposity Index	Bifidobacteriaceae	-0.445	1.92E-03	0.036
Subcutaneous	Verrucomicrobiaceae	0.445	1.95E-03	0.036
Subcutaneous	Rikenellaceae	-0.420	3.65E-03	0.036
iWAT	Bifidobacteriaceae	-0.389	7.58E-03	0.037
Gain weight	Bifidobacteriaceae	-0.388	7.63E-03	0.037
RWAT	Bifidobacteriaceae	-0.375	1.03E-02	0.037
iWAT	Christensenellaceae	-0.374	1.03E-02	0.038
mWAT	Bifidobacteriaceae	-0.363	1.33E-02	0.038
Subcutaneous	Anaeroplasmataceae	-0.355	1.54E-02	0.038
Subcutaneous	Bifidobacteriaceae	-0.355	1.55E-02	0.039
Adiposity Index	Christensenellaceae	-0.338	2.18E-02	0.039
Adiposity Index	Prevotellaceae	-0.336	2.25E-02	0.039
RWAT	Dehalobacteriaceae	0.335	2.29E-02	0.040
Subcutaneous	Pasteurellaceae	0.321	2.95E-02	0.040
Fat mass	Dehalobacteriaceae	0.319	3.07E-02	0.040
mWAT	Prevotellaceae	-0.317	3.21E-02	0.041
iWAT	Dehalobacteriaceae	0.316	3.24E-02	0.041
Subcutaneous	Prevotellaceae	-0.316	3.27E-02	0.041
Fat mass	Christensenellaceae	-0.313	3.39E-02	0.042
Fat mass	Prevotellaceae	-0.306	3.88E-02	0.042
Adiposity Index	Pasteurellaceae	0.302	4.10E-02	0.042
	GENUS			
eWAT	SMB53	-0.755	1.30E-09	1.54E-04
Gain weight	Oscillospira	-0.732	7.57E-09	3.09E-04
Fat mass	SMB53	-0.729	9.16E-09	4.63E-04
Visceral fat	SMB53	-0.725	1.25E-08	0.001
eWAT	Oscillospira	-0.717	2.12E-08	0.001
Fat mass	Oscillospira	-0.717	2.14E-08	0.001
Visceral fat	Oscillospira	-0.714	2.46E-08	0.001
eWAT	Clostridium	-0.711	3.05E-08	0.001
Adiposity Index	SMB53	-0.707	3.96E-08	0.001
iWAT	Lactococcus	-0.706	4.11E-08	0.002
Adiposity Index	Clostridium	-0.705	4.56E-08	0.002
Adiposity Index	Oscillospira	-0.703	5.04E-08	0.002
Visceral fat	Clostridium	-0.701	5.66E-08	0.002
RWAT	SMB53	-0.701	5.80E-08	0.002
Fat mass	Clostridium	-0.701	5.83E-08	0.002
RWAT	Oscillospira	-0.698	6.85E-08	0.002
Gain weight	Lactococcus	-0.688	1.24E-07	0.003
Fat mass	Anaerostipes	-0.683	1.72E-07	0.003
Fat mass	Lactococcus	-0.680	2.03E-07	0.003
Adiposity Index	Anaerostipes	-0.674	2.84E-07	0.003
Gain weight	SMB53	-0.671	3.27E-07	0.003
RWAT	Lactococcus	-0.655	7.74E-07	0.003
Subcutaneous	Oscillospira	-0.654	8.26E-07	0.004
Visceral fat	Anaerostipes	-0.647	1.17E-06	0.004

eWAT	Anaerostipes	-0.644	1.35E-06	0.004
mWAT	SMB53	-0.642	1.53E-06	0.004
Adiposity Index	Lactococcus	-0.639	1.78E-06	0.004
eWAT	Ruminococcus	-0.638	1.88E-06	0.004
Adiposity Index	Ruminococcus	-0.637	1.89E-06	0.004
eWAT	Moryella	-0.634	2.25E-06	0.005
Fat mass	Ruminococcus	-0.629	2.88E-06	0.005
eWAT	Lactococcus	-0.628	2.97E-06	0.005
RWAT	Moryella	-0.627	3.11E-06	0.005
Visceral fat	Lactococcus	-0.626	3.27E-06	0.005
mWAT	Oscillospira	-0.625	3.38E-06	0.005
Gain weight	Bilophila	-0.623	3.70E-06	0.006
Visceral fat	Ruminococcus	-0.620	4.28E-06	0.006
Visceral fat	Bilophila	-0.620	4.33E-06	0.006
RWAT	Anaerostipes	-0.618	4.76E-06	0.006
RWAT	Clostridium	-0.615	5.37E-06	0.006
Fat mass	Moryella	-0.614	5.72E-06	0.006
iWAT	Anaerostipes	-0.613	5.81E-06	0.006
Fat mass	Bilophila	-0.613	5.85E-06	0.007
Subcutaneous	SMB53	-0.612	6.15E-06	0.007
mWAT	Lactococcus	-0.610	6.89E-06	0.007
iWAT	SMB53	-0.605	8.47E-06	0.007
iWAT	Ruminococcus	-0.603	9.17E-06	0.007
eWAT	Bilophila	-0.602	9.57E-06	0.007
iWAT	Oscillospira	-0.601	1.02E-05	0.008
Gain weight	Clostridium	-0.598	1.16E-05	0.008
Adiposity Index	Bilophila	-0.596	1.25E-05	0.008
Adiposity Index	Moryella	-0.593	1.39E-05	0.008
Gain weight	Ruminococcus	-0.592	1.49E-05	0.008
mWAT	Clostridium	-0.591	1.55E-05	0.008
Visceral fat	Moryella	-0.591	1.56E-05	0.008
Subcutaneous	Anaerostipes	-0.588	1.72E-05	0.009
RWAT	Anaeroplasma	-0.579	2.50E-05	0.009
Gain weight	Moryella	-0.576	2.83E-05	0.009
iWAT	Moryella	-0.576	2.84E-05	0.009
mWAT	Bilophila	-0.562	4.91E-05	0.009
RWAT	Bilophila	-0.560	5.27E-05	0.009
Subcutaneous	Lactococcus	-0.551	7.23E-05	0.010
mWAT	Anaerostipes	-0.548	8.10E-05	0.010
mWAT	Moryella	-0.548	8.16E-05	0.010
Subcutaneous	Clostridium	-0.538	1.15E-04	0.010
Gain weight	Anaerostipes	-0.537	1.19E-04	0.010
RWAT	Ruminococcus	-0.535	1.26E-04	0.010
Subcutaneous	Bilophila	-0.534	1.30E-04	0.010
mWAT	Anaeroplasma	-0.530	1.53E-04	0.011
iWAT	Anaeroplasma	-0.529	1.57E-04	0.011
Subcutaneous	Moryella	-0.527	1.65E-04	0.011
Subcutaneous	Ruminococcus	-0.522	1.96E-04	0.011
iWAT	Bilophila	-0.519	2.19E-04	0.011
Fat mass	Anaeroplasma	-0.519	2.22E-04	0.011

Visceral fat	Anaeroplasma	-0.513	2.64E-04	0.012
Adiposity Index	Anaeroplasma	-0.510	2.97E-04	0.012
Fat mass	Rothia	-0.507	3.27E-04	0.012
iWAT	Clostridium	-0.505	3.45E-04	0.012
Visceral fat	Rothia	-0.504	3.60E-04	0.012
mWAT	Ruminococcus	-0.500	3.99E-04	0.012
mWAT	Roseburia	0.502	3.79E-04	0.013
iWAT	Butyrivibrio	0.502	3.73E-04	0.013
RWAT	Xenorhabdus	0.504	3.60E-04	0.013
mWAT	Escherichia	0.510	2.99E-04	0.013
Gain weight	Escherichia	0.510	2.95E-04	0.013
eWAT	Klebsiella	0.511	2.87E-04	0.013
mWAT	Xenorhabdus	0.517	2.31E-04	0.013
Visceral fat	Anaerofustis	0.518	2.30E-04	0.014
Fat mass	Anaerofustis	0.519	2.16E-04	0.014
Visceral fat	Klebsiella	0.521	2.07E-04	0.014
Adiposity Index	Enterobacter	0.521	2.06E-04	0.014
Fat mass	Enterobacter	0.522	2.00E-04	0.014
eWAT	Enterobacter	0.531	1.48E-04	0.014
mWAT	Butyrivibrio	0.534	1.30E-04	0.015
mWAT	Coprococcus	0.536	1.22E-04	0.015
RWAT	Anaerotruncus	0.541	1.05E-04	0.015
eWAT	Anaerotruncus	0.543	9.65E-05	0.015
Visceral fat	Anaerotruncus	0.544	9.24E-05	0.015
iWAT	Coprococcus	0.545	9.09E-05	0.015
Subcutaneous	Bacteroides	0.546	8.68E-05	0.015
Adiposity Index	Anaerofustis	0.548	8.12E-05	0.016
iWAT	Bacteroides	0.549	7.91E-05	0.016
iWAT	Escherichia	0.554	6.59E-05	0.016
Visceral fat	Enterobacter	0.554	6.53E-05	0.016
Subcutaneous	Butyrivibrio	0.558	5.66E-05	0.016
Fat mass	Anaerotruncus	0.558	5.61E-05	0.016
Adiposity Index	Anaerotruncus	0.558	5.53E-05	0.017
mWAT	Akkermansia	0.559	5.49E-05	0.017
RWAT	Anaerofustis	0.560	5.16E-05	0.017
RWAT	Akkermansia	0.562	4.82E-05	0.017
Gain weight	Dorea	0.563	4.71E-05	0.017
Adiposity Index	Butyrivibrio	0.566	4.14E-05	0.017
Adiposity Index	Akkermansia	0.567	4.03E-05	0.017
Visceral fat	Coprococcus	0.568	3.83E-05	0.018
RWAT	Butyrivibrio	0.568	3.81E-05	0.018
Visceral fat	Butyrivibrio	0.573	3.14E-05	0.018
Adiposity Index	Escherichia	0.577	2.68E-05	0.018
Fat mass	Escherichia	0.578	2.61E-05	0.018
Subcutaneous	Parabacteroides	0.578	2.55E-05	0.018
eWAT	Butyrivibrio	0.580	2.36E-05	0.019
Fat mass	Butyrivibrio	0.582	2.25E-05	0.019
eWAT	Coprococcus	0.585	1.97E-05	0.019
Fat mass	Akkermansia	0.585	1.94E-05	0.019
Visceral fat	Akkermansia	0.586	1.90E-05	0.019

RWAT	Coprococcus	0.586	1.85E-05	0.019
Subcutaneous	Coprococcus	0.590	1.62E-05	0.019
Fat mass	Xenorhabdus	0.590	1.62E-05	0.020
Gain weight	Coprococcus	0.595	1.28E-05	0.020
Gain weight	Butyrivibrio	0.602	9.79E-06	0.020
Adiposity Index	Xenorhabdus	0.604	8.74E-06	0.020
eWAT	Escherichia	0.605	8.27E-06	0.020
iWAT	Akkermansia	0.607	7.60E-06	0.020
Visceral fat	Escherichia	0.611	6.39E-06	0.021
Adiposity Index	Coprococcus	0.615	5.44E-06	0.021
Fat mass	Coprococcus	0.619	4.50E-06	0.021
mWAT	Parabacteroides	0.629	2.91E-06	0.021
eWAT	Akkermansia	0.629	2.85E-06	0.021
iWAT	Parabacteroides	0.635	2.09E-06	0.021
Visceral fat	Bacteroides	0.640	1.67E-06	0.021
Visceral fat	Xenorhabdus	0.646	1.27E-06	0.022
mWAT	Bacteroides	0.646	1.22E-06	0.022
Adiposity Index	Bacteroides	0.647	1.21E-06	0.022
Fat mass	Bacteroides	0.656	7.46E-07	0.022
eWAT	Bacteroides	0.658	6.64E-07	0.022
eWAT	Xenorhabdus	0.659	6.40E-07	0.022
Gain weight	Bacteroides	0.660	6.15E-07	0.023
iWAT	Blautia	0.661	5.71E-07	0.023
RWAT	Parabacteroides	0.667	4.17E-07	0.023
Gain weight	Parabacteroides	0.670	3.46E-07	0.023
RWAT	Bacteroides	0.678	2.25E-07	0.023
Subcutaneous	Blautia	0.678	2.20E-07	0.023
eWAT	Parabacteroides	0.681	1.89E-07	0.023
Fat mass	Parabacteroides	0.690	1.16E-07	0.024
Adiposity Index	Parabacteroides	0.692	1.02E-07	0.024
Subcutaneous	Sutterella	0.695	8.13E-08	0.024
Visceral fat	Parabacteroides	0.703	5.24E-08	0.024
mWAT	Blautia	0.710	3.22E-08	0.024
mWAT	Sutterella	0.724	1.26E-08	0.024
Gain weight	Blautia	0.735	6.13E-09	0.025
eWAT	Blautia	0.736	5.44E-09	0.025
Adiposity Index	Blautia	0.740	4.35E-09	0.025
eWAT	Sutterella	0.741	3.94E-09	0.025
Visceral fat	Blautia	0.742	3.73E-09	0.025
iWAT	Sutterella	0.742	3.49E-09	0.025
Visceral fat	Sutterella	0.752	1.74E-09	0.025
Fat mass	Blautia	0.754	1.42E-09	0.026
RWAT	Sutterella	0.760	9.30E-10	0.026
Gain weight	Sutterella	0.760	9.20E-10	0.026
RWAT	Blautia	0.767	5.13E-10	0.026
Adiposity Index	Sutterella	0.768	4.55E-10	0.026
Fat mass	Sutterella	0.773	3.19E-10	0.026
eWAT	Anaeroplasma	-0.499	4.17E-04	0.027
Adiposity Index	Rothia	-0.496	4.59E-04	0.027
eWAT	Bifidobacterium	-0.475	8.44E-04	0.027

Fat mass	Bifidobacterium	-0.471	9.55E-04	0.027
Gain weight	Anaeroplasma	-0.466	1.10E-03	0.027
Visceral fat	Bifidobacterium	-0.455	1.51E-03	0.027
Subcutaneous	Rothia	-0.452	1.61E-03	0.027
Adiposity Index	Bifidobacterium	-0.445	1.92E-03	0.028
eWAT	Rothia	-0.433	2.62E-03	0.028
RWAT	Rothia	-0.419	3.75E-03	0.028
mWAT	Rothia	-0.414	4.27E-03	0.028
Gain weight	Rothia	-0.397	6.35E-03	0.028
iWAT	Bifidobacterium	-0.389	7.58E-03	0.028
Gain weight	Bifidobacterium	-0.388	7.63E-03	0.029
RWAT	Bifidobacterium	-0.375	1.03E-02	0.029
mWAT	Bifidobacterium	-0.363	1.33E-02	0.029
Subcutaneous	Anaeroplasma	-0.355	1.54E-02	0.029
Subcutaneous	Bifidobacterium	-0.355	1.55E-02	0.029
iWAT	Rothia	-0.335	2.27E-02	0.029
Visceral fat	Dehalobacterium	0.297	4.50E-02	0.029
mWAT	Dehalobacterium	0.302	4.15E-02	0.030
Subcutaneous	Streptococcus	0.308	3.72E-02	0.030
Subcutaneous	Aggregatibacter	0.311	3.55E-02	0.030
eWAT	Allobaculum	0.313	3.44E-02	0.030
eWAT	Streptococcus	0.314	3.37E-02	0.030
eWAT	Dehalobacterium	0.315	3.30E-02	0.030
Subcutaneous	Dehalobacterium	0.316	3.22E-02	0.031
Adiposity Index	Dehalobacterium	0.322	2.89E-02	0.031
iWAT	Roseburia	0.332	2.41E-02	0.031
Visceral fat	Shuttleworthia	0.335	2.28E-02	0.031
Subcutaneous	Shuttleworthia	0.337	2.19E-02	0.031
mWAT	Allobaculum	0.341	2.05E-02	0.031
iWAT	Allobaculum	0.343	1.97E-02	0.031
eWAT	Roseburia	0.351	1.69E-02	0.032
Subcutaneous	Klebsiella	0.355	1.55E-02	0.032
Fat mass	Shuttleworthia	0.355	1.53E-02	0.032
iWAT	Dehalobacterium	0.357	1.49E-02	0.032
Fat mass	Dehalobacterium	0.359	1.43E-02	0.032
Gain weight	Allobaculum	0.365	1.26E-02	0.032
iWAT	Klebsiella	0.367	1.22E-02	0.033
RWAT	Dehalobacterium	0.370	1.13E-02	0.033
Adiposity Index	Shuttleworthia	0.372	1.08E-02	0.033
Gain weight	Anaerofustis	0.378	9.70E-03	0.033
Gain weight	Klebsiella	0.382	8.76E-03	0.033
Subcutaneous	Escherichia	0.392	7.11E-03	0.033
Subcutaneous	Roseburia	0.392	6.99E-03	0.033
Visceral fat	Roseburia	0.397	6.23E-03	0.034
iWAT	Enterobacter	0.399	6.04E-03	0.034
Adiposity Index	Roseburia	0.405	5.30E-03	0.034
eWAT	Dorea	0.411	4.58E-03	0.034
Subcutaneous	Enterobacter	0.414	4.25E-03	0.034
RWAT	Klebsiella	0.416	4.05E-03	0.034
Fat mass	Roseburia	0.417	3.94E-03	0.035

iWAT	Xenorhabdus	0.421	3.56E-03	0.035
mWAT	Klebsiella	0.435	2.51E-03	0.035
mWAT	Anaerofustis	0.435	2.49E-03	0.035
Gain weight	Anaerotruncus	0.444	1.97E-03	0.035
Subcutaneous	Dorea	0.445	1.96E-03	0.035
Subcutaneous	Akkermansia	0.445	1.95E-03	0.035
RWAT	Enterobacter	0.451	1.64E-03	0.036
RWAT	Roseburia	0.456	1.44E-03	0.036
RWAT	Escherichia	0.456	1.44E-03	0.036
Gain weight	Roseburia	0.459	1.34E-03	0.036
Adiposity Index	Dorea	0.461	1.27E-03	0.036
iWAT	Dorea	0.461	1.27E-03	0.036
Subcutaneous	Xenorhabdus	0.462	1.23E-03	0.037
Subcutaneous	Anaerofustis	0.462	1.23E-03	0.037
Gain weight	Enterobacter	0.464	1.17E-03	0.037
Visceral fat	Dorea	0.464	1.17E-03	0.037
mWAT	Enterobacter	0.470	9.69E-04	0.037
mWAT	Anaerotruncus	0.472	9.21E-04	0.037
Fat mass	Dorea	0.474	8.71E-04	0.038
Gain weight	Akkermansia	0.477	8.11E-04	0.038
iWAT	Anaerofustis	0.477	7.97E-04	0.038
Fat mass	Klebsiella	0.479	7.62E-04	0.038
Gain weight	Xenorhabdus	0.485	6.42E-04	0.038
mWAT	Dorea	0.486	6.11E-04	0.038
iWAT	Anaerotruncus	0.486	6.09E-04	0.038
Adiposity Index	Klebsiella	0.493	4.98E-04	0.039
RWAT	Dorea	0.494	4.86E-04	0.039
eWAT	Anaerofustis	0.498	4.34E-04	0.039
Subcutaneous	Anaerotruncus	0.499	4.13E-04	0.039

[a]Spearman's rank-order correlation coefficient (rho).

[b]The correlations were significant when the P-value and FDR (False Disvory Ratio) was < 0.05. (n=7-8).

Manuscript 2

Objective: To elucidate the influence of photoperiods and gut microbiota interaction on serum corticosterone hormone and seasonal and circadian clock genes expression

Photoperiod effects on corticosterone and seasonal clocks in obese Fischer 344 rats are influenced by gut microbiota

Arreaza-Gil V[1,2,3], Escobar-Martínez[1] I, Soliz-Rueda JR[1,2,3], Suárez M[1], Schellekens H[2]*, Torres-Fuentes C[1]* and Arola-Arnal A[1].

[1]Nutrigenomics Research Group, Departament de Bioquímica i Biotecnologia, Universitat Rovira i Virgili, 43007 Tarragona, Spain.

[2] Department of Anatomy and Neuroscience, University College Cork, Cork, Ireland.

[3] APC Microbiome Ireland, Cork, Ireland.

*Corresponding author

Submitted to the FASEB journal.

RESULTS

Abstract

Seasonal rhythms have been shown to influence gut microbiota composition, which can impact several metabolic and physiological processes. Although the specific mechanisms for this interaction are still poorly understood, corticosterone may play an important role as it is an essential hormone for homeostasis maintenance and its production is modulated by gut microbiota. Moreover, seasonal rhythms affect corticosterone production through the hypothalamus-pituitary-adrenal axis, and at the same time, corticosterone is involved in the regulation of central and peripheral clock genes. Hence, there may be a link between seasonal rhythms and gut microbiota at hormonal and molecular levels. Thus, the aim of this study was to investigate if the effects of seasonal rhythms on corticosterone and on circadian and seasonal clocks in the pituitary gland and colon tissue is influenced by gut microbiota in obese rats. Fischer 344 rats were housed under three different photoperiods (L6: 6 h of light, L12: 12h of light and L18: 18 h of light) for 9 weeks and randomly distributed in three groups for each photoperiod condition: standard-chow diet-fed rats, cafeteria (CAF)-fed rats and CAF-fed rats treated with an antibiotic cocktail (ABX) in drinking water for the last 4 week of the experiment. The results showed a photoperiod effect on corticosterone levels only in ABX-treated rats, increasing under L6 and decreasing under L18 conditions. No ABX effects were observed in the circadian clock, but it significantly altered seasonal clock depending on the photoperiod conditions. Hence, these results indicate that gut bacteria influence photoperiod effects on corticosterone, as well as on the seasonal clock in obese rats.

Keywords: corticosterone, *Eya3*, *Chga*, antibiotic, seasonal rhythms

RESULTS

1. Introduction

Seasonal rhythms, which are normally entrained by annual changes in day length (photoperiod) and daily light/dark cycles are emerging as key factors modulating several physiological and metabolic processes [1]. Thus, seasonal rhythms drive processes such as neuroendocrine regulation, metabolism, fattening and reproductive activity throughout the year [2]. These rhythms are normally entrained by annual changes in day length (photoperiod), allowing animals synchronize their physiological and metabolic activities to the time of year (seasonal rhythms) [1]. The seasonal clock is located in the pituitary gland (also known as hypophysis), concretely in the melatonin-responsive thyrotroph cells (calendar cells). These calendar cells operate as a binary switch mechanism, regulating the transcription of both the co-activator eyes-absent-3 (*Eya3)* and the chromogranin-A (*Chga*) in a photoperiod-dependent manner, initiating the pituitary gland a cascade of molecular events which translates to seasonal changes of neuroendocrine activity in the hypothalamus [3]. On the other hand, the variations of the light/dark outputs among seasons are the external driver of the central pacemaker of circadian rhythms. Hence, seasonal and circadian rhythms are closely interrelated [4–6]. In this context, circadian rhythms are driven by clock genes found in the suprachiasmatic nucleus (SCN) (central clock) and peripheral tissues [7]. These molecular clocks consist of an autoregulatory transcription-translation feedback loop formed by *Bmal1* (brain and muscle aryl hydrocarbon receptor nuclear translocator-like 1) and *Clock* (circadian locomotor output cycles kaput), which once reaching heterodimerization activates the transcription of period (*Per*) and cryptochrome (*Cry*) genes. In turn, the protein accumulation of PER and CRY result in a feedback inhibition of BMAL1/CLOCK activity. Moreover, secondary regulatory loops modulate the activity of this molecular clock. Thus, *Bmal1* gene is inhibited by the nuclear receptors REV-ERBα and β (Nuclear Receptor Subfamily 1 Group D Member 1 α and β) and activated by RAR-orphan receptor α and γ (RORα and –γ) [8]. The central clock synchronizes peripheral clocks

found in different tissues of the organism. However, these peripheral clocks are capable of autonomous regulation and these can be affected by other external signals such as diet and fasting/feeding states [9,10]. In fact, high fat diet feeding has been linked to alterations of clock genes expression in liver, adipose tissue, intestine and even hypothalamus, promoting metabolic disorders [11,12].

Seasonal rhythms have been reported to influence gut microbiota composition [13–17]. Thus, it has been shown that gut bacteria follow diurnal and season oscillations [13,18–20]. This is of interest as gut microbiota plays a crucial role in host metabolism and homeostasis maintenance and its alteration promote the development of metabolic disease such as obesity and metabolic syndrome [21–24]. Indeed, aberrant microbiota diurnal fluctuations and dysbiosis caused by external cues such as high fat diet or antibiotic intake have been linked to altered clock genes expression in colon and to obesity development [25]. Hence, gut bacteria have attracted the attention of scientists in the last years and several investigations have been carried out in order to elucidate the potential mechanisms involved in their interaction with the host. In this context, it is known that bacteria release bioactive metabolites that signal to the host via de gut-brain axis, a bidirectional network that allows for direct communication between gut bacteria and the brain [23]. In this regard, the hypothalamus-pituitary-adrenal (HPA) axis plays an important role as one of the most important components of the gut-brain axis [26]. The HPA axis provides response to stressful stimuli via de production of cortisol (corticosterone in rodents). This hormone is produced by the adrenal cortex and is essential for the maintenance of metabolic homeostasis [27]. Indeed, high corticosterone levels are linked to a variety of diseases, including obesity, dyslipidemia, fatty liver and glucose intolerance [28–30]. An excess of corticosterone results in an increase of circulating free fatty acids and induce adipocyte differentiation in adipose tissue, leading to increased adiposity and insulin resistance [31,32]. Recently, it has been shown that gut microbiota affects corticosterone

production in the murine small and colon intestine [33,34]. Moreover, recent studies have shown that glucocorticoids may regulate some physiological effects through the gut microbiota [35,36]. Hence, this hormone plays an important role in obesity and in gut microbiota-mediated effects in the host and, therefore, understanding the factors involved in their regulation is important. Interestingly, seasonal rhythms have been shown to modulate corticosterone production through the HPA axis [37,38]. At the same time, corticosterone is also involved in the regulation of central and peripheral clock genes [39,40].

Taking all together, we hypothesize that there may be a link between seasonal rhythms and gut microbiota at hormonal and molecular levels. Thus, the aim of this study was to investigate if the effects of seasonal rhythms on corticosterone levels, as well as in circadian and seasonal clocks in pituitary gland and colon tissues is influenced by gut microbiota in obese rats. To this aim, Fischer 344 rats were housed under different photoperiod conditions, which mimics seasonal changes, and administered a cafeteria diet (CAF) to induce obesity and an antibiotic cocktail to disturb gut microbiota. Moreover, standard diet (STD)-fed rats were included as healthy control.

2. Materials and methods

2.1. Experimental procedure.

Thirteen weeks-old male Fischer 344 rats (*n* = 72) from Janvier Laboratories (France) were pair-housed at standard conditions (22ºC, 65% relative humidity and 12:12 hour light/dark cycle) with ad libitum access to water and standard chow diet for one week. After this week of adaptation to the facilities, rats were weighted and randomized distributed into three different light-dark cycles (photoperiods) conditions to mimic seasonal day lengths for 9 weeks: short photoperiod [L6, 6 h light/18 h darkness], standard photoperiod [L12, 12 h light/12 h darkness], or long photoperiod [L18, 18 h light/6 h darkness].

Rats were further randomly divided in three groups (*n* = 8) for each photoperiod condition: (1) rats fed a standard chow diet (STD) (72% carbohydrate, 8% lipid, and 19% protein; Safe-A04c, Germany), (2) rats fed a cafeteria diet (CAF) (58% CH, 31% lipid, and 11% protein), and (3) CAF-fed rats treated with an antibiotic cocktail (ABX) during the last 4-weeks. CAF was freshly prepared every day and included the following (grams per rat and per day): biscuits with pâté and cheese (15-17 g), bacon (7-10 g), ensaimada (pastry) (10-15 g), carrot (11-12 g), standard chow (20-25 g) and milk containing 22% sucrose (w/v). The antibiotic cocktail (0.5 g/l ampicillin, 0.250 g/l vancomycin and 0.125 g/l imipenem; Discovery fine chemicals Ltd, United Kingdom) was freshly prepared every day and administered in drinking water. Body weight (BW) was recorded weekly during the whole experimental procedure. Oral glucose tolerance test (OGTT) was carried out at last week of the experiment. Glucose was orally administered after 6 h fasting (2 g/kg body weight, 50% w/v) and blood glucose levels were measured with a glucometer (Glucocard SM, Menarini Diagnostics, Italy) at 0, 15, 30, 60 and 120 min after glucose administration (**Figure S1**).

Animals were sacrificed by decapitation. Pituitary gland and colon tissue were freshly collected and immediately snap-frozen in liquid nitrogen and stored at -80ºC until further analysis. The blood was collected from the neck, in non-heparinized tubes, incubated for 1 h at room temperature and immediately centrifuged at 1200x g for 15 min to collect the serum. The Animal Ethics Committee of the University Rovira i Virgili (Tarragona, Spain) and the Generalitat de Catalunya approved all the procedures (number reference 9495) in accordance with the EU Directive 2010/63/EU for animal experiments.

2.2. Corticosterone levels analysis.

Corticosterone serum hormone concentration was measured by liquid chromatography coupled to a triple quadrupole mass spectrometer (LC-QqQ). 250 µL of methanol containing the internal standard (2 ng/mL) was added to 50 µL of serum. This mixture was vortexed and centrifuged for 5 min at 4 ◦C and 252× g. The supernatant was transferred to a new tube and mixed with 700 µL of 0.1% formic acid in water. The sample was loaded to a SPE system previously conditioned with methanol and 0.1% formic acid in water. The cartridge was washed with 0.1% formic acid in water and dried under high vacuum. The compounds were eluted with 500 µL of methanol using a Zorbax Eclipse C18 (150 × 2.1 mm) column (Agilent Technologies). Samples were evaporated in a SpeedVac at 45 ◦C and reconstituted with 50 µL of water:methanol (60:40, v/v) for the analysis.

2.3. RNA isolation and Real-time polymerase chain reaction quantification.

Total RNA was isolated from colon and pituitary gland samples using Total RNA kit I (Omega Bio-Tek, Inc., Norcross, GA, USA) according to the manufacturer protocol. RNA quality was determined using a NanoDrop ND2000 spectrophotometer (Thermo Fisher Scientific, Massachusetts, USA). RNA of suitable quality was reverse transcribed using a high-capacity complementary DNA reverse-transcription kit (Thermo Fisher, Madrid, Spain). Quantitative real-time polymerase chain reaction (qPCR) was performed using SYBR Green Master Mix on a CFX96 Real-time PCR detection system-IVD (Bio-Rad Laboratoires, Inc, Barcelona, Spain). The thermal-cycle program used in all qPCRs was 30 s at 90 ◦C, 40 cycles of 15 s at 95 ◦C and 1 min at 60 ◦C. The different analyzed genes were quantified using peptidylprolil isomerase A (*Ppia*) as housekeeping gene for normalization. The primers used for each gene were obtained from eurofins Genomics (Wolverhampton, United Kingdom) and are shown in

Table 1. Cycle threshold (Ct) values were recorded, normalized to housekeeping gene expression and transformed to relative gene expression value using the $2^{-\Delta\Delta Ct}$ method (REF: Livak and Schmittgen, 2001).

Table 1. Primer sequences for gene expression analysis.

Target	Forward 5'-3'	Reverse 5'-3'
Eya3	TTTGAGTGCCCACAGGACTC	CTGAAGAGGCCAAAGGAGGG
Chga	CAGGAGCTGGAACGTAAGCA	CCATCGCTTGTCCTCCCATT
Nr3c1	AGCATTACCACAGCTCACCC	CTGCATACAACACCTCGGGT
Bmal1	GGCGTCGGGACAAAATGAAC	AACTTCCGGGACATCGCATT
Per1	CAGTGAGGAGTCTGCTGAGC	GGAGCCTGAAAGTGCATCCT
Cry1	GGACAAGAATCCCGAGGCTC	CATGATGGCGTCAATCCACG
Clock	TCCTTCAGTTCAGCAGCCAG	ATTCCCATGGAGCAACCGAG
Rorα	GTGCGTGTCCTTGCATTGTT	GAGAGGGCTCACACACAGGAAC
Rev-erbα	GCGTCTGGGTGCTTCATTTC	CGGGRGCAAAAGTCCCAAAG

Eya3: Eyes Absent Homolog 3; Chga: Chromogranin A; Nr3c1: Nuclear Receptor Subfamily 3 Group C Member 1 (Glucocorticoid Receptor); Bmal1: Brain and muscle Aryl Hydrocarbon Receptor Nuclear Translocator Like 1; *Per1*: period circadian regulator 1; *Cry1*: Cryptochrome 1; *Clock:* circadian locomotor output cycles kaput; *RORα*: Orphan nuclear receptor α; *Rev-erbα:* Nuclear Receptor Subfamily 1 Group D Member 1.

2.4. Statistical Analysis.

Data were plotted using Graphpad Prism 8.0 software (Graphapad software Inc, San Diego, CA, USA) showing mean ± standard mean error (SEM) of each group. Statistical analysis was performed using SPSS software (IBS SPSS statistics 25). Normality as well as homogeneity of variance were tested by Shapiro-Wilk test and Levene test, respectively. BW gain and OGTT over time were analyzed using repeated-measured ANOVA followed by LSD post hot test at each individual time point. For the AUC of BW gain and OGTT, intake, fat parameters, corticosterone levels and gene expression, the differences between groups were

assessed by two-way ANOVA followed by LSD post hoc test. The two-way ANOVA was performed depending on the factor evaluated: diet and photoperiod factors or ABX and photoperiod factor. Additionally, when LSD post hoc test showed tendency ($0.05>p<0.1$), diet or ABX effect was analyzed by Student's t-test.

The statistical test used for individual analysis, as well as the statistical significances are provided in the figure legends.

3. Results

3.1. Corticosterone serum levels were influenced by photoperiod only in ABX-treated rats.

Corticosterone serum levels were analyzed in order to elucidate the effects of CAF feeding and ABX treatment in this hormone under different photoperiod conditions. CAF-fed rats showed similar serum levels of corticosterone independently of the photoperiod conditions. When comparing with STD-fed rats, a no significant increase in corticosterone levels was observed in CAF-fed rats housed under L6 and L12 conditions but not in L18. On the other hand, ABX-treatment did not show any significant effect in corticosterone levels. However, although it was not significant, increased levels of this hormone was observed under L6 and L12, while a decrease was observed under L18. Additionally, a photoperiod effect was found only in CAF+ABX rats, being serum corticosterone levels higher in rats housed under L6 or L12 compared to those housed under L18 conditions (**Figure 1a**). Interestingly, CAF-fed rats showed higher levels of corticosterone under L6 and L12 when treated with ABX, but the opposite was observed under L18 conditions.

Moreover, the gene expression of the glucocorticoids receptor (GR), also known as nuclear receptor subfamily 3, group C, member 1 (NR3C1), was analyzed in pituitary gland and colon tissue. In the pituitary gland, CAF

feeding did not have any effect in *Nr3c1* gene expression (**Figure 1b**). Furthermore, CAF+ABX rats showed decreased expression of *Nrc3c1* compared to CAF rats only when housed under L12. Additionally, CAF+ABX rats housed under L12 conditions showed decreased expression of this GR compared to those exposed to L6 conditions. Interestingly, the effects observed in *Nr3c1* expression in colon were different to those found in the pituitary gland. Moreover, colonic *Nr3c1* gene expression increased in CAF-fed rats housed under L12 and L18 conditions. Furthermore, CAF-fed rats showed lower expression of GR under L6 compared to rats housed under L12 conditions.

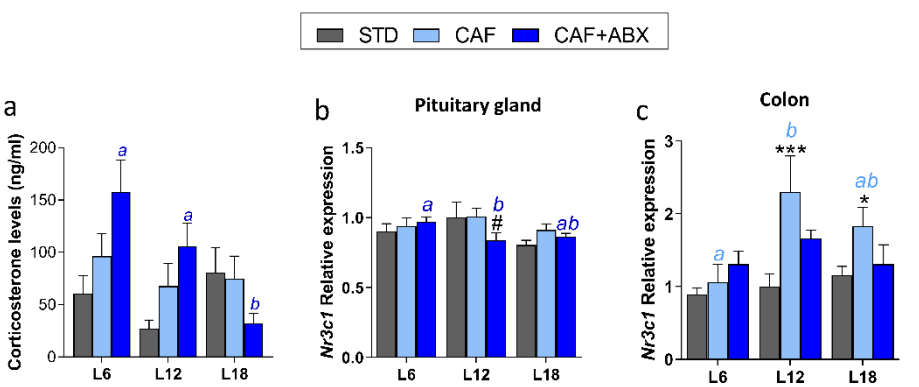

Figure 1. Corticosterone serum levels and glucocorticoids receptors expression*. (a) Corticosterone serum levels in STD, CAF and CAF+ABX rats housed under three different photoperiods (L6, L12 and L18). (b) Relative glucocorticoid receptor expression in pituitary gland; (c) Relative gene expression of the glucocorticoid receptor (Nr3c1) in colon tissue; Data were analyzed by two-way ANOVA followed by LSD post hoc test; * indicates CAF effect (*p<0.05; **p≤0.01; ***p≤0.001), # indicates ABX effect (# p<0.05) and ab letters indicate photoperiod effect; Data are plotted as the mean ± SEM (n=7-8). L6: 6h light/18h darkness; L12: 12h light/12h darkness; L18: 18h light/6h darkness; STD: standard chow diet; CAF: cafeteria diet; ABX: antibiotic cocktail (0.5 g/l ampicillin, 0.250 g/l vancomycin and 0.125 g/l imipenem). Nr3c1: nuclear receptor subfamily 3, group C, member 1.*

3.2. ABX treatment in CAF-fed rats altered seasonal clock in pituitary gland in a photoperiod-dependent manner.

The effects of CAF feeding and ABX administration in the relative expression of *Eya3* and *Chga* in the pituitary gland under different

photoperiod conditions were also evaluated. The relative expression of *Eya3* was not affected by CAF feeding (**Figure 2a**). However, CAF-fed rats showed increased *Chga* relative expression compared to STD-fed rats only under L18. Interestingly, ABX administration decreased *Eya3* and *Chga* expression in CAF-fed rats under L12 and L18 conditions respectively (**Figure 2b**).

Regarding photoperiod effects, the relative expression of *Eya3* was higher in L18 conditions, independently of the diet or ABX treatment (**Figure 2a**). In the case of *Chga*, its relative expression was affected by photoperiod in CAF-fed rats, being higher under L18 conditions compared to L12. When comparing with CAF-fed rats housed under L6, this increase in L18 was not significant but a trend was observed (p=0.07). Moreover, ABX administration to CAF-fed rats led to significantly decreased *Chga* expression under L18 conditions (**Figure 2b**).

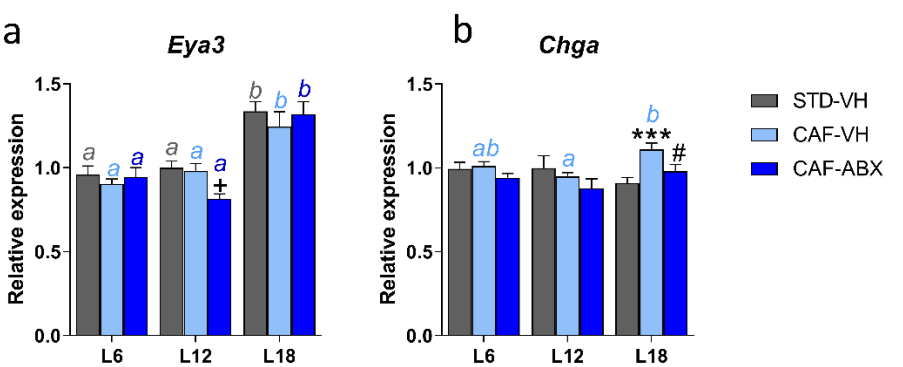

Figure 2. Seasonal genes expression in the pituitary gland. *(**a**) Relative expression of Eya3 and (**b**) Chga in STD, CAF and CAF+ABX rats housed under different photoperiods (L6, L12 and L18). Data were analyzed by two-way ANOVA followed by LSD post hoc test; * indicates diet effect (***p≤0.001), # indicates ABX effect (# p<0.05) and ab letters indicate photoperiod effect; + indicates ABX effect analyzed by student's t-test (p<0.01). Data are plotted as the mean ± SEM (n=7-8). L6: 6h light/18h darkness; L12: 12h light/12h darkness; L18: 18h light/6h darkness; STD: standard chow diet; CAF: cafeteria diet; ABX: antibiotic cocktail (0.5 g/l ampicillin, 0.250 g/l vancomycin and 0.125 g/l imipenem).*

3.3. Clock genes expression in pituitary gland and colon was differently affected by photoperiods but not by ABX treatment.

Finally, the effects of CAF feeding and ABX treatment in peripheral clock genes expression under different photoperiod conditions were also evaluated. In particular, these were analyzed in the pituitary gland and in colon tissue, two important peripheral clocks. In the pituitary gland, CAF feeding increased the relative expression of *Bmal1 and Clock* under L18 condition, *Rorα* under both L12 and L18 conditions and *Rev-erbα* under L6 conditions compared to STD-fed rats (**Figure 3**). Moreover, relative clock genes expression in colon tissue were also affected by CAF feeding (**Figure 4**). Thus, CAF feeding significantly increased the relative expression of *Bmal1* under L12 and L18 conditions, trended to increase the expression of *Clock* under L12 condition, significant decreased *Per1* expression under L12 condition and led a significant increase of *RORα* under L12 conditions. However, any significant ABX effect was observed in neither the pituitary gland nor in colon.

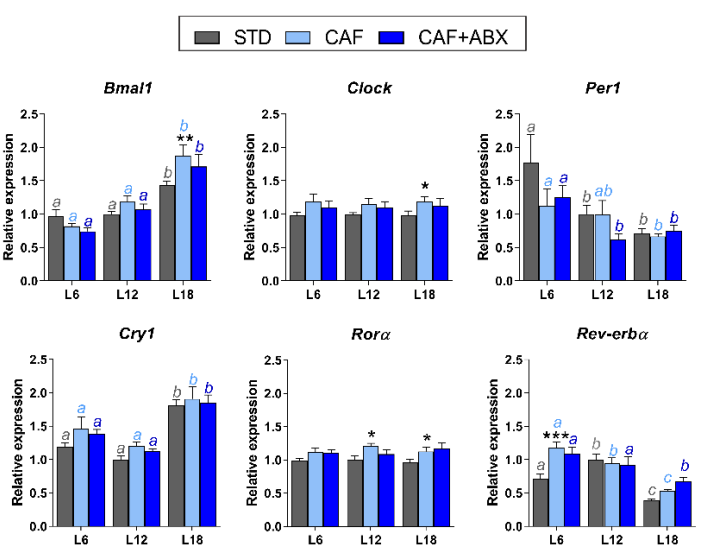

Figure 3. Clock genes expression in pituitary gland. *Data were analyzed by two-way followed by LSD post hoc test; * indicates diet effect (***p≤0.001), and ab letters indicate photoperiod effect; Data are plotted as the mean ± SEM (n=7-8). L6: 6h light/18h darkness; L12: 12h light/12h darkness; L18: 18h light/6h darkness; STD: standard chow diet; CAF: cafeteria diet; ABX: antibiotic cocktail.*

Additionally, a photoperiod effect was found in clock genes expression in both pituitary gland and colon tissue. In the pituitary gland, *Bmal1*, *Per1*, *Cry1* and *Rev-erbα* showed significant changes in their expression in STD, CAF and CAF+ABX rats depending on the photoperiod conditions, while *Clock* and *Rorα* did not show any photoperiod effect. In particular, *Bmal1* and *Cry1* expression was significantly higher under L18 independently of CAF feeding and ABX treatment, while *Rev-erbα* showed a lower expression under L18 conditions and *Per1* a higher expression under L6 (**Figure 3**). In contrast, in colon tissue only *Cry1* and *Rev-erbα* showed a photoperiod effect independently of the experimental group, while *Clock* only showed a photoperiod effect in CAF-fed rats and Bmal1 in CAF and CAF-ABX rats and *Per1* and *Rorα* did not show a photoperiod effect. Thus, *Bmal1* expression was significantly lower under L6 in CAF-fed rats (CAF and CAF+ABX rats) and *Clock* expression was higher under L12 only in CAF-fed rats. Furthermore, *Cry1* and *Rev-erbα* showed a higher and lower expression respectively under L18 compared to L6 (**Figure 4**).

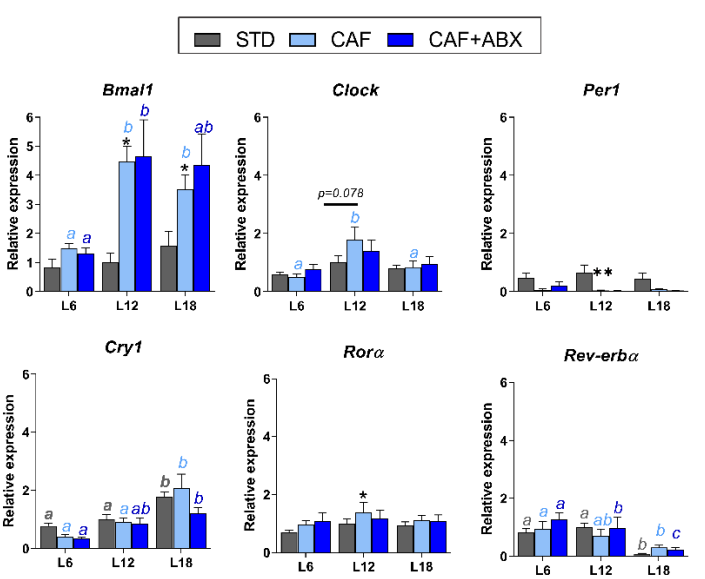

***Figure 4. Clock genes expression in colon**. Data were analyzed by two-way followed by LSD post hoc test; * indicates diet effect (*p<0.05; **p≤0.01), and ab letters indicate photoperiod effect; Data are plotted as the mean ± SEM (n=7-8). L6: 6h light/18h darkness; L12: 12h light/12h darkness; L18: 18h light/6h darkness; STD: standard chow diet; CAF: cafeteria diet; ABX: antibiotic cocktail.*

4. Discussion

Seasonal rhythms have been shown to modulate gut microbiota composition which can affect several metabolic and physiological processes influencing the risk for the development of disorders such as obesity [13]. However, the potential mechanisms involved are not well understood yet. In this regard, corticosterone signaling may be playing an important role. Thus, corticosterone is one of the main hormones involved in gut microbiota-mediated effects [35,36] and, at the same time, gut microbiota is involved in corticosterone production via the HPA axis, playing an important role in the corticosterone secretion [35]. Moreover, high levels of corticosterone has been linked to obesity development, hyperglycemia and insulin resistance affecting key metabolic organs such as pancreas, liver, muscle and adipose tissue [28–30,41–43]. Moreover, it has been shown to be modulated by seasonal rhythms through the HPA [44,45] and is also involved in the regulation of clock genes [46]. Therefore, there may be a link between seasonal rhythms and gut bacteria at hormonal and molecular levels. Hence, in this study we investigated the influence of gut microbiota disruption induced by ABX treatment on photoperiod-mediated oscillations of corticosterone as well as of circadian and seasonal clocks in obese rats.

To induce obesity, animals were fed a cafeteria diet, which consists in high palatable foods regularly consumed by humans, leading to a more robust model for human obesity in comparison with other high fat diets traditionally used [47]. Thus, CAF feeding has been shown to effectively induce obesity, diabetes and other disorders associated to the metabolic syndrome, significantly altering gut microbiota composition [47–49]. Indeed, CAF-fed rats showed higher body weight gain, lower glucose tolerance, higher fat accumulation, higher food intake and lower microbial alpha diversity compared to STD-fed rats (Figure S2; Figure S3

[13,50]. In this study, although no effects of photoperiod were observed in CAF-fed rats, a no significant increase of corticosterone levels was observed compared to STD-fed rats under L6 and L12 conditions. This is in agreement with other studies which have reported increased levels of this hormone in obesity [51]. Interestingly, this difference in corticosterone levels between STD- and CAF-fed rats was not observed when rats were housed under L18 conditions, indicating that photoperiod conditions can influence the variations in corticosterone levels associated to obesity development. Indeed, it is known that endogenous corticosterone secretion is governed by the seasonal and the circadian system, being regular corticosterone secretion an important factor in the synchronization between central and peripheral clocks in order to maintain physiological and metabolic homeostasis [52]. Hence, photoperiods have been reported as key modulators of corticosterone levels, showing lower basal levels in long photoperiod compared to short photoperiod conditions in studies carried out in healthy mice [53], F344 rats fed a low caloric diet [54] and goats [38]. In this case, although it was not significant, corticosterone levels were lower in L12 compared to L6 conditions in STD-fed rats, but this was not observed in L18. Interestingly, we have previously shown that L18 conditions led to the greatest changes in the gut microbiota of both STD-fed rats included in this study, suggesting a role for these bacteria in the effects of this photoperiod on corticosterone levels [13]. Moreover, CAF-fed rats did not show any photoperiod effect in corticosterone levels, indicating that the seasonal rhythm of this hormone is altered in obesity conditions. Indeed, obesity has been reported to disrupt biological rhythms [55]. Thus, disruption in the circadian rhythm of cortisol has been reported in animal models of obesity [56] and also in obese women [57], adolescents [58] and children [59]. Moreover, it is worth highlighting that corticosterone levels in CAF-fed rats treated with ABX showed a completely different pattern depending on the photoperiod

conditions. Thus, while the disruption of gut microbiota by ABX treatment led to increased corticosterone levels in CAF-fed rats housed under L6 and L12 conditions, this was the opposite in rats housed under L18. Hence, these results support that gut bacteria influence corticosterone production in a photoperiod dependent manner, having different effects in long photoperiod conditions compared to short and standard photoperiods. These findings are in line with what has been observed in relation to circadian corticosterone rhythms in intestine. Thus, an important role for commensal bacteria in the circadian regulation of intestinal glucocorticoid production has been reported [60]. In particular, the depletion of the intestinal microbiota completely disrupted the phasic intestinal production of corticosterone, leading to increased levels of this hormone that was linked with the development of hyperglycemia, insulin resistance, and increased triglycerides and free fatty acids. Hence, here we report for the first time to our knowledge that similar effects are found in the case of exposure to different photoperiods. In this study, the changes in corticosterone levels caused by ABX-mediated gut microbiota alteration also correlated with glucose tolerance and BW gain in CAF-fed rats. Hence, the higher corticosterone levels observed in ABX-treated CAF-fed rats housed under L6 conditions correlated with higher glucose intolerance in these conditions compared to L18 conditions where rats showed lower levels of this hormone. Moreover, ABX-CAF rats housed under L18 conditions showed a trend towards lower body weight gain.

Corticosterone mediates many of its effects by altering gene transcription through its interaction with its receptor [61]. It is known that peripheral tissues have high GR levels, which influence the expression of circadian rhythm-related genes. Interestingly, no photoperiod effects were observed for GR receptor in the pituitary gland except for ABX-treated CAF-fed rats, which showed higher levels under L6 compared to L12 and L18 conditions. Moreover, ABX treatment also decreased GR expression in CAF-fed rats only when housed under L12 conditions. This reinforce a

potential role for gut bacteria in corticosterone signaling which is influenced by photoperiod conditions. In the case of colon tissue, GR expression was significantly affected by photoperiod in CAF-fed rats, being lower when rats were housed under short photoperiod conditions. These effects were not observed in the colonic expression of GR in STD-fed rats. This could be due to the fact that CAF feeding can decrease intestinal barrier integrity promoting inflammation and increasing the glucocorticoid receptor expression [62,63]. Moreover, gut microbiota dysbiosis induced by CAF feeding can also contribute to this increased inflammation and GR expression in colon. Thus, as we have previously reported, CAF feeding significantly altered phyla such as *Proteobacteria*, which has been linked to high grade of inflammation and risk of metabolic disorders [64].

Moreover, the effects of the different treatments on seasonal and circadian clocks were investigated. The seasonal clock is located in the pituitary gland as previously mentioned and modulates different pathways that translates to seasonal changes of neuroendocrine activity in the hypothalamus [3]. Summer-like photoperiod signals activate *Eya3* gene transcription and suppresses *Chga* gene transcription in the pituitary gland, which expression would indicate winter-like state [3,65]. A clear photoperiod effect was observed for *Eya3* gene expression as expected [3,66] . Interestingly, depletion of gut microbiota by ABX treatment led to decreased levels of this gene only under L12 conditions. Moreover, ABX administration to CAF-fed rats led to decreased *Chga* expression, another important seasonal clock gene, being significant only under L18 conditions. However, CHGA has been reported to be activated under short photoperiod conditions [3,67] and here this was not observed. Therefore, this needs to be further investigated in order to elucidate the role of CHGA in this system and the potential role of gut microbiota in its regulation. Regarding clock genes, which orchestrate circadian oscillations of several metabolic and physiological processes as above mentioned [7], different photoperiod effects

were observed but no differences were found in ABX-treated rats. This is in contrast to other studies that have reported disruption of clock genes such as *Bmal1*, *Cry1*, *Per1*, and *Per2*, in intestine and liver in germ-free and antibiotic-treated mice [46,68]. However, these studies were not done in obese animals, and this may explain the differences observed for the effect of ABX. Hence, both CAF feeding and ABX treatment led to gut microbiota alterations, and it may be that the dysbiosis developed in both cases could have similar effects on clock genes expression. Indeed, some clock genes such as *Bmal1* showed an altered expression in the pituitary and colon tissue in CAF-fed rats compared to STD-fed rats. This effect was also dependent of photoperiods, reinforcing their influence on clock gene expression in peripheral tissues under obesogenic conditions.

In conclusion, these results suggest that gut microbiota influence photoperiod effects on corticosterone and colonic GR expression levels as well as on seasonal clock in obesity. However, it has little impact on circadian clocks in the pituitary and in colon tissue in obese rats. This interaction between gut microbiota, seasonal rhythms and corticosterone and seasonal clock signaling may be one of the main mechanisms driving seasonal oscillations of several metabolic and physiologic processes involved in obesity development. These results reinforce the importance of biological rhythms and gut microbiota when investigating metabolic-related pathologies. Further studies are needed to elucidate the potential mechanisms involved.

Data Availability Statement

The data that support the findings of this study are available in the methods and/or supplementary material of this article.

Conflict of Interest Statement

The authors declare no conflicts of interest.

Author Contributions

Conceptualization: V.A.-G., A.A.-A. and C.T.-F.; Formal analysis: V.A.-G., I.E.-M. and J.R. S-R; Data curation: V.A.-G; Investigation: V.A.-G., I.E.-M., J.R S-R., M.S., H.S., A.A.-A. and C.T.-F.; Methodology: V.A.-G., J.R. S-R., A.A.-A. and C.T.-F.; Funding acquisition: M.S., H.S., A.A.-A. and C.T-F.; Project administration: M.S., H.S., A.A.-A. and C.T-F.; Resources: M.S., H.S., A.A.-A. and C.T-F.; Software: V.A-G; Visualization: V.A.-G.; Supervision: A.A.-A. and C.T-F; Validation: V.A.-G., A.A.-A. and C.T.-F.; Writing original draft: V.A.-G.; Writing review & editing: A.A.-A. and C.T.-F.

Acknowledgments

This work was supported by MCIN/AEI/10.13039/501100011033/ FEDER "Una manera de hacer Europa" (AGL2016-77105-R) and "2021/22 Development of a prototype for the establishment of a dysbiosis (alteration) in the intestinal microbiota", co-financed by Diputació de Tarragona (2021PGR-DIPTA-URV09). V.A.-G. was supported by the Martí i Franquès Doctoral Fellowships Programme, Universitat Rovira i Virgili (PMF-PIPF-35); I.E.-M. was supported by the Youth Employment Initiative from the European Social Fund, Ministry of Science, The State Research Agency and Universitat Rovira i Virgili (PEJ2018-002778-A); J.R.S-R is the recipient of a grant for the hiring of predoctoral research staff (FPI) (Grant number: BES-2017-080919) from the Spanish Ministry of Science and Innovation MCIN/AEI/10.13039/ 501100011033 and FSE "El FSE invierte en tu futuro". A.A-A were supported by the Serra Húnter Programme, Government of Catalonia; C.T.-F. was supported by Beatriu de Pinós Postdoctoral Programme of the Government of Catalonia's Secretariat for Universities and Research of the Ministry of Economy and Knowledge. The authors would like to thank Niurka Dariela Llópiz and Rosa Pastor for their assistance.

REFERENCES

[1] Wood S, Loudon A. Clocks for all seasons: Unwinding the roles and mechanisms of circadian and interval timers in the hypothalamus and pituitary. J Endocrinol 2014;222. https://doi.org/10.1530/JOE-14-0141.

[2] Helm B, Ben-Shlomo R, Sheriff MJ, Hut RA, Foster R, Barnes BM, et al. Annual rhythms that underlie phenology: biological time-keeping meets environmental change. Proc R Soc B Biol Sci 2013;280. https://doi.org/10.1098/RSPB.2013.0016.

[3] Wood SH, Christian HC, Miedzinska K, Saer BRC, Johnson M, Paton B, et al. Binary Switching of Calendar Cells in the Pituitary Defines the Phase of the Circannual Cycle in Mammals. Curr Biol 2015;25:2651–62. https://doi.org/10.1016/j.cub.2015.09.014.

[4] Coomans CP, Ramkisoensing A, Meijer JH. The suprachiasmatic nuclei as a seasonal clock. Front Neuroendocrinol 2015;37:29–42. https://doi.org/10.1016/j.yfrne.2014.11.002.

[5] Tackenberg MC, McMahon DG. Photoperiodic Programming of the SCN and Its Role in Photoperiodic Output. Neural Plast 2018;2018. https://doi.org/10.1155/2018/8217345.

[6] Johnston JD. Measuring seasonal time within the circadian system: Regulation of the suprachiasmatic nuclei by photoperiod. J Neuroendocrinol 2005;17:459–65. https://doi.org/10.1111/j.1365-2826.2005.01326.x.

[7] Reppert SM, Weaver DR. Coordination of circadian timing in mammals. Nat 2002 4186901 2002;418:935–41. https://doi.org/10.1038/nature00965.

[8] Takahashi JS. Transcriptional architecture of the mammalian circadian clock. Nat Rev Genet 2016 183 2016;18:164–79. https://doi.org/10.1038/nrg.2016.150.

[9] Gagliano O, Luni C, Li Y, Angiolillo S, Qin W, Panariello F, et al. Synchronization between peripheral circadian clock and feeding-fasting cycles in microfluidic device sustains oscillatory pattern of transcriptome. Nat Commun 2021 121 2021;12:1–12. https://doi.org/10.1038/s41467-021-26294-9.

[10] Pickel L, Sung HK. Feeding Rhythms and the Circadian Regulation of Metabolism. Front Nutr 2020;7:39. https://doi.org/10.3389/FNUT.2020.00039.

[11] Kohsaka A, Laposky AD, Ramsey KM, Estrada C, Joshu C, Kobayashi Y, et al. High-Fat Diet Disrupts Behavioral and Molecular Circadian Rhythms in Mice. Cell Metab 2007;6:414–21. https://doi.org/10.1016/J.CMET.2007.09.006/ATTACHMENT/B1B506A6-A0E7-41A3-8740-7BD6B88664DF/MMC1.PDF.

[12] Barnea M, Madar Z, Froy O. High-Fat Diet Delays and Fasting Advances the Circadian Expression of Adiponectin Signaling Components in Mouse Liver. Endocrinology 2009;150:161–8. https://doi.org/10.1210/EN.2008-0944.

[13] Arreaza-Gil V, Escobar-Martínez I, Suárez M, Bravo F, Muguerza B, Arola-Arnal

A, et al. Gut Seasons: Photoperiod Effects on Fecal Microbiota in Healthy and Cafeteria-Induced Obese Fisher 344 Rats. Nutrients 2022;14:722. https://doi.org/10.3390/NU14030722.

[14] Shor EK, Brown SP, Freeman DA. A novel role for the pineal gland: Regulating seasonal shifts in the gut microbiota of Siberian hamsters. J Pineal Res 2020;69:e12696. https://doi.org/10.1111/jpi.12696.

[15] Bailey MT, Walton JC, Dowd SE, Weil ZM, Nelson RJ. Photoperiod modulates gut bacteria composition in male Siberian hamsters (Phodopus sungorus). Brain Behav Immun 2010;24:577–84. https://doi.org/10.1016/j.bbi.2009.12.010.

[16] Fan C, Zhang L, Jia S, Tang X, Fu H, Li W, et al. Seasonal variations in the composition and functional profiles of gut microbiota reflect dietary changes in plateau pikas. Integr Zool 2022. https://doi.org/10.1111/1749-4877.12630.

[17] Maurice CF, Cl Knowles S, Ladau J, Pollard KS, Fenton A, Pedersen AB, et al. Marked seasonal variation in the wild mouse gut microbiota. ISME J 2015;9:2423–34. https://doi.org/10.1038/ismej.2015.53.

[18] Thaiss CA, Levy M, Korem T, Dohnalová L, Shapiro H, Jaitin DA, et al. Microbiota Diurnal Rhythmicity Programs Host Transcriptome Oscillations. Cell 2016;167:1495-1510.e12. https://doi.org/10.1016/J.CELL.2016.11.003.

[19] Thaiss CA, Zeevi D, Levy M, Zilberman-Schapira G, Suez J, Tengeler AC, et al. Transkingdom control of microbiota diurnal oscillations promotes metabolic homeostasis. Cell 2014;159:514–29. https://doi.org/10.1016/j.cell.2014.09.048.

[20] Teichman EM, O'Riordan KJ, Gahan CGM, Dinan TG, Cryan JF. When Rhythms Meet the Blues: Circadian Interactions with the Microbiota-Gut-Brain Axis. Cell Metab 2020;31:448–71. https://doi.org/10.1016/j.cmet.2020.02.008.

[21] Crovesy L, Masterson D, Rosado EL. Profile of the gut microbiota of adults with obesity: a systematic review. Eur J Clin Nutr 2020;74:1251–62. https://doi.org/10.1038/s41430-020-0607-6.

[22] Saad MJA, Santos A, Prada PO. Linking gut microbiota and inflammation to obesity and insulin resistance. Physiology 2016;31:283–93. https://doi.org/10.1152/PHYSIOL.00041.2015/ASSET/IMAGES/LARGE/PHY0041603360003.JPEG.

[23] Torres-Fuentes C, Schellekens H, Dinan TG, Cryan JF. The microbiota–gut–brain axis in obesity. Lancet Gastroenterol Hepatol 2017;2:747–56. https://doi.org/10.1016/S2468-1253(17)30147-4.

[24] Rea K, Dinan TG, Cryan JF. The microbiome: A key regulator of stress and neuroinflammation. Neurobiol Stress 2016;4:23–33. https://doi.org/10.1016/J.YNSTR.2016.03.001.

[25] Murakami M, Tognini P. The Circadian Clock as an Essential Molecular Link Between Host Physiology and Microorganisms. Front Cell Infect Microbiol 2020;9:1–9. https://doi.org/10.3389/fcimb.2019.00469.

[26] de Weerth C. Do bacteria shape our development? Crosstalk between intestinal microbiota and HPA axis. Neurosci Biobehav Rev 2017;83:458–71. https://doi.org/10.1016/J.NEUBIOREV.2017.09.016.

[27] Kokkinos A, Lambadiari V, Cooney GJ, Rutter GA, Akalestou E, Genser L. Glucocorticoid Metabolism in Obesity and Following Weight Loss. Front Endocrinol | WwwFrontiersinOrg 2020;11:59. https://doi.org/10.3389/fendo.2020.00059.

[28] Acute Severe Steatohepatitis Related To Prednisolone Therapy : Official journal of the American College of Gastroenterology | ACG n.d. https://journals.lww.com/ajg/Citation/2002/04000/Acute_Severe_Steatohepatitis_Related_To.68.aspx (accessed May 31, 2022).

[29] Dimitriadis G, Leighton B, Parry-Billings M, Sasson S, Young M, Krause U, et al. Effects of glucocorticoid excess on the sensitivity of glucose transport and metabolism to insulin in rat skeletal muscle. Biochem J 1997;321:707–12. https://doi.org/10.1042/BJ3210707.

[30] Samuel VT, Petersen KF, Shulman GI. Lipid-induced insulin resistance: unravelling the mechanism. Lancet 2010;375:2267–77. https://doi.org/10.1016/S0140-6736(10)60408-4.

[31] Gathercole LL, Morgan SA, Bujalska IJ, Hauton D, Stewart PM, Tomlinson JW. Regulation of Lipogenesis by Glucocorticoids and Insulin in Human Adipose Tissue. PLoS One 2011;6:e26223. https://doi.org/10.1371/JOURNAL.PONE.0026223.

[32] Hauner H, Schmid P, Pfeiffer EF. Glucocorticoids and Insulin Promote the Differentiation of Human Adipocyte Precursor Cells into Fat Cells. J Clin Endocrinol Metab 1987;64:832–5. https://doi.org/10.1210/JCEM-64-4-832.

[33] Ergang P, Vagnerová K, Hermanová P, Vodička M, Jágr M, Šrůtková D, et al. The Gut Microbiota Affects Corticosterone Production in the Murine Small Intestine. Int J Mol Sci 2021;22. https://doi.org/10.3390/IJMS22084229.

[34] Vagnerová K, Vodička M, Hermanová P, Ergang P, Šrůtková D, Klusoňová P, et al. Interactions Between Gut Microbiota and Acute Restraint Stress in Peripheral Structures of the Hypothalamic–Pituitary–Adrenal Axis and the Intestine of Male Mice. Front Immunol 2019;10:1–10. https://doi.org/10.3389/fimmu.2019.02655.

[35] Farzi A, Fröhlich EE, Holzer P. Gut Microbiota and the Neuroendocrine System n.d. https://doi.org/10.1007/s13311-017-0600-5.

[36] Vodička M, Ergang P, Hrnčíř T, Mikulecká A, Kvapilová P, Vagnerová K, et al. Microbiota affects the expression of genes involved in HPA axis regulation and local metabolism of glucocorticoids in chronic psychosocial stress. Brain Behav Immun 2018;73:615–24. https://doi.org/10.1016/J.BBI.2018.07.007.

[37] Otsuka T, Goto M, Kawai M, Togo Y, Sato K, Katoh K, et al. Photoperiod Regulates Corticosterone Rhythms by Altered Adrenal Sensitivity via Melatonin-Independent Mechanisms in Fischer 344 Rats and C57BL/6J Mice. PLoS One 2012;7:e39090. https://doi.org/10.1371/JOURNAL.PONE.0039090.

[38] Alila-Johansson A, Eriksson L, Soveri T, Laakso ML. Serum Cortisol Levels in Goats Exhibit Seasonal But Not Daily Rhythmicity. Https://DoiOrg/101081/CBI-120017684 2009;20:65–79. https://doi.org/10.1081/CBI-120017684.

[39] Bering T, Hertz H, Rath MF. Rhythmic Release of Corticosterone Induces Circadian Clock Gene Expression in the Cerebellum. Neuroendocrinology 2020;110:604–15. https://doi.org/10.1159/000503720.

[40] Mavroudis PD, Scheff JD, Calvano SE, Lowry SF, Androulakis IP. Entrainment of peripheral clock genes by cortisol. Physiol Genomics 2012;44:607. https://doi.org/10.1152/PHYSIOLGENOMICS.00001.2012.

[41] Liu Y, Nakagawa Y, Wang Y, Liu L, Du H, Wang W, et al. Reduction of hepatic glucocorticoid receptor and hexose-6-phosphate dehydrogenase expression ameliorates diet-induced obesity and insulin resistance in mice. J Mol Endocrinol 2008;41:53–64. https://doi.org/10.1677/JME-08-0004.

[42] Kotelevtsev Y, Holmes MC, Burchell A, Houston PM, Schmoll D, Jamieson P, et al. 11β-Hydroxysteroid dehydrogenase type 1 knockout mice show attenuated glucocorticoid-inducible responses and resist hyperglycemia on obesity or stress. Proc Natl Acad Sci U S A 1997;94:14924–9. https://doi.org/10.1073/PNAS.94.26.14924/ASSET/CCF71866-A747-427A-B4EB-F90F158C0802/ASSETS/GRAPHIC/PQ2673529004.JPEG.

[43] Alberts P, Nilsson C, Selén G, Engblom LOM, Edling NHM, Norling S, et al. Selective Inhibition of 11β-Hydroxysteroid Dehydrogenase Type 1 Improves Hepatic Insulin Sensitivity in Hyperglycemic Mice Strains. Endocrinology 2003;144:4755–62. https://doi.org/10.1210/EN.2003-0344.

[44] Otsuka T, Goto M, Kawai M, Togo Y, Sato K, Katoh K, et al. Photoperiod regulates corticosterone rhythms by altered adrenal sensitivity via melatonin-independent mechanisms in fischer 344 rats and C57BL/6J mice. PLoS One 2012;7:1–8. https://doi.org/10.1371/journal.pone.0039090.

[45] Lind CM, Moore IT, Vernasco BJ, Farrell TM. Seasonal testosterone and corticosterone patterns in relation to body condition and reproduction in a subtropical pitviper, Sistrurus miliarius. Gen Comp Endocrinol 2018;267:51–8. https://doi.org/10.1016/j.ygcen.2018.05.027.

[46] Mukherji A, Kobiita A, Ye T, Chambon P. Homeostasis in intestinal epithelium is orchestrated by the circadian clock and microbiota cues transduced by TLRs. Cell 2013;153:812–27. https://doi.org/10.1016/j.cell.2013.04.020.

[47] Sampey BP, Vanhoose AM, Winfield HM, Freemerman AJ, Muehlbauer MJ, Fueger PT, et al. Cafeteria diet is a robust model of human metabolic syndrome with liver and adipose inflammation: comparison to high-fat diet. Obesity (Silver Spring) 2011;19:1109–17. https://doi.org/10.1038/OBY.2011.18.

[48] Del Bas JM, Guirro M, Boqué N, Cereto A, Ras R, Crescenti A, et al. Alterations in gut microbiota associated with a cafeteria diet and the physiological consequences in the host. Int J Obes 2018;42:746–54. https://doi.org/10.1038/ijo.2017.284.

[49] Gual-Grau A, Guirro M, Mayneris-Perxachs J, Arola L, Boqué N. Impact of

different hypercaloric diets on obesity features in rats: a metagenomics and metabolomics integrative approach. J Nutr Biochem 2019;71:122–31. https://doi.org/10.1016/j.jnutbio.2019.06.005.

[50] Arreaza-Gil, V, Escobar-Martínez I, Muguerza B, Aragonès G, Suárez M, Torres-Fuentes C, Arola-Arnal A. The effects of Grape Seed Proanthocyanidins in cafeteria diet-induced obese Fischer 344 rats are influenced by fecal microbiota in a photoperiod-dependent manner. Food & Function, 2022; Article in press.

[51] Hewagalamulage SD, Lee TK, Clarke IJ, Henry BA. Stress, cortisol, and obesity: a role for cortisol responsiveness in identifying individuals prone to obesity. Domest Anim Endocrinol 2016;56:S112–20. https://doi.org/10.1016/J.DOMANIEND.2016.03.004.

[52] Pierre K, Rao RT, Hartmanshenn C, Androulakis IP. Modeling the Influence of Seasonal Differences in the HPA Axis on Synchronization of the Circadian Clock and Cell Cycle. Endocrinology 2018;159:1808–26. https://doi.org/10.1210/en.2017-03226.

[53] Oyola MG, Johnson RC, Bauman BM, Frey KG, Russell AL, Cho-Clark M, et al. Gut microbiota and metabolic marker alteration following dietary isoflavone-photoperiod interaction. Endocrinol Diabetes Metab 2021;4:e00190. https://doi.org/10.1002/EDM2.190.

[54] Togo Y, Otsuka T, Goto M, Furuse M, Yasuo S. Photoperiod regulates dietary preferences and energy metabolism in young developing Fischer 344 rats but not in same-age Wistar rats. Am J Physiol - Endocrinol Metab 2012;303:777–86. https://doi.org/10.1152/ajpendo.00209.2012.

[55] Pereira LR, Moreira FP, Reyes AN, Bach SDL, Amaral PL Do, Motta JDS, et al. Biological Rhythm Disruption Associated with Obesity in School Children. Https://HomeLiebertpubCom/Chi 2019;15:200–5. https://doi.org/10.1089/CHI.2018.0212.

[56] Cano P, Jiménez-Ortega V, Larrad Á, Toso CFR, Cardinali DP, Esquifino AI. Effect of a high-fat diet on 24-h pattern of circulating levels of prolactin, luteinizing hormone, testosterone, corticosterone, thyroid-stimulating hormone and glucose, and pineal melatonin content, in rats. Endocrine 2008;33:118–25. https://doi.org/10.1007/S12020-008-9066-X/TABLES/1.

[57] Al-Safi ZA, Polotsky A, Chosich J, Roth L, Allshouse AA, Bradford AP, et al. Evidence for Disruption of Normal Circadian Cortisol Rhythm in Women with Obesity. Gynecol Endocrinol 2018;34:336. https://doi.org/10.1080/09513590.2017.1393511.

[58] Berdina O, Madaeva I, Bolshakova S, Sholokhov L, Rychkova L. Circadian Rhythm of Salivary Cortisol in Obese Adolescents With and Without Apnea: A Pilot Study. Front Pediatr 2022;0:537. https://doi.org/10.3389/FPED.2022.795635.

[59] Yu T, Zhou W, Wu S, Liu Q, Li X. Evidence for disruption of diurnal salivary cortisol rhythm in childhood obesity: Relationships with anthropometry, puberty and physical activity. BMC Pediatr 2020;20:1–10. https://doi.org/10.1186/S12887-020-02274-8/TABLES/5.

[60] Henao-Mejia J, Strowig T, Flavell RA. Microbiota Keep the Intestinal Clock Ticking. Cell 2013;153:741–3. https://doi.org/10.1016/J.CELL.2013.04.043.

[61] De Guia RM, Rose AJ, Herzig S. Glucocorticoid hormones and energy homeostasis. Horm Mol Biol Clin Investig 2014;19:117–28. https://doi.org/10.1515/HMBCI-2014-0021.

[62] Ayroldi E, Soma KK, Brunner T, Ahmed A, Schmidt C. Extra-Adrenal Glucocorticoid Synthesis in the Intestinal Mucosa: Between Immune Homeostasis and Immune Escape. Front Immunol | WwwFrontiersinOrg 2019;1:1438. https://doi.org/10.3389/fimmu.2019.01438.

[63] Tang S, Zhang Z, Oakley RH, Li W, He W, Xu X, et al. Intestinal epithelial glucocorticoid receptor promotes chronic inflammation–associated colorectal cancer. JCI Insight 2021;6. https://doi.org/10.1172/JCI.INSIGHT.151815.

[64] Shin NR, Whon TW, Bae JW. Proteobacteria: microbial signature of dysbiosis in gut microbiota. Trends Biotechnol 2015;33:496–503. https://doi.org/10.1016/J.TIBTECH.2015.06.011.

[65] Lincoln G. A brief history of circannual time. J Neuroendocrinol 2019;31:1–12. https://doi.org/10.1111/jne.12694.

[66] Masumoto KH, Ukai-Tadenuma M, Kasukawa T, Nagano M, Uno KD, Tsujino K, et al. Acute induction of Eya3 by late-night light stimulation triggers TSHβ expression in photoperiodism. Curr Biol 2010;20:2199–206. https://doi.org/10.1016/J.CUB.2010.11.038.

[67] Dardente H, Wyse CA, Birnie MJ, Dupré SM, Loudon ASI, Lincoln GA, et al. A molecular switch for photoperiod responsiveness in mammals. Curr Biol 2010;20:2193–8. https://doi.org/10.1016/J.CUB.2010.10.048/ATTACHMENT/25AEE83E-6383-4714-ABB1-95D107956508/MMC1.PDF.

[68] Leone V, Gibbons SM, Martinez K, Hutchison AL, Edmond Y, Cham CM, et al. on Host Circadian Clock Function and Metabolism. Cell Host Microbe 2016;17:681–9. https://doi.org/10.1016/j.chom.2015.03.006.Effects.

SUPPLEMENTARY MATERIAL

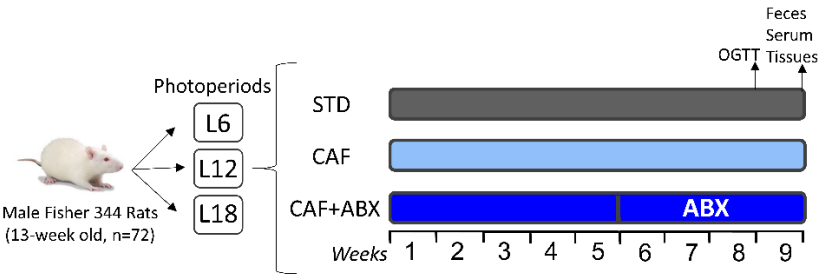

Figure S1. Experimental design. *13-week-old male Fischer 344 rats were pair-housed under three different photoperiods (6, 12 or 18 h of light per day) for 9 weeks. In each photoperiod, rats were fed a STD or CAF diet. During the last 4 weeks, a group of CAF-fed rats were treated with an antibiotic cocktail (ABX) in drinking water (ampicillin: 0.5g/l, vancomycin: 0.25 g/l, imipenem: 0.125 g/l). OGTT: oral glucose tolerance test; L6: 6h light/18h darkness; L12: 12h light/12h darkness; L18: 18h light/6h darkness; STD: standard chow diet; CAF: cafeteria diet; VH: vehicle.*

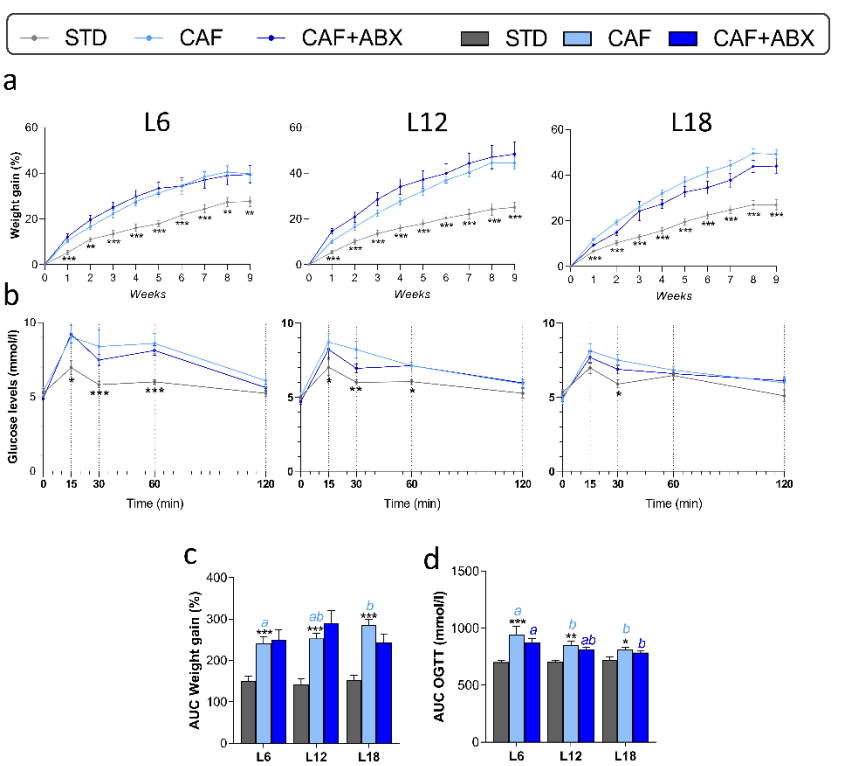

Figure S2. Phenotypic characteristic of STD, CAF and CAF+ABX rats. *(**a**) Body weight change in STD, CAF and CAF+ABX rats under the different photoperiods (L6, L12, L18) across the 9 weeks of the experiment; (**b**): Oral glucose tolerance test (OGTT) in STD, CAF and CAF+ABX rats under the different photoperiod (L6, L12, L18); (**c** and **d**) Area under the curve (AUC) for body weight gain and OGTT of*

*the STD, CAF and CAF+ABX rats under L6, L12 and L18 conditions; BW gain and OGTT were analyzed by measures-repeated ANOVA followed by LSD post hoc test; AUC, fat mass and adiposity index percentage were analyzed by two-way followed by LSD post hoc test; * indicates diet effect (*p<0.05; **p≤0.01; ***p≤0.001), and ab letters indicate the photoperiod effect into each experimental group. Significant ABX effect was not found (p>0.05). Data are plotted as the mean ± SEM (n=7-8). L6: 6h light/18h darkness; L12: 12h light/12h darkness; L18: 18h light/6h darkness; STD: standard chow diet; CAF: cafeteria diet; ABX: antibiotic cocktail.*

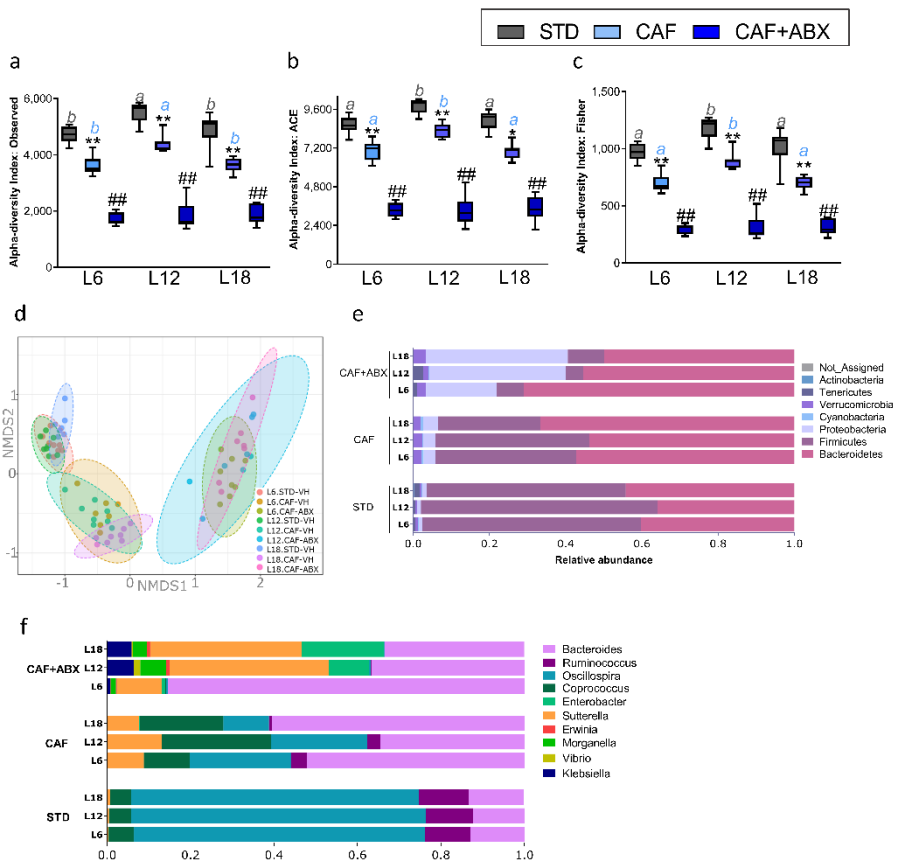

Figure S3. Diet, ABX and photoperiod effect on fecal microbiota composition. *(**a** to **c**): α-diversity index calculate by observed operational taxonomic unit (a); ACE (b); and Fisher (c); * and # indicate diet and ABX effect respectively analyzed by U-Mann Whitney test (*p<0.05; **p≤0.01; ***p≤0.001; ## p≤0.001); ab letters indicate photoperiod effect, analyzed by Kruskal-Wallis test followed by Bonferroni correction for multiple comparisons (p<0.016) (**d**): β-diversity based on Bray-Curtis distances and visualized by a Non-Metric Multidimensional Scaling (NMDS) 2D plot (PERMANOVA, p<0.001); (c): Stacked bar plots showing the relative abundance of each taxa at phylum level; (d) Stacked bar plots showing the relative abundance of each taxa at genera level.*

RESULTS

CHAPTER 2

To investigate the influence of the interaction between seasonal rhythms and gut microbiota in the functionality and bioavailability of PAs in a cafeteria-induced obese F344 rats

RESULTS

Manuscript 3

Objective: To elucidate if GSPE anti-obesity effects can be modulated by gut microbiota in a photoperiod dependent manner.

The effects of Grape Seed Proanthocyanidins in cafeteria diet-induced obese Fischer 344 rats are influenced by fecal microbiota in a photoperiod dependent manner

Arreaza-Gil V, Escobar-Martínez I, Muguerza B, Aragonès G, Suárez M, Torres-Fuentes C*, Arola-Arnal A.

Universitat Rovira i Virgili, Department de Biochemistry and Biotechnology, Nutrigenomics Research Group, Tarragona, 43007, Spain

*Corresponding author

In press in *Food & Function*. Impact Factor (2021): 6.317. SI Journal Citation Reports © Ranking 67/296 (Q1) in Biochemistry & molecular biology and 24/143 in Food science & Technology

RESULTS

ABSTRACT

Polyphenols are of high interest due to their beneficial health effects, including anti-obesity properties. Gut microbiota may play an important role in polyphenols-mediated effects as these bacteria are significantly involved in their metabolism. Moreover, seasonal rhythms have been demonstrated to influence both gut microbiota composition and polyphenols bioavailability. Thus, the goal of this study was to evaluate the impact of photoperiods and microbiota on polyphenols functionality under an obesogenic context. To this aim, cafeteria diet-fed Fischer 344 rats were housed under three different photoperiod conditions (L6: 6 h of light, L12: 12 h of light and L18: 18 h of light) for 9 weeks. During the last 4 weeks of the experiment, rats were daily administered with an oral dose of a grape seed proanthocyanidin extract (GSPE) (25 mg/kg body weight). Additionally, rats treated with GSPE and an antibiotic cocktail (ABX) in their drinking water were included for a better understanding of the gut microbiota role in GSPE functionality. Vehicle and non-ABX treated rats were included as controls. GSPE decreased body weight gain and fat depots only under L18 conditions. Interestingly, gut microbiota composition was strongly altered in this photoperiod. GSPE+ABX-treated rats gained significantly less body weight compared to the rest of treatments under L18 conditions. These results suggest that GSPE functionality is modulated by gut microbiota in a photoperiod dependent manner. These novel findings corroborate seasonal rhythms as key factors that must be taken into account when investigating the effects of polyphenols in the treatment or prevention of chronic diseases.

Keywords**:** GSPE, Gut microbiota, Obesity, Polyphenols, Seasonal rhythms, fat depots.

RESULTS

1. Introduction

Polyphenols have attracted increasing scientific attention due to their beneficial role in human health. They are the most common plant-derived bioactive component in our diet, being widely present in a variety of food such as fruits, vegetables, cereals, tea, coffee and wine [1,2]. In this context, grape seed proanthocyanidins (GSPE) have shown several beneficial effects against obesity and metabolic syndrome (MetS) development [3]. Thus, it was found that GSPE can improve lipid metabolism by reducing fat depots [4] and improving insulin resistance [5], preventing the increase in blood of glucose, triglycerides, and insulin levels by increasing adipokine secretion and decreasing oxidative stress pathways [6,7]. Furthermore, GSPE can reduce lipid accumulation through inhibiting preadipocyte differentiation, reducing the formation of new adipocytes and regulating white adipose tissue (WAT) hypertrophy and proliferation, improving therefore WAT function [4,8,9]. Hence, GSPE can effectively prevent obesity through different mechanisms [10].

In this context, it was also reported that the administration of GSPE improved the structural diversity of gut microbiota in high fat diet (HFD)-fed mice, increasing the relative abundance of *Faecalibaculum*, *Bacteroides* and *Akkermansia* as well as, the levels of butyric and propionic acids, changes that correlated with reduced final body weight, decreased insulin resistance and elevated levels of adiponectin and leptin [11]. Furthermore, GSPE ameliorated plasma levels of inflammatory factors such as interleukin-6 or tumor necrosis factor-alpha, reduced epididymal fat mass and improved insulin sensitivity by modulating bacterial content such as *Clostridium*, *Roseburia* and *Prevotella* in HFD mice [12]. This fact is of relevance as gut microbiota has been described as critical for the maintenance of the homeostasis and metabolic functions in the host [13] and alteration in its composition, also known as dysbiosis, can contribute to the development of metabolic diseases such as obesity and MetS [14]. Thus, gut microbiota composition may be another of the mechanisms by

which GSPE affects metabolism preventing obesity. Additionally, it is worth mentioning that about 90-95% of the total ingested polyphenols reach the colon and undergo extensive transformation by gut microbiota [15,16]. Thus, alterations in gut bacteria composition may significantly impact polyphenols functionality since it is believed that the effects of polyphenols are basically driven by its metabolized forms [17]. Therefore, evidence suggests that polyphenols can modulate gut microbiota composition and, at the same time, intestinal bacteria can modulate the metabolism of phenolic compounds, showing a bidirectional interaction that may have a significant impact on phenolic compounds bioactivity.

Seasonal rhythms have been recently reported as a key factor affecting the bioavailability and functionality of polyphenols [18–20], but also gut microbiota composition [19–21]. In this context, fluctuations in environmental cues, mainly driven by the length of the daylight phase, have been linked to changes in gut microbiota [22,23]. In fact, a study carried out in Siberian hamsters revealed that intestinal microbiota is responsive to changes in photoperiods. These changes in bacterial abundance were associated with the elevated body and fat masses observed in animals housed under long summer-like day length conditions (LD) compared to animals housed under short winter-like day length (SD) [21]. Regarding seasonal rhythms effects on polyphenols functionality, cafeteria diet-induced obese rats supplemented with polyphenol-rich fruits showed higher leptin sensitivity only under SD photoperiod [24]. Moreover, normoweight rats housed under different photoperiods and treated with red grapes presented a higher bioavailability of grape phenolic acids under SD photoperiod [18]. In addition, it was recently published that animals fed with a diet containing isoflavones and housed under different photoperiod conditions showed an association between the gut bacterial communities, photoperiod length and isoflavone compounds [25].

Therefore, photoperiods seem to be a key factor in modulating the bidirectional interaction between dietary polyphenols and gut microbiota. However, this

association is still poorly understood and further investigations are needed. Therefore, the aim of this study was to evaluate if GSPE anti-obesity effects can be modulated by gut microbiota in a photoperiod dependent manner.

2. Materials and methods

2.1. Experimental design.

Thirteen weeks-old male F344 rats (n=96) were obtained from Janvier Laboratories, France. Initially rats were pair-housed at standard conditions (22±1ºC, 50-65% relative humidity and 12:12 hour light/dark cycle) with ad libitum access to water and standard chow diet for one week. After this acclimation period, rats were weighted and randomized distributed into three different light-dark cycles (photoperiods) conditions to mimic seasonal day lengths for 9 weeks: short photoperiod [L6, 6 h light/18 h darkness], standard photoperiod [L12, 12 h light/12 h darkness], or long photoperiod [L18, 18 h light/6 h darkness]. Rats were fed a cafeteria diet (CAF) composed of highly palatable and energy-dense human foods (58% CH, 31% lipid, and 11% protein). CAF was freshly prepared every day and included the following (grams per rat and per day): biscuits with pâté and cheese (15-17 g), bacon (7-10 g), ensaimada (pastry) (10-15 g), carrot (11-12 g), standard chow (20-25 g) (Safe-A04c, Germany) and milk containing 22% sucrose (w/v).

Rats were further randomly distributed in four groups (n=8) for each photoperiod condition according to the treatment administrated in the last-4 weeks of the experiment (weeks 5-9) (Fig. 1): 1) vehicle (VH, condensed milk diluted with water in 1:5 proportion), 2) grape seed proanthocyanin extract (GSPE) (25 mg/kg body weight dissolved in VH), 3) VH and an antibiotic cocktail (ABX), and 4) combination of GSPE and ABX. VH and GSPE were daily administered orally one hour after the light was turned on. The antibiotic cocktail (0.5 g/l ampicillin, 0.250 g/l vancomycin and 0.125 g/l imipenem; Discovery fine chemicals Ltd, United Kingdom) was freshly prepared every day

and administered in drinking water. Body weight (BW) was recorded weekly during the whole experimental procedure.

Animals were sacrificed by decapitation following 3 h fasting after the administration of the last dose. Fecal samples for microbiota analysis were freshly collected from the colon and immediately snap-frozen until further analysis. The cecum as well as WAT depots including mesenteric (mWAT), retroperitoneal (RWAT), inguinal (iWAT), epididymal (eWAT) and subcutaneous were collected, weighed and immediately frozen in liquid nitrogen. The visceral mass was calculated as the sum of visceral adipose tissue depots (mWAT, RWAT and eWAT). Total body fat mass was measured as the sum of the visceral fat and subcutaneous fat (iWAT and Subcutaneous). The Adiposity Index was expressed as total body fat mass/final body weight. All the samples were stored at -80°C until further analyses. The Animal Ethics Committee of the University Rovira i Virgili (Tarragona, Spain) and the Generalitat de Catalunya approved all the procedures (number reference 9495) in accordance with the EU Directive 2010/63/EU for animal experiments.

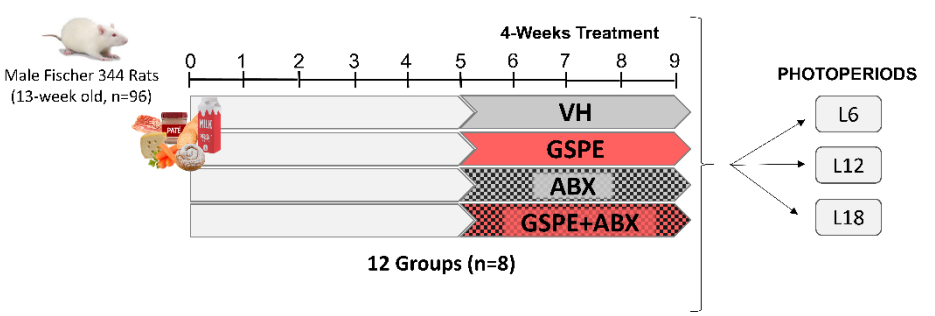

Figure 1. Animal experimental design. *CAF-fed 13-week-old male Fischer 344 rats were pair-housed under three different photoperiods (6, 12 or 18 h of light per day) for 9 weeks. During the last 4 weeks, animals were daily administered with either an oral dose of GSPE (grape seed proanthocyanidin extract) (25mg/kg) dissolved in a solution of water and condensed milk (5:1, VH), or a combination of GSPE and an antibiotic cocktail (ABX) in drinking water (ampicillin: 0.5g/l, vancomycin: 0.25 g/l, imipenem: 0.125 g/l). Vehicle and ABX-treated animals were included as controls. L6: 6h light/18h darkness; L12: 12h light/12h darkness; L18: 18h light/6h darkness; CAF: cafeteria diet; VH: vehicle.*

2.2. Biochemical serum parameters Analysis.

Serum samples were obtained from the blood collected from the neck, in non-heparinized tubes. The blood was incubated for 1 h at room temperature and immediately centrifuged at 1200x g for 15 min to collect the serum. Levels of triglycerides, total cholesterol, glucose (QCA, Barcelona, Spain), and non-esterified free fatty acids (NEFAs) (WAKO, Neuss, Germany) were analyzed in serum samples by enzymatic colorimetric assays. Serum insulin levels were analyzed using a rat insulin ELISA kit (Millipore, Barcelona, Spain) according to the manufacturers' instructions.

2.3. Oral Glucose Tolerance Test.

Oral Glucose tolerance test (OGTT) were performed at the last week. Glucose was orally administered after 6 h fasting (2 g/kg body weight, 50% w/v) and blood glucose levels were measured with a glucometer (Glucocard SM, Menarini Diagnostics, Italy) at 0, 15, 30, 60 and 120 min after glucose administration.

2.4. 16S rRNA analysis.

Fecal DNA was isolated using a QiAamp Fast DNA Stool mini kit (Qiagen Inc., Hilden, Germany) and kept at -20°C until further analysis. Isolated DNA was quantified using a NanoDrop ND2000 spectrophotometer (Thermo Fisher Scientific, Massachusetts, USA) and used for 16S ribosomal RNA sequencing by Ion S5 system (Life Technologies, California, USA) as described previously [26].

2.5. Statistical Analysis.

BW gain and OGTT data were plotted using Graphpad Prism 8.0 software (Graphapad software Inc, San Diego, CA, USA) showing mean ± standard error of the mean (SEM). Statistical analysis was performed using SPSS software (IBS SPSS statistics 25). Normality as well as homogeneity of variance were tested by Shapiro-Wilk test and Levene test respectively for

BW gain, OGTT, biochemical serum parameters and fats depots data. BW gain and OGTT over time was analyzed using repeated-measured ANOVA followed by Tukey HSD/Kramer post hot test at each individual time point. The correspondence area under the curve (AUC) of BW gain and the OGTT, biochemical serum parameters and fats depots data were analyzed by two way ANOVA (factors: GSPE and ABX) followed by Tukey HSD/kramer to evaluate the treatments effect in each photoperiod and by one-way ANOVA followed by Tukey HSD/kramer post hot test to evaluate the photoperiod effect in each group. Additionally, when Tukey HSD/kramer post hoc test showed tendency ($0.05>p<0.1$), effects of treatments were analyzed by Student's t-test.

MicrobiomeAnalyst web-based tool [27,28] was used for faucal microbiota analysis. Features remaining was 34257, after filter features that no contained at least 2 count in 10% of the samples. α-diversity was calculated by Chao1 index and analyzed by Kruskal-Wallis test to elucidate differences between groups. β-diversity was measured based on Bray-Curtis distances and analyzed by permutational multivariate analysis of variance (PERMANOVA) to assess the dissimilarity of faucal microbiota composition among different groups. Afterwards, the nonparametric Mann-Whitney/Kruskal-Wallis test followed by Dunn's multiple comparison and Bonferroni adjustment of P values was performed to elucidate pairwise differences in specific bacteria relative abundance between groups.

The statistical test used for individual analysis is provided in the figure legends.

3. Results

3.1. Grape Seed Proanthocyanidins effects on biometrics and biochemical serum parameters levels were photoperiod dependent.

BW gain, fat depots and biochemical serum parameters were analyzed to elucidate the impact of GSPE treatment and photoperiod exposure on obesity development.

GSPE treatment led to a significant reduction of BW gain only when rats were housed under L18 conditions ($p<0.05$) (**Figure 2**). Furthermore, GSPE-treated rats showed a non-significant decrease in fat depots accumulation compared to VH-treated rats only under L18 conditions ($p>0.05$) (**Table 1**). In contrast, GSPE-treated rats showed higher glucose tolerance after 60 min of glucose administration only under L6 conditions (**Figure 3A, D**). Interestingly, GSPE treatment abolished the photoperiod effect observed on BW and fat depots in VH-treated rats, which showed higher BW gain and fat depots under L18 and higher glucose intolerance under L6 conditions (**Figure 2D; Figure 3D; Table 1**). In addition, GSPE-treated rats showed higher cholesterol and NEFAs levels under L18 conditions compared to VH-treated rats. GSPE-treated rats showed significant higher levels of triglycerides, total cholesterol and NEFAs when rats were housed under L18 compared to rats housed under L6 conditions. In contrast, VH-treated rats showed significant lower levels of triglycerides, total cholesterol and NEFAs under L18 compared to L6 conditions. Glucose and insulin levels did not change due to photoperiod conditions in any treated group (**Table 1**).

Additionally, to evaluate the impact of the gut microbiota on GSPE effects and its interaction with photoperiods, rats were treated with ABX for the last 4 weeks. Rats treated with the combination of GSPE and ABX showed a significant decreased in BW gain by 21% ($p<0.05$) and lower fat depots ($p<0.05$) compared to ABX-treated rats only under L18 conditions. In fact, under L18 photoperiod, ABX-treated rats trended to decrease BW gain by 15% ($p=0.065$) compared to VH-treated rats. Besides this decrease in BW gain, ABX-treated rats did not show any change in fat depots accumulation compared to VH-treated rats (**Figure 2C-D; Table 1**). Moreover, GSPE+ABX-treated rats showed higher glucose tolerance after 60 min of glucose administration compared to ABX-

treated rats only under L6 photoperiods (**Figure 3A**). No significant effects were found in biochemical parameters in GSPE+ABX rats compared to ABX-treated rats. However, significant higher levels of total cholesterol were observed in ABX-treated rats compared to VH-treated rats when housed under L18 conditions (**Table 1**).

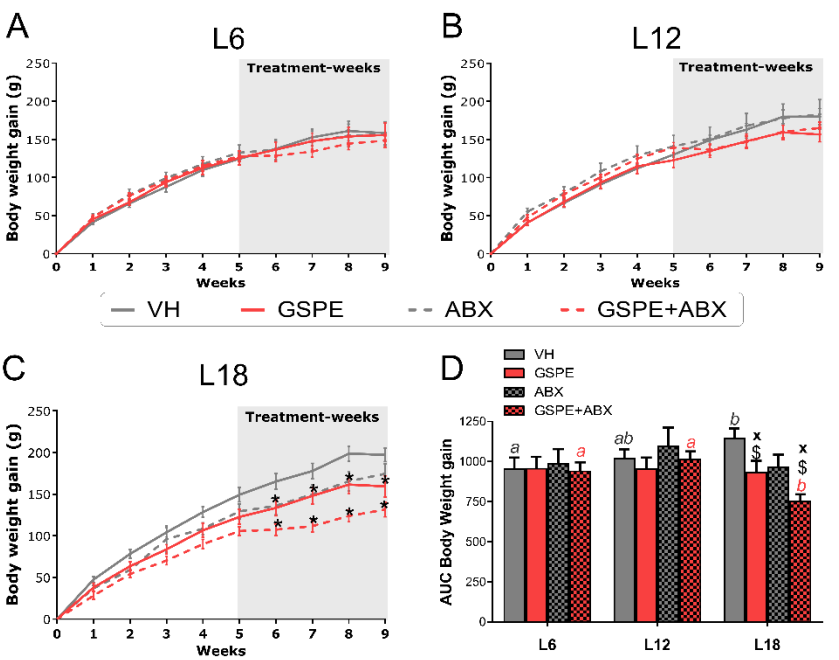

***Figure 2. Effects of photoperiods and treatments on body weight gain**. (**A** to **C**): Body weight gain under (**A**) short (L6), (B) standard (L12), and (**C**) long (L18) photoperiod conditions. * indicates significant GSPE effect, analyzed by measured-repeated ANOVA followed by Tukey HSD/kramer post hoc test (p<0.05); (**D**) Area under the curve (AUC) of body weight gain. $ indicate tendency analyzed by 2-way ANOVA followed by Tukey HSD/kramer post hoc test (0.05>p<0.1); x indicate significant GSPE effect analyzed by Student's t-test (p<0.05); and ab letters indicate photoperiod effect analyzed by one-way ANOVA followed by Tukey HSD/kramer post hoc test (p<0.05).Data are plotted as the mean ± SEM (n=8, except in L6.VH rats n=7). L6: 6h light/18h darkness; L12: 12h light/12h darkness; L18: 18h light/6h darkness; CAF: cafeteria diet; VH: vehicle; GSPE: grape seed proanthocyanidin extract; ABX: antibiotic cocktail.*

Interestingly, GSPE treatment abolished the photoperiod effect observed on BW and fat depots in VH-treated rats, which showed higher BW gain and fat depots under L18 and higher glucose intolerance under L6 conditions (**Figure 2D; Figure 3D; Table 1**). In addition, GSPE-treated rats

showed higher cholesterol and NEFAs levels under L18 conditions compared to VH-treated rats. GSPE-treated rats showed significant higher levels of triglycerides, total cholesterol and NEFAs when rats were housed under L18 compared to rats housed under L6 conditions. In contrast, VH-treated rats showed significant lower levels of triglycerides, total cholesterol and NEFAs under L18 compared to L6 conditions. Glucose and insulin levels did not change due to photoperiod conditions in any treated group (**Table 1**).

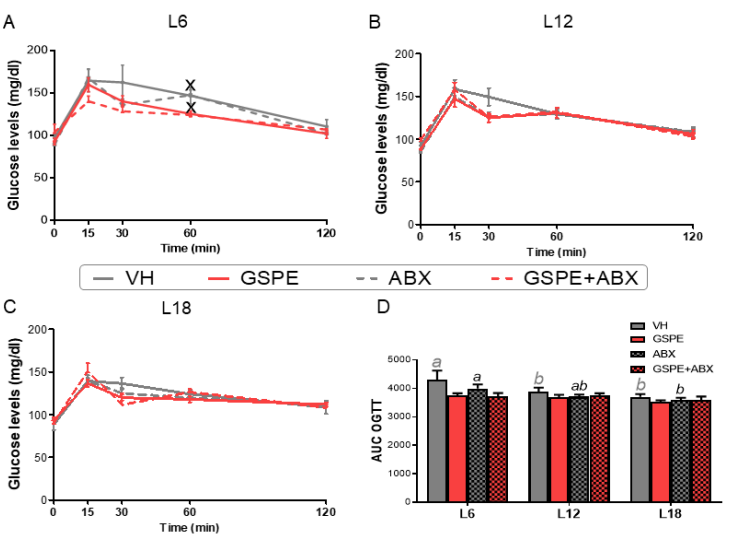

Figure 3. Effects of GSPE and photoperiods on glucose levels. *(**A** to **C**): Oral glucose tolerance test under (**A**) short (L6), (**B**) standard (L12), and (**D**) long (L18) photoperiod conditions. Measured-repeated ANOVA followed by Tukey-kramer post hoc test (p>0.05); x indicates GSPE effect analyzed by Student's t-test at each point (p<0.05); (**D**) Area under the curve (AUC) of glucose tolerance test. ab indicate significant GSPE and Photoperiod effect respectively, analyzed by one-way ANOVA followed by Tukey-kramer post hoc test (p<0.05). Data are plotted as the mean ± SEM (n=8, except in L6.VH n=7). L6: 6h light/18h darkness; L12: 12h light/12h darkness; L18: 18h light/6h darkness; CAF: cafeteria diet; VH: vehicle; GSPE: grape seed proanthocyanidin extract; ABX: antibiotic cocktail.*

Interestingly, a photoperiod effect was found in BW gain in rats treated with GSPE+ABX. Thus, GSPE+ABX-treated rats housed under L18 showed lower BW gain compared to those housed under both L6 and L12 conditions. In contrast, ABX-treated rats did not show any photoperiod effect on BW gain (**Figure 2D**). Furthermore, ABX-treated rats housed under L18 conditions showed

significantly higher iWAT, fat mass and adiposity index compared to those housed under L6 ($p<0.05$) (**Table 1**). Interestingly, GSPE treatment abolished this photoperiod effect in ABX-treated rats. Finally, a significant interaction effect was observed between photoperiod and GSPE in most of the fat depots parameters (iWAT, RWAT, fat mass, adiposity index and visceral mass) (Photoperiod*GSPE, $p<0.05$).

3.1. Grape Seed Proanthocyanidins affects faucal microbiota composition in a photoperiod-dependent manner.

Fecal microbiota composition of the different experimental groups was analyzed in order to evaluate if GSPE modulates it differently depending on the photoperiod conditions, which may explain the photoperiod dependent GSPE effects presented above.

Overall changes in faucal microbiota communities were observed by assessing microbial beta-diversity using a principal coordinates analysis (PCoA) based on Bray Curtis dissimilarity. Regarding GSPE treatment, it did not result in significant clusters (PERMANOVA, $p>0.05$) in any photoperiod conditions (**Figure 4A-B**). However, when analyzing each photoperiod independently, rats treated with GSPE tended to cluster differently from rats treated with VH when housed under L12 conditions (PERMANOVA, $p<0.063$) and L18 conditions (PERMANOVA, p-value<0.077) (**Figure 4A; Figure S1**), suggesting that GSPE may alter gut microbiota depending on photoperiod exposure. Moreover, when comparing GSPE-treated rats with GSPE+ABX-treated rats, a cluster according to ABX treatment was observed, indicating an ABX effect in GSPE-treated rats under the different photoperiod conditions (**Figure 4C**). In addition, GSPE treatment did not alter the α-diversity, Firmicutes-to-Bacteroidetes (F/B) ratio or Proteobacteria-to-Firmicutes (P/F) ratio, which were decreased only by ABX effect (**Figure 4D; Figure 5C-D**).

Table 1. Fat parameters and biochemical serum levels of different CAF-treated groups under the three-photoperiod conditions.

	VH (n=7)			GSPE (n=8)			ABX (n=8)			GSPE+ABX (n=8)			2-way ANOVA (ABX / GSPE)		
	L6	L12	L18	L6	L12	L18	L6	L12	L18	L6	L12	L18			
Biometric Parameters (g)													*L6*	*L12*	*L18*
MWAT	12.2 ± 1.8	14.2 ± 1.6	15.43 ± 0.25	12.72±1.29	15.59±1.68	14.15±1.33	12.75 ± 1.4	13.17 ± 1.7	16.43 ± 1.6	10.25±0.80	13.65±1.48	12.09±1.29*	ns	ns	G
eWAT	16.03 ± 1.8	18.9 ± 0.1	19.69 ± 1.59	18.65±1.10	18.10±1.01	16.47±1.75	17.77 ± 1.2	18.59 ± 1.9	18.63 ± 1.62	15.72±0.78	18.75±0.76	14.86±0.54	ns	ns	ns
iWAT	8.27 ± 1.5	8.64 ± 0.8	9.24 ± 1.39	7.28±0.90	9.44±1.06	7.05±1.00	8.77 ± 0.9	8.41 ± 0.9	11.71 ± 1.2	8.71±0.58	8.98±1.36	7.56±1.23	ns	ns	ns
RWAT	16.81 ± 1.7***a***	21.1 ± 1.2a***b***	22.01 ± 1.5***b***	18.49±1.50	18.44±1.48	19.67±1.44	20.24 ± 1.2	20.91 ± 1.9	23.75 ± 1.4	17.65±0.96	20.58±1.14	16.39±1.53*	ns	ns	G
Subcutaneous	22.50 ± 4.8	19.59 ± 2.6	27.73 ± 3.28	17.98±2.75	19.70±2.21	24.20±2.69	17.95 ± 1.2	18.65 ± 2.8	24.31 ± 2.58	22.61±2.47	19.52±1.93	16.60±1.72*	ns	ns	G
Fat Mass	73.45 ± 9.4***a***	82.56 ± 5.3***ab***	94.09 ± 5.3***b***	75.12±5.85	81.28±4.82	81.54±6.87	75.25 ± 4.6	79.73 ± 7.5	94.84 ± 5.28	74.94±4.34	81.48±5.21	67.50±5.10*	ns	ns	G
Visceral Fat	42.67 ± 4.9***a***	54.33 ± 3.4***ab***	57.13 ± 3.96***b***	49.86±3.61	52.13±3.43	50.29±4.24	50.77 ± 3.1	52.68 ± 5.3	58.82 ± 2.91	43.62±2.01	52.97±2.98	43.34±3.19*	ns	ns	G
Adiposity Index	0.13 ± 0.01***a***	0.14 ± 0.01***ab***	0.16 ± 0.01***b***	0.14±0.01	0.15±0.01	0.14±0.01	0.13 ± 0.01	0.14 ± 0.01	0.16 ± 0.01	0.14±0.01	0.14±0.01	0.12±0.01*	ns	ns	G
Cecum	4.45 ± 0.3	5.08 ± 0.3	5.15 ± 0.38	4.49±0.45	4.52±0.31	4.02±0.24	7.68 ± 0.5#	8.12 ± 0.4#	7.28 ± 0.53#	8.82±0.55#	7.54±0.64#	8.60±0.84#	ns	ns	G
Serum levels (mg/dl)															
Triglycerides	214.77 ± 24.9	201.75 ± 15.7	166.73 ± 22.9	132.49 ± 18.07*****	161.55±14.54	193.54±21.21	184.31 ± 19.2	215.27 ± 26.5	176.08 ± 12.9	179.59± 11.41	196.46±26.92	163.16±15.09	ns	ns	ns
Total Chol.	121.21 ± 16.5***a***	137.03 ± 24.9***b***	104.9 ± 8.9***a***	102.09 ± 12.43***a***	109.12±8.02***ab***	139.29±7.21****b***	113.70 ± 10.3	138.18 ± 12.3	142.66 ± 13.4	116.84 ± 6.77	131.14±17.81	114.19±5.53	ns	ns	G*A
Glucose	135 ± 7.2	144.76 ± 6.2	129.13 ± 4.2	125.53± 8.06	127.91±8.52	137.57±2.96	146.28 ± 4.9	130.09 ± 7.3	140.50 ± 4.6	133.43 ± 4.91	139.18±8.91	129.85±5.20	ns	ns	ns
NEFAs	26.36 ± 2.7***a***	33.17 ± 3.4***a***	20.69 ± 0.7***b***	19.38 ± 1.69***a***	23.37±1.92***ab***	29.26±2.91***b***	25.98 ± 3.6	25.04 ± 3.03	25.98 ± 3.7	24.51 ± 2.07	24.57±1.98	25.75±4.17	ns	ns	ns
Insulin (ng/ml)	13.06 ± 2.8	12.61 ± 1.9	10.17 ± 2.2	13.62 ± 2.49	14.05±2.54	8.52±1.92	17.35 ± 3.9	14.81 ± 3.7	10.95 ± 1.6	11.06± 3.01	11.02±1.21	10.99± 1.61	ns	ns	ns

*Data are expressed as the mean ± SEM. * and # indicate significant GSPE and ABX effects respectively in each photoperiod condition, analyzed by two-way ANOVA (factors: ABX and GSPE) followed by Tukey-kramer post hoc test. ns: no significant effect, G: GSPE effect, G*A, interaction between GSPE and ABX, *p<0.05, #p<0.05; ab letters indicate significant photoperiod effect in each treated group, analyzed by one-way ANOVA followed by Tukey-kramer post hoc test (p<0.05); mWAT, mesenteric white adipose tissue; eWAT, epididymal white adipose tissue; iWAT, inguinal white adipose tissue; RWAT, retroperitoneal white adipose tissue; Chol, cholesterol; NEFAs, non-esterified free fatty acid; L6: 6h light/18h darkness; L12: 12h light/12h darkness; L18: 18h light/6h darkness; CAF: cafeteria diet; VH: vehicle; GSPE: grape seed proanthocyanidin extract; ABX: antibiotic cocktail; Ph: photoperiod.*

Remarkably, photoperiod effects were observed in microbial beta-diversity of VH-treated rats. Thus, VH-treated rats housed under L18 conditions clustered differently from rats housed under either L6 or L12 conditions, which clustered together (**Figure 4A**). Interestingly, this marked L18 photoperiod effect was not observed in GSPE-treated rats which did not cluster differently from rats housed under L6 or L12 conditions (**Figure 4A**), indicating that GSPE may be able to modulate photoperiod effects on gut microbiota composition. This L18 photoperiod effect was less obvious in rats treated with ABX, although certain degree of separation could be observed along the axis 1 independently of VH or GSPE treatment (**Figure 4B**). When analyzing microbial beta-diversity of GSPE-treated rats versus GSPE+ABX-treated rats, a strong L18 photoperiod effect was observed for those receiving GSPE+ABX co-treatment (**Figure 4C**). Thus, GSPE+ABX-treated rats housed under L18 conditions clustered differently from both GSPE- and GSPE+ABX-treated rats housed under L6 and L12 conditions (**Figure 4C**). In addition, the photoperiod effect observed in CAF-fed rats under L12, which showed a significant higher alpha diversity than rats under L6 and L18, was abolished by GSPE, GSPE+ABX, but also by ABX treatments (**Figure 4D**).

Fecal composition was also analyzed at different taxonomic levels. GSPE effect on faucal microbiota composition was different depending on photoperiod conditions (**Figure 6; Table S1**). Thus, although GSPE did not cause changes at phylum level (**Figure 5A**) and at class level only *Bacilli* ($p<0.05$) under L12 and *Actinobacteria* ($p<0.05$) under L18 were affected, several bacteria at order, family and genera levels were significantly altered. For instance, GSPE treatment significantly increased *Bacillales* under L6, *Lactobacillales* under L12 and *Bifidobacteriales* and *Enterobacteriales* orders under L18 condition (**Table S1**). At family level, GSPE treatment significantly decreased *Porphyromonadaceae* under L6 and *Lactobacillaceae* and *Christensenellaceae* under L12 while increased *Prevotellaceae* under L6, and *Bifidobacteriaceae, Enterococcaceae* and *Enterobacteriaceae* under L18 conditions. Finally, among

bacteria genera levels, GSPE significantly decreased *Parabectoroides* and significantly increased *Bacillus, Butyrivibrio* and *Coprococcus* under L6, while significantly decreased *Lactobacillus, Lactococcus* and *Ruminococcus* under L12, and increased *Bifidobacterium* and decreased *Kleibsella* under L18 conditions.

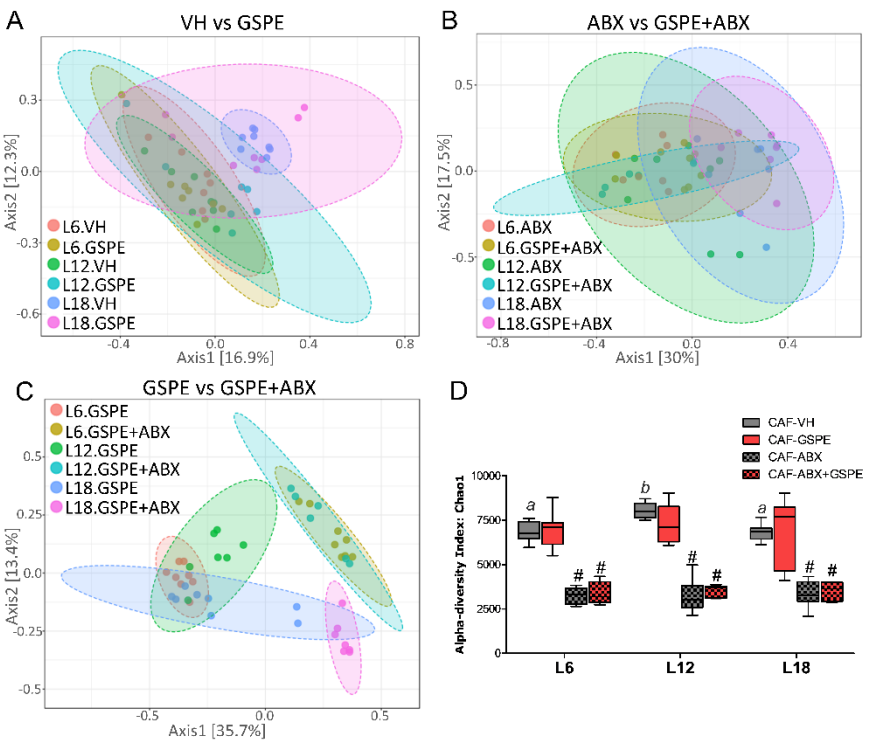

Figure 4. Photoperiod effects on β- and α-diversity. *(**A** to **B**): β-diversity based on Bray-Curtis distances and visualized by a Principal Coordinates Analysis (PCoA) 2D plot (PERMANOVA, p<0.001) in rats treated with (**A**) VH or GSPE and (**B**) ABX or GSPE+ABX under different photoperiod (L6, L12 and L18). (**C**) β-diversity to compare GSPE and GSPE+ABX treatments under different photoperiods (L6, L12 and L18); (**D**): Alpha diversity calculated by chao-1 index in all CAF-groups under different photoperiod conditions. Data are plotted as box and whiskers (median with interquartile ranges). # indicates significant ABX effect between VH- and ABX-treated rats under same photoperiod conditions, analyzed by U-Mann Whitney (p<0.05); ab letters indicate significant photoperiod effect analyzed by Kruskal-Wallis test followed by Bonferroni correction for multiple comparisons (p<0.016). (n=8, except L6.CAF-VH n=7). L6: short photoperiod (6h light/18h dark); L12: standard photoperiod (12h light/12h dark); L18: long photoperiod (18h light/6h dark); L6: 6h light/18h darkness; L12: 12h light/12h darkness; L18: 18h light/6h darkness; CAF: cafeteria diet; VH: vehicle; GSPE: grape seed proanthocyanidin extract; ABX: antibiotic cocktail.*

Interestingly, photoperiod housing conditions also significantly affected several bacterial genera relative abundance in GSPE-treated rats (**Figure 7; Table S1**).

In CAF-fed rats receiving GSPE, photoperiod effects were observed for low abundance genera belonging to the Firmicutes phyla such as *Butyricimonas*, *Coprobacillus*, *Rummelibacillus* and *Lachnobacterium*, which showed higher levels in rats housed under L18 compared to those housed under L6 conditions. GSPE treatment also altered genera belonging to Proteobacteria phyla such as *Enterobacter*, *Erwinia* and *Kleibsella*, increasing their levels under L18 compared to L6. Interestingly, GSPE treatment abolished the photoperiod effect observed in the most abundant bacterial genera compared to VH rats. Thus, *Bacteroides*, *Oscillospira*, *Sutterella*, *Coprococcus* and *Ruminococcus* did not show photoperiod effect in these GSPE-treated rats.

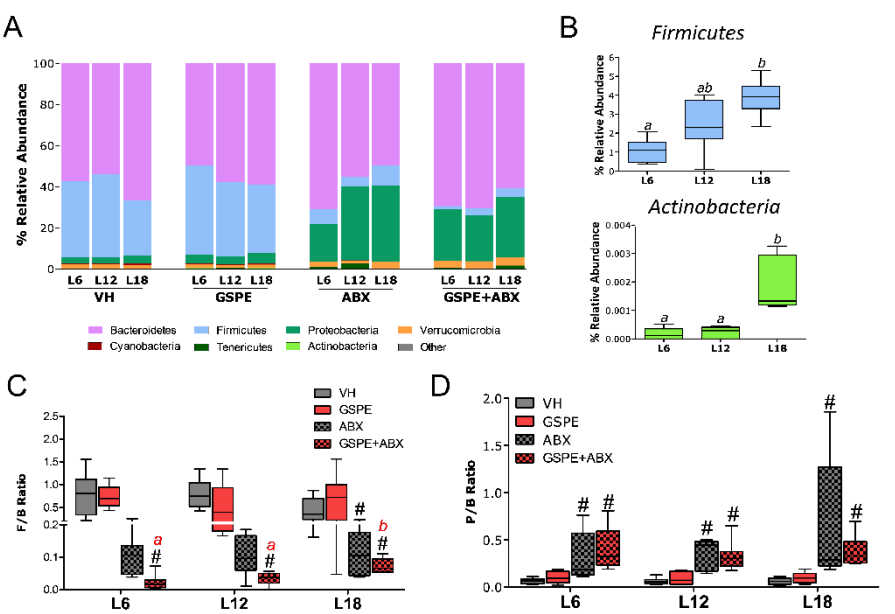

Figure 5. Effect of photoperiods on bacteria phyla relative abundance. (**A**) Stacked bar plots showing the relative abundance of taxa at phylum level. (**B**) Box and whiskers plots with interquartile ranges for Firmicutes and Actinobacteria relative abundance of GSPE+ABX rats under different photoperiods; (**C**) Box and whiskers plots (median with interquartile ranges) for Firmicutes-to-Bacteroidetes (F/B) ratio and (**D**) for Proteobacteria-to-Bacteroidetes (P/B) ratio; # and ab letters indicate ABX and photoperiod significant effects respectively, analyzed by Kruskal-Wallis followed by Bonferroni correction for multiple comparisons ($p<0.016$). (n=8, except L6.CAF-VH n=7). L6: short photoperiod (6h light/18h dark); L12: standard photoperiod (12h light/12h dark); L18: long photoperiod (18h light/6h dark). L6: 6h light/18h darkness; L12: 12h light/12h darkness; L18: 18h light/6h darkness; CAF: cafeteria diet; VH: vehicle; GSPE: grape seed proanthocyanidin extract; ABX: antibiotic cocktail.

On the other hand, several bacteria at the different taxonomic levels were altered by the combination of GSPE and ABX treatments compared to ABX-treated rats, also depending on photoperiod conditions (**Figure 6; Table S1**).Thus, when analyzing GSPE effects in ABX-treated rats (GSPE+ABX compared to ABX group) a significant decrease in *Firmicutes* relative abundance ($p<0.05$) and a tendency to increase *Proteobacteria* relative abundance ($p=0.059$) were observed only when rats were housed under L6 conditions (**Figure 5A**). In addition, GSPE treatment increased the relative abundance of *Clostridia* class under L6 and of *Actinobacteria* class under L18, while no bacteria class was affected under L12 conditions. At order level, *Bacillales* was significantly increased and *Clostridiales*, *Rhizobiales* and *Rhodospirillaled* were significantly decreased under L6, *Aeromonadales* was decreased under L12 and *Bifidobacteriales* were increased under L18. At family level, *Lactobacillaceae* were increased under L6, *Lachnospiraceae* and *Aeromonadaceae* were decreased under L12, and *Bifidobacteriaceae, Porphyromonadaceae* and *Lachnospiraceae* were increased under L18 conditions. Finally, among bacteria genera, GSPE+ABX decreased *Bacteroides* and *Lactobacillus* and increased *Ruminococcus* under L6, decreased *Coprococcus, Prevotella* and *Ruminococcus* and increased *Bacteroides* and *Bilophila* under L12, and increased *Bifidobacterium*, *Parabacteroides*, *Blautia* and *Bilophila* under L18 conditions (**Figure 6; Table S1**).

Additionally, in GSPE+ABX-treated rats, the major photoperiod effects were found in genera belonging to the Proteobacteria, Firmicutes and Actinobacteria phyla, being mostly altered in rats housed under L18 conditions. Interestingly, a photoperiod effect was also observed in ABX-treated rats. Thus, *Bacteroides,* one of the most abundant genera, showed significant higher levels under L6 compared to both L12 and L18 in ABX-treated rats. However, when GSPE+ABX was administered, *Bacteroides* levels were increased under L12 compared to L18 conditions. *Sutterella* and *kleibsella* showed significant lower abundance under L6 compared to both L12 and L18 in ABX-treated rats. In contrast, rats

treated with GSPE+ABX did not show any photoperiod effect in these bacteria genera, but showed a no significant increase of *Sutterella* levels under L6 and a no significant decrease of *Kleibsella* levels under L18. *Enterobacter*, which was altered in all groups, was higher under L18 compared to L6 and L12 photoperiods in both ABX and ABX+GSPE treated rats. Finally, it is worth highlighting that GSPE+ABX treatment also altered other bacteria genera with lower abundance, such as *Bifidobacterium* and *Lysinibacillus,* which were increased under L18 conditions. This effect was not observed when rats were treated with ABX only (**Figure 7; Table S1**).

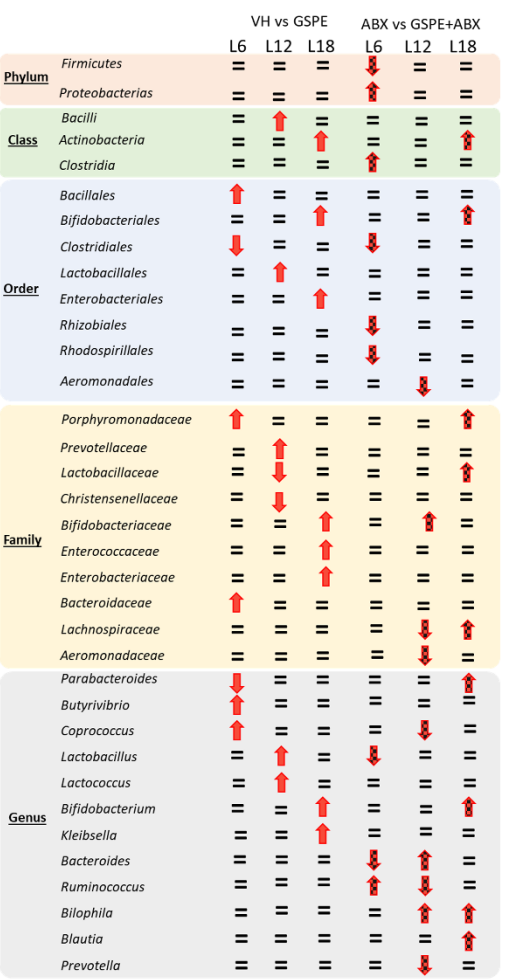

Figure 6. GSPE effects depended on photoperiod conditions. *Summary of significant GSPE effects in the different photoperiod conditions, when comparing VH versus GSPE-treated rats and ABX versus GSPE+ABX-treated rats.*

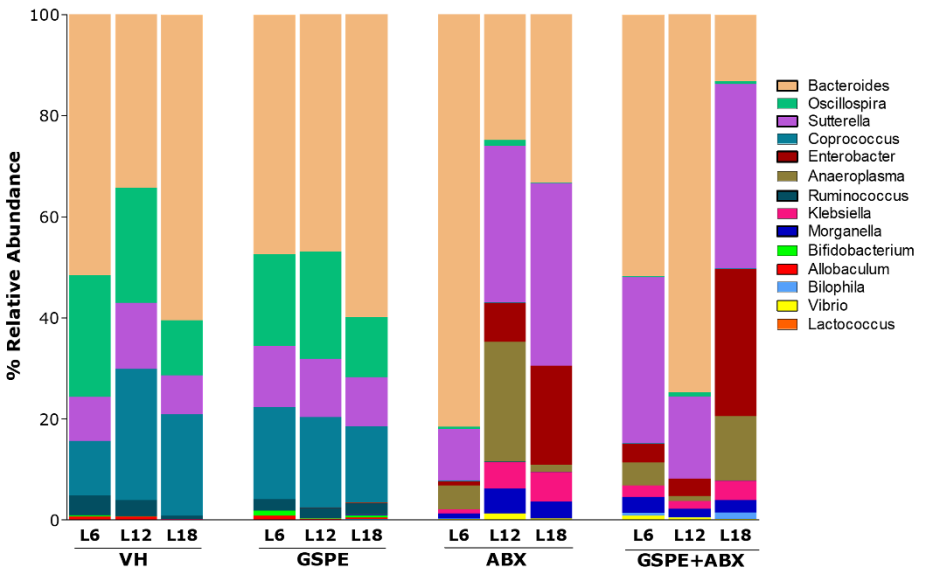

Figure 7. Relative abundance at genus level of the 14 most abundant genera. *Stacked bar plots showing the relative abundance of taxa at genus level (n=8, except L6.VH n=7)); L6: 6h light/18h darkness; L12: 12h light/12h darkness; L18: 18h light/6h darkness; CAF: cafeteria diet; VH: vehicle; GSPE: grape seed proanthocyanidin extract; ABX: antibiotic cocktail.*

4. Discussion

Dietary polyphenols naturally present in fruits and vegetables are gaining increasing attention due to their beneficial health effects on obesity and MetS development [29,30]. Hence, the study of factors affecting polyphenols bioactivities is of high interest nowadays. Gut microbiota is one of the main factors that may be playing an important role on polyphenols functionality. Thus, gut bacteria are significantly involved in polyphenols metabolism. Moreover, recent studies indicate that dietary polyphenols are relevant in the modulation of gut microbiota composition, which are crucial for the maintenance of homeostasis and metabolic function in the host [31,32]. Additionally, seasonal rhythms have recently been established as key factors in the modulation of the gut microbial and, interestingly, also in the metabolism of polyphenols [20,33]. However, the interaction between polyphenols, gut microbiota and photoperiods is poorly understood and further investigations are needed. Thus, the purpose of this study was to evaluate if the beneficial

anti-obesity effects of GSPE are modulated by gut microbiota in a photoperiod dependent manner.

Different photoperiod conditions were used to mimic seasonal rhythms. The short photoperiod conditions emulated the hours of light in short days typical of the winter season, while the long photoperiod conditions simulated the long days typical of the summer season. GSPE was orally administered at 25 mg/kg/day which is within the estimated range of polyphenols intake in humans. This is equivalent to the daily intake of 367 mg for a person of 70 kg [34], which is easy to achieve with a polyphenol-rich diet [35–37]. Furthermore, the use of low doses of GSPE have shown beneficial effects on obesity development, not being necessary the administration of high doses in order to get a positive effect [5]. Thus, GSPE has been proven to have lipolytic properties and to be an effective anti-obesity agent when administered at this low dose [38]. Moreover, administration of 25 mg/kg/day of GSPE to CAF-fed Wistars rats during 3 weeks decreased body weight gain and adipose depots accumulation [39]. Furthermore, the same doses administered for 2 weeks significantly reduced adiposity index in hamster fed with a high fat diet, although BW gain was not affected [6]. However, GSPE administration at the same dose for 30 days did not significant decrease body weight or fat depots in diet-induced obese female Wistars rats [5]. In this study, the results did not show a significant reduction of BW gain or fat depots in standard conditions (L12 photoperiod) by GSPE treatment. These discrepancies regarding the GSPE effect on BW gain and fat depots may result from the use of animals of different age, sex and strains as well as, from the duration of the treatment.

In our study, rats housed under L18 conditions gained more BW compared to rats housed under L6 or L12 conditions. Interestingly, GSPE treatment decreased significantly this BW gain observed in this long photoperiod. The higher BW gain under long photoperiod conditions is in accordance with other studies reporting increased BW gain in rats held under photoperiods of more than 12 h of light/day compared to rats held under photoperiods of less than

10 h of light/day [40]. Indeed, increased BW under long photoperiods is common in mammals, who are able to adapt to changes in the light and dark cycle during the different seasons, and it is associated with a more efficient pattern of energy harvesting from the consumed food [41,42].

Interestingly, the GSPE effects observed in L18 can be associated with changes in fecal microbiota composition. Hence, GSPE altered gut microbiota composition differently depending on the photoperiod conditions. Thus, GSPE increased levels of *Bifidobacterium* and *Coprobacillus* and decreased *Kleibsella* genera only under L18. These bacteria genera levels are linked to lower body weight gain and non-obese phenotypes [43,44]. In contrast, decreased *Parabacteroides* under L6 and *Lactobacillus, Lactococcus* and *Ruminococcus* under L12. Strains belonging to *Parabacteroides* genera such as *P. goldsteinii* and *P. distasonis* have been described as important bacteria with anti-obesity effects [45,46]. Furthermore, strains of *Lactobacillus, Lactococcus* and *Ruminococcus* genera, belonging to Firmicutes phyla, have been associated with lower BW gain. Thus, *Lactobacillus* strains are able to alleviate obesity in mice induced by high-fat diet via relieving fat accumulation, lipid metabolism and regulating the content of leptin and adiponectin [47], *Lactococcus* reduce weight gain and lipid accumulation and regulating leptin and adipokine secretion [48], and *Ruminococcus* genera has been shown to decreased in obese subjects and is known as potential butyrate producer, which exert beneficial effects against obesity by increasing lipid oxidation [49,50]. Therefore, these changes in the gut microbiota composition by GSPE depending on photoperiod may help to explain the difference of BW gain in GSPE-treated rats under L18 compared to both L6 and L12 conditions.

In addition, the differences in BW gain depending on photoperiod conditions have been linked with changes in gut microbiota composition correlated with higher capacity to harvest energy from diet and increase glucose and fatty acid absorption [51]. Thus, evidence in Siberian hamster [19], broiler roosters [52], Sprague-Dawley rats [53] and humans [54] have shown different gut

microbiota composition depending on photoperiod exposure. In this context, GSPE decreased the photoperiod effect observed on faucal microbiota composition in VH-treated rats, showing similar beta- and alpha-diversity independently of photoperiod conditions, and modulating the most abundant genera. Accordingly, *Bacteroides*, *Oscillospira*, *Coprococcus* and *Ruminococcu*s genera levels, which were associated with higher BW gain and fat depots accumulation under L18 in VH-treated rats [26], did not show any photoperiod effect in GSPE-treated rats. Therefore, GSPE affected BW gain and gut microbiota composition in a photoperiod dependent manner, suggesting a potential interaction among GSPE, gut microbiota and photoperiod conditions.

To further evaluate the role of gut microbiota on GSPE effects in the different photoperiod conditions, rats were treated with an ABX cocktail. The effects of this cocktail on gut microbiota were consistent with previous studies [55,56]. Remarkably, the effect of GSPE on BW gain observed in L18 conditions was potentiated in ABX-treated rats. Furthermore, GSPE also significant decreased fat depots accumulation only under L18 in ABX-treated rats. Moreover, GSPE+ABX-treated rats showed a significant L18 effect on faucal microbiota composition. Therefore, the differences in GSPE anti-obesity effects observed in this group under L18 could be due to changes in the bioavailability of GSPE mediated by more pronounced changes in gut microbiota observed in these conditions [12,57]. Thus, it has been estimated that the 90-95% of the total polyphenol intake remain unabsorbed in the small intestine and they are metabolized by the gut microbiota in the colon [15,16]. The gut microbiota therefore play an important role in the extensive breakdown of polyphenols into a low-molecular-weight phenolic acids and other microbial-derived metabolites that can be absorbed into the circulatory system and confer health benefits [17]. Thus, changes in the gut microbiota composition mediated by ABX treatment and photoperiod conditions, may change microbial-derived GSPE metabolites, altering the bioactivities of this polyphenol extract. Indeed, ABX+GSPE treatment led to significant photoperiod effect on *Firmicutes* and

Actinobacteria phyla, increasing both of them under L18. These high levels of *Firmicutes* under L18 promoted an increase in F/B ratio, which could be associated to lower body mass in these rats. In fact, other studies using cafeteria diet reported that the F/B ratio is decreased in these induced-obese rats due to the differences in the type of fat present in this diet, mainly lard and milk-derived fat, in comparison with other high fat diets induced obesity models [58,59]. In addition, the increase of *Actinobacteria* in L18 led to significant higher levels of *Bifidobacterium* genera in this photoperiod. *Bifidobacterium* is the most studied genus of *Actinobacteria* phylum, showing a high versatility [60,61]. These bacteria metabolize dietary compounds and ferment non-digestible dietary foods resulting in the formation of SCFAs, and are able to displace harmful bacteria by competing with pathogens for nutrients [62]. Likewise, *Bifidobacterium* has been reported to exert anti-obesity effects [63–65], which is in concordance with our previous results where this bacterium taxon was associated with decreased body mass. Therefore, we suggest that the strongest effect of GSPE in decreasing body weight gain in ABX-treated rats housed under L18 conditions may be mediated by these changes in gut microbiota observed in these photoperiod conditions.

It is also important to consider the effect of ABX administration on the body composition, since several studied have provided increasing evidence for an association between the ABX consumption and weight gain and fat accumulation [66–68]. However, our results did not show ABX effects on body weight gain, body composition nor serum parameters, which could be due to differences in the doses employed and/or the duration of the treatment.

5. Conclusions

GSPE administered together with ABX potentiated the decrease of BW gain and body composition only under L18 compared to when GSPE was administered alone, which suggests an interaction between polyphenols, gut microbiota, and photoperiods. Thus, GSPE anti-obesity effects were modulated by gut

microbiota in a photoperiod dependent manner. Therefore, seasonal rhythms and gut microbiota are key factors that must be taken into account when investigating the benefits of polyphenols in the organism.

Author Contributions

Conceptualization: V.A.-G., A.A.-A. and C.T.-F.; Formal analysis: V.A.-G. and I.E.-M.; Data curation: V.A.-G; Investigation: V.A.-G., I.E.-M., M.S., B.M., G.A., A.A.-A. and C.T.-F.; Methodology: V.A.-G., A.A.-A. and C.T.-F.; Funding acquisition: B.M., M.S., G.A., A.A.-A. and C.T-F.; Project administration: B.M., M.S., G.A.,A.A.-A. and C.T-F.; Resources: B.M., M.S., G.A., A.A.-A. and C.T-F.; Software: V.A-G; Visualization: V.A.-G.; Supervision: A.A.-A. and C.T-F; Validation: V.A.-G., A.A.-A. and C.T.-F.; Writing original draft: V.A.-G.; Writing review & editing: A.A.-A. and C.T.-F.

Conflict of interest

There are no conflicts to declare.

Acknowledgements

This work was supported by MCIN/AEI/10.13039/501100011033/ FEDER “Una manera de hacer Europa” (AGL2016-77105-R) and “2021/22 Development of a prototype for the establishment of a dysbiosis (alteration) in the intestinal microbiota”, co-financed by Diputació de Tarragona (2021PGR-DIPTA-URV09). V.A.-G. was supported by the Martí i Franquès Doctoral Fellowships Programme, Universitat Rovira i Virgili (PMF-PIPF-35); I.E.-M. was supported by the Youth Employment Initiative from the European Social Fund, Ministry of Science, The State Research Agency and Universitat Rovira i Virgili (PEJ2018-002778-A); G.A. and A.A-A were supported by the Serra Húnter Programme, Government of Catalonia; C.T.-F. was supported by Beatriu de Pinós Postdoctoral Programme of the Government of Catalonia’s Secretariat for Universities and Research of the Ministry of Economy and Knowledge. The

authors would like to thank Niurka Dariela Llópiz and Rosa Pastor for their assistance.

References

[1] Pérez-Jiménez J, Neveu V, Vos F, Scalbert A. Identification of the 100 richest dietary sources of polyphenols: an application of the Phenol-Explorer database. Eur J Clin Nutr 2010 643 2010;64:S112–20. https://doi.org/10.1038/ejcn.2010.221.

[2] Del Rio D, Rodriguez-Mateos A, Spencer JPE, Tognolini M, Borges G, Crozier A. Dietary (poly)phenolics in human health: structures, bioavailability, and evidence of protective effects against chronic diseases. Antioxid Redox Signal 2013;18:1818–92. https://doi.org/10.1089/ARS.2012.4581.

[3] Liu M, Yun P, Hu Y, Yang J, Khadka RB, Peng X. Effects of Grape Seed Proanthocyanidin Extract on Obesity. Obes Facts 2020;13:279–91. https://doi.org/10.1159/000502235.

[4] Pascual-Serrano A, Arola-Arnal A, Suárez-García S, Bravo FI, Suárez M, Arola L, et al. Grape seed proanthocyanidin supplementation reduces adipocyte size and increases adipocyte number in obese rats. Int J Obes 2017;41:1246–55. https://doi.org/10.1038/IJO.2017.90.

[5] Montagut G, Bladé C, Blay M, Fernández-Larrea J, Pujadas G, Salvadó MJ, et al. Effects of a grapeseed procyanidin extract (GSPE) on insulin resistance. J Nutr Biochem 2010;21:961–7. https://doi.org/10.1016/J.JNUTBIO.2009.08.001.

[6] Caimari A, Del Bas JM, Crescenti A, Arola L. Low doses of grape seed procyanidins reduce adiposity and improve the plasma lipid profile in hamsters. Int J Obes 2013 374 2012;37:576–83. https://doi.org/10.1038/ijo.2012.75.

[7] Caimari A, Mariné-Casadó R, Boqué N, Crescenti A, Arola L, Maria Del Bas J. Maternal intake of grape seed procyanidins during lactation induces insulin resistance and an adiponectin resistance-like phenotype in rat offspring OPEN n.d. https://doi.org/10.1038/s41598-017-12597-9.

[8] Guerrero L, Margalef M, Pons Z, Quiñones M, Arola L, Arola-Arnal A, et al. Serum metabolites of proanthocyanidin-administered rats decrease lipid synthesis in HepG2 cells. J Nutr Biochem 2013;24:2092–9. https://doi.org/10.1016/J.JNUTBIO.2013.08.001.

[9] Pinent M, Bladé MC, Salvadó MJ, Arola L, Hackl H, Quackenbush J, et al. Grape-seed derived procyanidins interfere with adipogenesis of 3T3-L1 cells at the onset of differentiation. Int J Obes 2005 298 2005;29:934–41. https://doi.org/10.1038/sj.ijo.0802988.

[10] Rodríguez-Pérez C, García-Villanova B, Guerra-Hernández E, Verardo V. Grape Seeds Proanthocyanidins: An Overview of In Vivo Bioactivity in Animal Models. Nutrients 2019;11. https://doi.org/10.3390/NU11102435.

[11] Du H, Wang Q, Li T, Ren D, Yang X. Grape seed proanthocyanidins reduced the

overweight of C57BL/6J mice through modulating adipose thermogenesis and gut microbiota. Food Funct 2021;12:8467–77. https://doi.org/10.1039/D1FO01361K.

[12] Liu W, Zhao S, Wang J, Shi J, Sun Y, Wang W, et al. Grape seed proanthocyanidin extract ameliorates inflammation and adiposity by modulating gut microbiota in high-fat diet mice. Mol Nutr Food Res 2017;61:1601082. https://doi.org/10.1002/MNFR.201601082.

[13] Patterson EE, Ryan PM, Cryan JF, Dinan TG, Paul Ross R, Fitzgerald GF, et al. Gut microbiota, obesity and diabetes. Postgrad Med J 2016;92:286–300. https://doi.org/10.1136/postgradmedj-2015-133285.

[14] Torres-Fuentes C, Schellekens H, Dinan TG, Cryan JF. The microbiota–gut–brain axis in obesity. Lancet Gastroenterol Hepatol 2017;2:747–56. https://doi.org/10.1016/S2468-1253(17)30147-4.

[15] Clifford MN. Diet-derived phenols in plasma and tissues and their implications for health. Planta Med 2004;70:1103–14. https://doi.org/10.1055/S-2004-835835/ID/2.

[16] Monagas M, Urpi-Sarda M, Sánchez-Patán F, Llorach R, Garrido I, Gómez-Cordovés C, et al. Insights into the metabolism and microbial biotransformation of dietary flavan-3-ols and the bioactivity of their metabolites. Food Funct 2010;1:233–53. https://doi.org/10.1039/c0fo00132e.

[17] Cardona F, Andrés-Lacueva C, Tulipani S, Tinahones FJ, Queipo-Ortuño MI. Benefits of polyphenols on gut microbiota and implications in human health. J Nutr Biochem 2013;24:1415–22. https://doi.org/10.1016/j.jnutbio.2013.05.001.

[18] Iglesias-Carres L, Mas-Capdevila A, Bravo FI, Arola L, Muguerza B, Arola-Arnal A. Exposure of Fischer 344 rats to distinct photoperiods influences the bioavailability of red grape polyphenols. J Photochem Photobiol B Biol 2019;199:111623. https://doi.org/10.1016/j.jphotobiol.2019.111623.

[19] Ren CC, Sylvia KE, Munley KM, Deyoe JE, Henderson SG, Vu MP, et al. Photoperiod modulates the gut microbiome and aggressive behavior in Siberian hamsters. J Exp Biol 2020;223. https://doi.org/10.1242/jeb.212548.

[20] Shor EK, Brown SP, Freeman DA. A novel role for the pineal gland: Regulating seasonal shifts in the gut microbiota of Siberian hamsters. J Pineal Res 2020;69:e12696. https://doi.org/10.1111/jpi.12696.

[21] Bailey MT, Walton JC, Dowd SE, Weil ZM, Nelson RJ. Photoperiod modulates gut bacteria composition in male Siberian hamsters (Phodopus sungorus). Brain Behav Immun 2010;24:577–84. https://doi.org/10.1016/J.BBI.2009.12.010.

[22] Fan C, Zhang L, Jia S, Tang X, Fu H, Li W, et al. Seasonal variations in the composition and functional profiles of gut microbiota reflect dietary changes in plateau pikas. Integr Zool 2022. https://doi.org/10.1111/1749-4877.12630.

[23] Yang X, Yao Y, Zhang X, Zhong J, Gao F, Zhang H, et al. Seasonal Changes in the Distinct Taxonomy and Function of the Gut Microbiota in the Wild Ground

Squirrel (Spermophilus dauricus). Anim an Open Access J from MDPI 2021;11. https://doi.org/10.3390/ANI11092685.

[24] Ibars M, Aragonès G, Ardid-Ruiz A, Gibert-Ramos A, Arola-Arnal A, Suárez M, et al. Seasonal consumption of polyphenol-rich fruits affects the hypothalamic leptin signaling system in a photoperiod-dependent mode. Sci Rep 2018;8. https://doi.org/10.1038/S41598-018-31855-Y.

[25] Oyola MG, Johnson RC, Bauman BM, Frey KG, Russell AL, Cho-Clark M, et al. Gut microbiota and metabolic marker alteration following dietary isoflavone-photoperiod interaction. Endocrinol Diabetes Metab 2021;4:e00190. https://doi.org/10.1002/EDM2.190.

[26] Arreaza-Gil V, Escobar-Martínez I, Suárez M, Bravo F, Muguerza B, Arola-Arnal A, et al. Gut Seasons: Photoperiod Effects on Fecal Microbiota in Healthy and Cafeteria-Induced Obese Fisher 344 Rats. Nutrients 2022;14:722. https://doi.org/10.3390/NU14030722.

[27] Chong J, Liu P, Zhou G, Xia J. Using MicrobiomeAnalyst for comprehensive statistical, functional, and meta-analysis of microbiome data. Nat Protoc 2020;15:799–821. https://doi.org/10.1038/s41596-019-0264-1.

[28] Dhariwal A, Chong J, Habib S, King IL, Agellon LB, Xia J. MicrobiomeAnalyst: A web-based tool for comprehensive statistical, visual and meta-analysis of microbiome data. Nucleic Acids Res 2017;45:W180–8. https://doi.org/10.1093/nar/gkx295.

[29] Ohishi T, Fukutomi R, Shoji Y, Goto S, Isemura M. The Beneficial Effects of Principal Polyphenols from Green Tea, Coffee, Wine, and Curry on Obesity. Mol 2021, Vol 26, Page 453 2021;26:453. https://doi.org/10.3390/MOLECULES26020453.

[30] Wang S, Moustaid-Moussa N, Chen L, Mo H, Shastri A, Su R, et al. Novel insights of dietary polyphenols and obesity. J Nutr Biochem 2014;25:1–18. https://doi.org/10.1016/J.JNUTBIO.2013.09.001.

[31] Man AWC, Xia N, Daiber A, Li H. The roles of gut microbiota and circadian rhythm in the cardiovascular protective effects of polyphenols. Br J Pharmacol 2020;177:1278–93. https://doi.org/10.1111/bph.14850.

[32] Song D, Yang CS, Zhang X, Wang Y. The relationship between host circadian rhythms and intestinal microbiota: A new cue to improve health by tea polyphenols. Crit Rev Food Sci Nutr 2020;0:1–10. https://doi.org/10.1080/10408398.2020.1719473.

[33] Bailey MT, Walton JC, Dowd SE, Weil ZM, Nelson RJ. Photoperiod modulates gut bacteria composition in male Siberian hamsters (Phodopus sungorus). Brain Behav Immun 2010;24:577–84. https://doi.org/10.1016/j.bbi.2009.12.010.

[34] Reagan-Shaw S, Nihal M, Ahmad N. Dose translation from animal to human studies revisited. FASEB J 2008;22:659–61. https://doi.org/10.1096/FJ.07-9574LSF.

[35] Saura-Calixto F, Serrano J, Goñi I. Intake and bioaccessibility of total

polyphenols in a whole diet. Food Chem 2007;101:492–501. https://doi.org/10.1016/J.FOODCHEM.2006.02.006.

[36] Wang Y, Chung SJ, Song WO, Chun OK. Estimation of Daily Proanthocyanidin Intake and Major Food Sources in the U.S. Diet. J Nutr 2011;141:447–52. https://doi.org/10.3945/JN.110.133900.

[37] Zamora-Ros R, Andres-Lacueva C, Lamuela-Raventós RM, Berenguer T, Jakszyn P, Barricarte A, et al. Estimation of Dietary Sources and Flavonoid Intake in a Spanish Adult Population (EPIC-Spain). J Am Diet Assoc 2010;110:390–8. https://doi.org/10.1016/J.JADA.2009.11.024.

[38] Salvadó MJ, Casanova E, Fernández-Iglesias A, Arola L, Bladé C. Roles of proanthocyanidin rich extracts in obesity. Food Funct 2015;6:1053. https://doi.org/10.1039/c4fo01035c.

[39] Pajuelo D, Quesada H, Díaz S, Fernández-Iglesias A, Arola-Arnal A, Bladé C, et al. Chronic dietary supplementation of proanthocyanidins corrects the mitochondrial dysfunction of brown adipose tissue caused by diet-induced obesity in Wistar rats. Br J Nutr 2012;107:170–8. https://doi.org/10.1017/S0007114511002728.

[40] Tavolaro FM, Thomson LM, Ross AW, Morgan PJ, Helfer G. Photoperiodic Effects on Seasonal Physiology, Reproductive Status and Hypothalamic Gene Expression in Young Male F344 Rats. J Neuroendocrinol 2015;27:79–87. https://doi.org/10.1111/jne.12241.

[41] Goldman BD. Mammalian photoperiodic system: Formal properties and neuroendocrine mechanisms of photoperiodic time measurement. J Biol Rhythms 2001;16:283–301. https://doi.org/10.1177/074873001129001980.

[42] Hut RA, Beersma DGM. Evolution of time-keeping mechanisms: Early emergence and adaptation to photoperiod. Philos Trans R Soc B Biol Sci 2011;366:2141–54. https://doi.org/10.1098/rstb.2010.0409.

[43] Yin YN, Yu QF, Fu N, Liu XW, Lu FG. Effects of four Bifidobacteria on obesity in high-fat diet induced rats. World J Gastroenterol 2010;16:3394–401. https://doi.org/10.3748/wjg.v16.i27.3394.

[44] Zeng Q, Li D, He Y, Li Y, Yang Z, Zhao X, et al. Discrepant gut microbiota markers for the classification of obesity-related metabolic abnormalities n.d. https://doi.org/10.1038/s41598-019-49462-w.

[45] Wu TR, Lin CS, Chang CJ, Lin TL, Martel J, Ko YF, et al. Gut commensal Parabacteroides goldsteinii plays a predominant role in the anti-obesity effects of polysaccharides isolated from Hirsutella sinensis. Gut 2019;68:248–62. https://doi.org/10.1136/GUTJNL-2017-315458.

[46] Wang K, Liao M, Zhou N, Bao L, Ma K, Zheng Z, et al. Parabacteroides distasonis Alleviates Obesity and Metabolic Dysfunctions via Production of Succinate and Secondary Bile Acids. Cell Rep 2019;26:222-235.e5. https://doi.org/10.1016/J.CELREP.2018.12.028.

[47] Wang M, Zhang B, Hu J, Nie S, Xiong T, Xie M. Intervention of five strains of

Lactobacillus on obesity in mice induced by high-fat diet. J Funct Foods 2020;72:104078. https://doi.org/10.1016/J.JFF.2020.104078.

[48] Zhang Q, Kim JH, Kim Y, Kim W. Lactococcus chungangensis CAU 28 alleviates diet-induced obesity and adipose tissue metabolism in vitro and in mice fed a high-fat diet. J Dairy Sci 2020;103:9803–14. https://doi.org/10.3168/JDS.2020-18681.

[49] Raman M, Ahmed I, Gillevet PM, Probert CS, Ratcliffe NM, Smith S, et al. Fecal microbiome and volatile organic compound metabolome in obese humans with nonalcoholic fatty liver disease. Clin Gastroenterol Hepatol 2013;11:868-875.e3. https://doi.org/10.1016/j.cgh.2013.02.015.

[50] Gao Z, Yin J, Zhang J, Ward RE, Martin RJ, Lefevre M, et al. Butyrate improves insulin sensitivity and increases energy expenditure in mice. Diabetes 2009;58:1509–17. https://doi.org/10.2337/db08-1637.

[51] Jumpertz R, Le DS, Turnbaugh PJ, Trinidad C, Bogardus C, Gordon JI, et al. Energy-balance studies reveal associations between gut microbes, caloric load, and nutrient absorption in humans. Am J Clin Nutr 2011;94:58–65. https://doi.org/10.3945/ajcn.110.010132.

[52] Lu W, Wang J, Nesengani LT, Gong Y, Yang Y. 6S rRNA gene sequencing reveals effects of photoperiod on cecal microbiota of broiler roosters n.d. https://doi.org/10.7717/peerj.4390.

[53] Liu J, Song Y, Lu X, Chen T, Guo W, Fan Z, et al. Seasonal Variation Influences on Intestinal Microbiota in Rats. Curr Microbiol 2018;75:1006–10. https://doi.org/10.1007/S00284-018-1480-6.

[54] Koliada A, Moseiko V, Romanenko M, Piven L, Lushchak O, Kryzhanovska N, et al. Seasonal variation in gut microbiota composition: Cross-sectional evidence from Ukrainian population. BMC Microbiol 2020;20:1–9. https://doi.org/10.1186/S12866-020-01786-8/TABLES/3.

[55] De Sá Del Fiol F, Tardelli Ferreira ACM, Marciano JJ, Marques MC, Sant'Ana LL. Obesity and the use of antibiotics and probiotics in rats. Chemotherapy 2014;60:162–7. https://doi.org/10.1159/000371737.

[56] Manichanh C, Reeder J, Gibert P, Varela E, Llopis M, Antolin M, et al. Reshaping the gut microbiome with bacterial transplantation and antibiotic intake. Genome Res 2010;20:1411–9. https://doi.org/10.1101/gr.107987.110.

[57] Ibars M, Ardid-Ruiz A, Suárez M, Muguerza B, Bladé C, Aragonès G. Proanthocyanidins potentiate hypothalamic leptin/STAT3 signalling and Pomc gene expression in rats with diet-induced obesity. Int J Obes (Lond) 2017;41:129–36. https://doi.org/10.1038/IJO.2016.169.

[58] Devkota S, Wang Y, Musch MW, Leone V, Fehlner-Peach H, Nadimpalli A, et al. Dietary-fat-induced taurocholic acid promotes pathobiont expansion and colitis in Il10-/- mice. Nature 2012;487:104–8. https://doi.org/10.1038/nature11225.

[59] Gual-Grau A, Guirro M, Mayneris-Perxachs J, Arola L, Boqué N. Impact of different hypercaloric diets on obesity features in rats: a metagenomics and

metabolomics integrative approach. J Nutr Biochem 2019;71:122–31. https://doi.org/10.1016/j.jnutbio.2019.06.005.

[60] Ghouri YA, Richards DM, Rahimi EF, Krill JT, Jelinek KA, DuPont AW. Systematic review of randomized controlled trials of probiotics, prebiotics, and synbiotics in infammatory bowel disease. Clin Exp Gastroenterol 2014;7:473–87. https://doi.org/10.2147/CEG.S27530.

[61] Salvini F, Riva E, Salvatici E, Boehm G, Jelinek J, Banderali G, et al. A specific prebiotic mixture added to starting infant formula has long-lasting bifidogenic effects. J Nutr 2011;141:1335–9. https://doi.org/10.3945/jn.110.136747.

[62] Tojo R, Suárez A, Clemente MG, De Los Reyes-Gavilán CG, Margolles A, Gueimonde M, et al. Intestinal microbiota in health and disease: Role of bifidobacteria in gut homeostasis. World J Gastroenterol 2014;20:15163–76. https://doi.org/10.3748/wjg.v20.i41.15163.

[63] Schellekens H, Torres-Fuentes C, van de Wouw M, Long-Smith CM, Mitchell A, Strain C, et al. Bifidobacterium longum counters the effects of obesity: Partial successful translation from rodent to human. EBioMedicine 2021;63. https://doi.org/10.1016/J.EBIOM.2020.103176.

[64] An HM, Park SY, Lee DK, Kim JR, Cha MK, Lee SW, et al. Antiobesity and lipid-lowering effects of Bifidobacterium spp. in high fat diet-induced obese rats. Lipids Health Dis 2011;10. https://doi.org/10.1186/1476-511X-10-116.

[65] Cani PD, Neyrinck AM, Fava F, Knauf C, Burcelin RG, Tuohy KM, et al. Selective increases of bifidobacteria in gut microflora improve high-fat-diet-induced diabetes in mice through a mechanism associated with endotoxaemia. Diabetologia 2007;50:2374–83. https://doi.org/10.1007/s00125-007-0791-0.

[66] Angelakis E, Merhej V, Raoult D. Related actions of probiotics and antibiotics on gut microbiota and weight modification. Lancet Infect Dis 2013;13:889–99. https://doi.org/10.1016/S1473-3099(13)70179-8.

[67] Cho I, Yamanishi S, Cox L, Methé BA, Zavadil J, Li K, et al. Antibiotics in early life alter the murine colonic microbiome and adiposity. Nature 2012;488:621–6. https://doi.org/10.1038/nature11400.

[68] Lange K, Buerger M, Stallmach A, Bruns T. Effects of Antibiotics on Gut Microbiota. Dig Dis 2016;34:260–8. https://doi.org/10.1159/000443360.

SUPPLEMENTARY MATERIAL

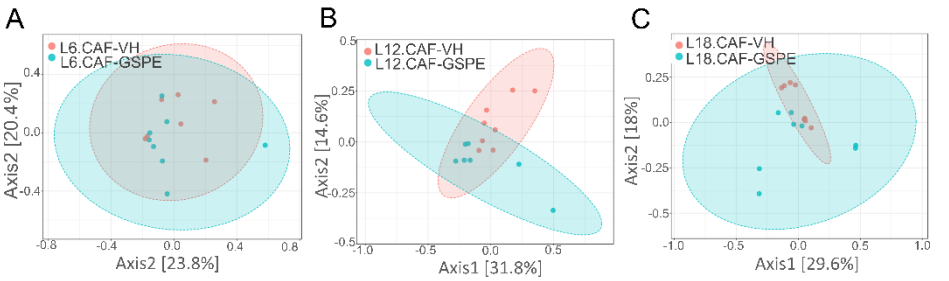

***Figure S1**. GSPE effects on β-diversity. (**A** to **B**): β-diversity based on Bray-Curtis distances and visualized by a Principal Coordinates Analysis (PCoA) 3D plot (PERMANOVA, p<0.001) in GSPE-treated rats under (**A**) L6; (**B**) L12; and (**C**) L18 conditions. (n=7-8); L6: 6h light/18h darkness; L12: 12h light/12h darkness; L18: 18h light/6h darkness; CAF: cafeteria diet; VH: vehicle; GSPE: grape seed proanthocyanidin extract;*

RESULTS

Table S1. Percentage of the relative abundance of GSPE- and GSPE+ABX-treated rats and their respective controls under short, standard and long photoperiod conditions at the different taxonomic levels.

	Ph	CAF-VH	*P-value Ph*[1]	CAF-GSPE	*P-value Ph*[1]	CAF-ABX	*P-value Ph*[1]	CAF-ABX+GSPE	*P-value Ph*[1]	*P-value Group*[2]	*P-value*[3]	
		Median(Q1-Q3)[4]		Median(Q1-Q3)[4]		Median(Q1-Q3)[4]		Median(Q1-Q3)[4]			VH vs GSPE	ABX vs GSPE
Phylum												
Actinobacteria	**L6**	0.08(0.04-0.18)	0.321	0.13(0.07-1.04)	0.111	2.82E-04(0-3.30E-04)#	0.801	1.17E-04(0-3.49E-04)# a	0.004	0.000	0.165	0.584
	L12	0.05(0.05-0.06)		0.04(0.04-0.15)		3.19E-04(0-8.09E-04)#		3.22E-04(6.05E-05-4.45E-04)# ab		0.000	0.418	0.831
	L18	0.06(0.03-0.06)		0.14(0.04-0.47)		4.47E-04(0-6.47E-04)		0.002(0.001-0.003) ***b $***		0.000	0.247	0.009
Bacteroidetes	**L6**	52.24(44.61-70.78)	0.084	50.44(44.02-61.95)	0.610	76.78(58.04-80.46)#	0.176	72.46(60.01-78.37)#	0.410	0.012	0.355	0.600
	L12	53.86(46.92-61.94)		55.71(38.91-81.32)		59.72(35.89-76.41)		71.04(63.72-75.88)		0.107	0.643	0.093
	L18	69.27(54.76-76.93)		52.97(46.68-78.57)		63.56(32.54-72.08)		66.55(55.82-68.73)		0.427	0.294	0.475
Cyanobacteria	**L6**	0.51(0.17-0.97)	0.538	0.41(0.13-0.59)	0.738	0.001(5.65E-04-0.009)#	0.664	1.84E-04(0-0.002)#	0.045	0.000	0.487	0.110
	L12	0.30(0.23-0.42)		0.22(0.08-0.50)		0.003(6.70E-04-0.01)#		7.40E-04(6.45E-05-0.001)#		0.000	0.563	0.131
	L18	0.41(0.30-0.57)		0.38(0.05-1.55)		0.001(8.95E-04-0.002)#		0.002(0.001-0.003)#		0.000	0.600	0.142
Firmicutes	**L6**	42.02(23.69-49.75)	0.072	38.17(33.76-47.92)	0.769	7.68(3.74-9.28)#	0.270	1.11(0.51-1.93)# ***a $***	0.015	0.000	0.643	0.002
	L12	40.02(32.87-48.83)		32.07(15.04-52.25)		4.43(2.44-6.61)#		2.50(1.77-3.95)# ***ab***		0.000	0.487	0.248
	L18	24.51(18.53-37.85)		39.09(13.63-46.36)		7.60(2.92-15.66)#		4.20(3.61-5.32)# ***b***		0.001	0.401	0.277
Proteobacteria	**L6**	3.02(2.22-3.71)	0.418	3.72(2.14-7.14)	0.449	13.77(10.11-31.59)#	0.135	22.64(17.84-35.39)#	0.537	0.000	0.418	0.059
	L12	3.26(1.89-3.98)		2.83(2.30-5.16)		27.04(17.49-58.26)#		20.80(16.05-25.96)#		0.000	0.728	0.248
	L18	4.23(2.06-5.26)		4.65(3.12-6.30)		22.14(16.12-60.41)#		26.58(17.02-38.82)#		0.000	0.345	0.949
Tenericutes	**L6**	7.66E-04(2.64E-04-0.009)	0.846	6.09E-04(6.98E-05-0.02)	0.480	0.48(2.91E-04-2.60)#	0.193	0.05(0.00-0.79)#	0.495	0.424	0.728	0.368
	L12	0.001(6.53E-05-0.003)		6.16E-04(0-0.04)		0.006(0.002-7.19)		0.07(7.24E-04-0.29)		0.203	0.907	0.674
	L18	7.92E-04(3.27E-04-0.002)		0.003(6.23E-04-0.08)		8.46E-04(5.55E-04-9.70E-04)		0.3011(0.0025-2.8275)		0.078	0.115	0.073

Verrucomicrobia	**L6**	1.92(1.23-2.26)	0.722	1.23(0.43-2.76)	0.974	1.97(0.32-3.96)#	0.583	2.96(1.50-5.32)#	0.543	0.282	0.247	0.345
	L12	1.63(0.71-3.76)		0.95(0.60-1.46)		0.54(0.01-3.60)		3.00(0.12-7.56)		0.550	0.247	0.345
	L18	1.13(0.92-1.83)		1.02(0.42-2.11)		0.022(0.005-6.840)		0.016(0.009-10.641)		0.572	0.529	0.848
Class												
Actinobacteria	**L6**	0.01(0-0.05)	0.413	0.08(0.01-0.65) ***a***	0.048	2.82E-04(0-3.30E-04)#	0.889	9.80E-05(0-3.34E-04)# ***a***	0.005	0.000	0.083	0.511
	L12	0.01(0-0.01)		0(0-0.01) ***b***		1.62E-04(0-8.09E-04)#		2.66E-04(5.72E-05-3.95E-04)# ***a***		0.000	0.908	0.746
	L18	0(0-0.01)		0.03(0.01-0.26) ***ab***		4.47E-04(0-6.47E-04)#		0(4.44E-04-0)# ***$ b***		0.000	0.021	0.047
Coriobacteriia	**L6**	0.04(0.03-0.06)	0.762	0.08(0.04-0.2)	0.537	0(0-0)#	0.631	0(0-0)#	0.069	0.000	0.165	0.927
	L12	0.05(0.04-0.06)		0.04(0.03-0.04)		0(0-0)#		0(0-1.72E-04)#		0.000	0.563	0.644
	L18	0.05(0.03-0.05)		0.05(0.02-0.11)		0(0-0)#		3.79E-04(0-8.88E-04)# ***$***		0.000	0.600	0.025
Bacteroidia	**L6**	52.24(44.61-70.78)	0.084	50.44(44.02-59.37)	0.610	76.76(58.02-80.46)	0.176	72.45(60-78.35)	0.219	0.012	0.355	0.600
	L12	53.86(46.92-61.94)		55.71(38.91-81.32)		59.72(35.89-76.4)		71.03(63.72-75.87)		0.107	0.643	0.093
	L18	69.27(54.76-76.93)		52.97(46.68-78.56)		63.56(32.51-72.07)		66.55(55.82-68.68)		0.541	0.294	0.749
Flavobacteriia	**L6**	0(0-0)	0.887	0(0-2.29E-04)	0.745	0(0-0)	0.150	0(0-0)	0.072	0.280	0.741	0.064
	L12	0(0-0)		0(0-0)		0(0-0)		0(0-0)		1.000	1.000	0.927
	L18	0(0-1.62E-04)		0(0-0)		0(0-0)		0(0-7.10E-04)		0.309	0.783	0.062
Sphingobacteriia	**L6**	0(0-0)	0.250	0(0-0)	0.112	0.01(0.01-0.02)#	0.291	0.01(0.01-0.01)#	0.061	0.000	0.350	0.600
	L12	0(0-1.67E-04)		2.26E-04(0-2.78E-04)		0(5.67E-05-0.01)#		0(0-0.01)#		0.001	0.103	0.916
	L18	0(0-2.15E-04)		2.95E-04(0-0)		0.01(0-0.03)#		0(0-0.02)#		0.043	0.104	0.477
Bacilli	**L6**	0.75(0.55-1.54)	0.090	1.64(0.43-3.62)	0.521	0.9(0.21-1.48)#	0.566	0.03(0.01-0.57)#	0.230	0.031	0.728	0.059
	L12	2.41(1.23-3.97)		0.95(0.78-1.27)***$***		0.31(0.03-2.01)#		0.39(0.01-1.53)#		0.028	0.015	0.600
	L18	0.71(0.22-2.38)		2.17(0.61-2.98)		0.23(0.03-4.96)		0.36(0.11-2.18)		0.431	0.345	0.655
Clostridia	**L6**	41.45(22.84-45.36) ***ab***	0.049	35.95(32.61-42.12)	0.626	6.88(2.15-8.94)#	0.426	0.55(0.34-1.35)# ***$***	0.044	0.000	0.908	0.003
	L12	36.98(30.67-44.22) ***a***		29.13(13.97-40.96)		2.79(1.19-5.58)#		2.2(1.14-2.67)#		0.000	0.487	0.294

	L18	23.94(17.64-29.23) ***b***		35.17(12.16-42.86)		2.8(1.6-15.42)#		3.2(2.03-4.12)#		0.001	0.208	0.655
Erysipelotrichi	**L6**	0.21(0.1-1.4)	0.153	0.65(0.22-1.49)	0.516	0.01(0-0.28)#	0.499	5.35E-04(7.35E-05-0.01)#	0.116	0.000	0.298	0.394
	L12	0.85(0.35-1.09)		0.28(0.21-0.67)		0(0-0.22)#		0.01(8.29E-04-0.19)#		0.001	0.165	0.834
	L18	0.37(0.13-0.52)		0.97(0.17-1.17)		0(2.78E-04-0.09)#		8.79E-04(0-0)#		0.000	0.208	0.653
Alphaproteobacteria	**L6**	0.48(0.14-0.7)	0.255	0.28(0.12-0.34)	0.138	0.01(0-0.01)#	0.270	8.77E-04(3.39E-04-0)# ***$ a***	0.037	0.000	0.247	0.002
	L12	0.22(0.16-0.34)		0.16(0.11-0.82)		0(0-0.01)#		0(8.27E-04-0)# ***ab***		0.000	0.817	0.172
	L18	0.56(0.19-1.08)		0.07(0.01-0.25)		0(0-0.01)#		0(0-0.01)# ***b***		0.001	0.046	0.655
Betaproteobacteria	**L6**	1.05(0.89-1.59)	0.976	1.83(0.8-5.33)	0.881	1.96(1.48-3.76)	0.065	3.63(2.91-4.25)	0.297	0.053	0.355	0.093
	L12	1.1(0.74-2.39)		1.33(0.69-2.51)		3.14(1.59-4.55)#		3.16(2.62-4.26)#		0.016	1.000	0.753
	L18	1.24(0.5-2.55)		1.65(0.83-3.34)		5.11(2.96-7.82)#		5.27(2.6-5.71)#		0.002	0.401	0.749
Deltaproteobacteria	**L6**	0.64(0.43-1.19)	0.586	0.78(0.23-1.47)	0.470	0.63(0.07-0.78)	0.920	0.12(0.07-0.53)	0.064	0.068	0.908	0.141
	L12	0.76(0.32-1.54)		0.72(0.31-1.52)		0.47(0.12-1.39)		0.49(0.32-0.84)		0.746	0.908	0.916
	L18	1.18(0.44-1.83)		1(0.62-1.34)		0.63(0.01-1.16)		0.31(0.26-0.87)		0.086	0.600	0.749
Mollicutes	**L6**	5.90E-04(2.64E-04-0.01)	0.871	6.09E-04(6.98E-05-0.02)	0.388	0.48(2.91E-04-2.6)	0.161	0.05(0-0.79)	0.495	0.423	0.908	0.368
	L12	5.80E-04(6.53E-05-0)		6.16E-04(0-0)		0.01(0-7.19)		0.07(6.63E-04-0.29)		0.100	0.726	0.674
	L18	6.75E-04(3.27E-04-0)		0(6.23E-04-0.02)		8.46E-04(2.78E-04-9.70E-04)		0.3(0-2.83)		0.065	0.115	0.073
Verrucomicrobiae	**L6**	1.92(1.23-2.26)	0.722	1.23(0.43-2.75)	0.974	1.97(0.32-3.96)	0.583	2.96(1.5-5.32)	0.543	0.282	0.247	0.345
	L12	1.63(0.71-3.76)		0.95(0.6-1.28)		0.54(0.01-3.6)		3(0.12-7.56)		0.550	0.247	0.345
	L18	1.13(0.92-1.83)		1.02(0.42-2.11)		0.02(0-6.84)		0.02(0.01-10.64)		0.572	0.529	0.848
Order												
Actinomycetales	**L6**	2.48E-03(1.80E-03-3.76E-03)	0.805	3.75E-03(2.80E-03-4.62E-03)	0.490	0(0-2.01E-04)#	0.790	0(0-0)#	0.173	0.000	0.105	0.644
	L12	3.54E-03(1.31E-03-3.68E-03)		1.75E-03(1.53E-03-6.78E-03)		0(0-0)#		2.51E-04(5.72E-05-3.38E-04)# ***$***		0.000	0.563	0.049
	L18	2.13E-03(1.18E-03-3.55E-03)		5.15E-03(1.50E-03-0.06)		0(0-3.23E-04)#		0(0-8.79E-04)#		0.000	0.172	0.413

Bifidobacteriales	**L6**	4.42E-03(5.27E-04-0.03)	0.528	0.08(5.05E-03-0.65)	0.075	1.48E-04(0-3.30E-04)#	0.903	0(0-2.25E-04)# ***a***	0.001	0.000	0.105	0.418
	L12	4.17E-03(1.12E-03-6.54E-03)		2.78E-03(3.82E-04-0.02)		0(0-3.48E-04)#		0(0-0)# ***a***		0.000	0.817	0.370
	L18	1.65E-03(5.12E-04-0.01)		0.02(4.28E-03-0.3)***$***		2.80E-04(0-4.47E-04)#		8.18E-04(4.44E-04-2.54E-03)# ***$ b***		0.001	0.036	0.012
Coriobacteriales	**L6**	0.04(0.03-0.09)	0.762	0.08(0.04-0.2)	0.537	0(0-0)#	0.631	0(0-0)#	0.069	0.000	0.165	0.927
	L12	0.05(0.03-0.06)		0.04(0.03-0.09)		0(0-0)#		0(0-1.72E-04)#		0.000	0.563	0.644
	L18	0.05(0.03-0.05)		0.05(0.02-0.18)		0(0-0)#		3.79E-04(0-8.88E-04)# ***$***		0.000	0.600	0.025
Bacteroidales	**L6**	52.24(44.61-72.07)	0.084	50.44(44.02-61.95)	0.610	76.76(58.02-80.46)#	0.176	72.45(60-78.35)#	0.219	0.012	0.355	0.600
	L12	56.3(50.77-62.99)		55.71(38.91-81.32)		59.72(35.89-76.4)		71.03(63.72-75.87)		0.107	0.643	0.093
	L18	67.68(52.56-77.02)		52.97(46.68-78.56)		63.56(32.51-72.07)		66.55(55.82-68.68)		0.541	0.294	0.749
YS2	**L6**	0.51(0.17-1.03)	0.538	0.41(0.13-0.59)	0.781	1.70E-04(0-7.96E-03)#	0.362	0(0-3.52E-04)# ***a***	0.014	0.000	0.563	0.487
	L12	0.3(0.22-0.45)		0.22(0.08-0.5)		2.48E-03(3.58E-04-9.38E-03)#		0(0-7.80E-04)# ***$ a***		0.000	0.563	0.027
	L18	0.44(0.3-0.58)		0.38(0.05-1.55)		5.55E-04(2.82E-04-1.08E-03)#		1.64E-03(8.88E-04-2.64E-03)# ***b***		0.000	0.600	0.085
Bacillales	**L6**	5.27E-04(4.14E-04-1.27E-03)***a***	0.030	3.39E-03(1.31E-03-0.03)***$ a***	0.015	7.59E-04(5.53E-04-1.14E-03)	0.064	2.02E-04(0-3.56E-04)# ***$***	0.132	0.001	0.005	0.026
	L12	6.37E-04(0-2.18E-03)***a***		8.65E-04(1.91E-04-1.11E-03) ***b***		1.13E-04(0-4.29E-04)		3.81E-04(7.76E-05-1.84E-03)		0.529	1.000	0.332
	L18	2.84E-03(1.19E-03-3.07E-03)***b***		1.72E-03(5.54E-04-2.98E-03) ***ab***		8.46E-04(2.78E-04-3.64E-03)		1.89E-03(0-4.71E-03)		0.859	0.401	0.748
Lactobacillales	**L6**	0.75(0.55-1.78)	0.090	1.64(0.4-3.62)	0.516	0.77(0.21-1.48)	0.586	0.03(6.42E-03-0.57)#	0.230	0.031	0.728	0.059
	L12	2.39(1.13-4.38)		0.95(0.77-1.27)		0.31(0.03-2.01)#		0.39(0.01-1.53)#		0.028	0.015	0.600
	L18	0.67(0.2-2.44)		2.17(0.61-3.49)		0.23(0.03-4.96)		0.36(0.1-2.18)		0.442	0.401	0.655
Clostridiales	**L6**	41.45(22.84-47.86)***a***	0.049	35.94(32.61-42.12)	0.626	6.88(2.15-8.94)#	0.426	0.55(0.34-1.35)# ***$ a***	0.044	0.000	0.908	0.003
	L12	34.62(30.25-44.44)***a***		29.13(13.97-50.43)		2.79(1.19-5.58)#		2.2(1.14-2.67)# ***ab***		0.000	0.487	0.294
	L18	25.57(19.07-29.34)***b***		35.17(12.16-42.86)		2.8(1.6-15.42)#		3.2(2.03-4.12)# ***b***		0.001	0.208	0.655
Erysipelotrichales	**L6**	0.21(0.1-1.5)	0.153	0.65(0.22-1.49)	0.516	0.01(0-0.28)#	0.499	5.35E-04(7.35E-05-0.01)#	0.116	0.000	0.298	0.394

RESULTS

	L12	0.8(0.27-1.13)		0.28(0.21-0.72)		2.81E-03(1.90E-03-0.22)#		0.01(8.29E-04-0.19)#		0.001	0.165	0.834
	L18	0.4(0.11-0.53)		0.97(0.17-1.17)		1.08E-03(2.78E-04-0.09)#		8.79E-04(0-2.90E-03)#		0.000	0.208	0.653
RF32	**L6**	0.47(0.14-0.97)	0.255	0.21(0.11-0.34)	0.147	2.92E-04(0-3.36E-04)#	0.303	0(0-4.41E-04)# ***a***	0.001	0.000	0.203	0.400
	L12	0.19(0.16-0.25)		0.16(0.11-2.06)		9.06E-04(2.01E-04-1.38E-03)#		0(0-0)# ***$ a***		0.000	0.817	0.008
	L18	0.46(0.16-1.11)		0.07(0.01-0.25) ***$***		3.59E-04(0-1.69E-03)#		8.88E-04(6.19E-04-2.84E-03)# ***b***		0.000	0.046	0.110
Rhizobiales	**L6**	1.05E-03(2.95E-04-1.46E-03)***a***	0.014	1.83E-03(0-0.05)	0.055	1.60E-03(5.66E-04-4.78E-03)# ***a***	0.014	0(0-2.94E-04)* # ***$***	0.076	0.032	0.814	0.003
	L12	0(0-0)***b***		0(0-0)		0(0-3.48E-04) ***b***		2.51E-04(0-4.32E-04)		0.067	0.350	0.537
	L18	5.07E-04(0-1.70E-03)***a***		4.65E-04(0-2.02E-03)		6.47E-04(5.64E-04-8.95E-04) ***ab***		1.09E-03(0-2.84E-03)		0.884	0.957	0.564
Rhodospirillales	**L6**	2.55E-04(0-4.19E-04)	0.389	2.92E-04(0-1.10E-03)	0.639	3.21E-03(1.42E-03-6.67E-03)#	0.657	2.88E-04(5.87E-05-1.78E-03)# ***$***	0.424	0.006	0.591	0.021
	L12	0(0-2.75E-04)		0(0-5.04E-04)		1.82E-03(4.41E-04-4.53E-03)#		1.50E-03(5.88E-04-2.61E-03)#		0.002	0.408	0.875
	L18	0(0-6.38E-04)		0(0-3.79E-04)		1.41E-03(7.18E-04-0.01)#		7.58E-04(0-1.64E-03)#		0.009	0.952	0.275
Rickettsiales	**L6**	3.32E-04(0-4.68E-04)	0.683	0(0-8.26E-04)	0.425	0(0-0)#	0.146	0(0-1.47E-04)	0.365	0.030	0.464	0.144
	L12	2.42E-04(0-4.46E-04)		0(0-2.88E-04)		0(0-2.01E-04)		0(0-1.72E-04)		0.184	0.232	0.890
	L18	2.44E-04(0-4.73E-04)		0(0-0)		0(0-2.82E-04)		0(0-0)		0.110	0.125	0.062
Burkholderiales	**L6**	1.05(0.89-2.18)	0.976	1.83(0.8-5.31)	0.881	1.96(1.48-3.76)	0.065	3.63(2.91-4.25)	0.297	0.052	0.355	0.093
	L12	0.91(0.71-2.74)		1.33(0.69-2.51)		3.14(1.59-4.54)#		3.16(2.62-4.26)#		0.016	1.000	0.753
	L18	1.21(0.44-2.64)		1.65(0.83-3.34)		5.11(2.96-7.82)#		5.27(2.6-5.71)#		0.002	0.401	0.749
Aeromonadales	**L6**	0(0-0)	0.141	0(0-0)	0.197	5.65E-04(2.91E-04-1.51E-03)# ***a***	0.004	1.35E-03(6.63E-04-2.13E-03)#	0.154	0.000	0.350	0.093
	L12	0(0-0)		0(0-0)		3.71E-03(2.10E-03-5.55E-03)# ***b***		6.94E-04(3.83E-04-1.62E-03)# ***$***		0.000	1.000	0.009
	L18	0(0-2.16E-04)		0(0-2.71E-04)		0.01(1.69E-03-0.02)# ***b***		1.89E-03(8.18E-04-2.47E-03)#		0.000	0.444	0.064
Enterobacteriales	**L6**	0.15(0.03-0.31)	0.361	0.22(0.07-0.68)	0.062	10.67(6.5-22.7)#	0.238	18.6(13.01-27.69)#	0.597	0.000	0.203	0.141

	L12	0.37(0.07-0.43)		0.15(0.07-0.22)		23.03(14.61-48.04)#		15.55(11-21.02)#		0.000	0.817	0.141
	L18	0.13(0.06-0.73)		0.73(0.27-2.36)		14.76(12.08-50.64)#		19.75(11.76-30.82)# ***$***		0.000	0.046	0.848
Pasteurellales	**L6**	7.66E-03(5.60E-03-0.02)	0.524	7.21E-03(4.20E-03-0.03)	0.653	0(0-0)#	1.000	0(0-0)#	0.141	0.000	0.908	1.000
	L12	8.63E-03(4.12E-03-0.01)		9.04E-03(3.82E-03-0.06)		0(0-0)#		0(0-2.81E-04)#		0.000	0.487	0.144
	L18	0.03(4.14E-03-0.03)		0.03(8.06E-03-0.07)		0(0-0)#		0(0-0)#		0.000	0.345	1.000
Pseudomonadales	**L6**	7.63E-03(2.69E-03-0.01)	0.834	0.01(2.70E-03-0.02) ***ab***	0.034	0.67(0.52-2.15)#	0.169	0.62(0.25-1.66)#	0.075	0.000	0.355	0.753
	L12	0.04(2.18E-03-0.05)		3.75E-03(9.54E-04-0.01) ***a***		1.61(0.7-2.35)#		0.84(0.29-1.68)#		0.000	0.355	0.529
	L18	8.53E-03(3.44E-03-0.03)		0.03(0.01-0.28) ***b***		1.43(0.85-3.2)#		1.8(0.91-2.08)#		0.000	0.093	0.949
Vibrionales	**L6**	0(0-0)	0.358	3.09E-04(0-6.20E-04)***$***	0.547	0.04(8.40E-03-0.08)# ***a***	0.014	0.1(0.05-0.15)#	0.058	0.000	0.016	0.115
	L12	0(0-6.69E-04)		0(0-2.52E-04)		0.11(0.07-0.26)# ***b***		0.05(0.02-0.12)#		0.000	0.882	0.074
	L18	0(0-2.37E-04)		1.19E-04(0-1.02E-03)		0.01(6.71E-03-0.07)# ***a***		0.02(5.71E-03-0.05)#		0.000	0.184	0.749
Xanthomonadales	**L6**	0(0-0)	0.392	1.13E-04(0-1.39E-03)***$ a***	0.014	2.85E-04(0-1.63E-03)#	0.112	0(0-0)* # ***$***	1.000	0.010	0.038	0.011
	L12	0(0-0)		0(0-0) ***b***		0(0-0)		0(0-0)		0.411	1.000	0.317
	L18	0(0-0)		0(0-0) ***b***		0(0-2.80E-04)		0(0-0)		0.214	0.317	0.142
Anaeroplasmatales	**L6**	2.64E-04(0-2.37E-03)	0.151	1.27E-04(0-4.10E-04) ***a***	0.014	0.48(7.39E-05-2.6)	0.164	0.05(0-0.79)	0.533	0.159	0.473	0.456
	L12	2.42E-04(0-4.25E-04)		6.16E-04(0-1.15E-03) ***ab***		4.52E-03(1.81E-03-7.19)#		0.07(4.88E-04-0.29)#		0.006	0.189	0.674
	L18	5.12E-04(2.65E-04-9.45E-04)		1.59E-03(5.54E-04-4.66E-03) ***a***		3.23E-04(2.78E-04-8.95E-04)#		0.3(2.47E-03-2.83)#		0.036	0.141	0.073
Verrucomicrobiales	**L6**	1.92(1.23-2.93)	0.722	1.23(0.43-2.76)	0.974	1.97(0.32-3.96)	0.583	2.96(1.5-5.32)	0.543	0.282	0.247	0.345
	L12	1.79(0.73-4.35)		0.95(0.6-1.46)		0.54(0.01-3.6)		3(0.12-7.56)		0.550	0.247	0.345
	L18	1.31(0.95-1.95)		1.02(0.42-2.11)		0.02(5.00E-03-6.84)		0.02(8.52E-03-10.64)		0.572	0.529	0.848
Family												

Corynebacteriaceae	**L6**	0(0-0)	0.196	2.69E-04(0-6.49E-04)	0.934	0(0-0)	1.000	0(0-0)	0.631	0.020	0.090	0.317
	L12	0(0-6.13E-05)		4.52E-04(0-5.02E-04)		0(0-0)		0(0-0)		0.039	0.346	0.317
	L18	3.35E-04(0-5.15E-04)		1.44E-04(0-3.57E-04)		0(0-0)		0(0-0)		0.014	0.826	1.000
Microbacteriaceae	**L6**	0(0-0)	0.150	0(0-0)	1.000	0(0-0)	1.000	0(0-0)	1.000	1.000	1.000	1.000
	L12	0(0-2.31E-04)		0(0-0)		0(0-0)		0(0-0)		0.027	0.082	1.000
	L18	0(0-0)		0(0-0)		0(0-0)		0(0-0)		0.432	0.317	1.000
Micrococcaceae	**L6**	2.36E-03(1.28E-03-2.80E-03)	0.278	3.07E-03(2.06E-03-3.45E-03)	0.703	0(0-0)	0.245	0(0-0)	0.141	0.000	0.355	0.317
	L12	2.22E-03(1.09E-03-3.04E-03)		1.26E-03(1.20E-03-1.46E-03)		0(0-0)		0(0-6.05E-05)		0.000	0.908	0.144
	L18	1.32E-03(6.91E-04-1.98E-03)		2.37E-03(1.61E-03-2.59E-03)		0(0-1.62E-04)		0(0-0)		0.001	0.248	0.142
Nocardiaceae	**L6**	0(0-0)	0.177	0(0-1.36E-03)	0.144	0(0-0)	0.392	0(0-0)	0.107	0.190	0.449	0.317
	L12	0(0-0)		0(0-0)		0(0-0)		0(0-0)		0.290	0.285	0.144
	L18	0(0-4.14E-04)		2.84E-03(0-0.02)		0(0-0)		0(0-6.44E-04)		0.046	0.104	0.062
Bifidobacteriaceae	**L6**	4.42E-03(1.06E-03-0.01)	0.528	0.08(9.54E-03-0.63)	0.075	1.48E-04(0-3.07E-04)	0.903	0(0-5.87E-05) ***a***	0.001	0.000	0.105	0.418
	L12	2.87E-03(1.31E-03-4.76E-03)		2.78E-03(9.40E-04-4.01E-03)		0(0-3.32E-04)		0(0-0) ***a***		0.000	0.817	0.370
	L18	1.59E-03(7.66E-04-4.58E-03)		0.02(6.07E-03-0.1)		2.80E-04(0-3.85E-04)		8.18E-04(6.01E-04-2.15E-03) ***b***		0.001	0.036	0.012
Coriobacteriaceae	**L6**	0.04(0.03-0.06)	0.762	0.08(0.05-0.14)	0.537	0(0-0)	0.631	0(0-0)	0.069	0.000	0.165	0.927
	L12	0.05(0.04-0.06)		0.04(0.03-0.04)		0(0-0)		0(0-5.72E-05)		0.000	0.563	0.644
	L18	0.05(0.03-0.05)		0.05(0.02-0.08)		0(0-0)		3.79E-04(0-8.06E-04)		0.000	0.600	0.025
Bacteroidaceae	**L6**	5.77(4.5-7.46)***ab***	0.004	3.97(2.28-6.77)	0.619	18.72(8.35-25.34) ***ab***	0.012	3.38(0.07-10.1) ***$***	0.067	0.190	0.487	0.027
	L12	4.37(2.99-4.51)***a***		6.35(5.04-10.42)		0.11(0.06-3.46)# ***a***		10.75(2.95-26.08)* # ***$***		0.036	0.105	0.016
	L18	10.09(8.24-10.94)***b***		5.99(4.61-12.1)		0.07(0.05-4.93)# ***b***		0.19(0.11-2.34)#		0.007	0.141	0.749

Porphyromonadaceae	**L6**	12.45(12.18-15.71)	0.774	9.32(8-9.63)***$***	0.063	43.49(31.76-50)#	0.865	51.18(43.92-57.58)#	0.541	0.000	0.015	0.141
	L12	16.87(8.52-17.98)		24.58(19.02-25.63)		41.9(23.15-57.03)#		48.36(35.59-52.28)#		0.003	0.064	0.600
	L18	16.29(11.48-22.04)		17.45(7.64-30.06)		36.03(25.01-44.6)#		55.29(49.01-66.11)* # ***$***		0.003	0.916	0.035
Prevotellaceae	**L6**	3.79(1.81-6)	0.367	1.78(1.38-4.69)	0.980	0.02(8.12E-03-0.07)#	0.954	4.23E-03(1.48E-03-0.06)#	0.398	0.000	0.298	0.294
	L12	7.76(4.87-8.95)		2.71(1.3-3.72)***$***		0.01(9.58E-03-0.94)#		9.16E-03(5.76E-03-0.06)#		0.000	0.037	0.345
	L18	6.06(4.15-9.14)		3.61(1.13-4.94)		0.02(9.67E-03-0.02)#		0.02(0.01-0.05)#		0.000	0.172	0.225
Rikenellaceae	**L6**	0.37(0.34-0.49)	0.159	0.37(0.28-0.65)	0.928	0.55(0.06-1.02)#	0.062	1.56E-03(2.69E-04-0.02)# ***$a***	0.018	0.024	0.817	0.036
	L12	0.28(0.17-0.4)		0.45(0.18-0.7)		2.48E-03(9.07E-04-5.93E-03)#		0.2(0.07-0.4)# ***$ b***		0.010	0.487	0.027
	L18	0.54(0.38-0.7)		0.39(0.24-0.88)		0.66(8.01E-03-1.03)#		3.19E-03(1.28E-03-0.02)# ***$ ab***		0.016	0.674	0.035
Paraprevotellaceae	**L6**	3.22(1.12-7.2)	0.632	0.38(0.09-1.3)	0.169	2.63E-03(1.24E-03-2.94E-03)	0.149	2.49E-03(1.40E-03-1.58)	0.740	0.003	0.049	0.674
	L12	1.59(0.65-3.08)		1.18(0.99-8.3)		0.01(3.32E-03-1.89)		8.85E-03(4.46E-03-1.43)		0.073	0.728	0.834
	L18	1.97(1.46-2.35)		1(0.4-1.24)		5.07E-03(4.45E-03-8.08E-03)		0.01(7.44E-03-0.03)		0.000	0.059	0.110
Bacillaceae	**L6**	0(0-0)	0.056	6.07E-04(2.07E-04-8.63E-04)	0.238	0(0-3.78E-04)	0.955	1.53E-04(0-3.32E-04)	0.947	0.044	0.012	0.817
	L12	0(0-3.51E-04)		0(0-2.52E-04)		0(0-5.67E-05)		1.55E-04(0-3.96E-04)		0.926	1.000	0.418
	L18	2.54E-04(1.78E-04-5.47E-04)		3.16E-04(0-4.44E-04)		0(0-2.24E-04)		0(0-2.22E-04)		0.678	0.915	0.710
Planococcaceae	**L6**	5.11E-04(2.07E-04-5.95E-04)	0.059	1.23E-03(2.60E-04-8.55E-03) ***a***	0.009	6.25E-04(0-9.05E-04)	0.054	0(0-0)# ***$ a***	0.030	0.014	0.245	0.026
	L12	1.38E-04(0-5.03E-04)		0(0-0) ***b***		0(0-0)		1.77E-04(0-7.24E-04) ***ab***		0.302	0.168	0.202
	L18	1.68E-03(4.98E-04-1.95E-03)		1.06E-03(6.24E-04-1.42E-03) ***a***		7.18E-04(4.61E-04-2.18E-03)		1.14E-03(4.44E-04-3.24E-03) ***b***		0.961	0.793	0.564
Enterococcaceae	**L6**	2.00E-04(0-7.63E-04)	0.461	7.70E-04(5.57E-04-1.22E-03)	0.333	4.70E-04(2.17E-04-1.67E-03)	0.581	4.90E-05(0-6.07E-04)	0.527	0.187	0.131	0.281
	L12	5.96E-04(2.35E-04-7.78E-04)		5.77E-04(2.65E-04-7.88E-04)		1.37E-03(2.35E-04-4.61E-03)		1.30E-04(0-5.71E-04)		0.263	0.954	0.067
	L18	1.22E-04(0-3.67E-04)		1.38E-03(3.79E-04-1.96E-03)***$***		5.55E-04(1.62E-04-7.25E-04)		8.88E-04(0-1.76E-03)		0.111	0.011	0.845

RESULTS

Lactobacillaceae	**L6**	0.69(0.56-1.09)	0.078	1.61(0.39-3.15)	0.516	0.76(0.23-1.43)	0.583	0.02(1.90E-03-0.34)# ***$***	0.272	0.030	0.728	0.046
	L12	2.38(1.4-3.1)		0.93(0.76-1.19)***$***		0.27(9.71E-03-1.17)#		0.38(1.40E-03-1.24)#		0.038	0.015	0.462
	L18	0.67(0.24-2.22)		2.11(1.08-2.4)		0.23(6.57E-03-2.72)		0.36(0.16-1.3)		0.481	0.401	0.655
Leuconostocaceae	**L6**	1.66E-03(6.31E-04-2.03E-03)	0.157	4.55E-03(2.32E-03-6.38E-03)	0.089	1.00E-03(4.78E-04-1.54E-03)***a***	0.003	2.47E-03(1.02E-03-8.60E-03)	0.807	0.067	0.064	0.074
	L12	2.96E-03(1.61E-03-4.38E-03)		5.04E-04(3.35E-04-5.30E-04)		4.27E-03(2.53E-03-5.48E-03)***b***		3.27E-03(1.27E-03-4.74E-03)		0.085	0.083	0.674
	L18	6.24E-03(4.39E-03-9.11E-03)		0.01(4.16E-03-0.01)		5.81E-03(3.74E-03-0.01)***b***		3.08E-03(2.47E-03-3.31E-03)		0.587	0.527	0.225
Christensenellaceae	**L6**	0.04(0.03-0.05)	0.058	0.06(0.03-0.11)	0.109	0(0-0)#	0.998	0(0-7.99E-05)#	0.107	0.000	1.000	0.644
	L12	0.03(0.02-0.03)		4.32E-03(1.03E-03-7.03E-03)***$***		0(0-0)#		0(0-0)#		0.000	0.037	0.317
	L18	0.01(0.01-0.02)		0.02(2.53E-03-0.02)		0(0-0)#		0(0-1.89E-03)#		0.001	0.753	0.174
Clostridiaceae	**L6**	0.01(7.96E-03-0.01) ***a***	0.005	0.01(3.54E-03-0.02)	0.373	1.23E-03(2.43E-04-1.93E-03)#	0.506	2.84E-04(0-5.36E-04)#	0.297	0.000	1.000	0.136
	L12	7.74E-03(3.96E-03-0.01) ***ab***		3.39E-03(1.83E-03-4.34E-03)		6.26E-04(2.67E-04-1.35E-03)#		2.51E-04(0-6.63E-04)#		0.002	0.563	0.286
	L18	2.99E-03(2.59E-03-3.91E-03) ***b***		3.71E-03(1.95E-03-5.22E-03)		3.23E-04(1.39E-04-8.18E-04)#		7.10E-04(4.26E-04-3.87E-03)#		0.019	0.875	0.275
Lachnospiraceae	**L6**	16.47(12.72-24.19)	0.118	26.23(21.87-27.74)	0.473	0.04(0.01-0.09)#	0.228	0.06(0.01-0.09)#	0.098	0.000	0.418	0.753
	L12	27.45(23.67-29.99)		17.9(11.74-22.04)		0.06(0.04-0.18)#		0.02(9.52E-03-0.03)*# ***$***		0.000	0.105	0.012
	L18	18.06(12.95-23.57)		25.99(14.63-29.28)		0.02(0.01-0.04)#		0.04(0.03-0.23)* # ***$***		0.000	0.401	0.048
Peptococcaceae	**L6**	0.15(0.04-0.2)	0.551	0.14(0.1-0.18) ***ab***	0.042	1.48E-04(0-3.02E-04)#	0.562	0(0-7.99E-05)# ***a***	0.001	0.000	0.908	0.452
	L12	0.08(0.04-0.09)		0.01(3.08E-04-0.02) ***a***		9.06E-04(2.67E-04-1.01E-03)#		0(0-0)# ***$ a***		0.001	0.247	0.008
	L18	0.06(0.03-0.09)		0.22(0.11-0.24) ***b***		3.59E-04(0-4.57E-04)#		4.44E-04(3.82E-04-2.76E-03)# ***b***		0.004	0.208	0.275
Ruminococcaceae	**L6**	5(4.28-6.48) ***a***	0.005	4.89(3.86-6.29)	0.434	0.03(6.54E-03-0.06)#	0.965	4.87E-03(3.52E-03-0.01)#	0.120	0.000	0.563	0.115
	L12	3.88(3.64-5.87) ***ab***		2.18(1.8-3.07)		0.02(9.49E-03-0.33)#		0.02(3.08E-03-0.17)#		0.000	0.355	0.600
	L18	2.66(2.38-3.09) ***b***		3.78(2-5.13)		0.03(0.02-0.04)#		0.03(0.02-0.22)#		0.000	0.600	0.655

Acidaminobacteraceae	**L6**	0(0-0)	1.000	0(0-0)	0.319	4.56E-04(0-6.99E-04)	0.800	0(0-0)	0.197	0.007	1.000	0.064
	L12	0(0-0)		0(0-0)		0(0-1.13E-04)		0(0-6.48E-05)		0.262	0.285	0.763
	L18	0(0-0)		0(0-0)		2.78E-04(0-2.79E-04)		0(0-0)		0.002	1.000	0.025
Mogibacteriaceae	**L6**	0.05(0.04-0.06)	0.091	0.05(0.03-0.06)	0.121	8.47E-04(2.44E-04-1.38E-03)#	0.468	2.51E-04(0-4.03E-04)#	0.622	0.000	0.728	0.110
	L12	0.03(0.02-0.06)		0.02(3.36E-03-0.02)		4.27E-04(3.22E-04-4.60E-04)#		1.21E-04(0-2.70E-04)#		0.000	0.132	0.070
	L18	0.02(0.02-0.02)		0.02(0.01-0.03)		0(0-1.79E-04)#		3.55E-04(0-1.10E-03)#		0.000	0.401	0.946
Erysipelotrichaceae	**L6**	0.21(0.14-0.82)	0.153	0.65(0.29-1.09)	0.516	0.01(0-0.13)#	0.499	5.35E-04(2.20E-04-5.59E-03)#	0.116	0.000	0.298	0.394
	L12	0.85(0.49-0.95)		0.28(0.22-0.48)		2.81E-03(1.93E-03-0.08)#		0.01(9.86E-04-0.13)#		0.001	0.165	0.834
	L18	0.37(0.17-0.49)		0.97(0.3-1.12)		1.08E-03(4.18E-04-0.05)#		8.79E-04(3.09E-04-1.89E-03)#		0.000	0.208	0.653
Bradyrhizobiaceae	**L6**	4.00E-04(0-5.95E-04) ***a***	0.043	6.10E-04(0-1.54E-03)	0.064	3.05E-04(0-3.22E-04)	0.146	0(0-0)***$ a***	0.029	0.067	0.542	0.011
	L12	0(0-0) ***b***		0(0-0)		0(0-0)		0(0-6.48E-05) ***a***		0.317	1.000	0.644
	L18	1.06E-04(0-5.72E-04) ***ab***		0(0-0)		3.23E-04(1.41E-04-4.03E-04)		3.79E-04(0-5.82E-04) ***b***		0.437	0.277	0.744
Phyllobacteriaceae	**L6**	0(0-0)	1.000	0(0-6.90E-05)	0.141	0(0-7.23E-05)	0.348	0(0-0)	0.092	0.247	0.171	0.144
	L12	0(0-0)		0(0-0)		0(0-0)		0(0-0)		1.000	1.000	1.000
	L18	0(0-0)		0(0-0)		0(0-0)		0(0-2.04E-04)		0.199	1.000	0.424
Rhizobiaceae	**L6**	0(0-9.99E-05)	0.514	6.10E-04(0-2.23E-03)	0.064	3.13E-04(2.89E-04-7.53E-04)***a***	0.011	0(0-0)$	0.550	0.068	0.315	0.012
	L12	0(0-0)		0(0-0)		0(0-0)***b***		0(0-2.32E-04)		0.308	0.350	0.301
	L18	0(0-4.37E-04)		0(0-0)		0(0-1.40E-04)***ab***		0(0-4.40E-04)		0.823	0.610	0.620
Rhodospirillaceae	**L6**	2.55E-04(0-2.75E-04)	0.470	2.92E-04(0-3.07E-04)	0.362	2.93E-03(1.41E-03-4.00E-03)#	0.652	2.88E-04(1.76E-04-6.21E-04)#	0.424	0.010	0.591	0.035
	L12	0(0-6.88E-05)		0(0-1.25E-04)		1.65E-03(2.01E-04-4.17E-03)#		1.50E-03(1.14E-03-1.64E-03)#		0.008	0.408	1.000
	L18	0(0-2.26E-04)		0(0-8.90E-05)		1.41E-03(7.75E-04-6.50E-03)#		3.79E-04(1.81E-04-1.26E-03)#		0.006	0.702	0.223

RESULTS

Alcaligenaceae	**L6**	1.05(0.91-1.32)	0.976	1.83(0.93-4.41)	0.881	1.95(1.58-3.18)	0.045	3.6(2.97-4)	0.297	0.055	0.418	0.093
	L12	1.1(0.79-1.68)		1.33(0.75-2.2)		3.11(1.57-3.31)#		3.12(2.7-3.81)#		0.016	1.000	0.753
	L18	1.24(0.61-2.37)		1.65(0.89-2.82)		5.08(3.21-6.86)#		5.27(3.35-5.33)#		0.002	0.401	0.749
Comamonadaceae	**L6**	4.00E-04(0-4.55E-04)	0.502	1.78E-03(0-5.35E-03)***a***	0.030	1.55E-03(8.98E-04-0.01)# ***a***	0.001	0(0-9.19E-05)# ***$ a***	0.006	0.019	0.370	0.002
	L12	1.12E-04(0-3.34E-04)		0(0-0)***$ b***		0(0-0) ***b***		0(0-1.72E-04) ***a***		0.142	0.038	0.441
	L18	3.38E-04(1.77E-04-1.11E-03)		4.15E-04(0-5.03E-04) ***ab***		3.23E-04(1.61E-04-7.00E-04) ***ab***		7.10E-04(4.26E-04-1.23E-03) ***b***		0.504	0.915	0.179
Oxalobacteraceae	**L6**	0(0-2.64E-04)	0.203	6.60E-04(2.29E-04-1.52E-03)	0.212	6.18E-03(4.23E-03-7.28E-03)#	0.002	0.02(0.01-0.03)# ***$***	0.564	0.000	0.088	0.016
	L12	3.51E-04(0-5.35E-04)		0(0-2.40E-04)		0.02(0.02-0.03)#		0.02(7.95E-03-0.03)#		0.000	0.329	0.529
	L18	0(0-5.93E-05)		5.50E-04(0-7.73E-04)***$***		7.42E-03(6.30E-03-0.01)#		0.01(0.01-0.01)#		0.000	0.049	0.142
Desulfovibrionaceae	**L6**	0.64(0.49-0.81)	0.586	0.78(0.26-1.37)	0.470	0.62(0.18-0.68)	0.928	0.12(0.08-0.38)	0.064	0.068	0.908	0.141
	L12	0.76(0.4-1.32)		0.72(0.44-1.34)		0.47(0.19-0.78)		0.49(0.33-0.65)		0.746	0.908	0.916
	L18	1.18(0.5-1.48)		1(0.67-1.29)		0.63(0.18-0.91)		0.31(0.28-0.61)		0.086	0.600	0.749
Aeromonadaceae	**L6**	0(0-0)	1.000	0(0-0)	0.408	5.65E-04(2.94E-04-8.46E-04)#	0.098	1.35E-03(9.68E-04-1.99E-03)#	0.302	0.000	0.350	0.115
	L12	0(0-0)		0(0-0)		2.13E-03(1.30E-03-2.30E-03)#		6.70E-04(3.46E-04-1.31E-03)# ***$***		0.000	1.000	0.036
	L18	0(0-0)		0(0-5.97E-05)		9.70E-04(5.78E-04-1.99E-03)#		1.33E-03(7.17E-04-1.54E-03)#		0.000	0.144	0.848
Enterobacteriaceae	**L6**	0.15(0.04-0.27)	0.361	0.22(0.08-0.45) ***ab***	0.022	10.67(7.12-12.78)#	0.238	18.6(13.57-22.76)#	0.597	0.000	0.203	0.141
	L12	0.26(0.07-0.39)		0.15(0.07-0.19) ***a***		23.03(18.86-23.71)#		15.55(11.31-18.49)#		0.000	0.817	0.141
	L18	0.2(0.07-0.49)		0.73(0.46-0.99) ***$ b***		14.76(12.28-39.02)#		19.75(12.51-19.88)#		0.000	0.046	0.848
Pasteurellaceae	**L6**	7.66E-03(6.11E-03-0.01)	0.524	7.21E-03(5.47E-03-0.03)	0.653	0(0-0)#	1.000	0(0-0)#	0.141	0.000	0.908	1.000
	L12	6.42E-03(3.48E-03-0.01)		9.04E-03(5.06E-03-0.04)		0(0-0)#		0(0-9.38E-05)#		0.000	0.487	0.144
	L18	0.02(5.64E-03-0.03)		0.03(0.02-0.04)		0(0-0)#		0(0-0)#		0.000	0.345	1.000

Pseudoalteromonadaceae	**L6**	0(0-0)	1.000	0(0-0)	0.562	3.32E-04(2.41E-04-2.86E-03)#	0.963	0(0-1.84E-04)#	0.308	0.003	1.000	0.125
	L12	0(0-0)		0(0-0)		7.14E-04(0-7.61E-03)#		2.70E-04(0-3.21E-04)#		0.019	0.285	0.258
	L18	0(0-0)		0(0-0)		2.82E-04(0-0.01)#		3.79E-04(1.81E-04-8.38E-04)#		0.008	0.317	0.948
Vibrionaceae	**L6**	0(0-0)	0.358	3.09E-04(0-3.85E-04)***$***	0.547	0.03(7.89E-03-0.04)# ***a***	0.014	0.1(0.05-0.14)#	0.051	0.000	0.016	0.059
	L12	0(0-1.67E-04)		0(0-1.26E-04)		0.1(0.08-0.12)# ***b***		0.05(0.02-0.11)#		0.000	0.882	0.093
	L18	0(0-5.93E-05)		1.19E-04(0-3.23E-04)		0.01(8.05E-03-0.03)# ***a***		0.02(6.85E-03-0.04)#		0.000	0.184	0.949
Xanthomonadaceae	**L6**	0(0-0)	0.392	1.13E-04(0-8.72E-04)***$ a***	0.014	2.85E-04(0-7.61E-04)#	0.112	0(0-0)#***$***	1.000	0.010	0.038	0.011
	L12	0(0-0)		0(0-0) ***b***		0(0-0)		0(0-0)		0.411	1.000	0.317
	L18	0(0-0)		0(0-0) ***b***		0(0-1.40E-04)		0(0-0)		0.214	0.317	0.142
Anaeroplasmataceae	**L6**	2.64E-04(9.99E-05-4.03E-04)	0.151	1.27E-04(0-2.61E-04) ***a***	0.014	0.48(2.22E-04-1)	0.164	0.05(0-0.13)	0.533	0.159	0.473	0.456
	L12	1.21E-04(0-2.88E-04)		6.16E-04(1.44E-04-8.12E-04) ***ab***		4.52E-03(2.20E-03-2.07)		0.07(5.48E-04-0.13)#		0.006	0.189	0.674
	L18	5.75E-04(4.22E-04-7.15E-04)		1.59E-03(9.55E-04-4.40E-03) ***b***		3.23E-04(2.79E-04-6.09E-04)		0.3(0.01-0.33)#		0.036	0.141	0.073
Verrucomicrobiaceae	**L6**	1.92(1.33-2.2)	0.722	1.23(0.69-1.74)	0.974	1.97(0.44-3.94)	0.583	2.96(1.61-4.16)	0.543	0.282	0.247	0.345
	L12	1.63(0.73-2.58)		0.95(0.71-1.12)		0.54(0.01-2.4)		3(0.35-6.35)		0.550	0.247	0.345
	L18	1.13(0.94-1.59)		1.02(0.52-2.07)		0.02(6.52E-03-5.44)		0.02(0.01-5.52)		0.572	0.529	0.848
Genus												
Other	**L6**	0.02(6.17E-03-0.02)	0.292	0.02(7.49E-03-0.03)	0.020	1.50E-04(0-3.28E-04)#	0.039	0(0-1.50E-04)#	0.081	0.000	0.563	0.487
	L12	0.01(4.73E-03-0.01)		7.05E-03(2.48E-03-0.01)		1.34E-04(0-4.43E-04)#		1.14E-04(0-3.59E-04)#		0.000	0.203	0.822
	L18	5.88E-03(5.23E-03-7.41E-03)		2.96E-03(2.26E-03-3.79E-03)***$***		1.08E-03(7.63E-04-2.99E-03)		2.22E-03(3.55E-04-7.56E-03)		0.061	0.012	0.564
Corynebacterium	**L6**	0(0-0)	0.196	2.69E-04(0-6.49E-04)	0.934	0(0-0)#	1.000	0(0-0)#	0.631	0.020	0.090	0.317
	L12	0(0-2.53E-04)		4.52E-04(0-5.02E-04)		0(0-0)#		0(0-0)#		0.039	0.346	0.317

RESULTS

	L18	3.35E-04(0-5.55E-04)		1.44E-04(0-5.98E-04)		0(0-0)#		0(0-0)#		0.014	0.826	1.000
Rothia	**L6**	1.24E-03(8.24E-04-1.38E-03)	0.050	1.76E-03(1.11E-03-2.42E-03)	0.642	0(0-0)#	1.000	0(0-0)#	0.392	0.000	0.298	1.000
	L12	8.67E-04(6.94E-04-1.07E-03)		5.73E-04(5.02E-04-2.41E-03)		0(0-0)#		0(0-0)#		0.000	0.908	0.317
	L18	3.72E-04(1.90E-04-5.75E-04)		1.42E-03(8.95E-04-1.61E-03)		0(0-0)#		0(0-0)#		0.001	0.057	1.000
Rhodococcus	**L6**	0(0-2.07E-04)	0.177	0(0-1.36E-03)	0.144	0(0-0)	0.392	0(0-0)	0.107	0.190	0.449	0.317
	L12	0(0-0)		0(0-0)		0(0-0)		0(0-8.87E-05)		0.290	0.285	0.144
	L18	0(0-4.14E-04)		2.84E-03(0-0.05)		0(0-0)		0(0-6.44E-04)#		0.046	0.104	0.062
Bifidobacterium	**L6**	4.42E-03(1.06E-03-0.04)	0.528	0.08(9.54E-03-0.63)	0.112	1.48E-04(0-3.10E-04)#	0.903	0(0-2.06E-04)# ***a***	0.001	0.000	0.180	0.418
	L12	2.87E-03(1.31E-03-6.06E-03)		2.78E-03(9.40E-04-0.01)		0(0-3.32E-04)#		0(0-0)# ***a***		0.000	0.817	0.370
	L18	1.59E-03(7.66E-04-4.58E-03)		0.02(6.07E-03-0.29) ***$***		2.80E-04(0-3.85E-04)#		8.18E-04(6.01E-04-2.15E-03)***$ b***		0.001	0.036	0.012
Enterococcus	**L6**	0(0-1.47E-04)	0.060	1.27E-04(0-2.88E-04)	0.455	0(0-0)	1.000	0(0-0)#	1.000	0.040	0.602	1.000
	L12	0(0-0)		0(0-9.54E-05)		0(0-0)		0(0-0)		0.234	0.563	1.000
	L18	2.60E-04(1.62E-04-4.82E-04)		0(0-7.22E-05)		0(0-0)#		0(0-0)		0.004	0.092	1.000
Bacteroides	**L6**	5.77(4.5-10.79) ***a***	0.004	3.97(2.28-13.54)	0.619	18.72(8.35-25.34) ***a***	0.012	3.38(0.07-10.1)***$***	0.067	0.190	0.487	0.027
	L12	4.37(2.99-4.66) ***a***		6.35(5.04-10.42)		0.11(0.06-3.46)# ***b***		10.75(2.95-26.08)* # ***$***		0.036	0.105	0.016
	L18	10.09(8.24-13.38) ***b***		5.99(4.61-12.1)		0.07(0.05-4.95)# ***b***		0.19(0.11-2.34)#		0.007	0.141	0.749
Parabacteroides	**L6**	12.45(12.17-15.71)	0.774	9.32(7.99-10.01) ***$***	0.063	43.46(31.73-49.99)#	0.865	51.15(43.9-57.57)#	0.541	0.000	0.015	0.141
	L12	16.87(8.52-19.54)		24.58(19.02-25.63)		41.89(23.12-57.02)#		48.36(35.57-52.27)#		0.003	0.064	0.600
	L18	16.29(11.48-22.04)		17.45(7.64-30.05)		36.03(25.01-50.82)#		55.29(49.01-66.11)# ***$***		0.003	0.916	0.035
Porphyromonas	**L6**	9.95E-04(2.07E-04-1.67E-03)	0.062	1.01E-04(0-2.48E-04)	0.134	9.43E-04(2.41E-04-0.02)#	0.400	0.01(7.13E-03-0.02)# ***a***	0.009	0.037	0.151	0.598
	L12	7.45E-04(0-1.22E-03)		1.39E-03(2.80E-04-1.59E-03)		2.40E-04(0-0.02)		5.03E-03(0-0.01) ***ab***		0.936	0.683	0.913

	L18	0(0-5.91E-05)		1.44E-04(0-4.13E-04)		0(0-1.47E-03)		0(0-0) ***b***		0.152	0.228	0.062
Prevotella	**L6**	2.39(1.44-5.64)	0.446	1.36(0.7-3.81)	0.981	0.02(7.18E-03-0.03)#	0.483	3.46E-03(1.11E-03-0.01)#	0.071	0.000	0.298	0.141
	L12	5.77(3.39-10.26)		1.47(1.06-3.31)		0.01(5.77E-03-0.5)***$***		4.55E-03(1.35E-03-8.02E-03)# ***$***		0.000	0.049	0.046
	L18	5.38(3.48-7.6)		2.95(0.85-4.07)		9.33E-03(5.77E-03-0.01)#		0.01(7.28E-03-0.05)#		0.000	0.115	0.142
Bacillus	**L6**	0(0-0) ***a***	0.046	6.07E-04(2.07E-04-6.78E-04)*** $***	0.309	0(0-3.78E-04)	0.955	1.53E-04(0-3.32E-04)#	0.947	0.023	0.006	0.817
	L12	0(0-2.96E-04) ***a***		0(0-3.65E-04)		0(0-2.59E-04)		1.55E-04(0-3.96E-04)		0.912	0.896	0.418
	L18	2.40E-04(0-3.17E-04) ***b***		3.16E-04(0-4.44E-04)		0(0-2.24E-04)		0(0-6.01E-04)		0.843	0.553	0.710
Enterococcus	**L6**	2.00E-04(0-8.70E-04)	0.461	7.70E-04(5.57E-04-1.22E-03)	0.333	4.70E-04(2.17E-04-1.67E-03)	0.581	4.90E-05(0-6.07E-04)	0.527	0.187	0.131	0.281
	L12	5.96E-04(2.35E-04-9.58E-04)		5.77E-04(2.65E-04-9.51E-04)		1.37E-03(2.35E-04-4.61E-03)		1.30E-04(0-5.71E-04)		0.263	0.954	0.067
	L18	1.22E-04(0-3.67E-04)		1.38E-03(3.79E-04-2.38E-03) ***$***		5.55E-04(1.62E-04-1.25E-03)		8.88E-04(0-2.08E-03)		0.111	0.011	0.845
Lactobacillus	**L6**	0.69(0.56-1.51)	0.078	1.61(0.39-3.15)	0.516	0.76(0.23-1.43)	0.583	0.02(1.90E-03-0.34)# ***$***	0.272	0.030	0.728	0.046
	L12	2.38(1.4-3.1)		0.93(0.76-1.19) ***$***		0.27(9.71E-03-1.17)#		0.38(1.40E-03-1.24)#		0.038	0.015	0.462
	L18	0.67(0.24-2.22)		2.11(1.08-3.24)		0.23(6.57E-03-2.72)		0.36(0.16-1.3)		0.481	0.401	0.655
Leuconostoc	**L6**	1.66E-03(6.31E-04-1.88E-03)	0.132	4.24E-03(2.32E-03-9.53E-03)	0.089	1.00E-03(4.03E-04-1.54E-03)***a***	0.003	2.47E-03(1.02E-03-8.60E-03)	0.867	0.053	0.056	0.059
	L12	2.41E-03(1.60E-03-5.68E-03)		5.04E-04(3.35E-04-8.43E-04)		4.27E-03(2.53E-03-6.62E-03)***b***		3.27E-03(1.27E-03-7.62E-03)		0.073	0.165	0.674
	L18	5.97E-03(4.27E-03-8.93E-03)		0.01(4.16E-03-0.02)		5.81E-03(3.20E-03-0.01)***b***		2.64E-03(2.29E-03-3.77E-03)		0.633	0.527	0.338
Lactococcus	**L6**	4.64E-03(2.87E-03-7.34E-03)	0.483	9.25E-03(5.29E-03-0.02) ***a***	0.016	0(0-0)#	0.631	0(0-0)#	0.562	0.000	0.083	0.317
	L12	6.39E-03(4.51E-03-0.01)		2.26E-03(1.22E-03-3.84E-03)***$ b***		0(0-0)#		0(0-0)#		0.000	0.049	0.927
	L18	0.01(3.04E-03-0.02)		0.02(9.68E-03-0.03)***a***		0(0-0)#		0(0-0)#		0.000	0.674	0.317
Blautia	**L6**	8.68(6.79-13.54)	0.610	10.51(6.34-17.38)	0.408	3.50E-03(6.27E-04-6.28E-03)#	0.063	4.99E-03(3.00E-03-0.02)#	0.133	0.000	0.817	0.401

RESULTS

	L12	8(6.99-10.18)		5.47(4.66-8.89)		0.03(0.01-0.04)#		7.51E-03(3.80E-03-0.01)#		0.000	0.165	0.059
	L18	7.48(4.64-10.24)		14.39(6.54-16.71)		3.95E-03(3.18E-03-6.81E-03)#		0.02(0.01-0.03)***$ #***		0.000	0.294	0.004
Butyrivibrio	**L6**	5.27E-04(4.21E-04-8.56E-04)	0.761	1.25E-03(1.11E-03-1.71E-03) ***$***	0.012	0(0-0)#	1.000	0(0-0)#	1.000	0.000	0.004	1.000
	L12	5.94E-04(3.93E-04-1.73E-03)		1.73E-03(1.45E-03-2.50E-03)		0(0-0)#		0(0-0)#		0.000	0.083	1.000
	L18	1.03E-03(4.32E-04-1.45E-03)		4.32E-04(2.11E-04-7.25E-04)		0(0-0)#		0(0-0)#		0.000	0.292	1.000
Coprococcus	**L6**	1.17(0.84-2.46)***a***	0.040	3.23(2.48-4.5)***$***	0.490	0.02(8.93E-04-0.04)	0.282	7.23E-03(1.03E-03-8.05E-03)	0.178	0.000	0.049	0.208
	L12	3.06(2.02-4.32)***ab***		1.94(1.65-4.28)		8.53E-03(4.35E-03-0.01)		1.19E-03(1.09E-03-2.98E-03)***$***		0.000	0.817	0.046
	L18	4.12(2.72-5.43)***b***		3.13(1.54-4.38)		1.94E-03(1.53E-03-3.49E-03)		3.27E-03(3.07E-03-0.02)		0.000	0.345	0.141
Ruminococcus	**L6**	0.74(0.22-1.13)***a***	0.025	0.97(0.65-1.52)	0.229	3.25E-04(2.17E-04-1.13E-03)# ***a***	0.005	2.97E-03(1.36E-03-0.03)#	0.110	0.000	0.298	0.009
	L12	3.61(1.37-4.21)***b***		1.02(0.68-1.24)***$***		3.20E-03(1.86E-03-0.04)# ***b***		9.50E-04(5.36E-04-1.91E-03)# ***$***		0.000	0.037	0.016
	L18	0.55(0.35-0.94)***ab***		0.5(0.3-1.04)		1.34E-03(8.62E-04-2.11E-03)#***ab***		2.22E-03(9.62E-04-6.03E-03)#		0.000	0.834	0.565
Oscillospira	**L6**	3.8(2.91-4.67)***a***	0.015	3.35(2.69-3.94)	0.311	0.02(3.97E-03-0.13)#	0.981	2.40E-03(2.10E-03-7.23E-03)#	0.134	0.000	0.563	0.115
	L12	2.65(2.25-3.22)***b***		1.61(1.32-4.52)		8.42E-03(6.49E-03-0.25)#		0.01(2.04E-03-0.16)#		0.000	0.355	0.674
	L18	2.03(1.8-2.34)***b***		1.89(1.12-3.67)		0.02(0.01-0.02)#		0.01(9.62E-03-0.12)#		0.000	0.834	0.749
Allobaculum	**L6**	0.09(9.14E-03-0.17)***a***	0.044	0.09(3.82E-03-0.15)	0.448	0(0-0)#	0.294	0(0-0)#	0.279	0.000	0.954	0.317
	L12	3.16E-03(7.50E-04-0.05)***b***		0.03(4.33E-04-0.05)		0(0-8.11E-05)#		1.21E-04(0-2.83E-04)#		0.000	0.643	0.469
	L18	4.53E-04(2.42E-04-1.04E-03)***ab***		7.92E-03(3.23E-04-0.11)		0(0-1.41E-04)#		0(0-0)#		0.009	0.270	0.657
Coprobacillus	**L6**	0(0-0.02)***a***	0.009	5.06E-04(2.57E-04-0.03)	0.028	0(0-0)#	1.000	0(0-0)#	0.392	0.002	0.346	0.317
	L12	0(0-5.31E-05)***a***		6.16E-04(1.26E-04-1.46E-03)* ***$***		0(0-0)#		0(0-0)#		0.002	0.024	1.000
	L18	1.33E-03(4.61E-04-5.60E-03)***b***		0(0-0)****$***		0(0-0)#		0(0-0)#		0.000	0.002	1.000

Sutterella	**L6**	1.05(0.91-1.46)	0.976	1.83(0.93-4.41)	0.881	1.95(1.58-3.18)***a***	0.045	3.6(2.97-4)	0.297	0.055	0.418	0.093
	L12	1.1(0.79-1.68)		1.33(0.75-2.2)		3.11(1.57-3.84)# ***b***		3.12(2.7-3.81)#		0.016	1.000	0.753
	L18	1.24(0.61-2.37)		1.65(0.89-2.82)		5.08(3.21-6.86)€ ***b***		5.27(3.35-5.55)#		0.002	0.401	0.749
Bilophila	**L6**	3.20E-03(1.51E-03-6.30E-03)	0.201	6.95E-04(2.07E-04-1.62E-03)	0.321	8.14E-03(2.09E-03-0.02)	0.022	9.60E-03(0-0.11)	0.099	0.398	0.131	1.000
	L12	1.29E-03(6.63E-04-2.05E-03)		5.77E-04(1.25E-04-2.33E-03)		0(0-7.13E-04)#		0.02(0.01-0.03)* # ***$***		0.007	0.815	0.004
	L18	9.70E-04(2.51E-04-1.74E-03)		2.00E-03(1.45E-03-4.54E-03)		4.47E-04(0-7.82E-04)#		0.16(0.05-0.28)* # ***$***		0.000	0.103	0.002
Enterobacter	**L6**	9.99E-04(3.56E-04-1.36E-03)***a***	0.009	1.30E-03(4.51E-04-2.45E-03)***a***	0.028	0.18(0.11-0.28)# ***a***	0.001	0.24(0.12-0.79)# ***a***	0.001	0.000	0.452	0.462
	L12	7.51E-04(2.57E-04-3.30E-03)***a***		1.75E-03(9.21E-04-2.40E-03)***ab***		0.68(0.35-0.98)# ***ab***		0.47(0.15-1.02)# ***a***		0.000	0.418	0.600
	L18	5.85E-03(4.44E-03-8.85E-03)***b***		0.01(5.77E-03-0.03)***b***		1.93(0.95-3.32)# ***b***		3.02(1.83-4.14)# ***b***		0.000	0.294	0.277
Erwinia	**L6**	2.55E-04(0-3.13E-04)	0.310	0(0-7.63E-05)***a***	0.012	0.02(0.01-0.04)#	0.067	0.05(0.03-0.07)#	0.339	0.000	0.361	0.074
	L12	2.44E-04(1.66E-04-6.45E-04)		0(0-2.20E-04)***a***		0.07(0.05-0.09)#		0.05(0.04-0.07)#		0.000	0.232	0.345
	L18	6.87E-04(1.90E-04-1.79E-03)		1.41E-03(6.47E-04-3.19E-03)***b***		0.04(0.02-0.07)#		0.03(0.02-0.05)#		0.000	0.343	0.655
Klebsiella	**L6**	4.49E-04(2.79E-04-1.72E-03)	0.751	1.53E-03(4.14E-04-4.03E-03)***a***	0.025	0.21(0.17-0.23)# ***a***	0.008	0.19(0.15-0.45)#	0.054	0.000	0.296	0.834
	L12	1.26E-03(0-6.48E-03)		4.52E-04(2.51E-04-1.53E-03)***a***		0.37(0.31-0.64)# ***ab***		0.25(0.12-0.45)#		0.000	0.770	0.345
	L18	1.23E-03(5.15E-04-2.46E-03)		0.01(4.44E-03-0.03)***$ b***		0.74(0.58-1.12)# ***b***		0.51(0.4-0.56)#		0.000	0.009	0.180
Vibrio	**L6**	0(0-0)	0.358	3.09E-04(0-6.10E-04)***$***	0.547	0.03(7.82E-03-0.06)#	0.014	0.1(0.05-0.14)#	0.051	0.000	0.016	0.059
	L12	0(0-1.67E-04)		0(0-1.26E-04)		0.1(0.08-0.15)#		0.05(0.02-0.11)#		0.000	0.882	0.141
	L18	0(0-5.93E-05)		1.19E-04(0-7.25E-04)		0.01(7.83E-03-0.03)#		0.02(6.85E-03-0.04)#		0.000	0.184	0.949
Anaeroplasma	**L6**	2.64E-04(9.99E-05-4.03E-04)	0.151	1.27E-04(0-3.23E-04)***a***	0.014	0.48(2.22E-04-2.27)	0.164	0.05(0-0.41)	0.533	0.159	0.473	0.456
	L12	1.21E-04(0-5.42E-04)		6.16E-04(1.44E-04-1.08E-03)***ab***		4.52E-03(2.20E-03-5.06)#		0.07(5.48E-04-0.25)#		0.006	0.189	0.674

RESULTS

	L18	5.75E-04(4.22E-04-1.20E-03)		1.59E-03(9.55E-04-4.40E-03)***b***		3.23E-04(2.79E-04-7.29E-04)#		0.3(0.01-1.59)#		0.036	0.141	0.073
Akkermansia	**L6**	1.92(1.33-2.2)	0.722	1.23(0.69-1.77)	0.974	1.97(0.44-3.94)	0.583	2.96(1.61-4.16)	0.543	0.282	0.247	0.345
	L12	1.63(0.73-2.58)		0.95(0.71-1.37)		0.54(0.01-2.4)		3(0.35-6.35)		0.550	0.247	0.345
	L18	1.13(0.94-1.59)		1.02(0.52-2.07)		0.02(6.52E-03-5.44)		0.02(0.01-5.52)		0.572	0.529	0.848

[1]P-value by Kruskal-Wallis test comparing photoperiods in each group. ab letters indicate significant photoperiods differences analyzed by Kruskal-Wallis test followed by Bonferroni p-values adjustment (p<0.016).

*[2]P-value by Kruskal-Wallis test comparing treatment effect into each group. * and # indicate significant GSPE and ABX effect respectively, analyzed by Kruskal-Wallis test followed by Bonferroni p-values adjustment (p<0.016).*

[3]P-Value by U-Mann Whitney test to analyze GSPE effect, comparing VH and GSPE-treated rats and ABX and GSPE+ABX-treated rats into each photoperiod. $ indicates significant GSPE effect using U-Mann Whitney test (p<0.05).

[4]Data shown as median (firts and third quartile) in percentage of relative abundance (n=7-8)

Ph:photoperiod condition; L6: 6h light/18h darkness; L12: 12h light/12h darkness; L18: 18h light/6h darkness; CAF: cafeteria diet; GSPE: grape seed proanthocyanidins extract; VH: vehicle; ABX: antibiotic cocktail;

Manuscript 4

Objective: To evaluate if GSPE bioavailability is influenced by different photoperiod exposure via gut microbiota modulation in an obesogenic context

Gut microbiota influences the photoperiod effects on proanthocyanidins bioavailability

Arreaza-Gil V[†], Escobar-Martínez I[†], Mulero M, Muguerza B, Suárez M, Anna Arola-Arnal* and Torres-Fuentes C.

Universitat Rovira i Virgili, Department de Biochemistry and Biotechnology, Nutrigenomics Research Group, Tarragona, 43007, Spain

*Corresponding author

[†]Co-authors

Manuscript in preparation.

RESULTS

ABSTRACT

Grape Seed Proanthocyanidins have health effects on metabolic syndrome and obesity in animal models. These effects are mainly attributed to polyphenols-derived metabolites generated after their gastrointestinal digestion where gut microbiota plays an important role. In addition, gut microbiota composition and polyphenols bioavailability have been shown to be affected by differences in day light length (photoperiod). Thus, the aim of this study was to evaluate if a grape seed proanthocyanidin extract (GSPE) bioavailability is influenced by different photoperiod exposure via gut microbiota in an obesogenic context. To this goal, male Fischer 344 rats fed a cafeteria diet were housed under three different photoperiod conditions (6, 12 or 18 h of light per day) for 9 weeks. During the last 4-weeks, animals were daily administered with GSPE (25 mg/kg) or the combination of GSPE and an antibiotic cocktail (ABX) in drinking water. Serum GSPE-derived metabolites were quantified by HPLC-MS/MS. A higher bioavailability was observed in rats housed under L6 conditions compared to L18 conditions. Individual metabolites, especially those derived by the gut microbiota, were affected by the different photoperiod conditions. Interestingly, ABX treatment altered these photoperiod-mediated changes. Therefore, these results indicate that gut microbiota play a key role in the effects that different day light lengths have on the bioavailability of GSPE in CAF rats.

Keywords: GSPE, bioavailability, obesity, gut microbiota, seasonal rhythms

1. Introduction

Proanthocyanidins (PAs) are the most common groups of polyphenols in the human diet [1].They are formed by oligomerization or polymerization of subunits of flavan-3-ols (catechin and epicatechin) and their gallic acid esters [2]. PAs exist ubiquitously in many edible plants sources including barley, hops, maize, apples, grapes, strawberries, cocoa, almond, cinnamon, peanuts, and tea. Grape seeds in particular provide a diverse source of PAs, whose consumption has been linked to a range of health benefits [3]. Specifically, a grape seed proanthocyanidin extract (GSPE) has demonstrated several beneficial effects on the health, improving insulin resistance [4], hypertension [5–7], oxidative stress [8], mitochondrial dysfunctionality [9] and lipid metabolism [10–12] in rats. Thus, showing the potential role of PAs in the prevention of metabolic syndrome and cardiovascular diseases.

Several studies attribute the beneficial health properties of polyphenols to the products derived from their metabolism [13]. Thus, once absorbed in the small intestine, phenolic compounds are recognized as xenobiotic and undergo extensive phase-II enzymatic detoxification, including glucuronidation, sulfation and/or methylation, in the small intestine or in the liver [14]. However, it is estimated that 90-95 % of dietary polyphenols reach the colon, where a wide range of enzymes produced by gut bacteria can hydrolyze, reduce, dehydroxylate, decarboxyalte and demethylate the polyphenols [14]. Because of this step, high molecular weight PAs are transformed into small phenolic acid microbial-derived metabolites (valerolactone compounds, phenylpropionic acids, phenylacetic acids, benzoic acids, and several conjugated phenolic acids) [15,16]. Part of these phenolic acid microbial metabolites are absorbable and can reach the liver for phase II metabolism. Subsequently, both phase II and microbial-derived metabolites reach the different tissues via systemic circulation [17–19]. Additionally, the metabolites in the liver can be excreted via the bile duct or be reabsorbed throughout the enterohepatic recirculation

[20]. Finally, the metabolites are excreted in the urine, and non-absorbed polyphenols are directly eliminated in the feces [14].

Photoperiods can affect the functionality and the bioavailability of polyphenols [21,22]. Thus, cafeteria diet-induced obese rats supplemented with polyphenol-rich fruits presented higher leptin sensitivity only under short winter-like day length (SD) [21]. Moreover, a higher bioavailability of phenolic acids was found in normoweight rats treated with red grapes housed under SD compared to rats housed under summer-like day length conditions (LD) [22]. However, the specific mechanism involved in these photoperiod-mediated effects on polyphenols bioavailability are not yet fully understood. In this regard, gut microbiota may be play an important role. Thus, as above mentioned, these bacteria are significantly involve in polyphenols metabolism and have been shown to be affected by different photoperiod conditions [23–27] . Indeed, it was recently published that animals fed with a diet containing isoflavones and housed under different photoperiod conditions showed an association between the gut bacterial communities, photoperiod length and isoflavone compounds [28].

Hence, the aim of this study was to evaluate if the serum bioavailability of GSPE is influenced by different photoperiods exposure via gut microbiota in cafeteria-induced obese rats.

2. Materials and methods

2.1. Grape seed proanthocyanidin extract.

Grape seed proanthocyanidin extract (GSPE) was obtained from white grape seed and provided by *Les Dérives Résiniques et Terpéniques* (Dax, France). According to the manufacturer, this flavanol-rich extract contained monomeric (25.0%), dimeric and trimeric (43.3%), and oligomeric (< 3 units; 31.7%) procyanidin. The main phenolic compounds (flavan-3-ols and phenolic acids) present in the extract are shown in **Table 1** [29].

Table 1. Main phenolic compounds (flavan-3-ols and phenolic acids) of the grape seed proanthocyanidin extract (GSPE) used in this study, analyzed by HPLC-MS/MS.

Phenolic compound	Concentration (mg/g)
Protocatechuic acid (PCA)	1.40 ± 0.25
Catechin	51.88 ± 5.56
Epicatechin	62.86 ± 8.32
3,4,5-trihydroxybenzoic acid	44.66 ± 7.76
Kaempferol-3-glucoside	0.50 ± 0.02
Naringenin-7-glucoside	0.64 ± 0.08
p-Coumaric acid	0.09 ± 0.01
Quercetin	0.05 ± 0.01
Quercetin-3-O-galactoside	0.43 ± 0.05
4-hydroxy-3-methoxybenzoic acid	0.09 ± 0.01
Procyanidin dimer	76.84 ± 15.76
Procyanidin trimer	13.04 ± 0.64
Procyanidin tetramer	5.14 ± 0.28
Dimer gallate	15.22 ± 2.72
Epicatechin gallate	14.24 ± 2.76
Epigallocatechin gallate	0.06 ± 0.01

Adapted from Rodríguez, MR. *et al.* (2022) [29]. Concentrations are expressed as mg of compound per gram of fresh extract (mean ± standard derivation).

2.2. Chemical and reagents.

Acetone, acetonitrile, phosphoric acid (Sigma-Aldrich, Madrid, Spain), glacial acetic acid (Panreac, Barcelona, Spain) and methanol (Scharlab S.L., Barcelona, Spain) were all of HPLC analytical grade. Ultrapure water was obtained from a MilliQ Advantage A10 system (Millipore, Madrid, Spain).

Individual standard stock solutions of 2000 mg/L of (+)-catechin, epigallocatechin gallate (EGCG), 3,4,5-trihydroxybenzoic acid, 4-hydroxy-3-methoxybenzoic acid, 3-hydroxybenzoic acid, 3'-hydroxyphenylacetic acid, 3’,4’-Dihydroxycinnamic acid, 3-(4'-hydroxyphenyl)propanoic acid, benzoic acid, hippuric acid, 4’-hydroxy-3’-methoxycinnamic acid and benzene-1,2-diol (internal standard; IS) (all purchased from Fluka / Sigma-Aldrich, Madrid, Spain),

and proanthocyanidin B2 (Extrasynthese Lyon, France), were prepared in methanol and stored in dark glass flasks at -20 °C. In addition, a stock solution containing all individual compounds was prepared weekly at a concentration of 2000 ppm in methanol. Standard compounds were mixed to create the calibration curve prepared in acetone/water/acetic acid (70:29.5:0.5, v:v:v). This solution was stored in dark glass containers at -20 °C until chromatographic analysis.

2.3. Experimental design.

Thirteen weeks old male Fischer 344 rats (F344) (n=96) were obtained from Janvier Laboratories (France). Rats were pair-housed at standard conditions (22±1ºC, 50-55% relative humidity and 12:12 hour light/dark cycle) with ad libitum access to water and standard chow diet for one week. After this acclimation week, rats were weighted and randomized distributed into three different photoperiods for 9 weeks: short photoperiod [L6, 6 h light/18 h darkness], standard photoperiod [L12, 12 h light/12 h darkness], or long photoperiod [L18, 18 h light/6 h darkness]. Into each photoperiod, rats were further randomly divided into four groups (n=8) depending on the treatment administered in the last four weeks. Thus, rats were administered with GSPE (25 mg/kg body weight dissolved in vehicle (VH, solution of water and condensed milk (5:1)) or with the combination of GSPE and an antibiotic cocktail (ABX) during the last four weeks. GSPE were orally and daily administered one hour after the light was turned on. Animals administered with VH or with VH and ABX were used to subtract any phenolic compound in serum no derived from the GSPE. During the whole experiment procedure, rats were fed a cafeteria diet (CAF) composed of highly palatable and energy-dense human foods (58% CH, 31% lipid, and 11% protein). CAF was freshly prepared every day and included the following (grams per rat and per day): biscuits with pâté and cheese (15-17 g), bacon (7-10 g), ensaimada (pastry) (10-15 g), carrot (11-12 g), standard chow (20-25 g) and milk containing 22% sucrose (w/v). The ABX (0.5

g/l ampicillin, 0.250 g/l vancomycin and 0.125 g/l imipenem; Discovery fine chemicals Ltd, United Kingdom) was freshly prepared every day and administered in drinking water.

Animals were sacrificed by decapitation, following a fasting period of three hours after the last dose administration. Serum samples were obtained from the blood collected from the neck, in non-heparinized tubes. The blood was incubated for 1 h at room temperature and immediately centrifuged at 1200x g for 15 min to collect the serum. The serum samples were stored at -80ºC until chromatographic analysis was performed (**Figure 1**). The Animal Ethics Committee of the University Rovira i Virgili (Tarragona, Spain) and the Generalitat de Catalunya approved all the procedures (number reference 9495) in accordance with the EU Directive 2010/63/EU for animal experiments.

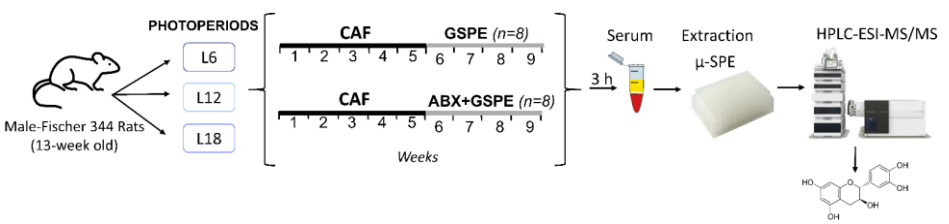

Figure 1. Experimental design. *13-week old male-Fischer 344 rats were housed under three different photoperiods (L6, L12 and L18) for 9 weeks. Into each photoperiod animals were fed a CAF and orally administered with GSPE (25 mg/kg) or with the combination of GSPE and ABX (0.5 g/l ampicillin, 0.250 g/l vancomycin and 0.125 g/l imipenem) daily in drinking water during the last 4-week of the experiment. L6: 6h light/18h darkness; L12: 12h light/12h darkness; L18: 18h light/6h darkness; CAF: cafeteria diet; GSPE: grape seed proanthocyanidin extract; ABX: antibiotic cocktail.*

2.4. Micro-solid phase serum phenolic metabolites extraction.

In order to analyze the content of polyphenols and its derivatives of the serum samples it was necessary to make an extraction to eliminate possible interferences. For this purpose, our previous developed methodology based on micro solid-phase extraction (μSPE) was performed using 30 μm OASIS HLB μ-Elution Plates (Waters, Barcelona, Spain) [30].

Briefly, the micro-cartridges were sequentially conditioned with 250 μL of methanol and 250 μL of 0.2% acetic acid. Serum samples (250 μL) were mixed

with 300 µL 4% H3PO4 and 50 µL IS at 20 ppm, and this mixture was loaded into the plates. Subsequently, a washing process was carried out to remove interferences that may have been retained in the plates with 200 µL Milli-Q water and then 200 µL acetic 0.2 %. Finally, the samples were eluted twice with 50 µL of acetone: water: acetic acid (70: 29.5: 0.5, v: v: v). The eluted solutions were directly injected into the chromatography equipment.

2.5. Chromatographic analysis (HPLC-ESI-MS/MS).

Chromatographic separation of phenolic compounds in µ-SPE eluted solutions was performed using an Agilent 1290 LC Series and Zorbax SB-Aq chromatographic column (150 mm x 21 mm i.d., 3.5 µm particle size, Agilent Technologies Palo Alto, CA, USA) at room temperature. The mobile phase consisted of 0.2 % acetic acid in water (solvent A) and 100 % acetonitrile (solvent B). The mobile phase gradient is summarized in **Table 2**. A post run of 10 min was applied for column equilibration. The flow rate was set at 0.4 mL/min and the injection volume was 2.5 µL for all runs. Quantification was performed by coupling the LC system to a 6490 (MS/MS) tandem mass spectrometer (Agilent Technologies) following the method described by Margalef *et al.* 2014 [30]. Negative electrospray (ESI) mode at unit resolution. Electrospray capillary voltage was 3000 V, source temperature was 200 ºC, and the flow rate was 14 L/min with a nebulizer gas pressure of 20 psi. The MS/MS data were acquired in "Multiple Reaction Monitoring" (MRM) mode. Optimized MRM conditions for the analysis were performed as previously reported for the quantification of phase-II and microbial flavan-3-ols metabolites in plasma [30].

Table 2. Applied HPLC Gradient Parameters for the Elution of GSPE metabolites.

Time (min)	Solvent A (%)	Solvent B (%)	Flow rate (mL/min)
0	95	5	0.4
10	45	55	0.4
12	20	80	0.4
15	20	80	0.4
16	95	5	0.4

2.6. Sample quantification.

For the quantification of the samples, control group blank serum was spiked with standard compounds at 8 different concentrations (20-5000 ppb) to obtain calibration curves. Concentrations of metabolites found in GSPE and GSPE+ABX groups were obtained by subtracting the concentrations of compounds quantified in VH and ABX groups respectively, in each photoperiod. Samples were quantified by interpolating the analyte/IS peak abundance ratio in the standards curves. All quality parameters are presented in **Table S1**. Data acquisition was performed by using MassHunter Software (Agilent Technologies, Palo Alto, CA, USA).

2.7. Statistical analysis.

Data are shown as median (first quartile and third quartile) and were plotted using Graphpad Prism 8.0 software (Graphapad software Inc, San Diego, CA, USA). Statistical analyses were carried out using SPSS software (IBS SPSS statistics 25, Chicago, IL, USA). Normality and homogeneity of variance were evaluated by Shapiro-Wilk and Levene's test respectively. Data were non-parametric because of the analysis were performed using non-parametric tests: photoperiod effect was analyzed by Kruskal Wallis test followed by Bonferroni p-values adjustment to comparison by pairwise ($p<0.016$), while the comparison between treatments in each photoperiod was analyzed by U Mann-Whitney test ($p<0.05$).

Principal component analysis (PCA) involving serum phenolic compounds data were analyzed and plotted using MetaboAnalyst v.5.0 [31]. Missing values were replaced by the half of the minimum positive values in the data, assuming that most missing values are caused by low abundance metabolites.

Statistical significances are subsequently depicted as follows: * indicating differences between experimental groups (GSPE vs GSPE+ABX) in each

photoperiod ($p \leq 0.05$), and *ab* letters indicating photoperiod effect ($p \leq 0.05$). The statistical test used for individual analysis is provided in the figure legends.

3. Results

To evaluate the role of the gut microbiota in the effect of different photoperiod conditions on the bioavailability and metabolism of GSPE in an obesogenic context, male Fischer 344 rats exposed to 6, 12 or 18 h of daily light (emulating winter, autumn and spring, or summer light conditions, respectively) were chronically administered with GSPE (25 mg/kg) for four weeks. The circulating levels of phenolic compounds (flavan-3-ols and phenolic acids, phase II and microbial-derived metabolites) were analyzed in serum.

3.1. Total serum phenolic profile.

Different photoperiod effects were observed in total serum phenolic profile (**Figure 2**). Interestingly, rats housed under L6 conditions showed higher levels of metabolites and a different profile compared to those housed under either L6 or L12 conditions. This photoperiod effect was due to the decrease of the glucuronidated metabolites (catechin and epicatechin glucuronide), which were not detected under L12 and L18 conditions. This fact increased the proportion of those metabolites classified as other metabolites, which included cinnamic acids, hippuric acid and valerolatone and valeric acid derivates. This group of metabolites accounted for the highest serum proportion in rats without ABX housed under L12 and L18 conditions and mainly consisted on hippuric acid and 3',4'-Dihydroxycinnamic acid, which were not detected under L6. Interestingly, this photoperiod effect was lost when treating with ABX. Moreover, ABX-treated rats showed increased total phenolic metabolites in rats housed under L12 and L18 conditions compared to those rats without ABX. However, rats under L6 administered with ABX showed lower total metabolites than those housed under the same conditions without ABX. Nevertheless, same

tendency towards decreased levels of metabolites as the hours of day light increased were observed in ABX-treated rats.

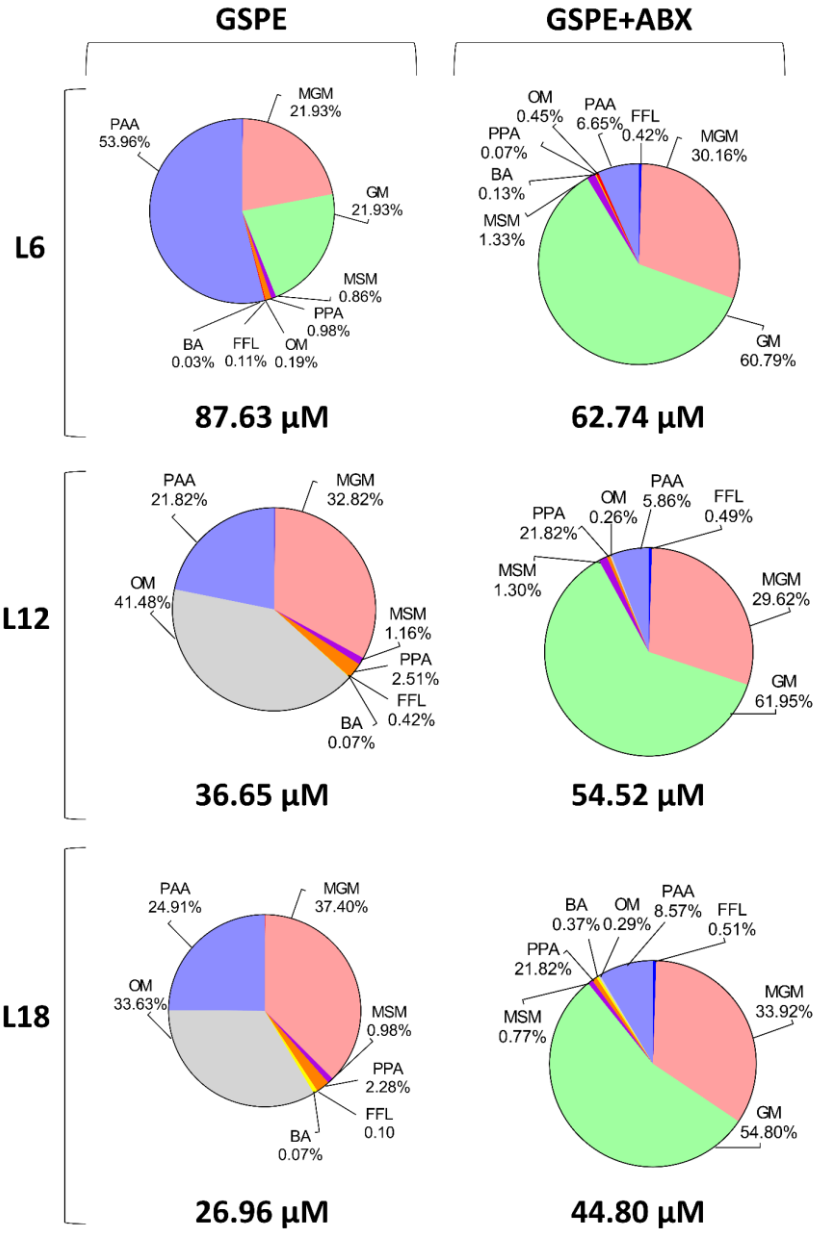

Figure 2. Distribution of phenolic serum metabolites in rats administered with GSPE (25 mg/Kg bw) and exposed to different photoperiods. *BA: benzoic acids; FFL: free flavonols; GM: glucuronidated metabolites; MGM: Methyl-glucuronidated metabolites; MSM: Methyl-sulfated metabolites; PAA: Phenylacetic acids; PPA: Phenylpropionic acids; OM: other metabolites; L6: short photoperiod (6h light/18h dark); L12: standard photoperiod (12h light/12h dark); L18: long photoperiod (18h light/6h dark). GSPE: grape seed proanthocyanidin extract; ABX: antibiotic cocktail.*

3.2. Flavan-3-ols and Phenolic Acids.

Flavan-3-ols and phenolic acids, which are present in the GSPE, were also quantified in serum in their non-metabolized form (**Figure 3a** and **Table 3)**. Remarkably, although the total levels of these compounds were affected by photoperiod conditions, increasing under L6, any photoperiod effect was observed in the individual compounds. Additionally, rats administered with the combination of GSPE and ABX did not show any photoperiod effect in these compounds. Interestingly, most of the phenolic metabolites of this group were significantly increased by the administration of GSPE and ABX independently of the photoperiod conditions compared to GSPE treatment. Thus, overall GSPE+ABX effect was the main factor affecting the flavan-3-ols and phenolic acids. Indeed, rats treated with GSPE+ABX tended to cluster separately from GSPE-treated rats when data were visualized by PCA. However, no cluster was observed by photoperiod effect (**Figure 3b**).

3.3. Flavan-3-ols-Phase II Metabolites.

The concentrations of the different flavan-3-ols-phase II metabolites are shown in the **Figure 3c** and **Table 3**. An interesting photoperiod effect was found in this group of metabolites. Rats administered with GSPE (without ABX) and housed under L12 and L18 conditions showed an overall decreased of phase II metabolites levels compared to rats housed under L6. Thus, the concentration of the total phase II metabolites, methyl-epicatechin glucuronide and 3-o-methyl gallic metabolites, were significantly lower under L18 conditions compared to L6 and lower under L12 than under L6. Interestingly, the concentration of both catechin glucuronide and epicatechin glucuronide was higher under L6 conditions while under L12 and L18 conditions, these metabolites were not detected. However, GSPE+ABX-treated rats showed a lower photoperiod effect, being only the most abundant phase-II metabolites (catechin glucuronide and epicatechin glucuronide) decreased under L18 compared to L6 condition ($p<0.016$) and lower under L12 than under L6.

However, this photoperiod effect was not strong enough to cluster differently either GSPE or GSPE+ABX-treated rats according to the photoperiod condition by PCA analysis. (**Figure 3d**).

In addition, the serum GSPE metabolites derived from ABX administration tended to cluster differently from those without ABX administration (**Figure 3d**). Thus, the ABX administration produced an overall significant increase of total phase II metabolites. In this context, catechin glucuronide increased under both L12 and L18, epicatechin glucuronide increased independently of the photoperiod conditions and of 3-O methyl epicatechin and methyl-epicatechin glucuronide were only increased under L18 (**Figure 3c**; **Table 3**).

3.4. Microbial-derived metabolites.

The microbial-derived metabolites group was the second largest group detected in the samples **(Figure 3e** and **Table 3)**. This group of metabolites was importantly modified by the different photoperiod conditions and by ABX administration. Regarding to photoperiod effect, 4'-Hydroxy-3'-methoxyphenylacetic acid was the unique microbial-derived metabolite found under L6 whereas, 3'-Hydroxyphenylacetic acid was the unique metabolite found in L12 conditions. Furthermore, these two metabolites were not present in serum of rats exposed to other photoperiod conditions. On the other hand, more metabolites were present under L18 conditions. Thus, hippuric acid, 3'-4'-dihydroxycinnamic acid, 4'-hidroxy-3'-methoxycinnamic acid and 4-hidroxyphenylpropionic acid metabolites were only found under L18 conditions. In this context, an overall photoperiod effect was observed only in rats not administered with ABX under L6, which cluster separately from rats housed under both L12 and L18 conditions (**Figure 3f**). However, when rats were administered with ABX, only phenilacetic acid metabolite was affected by photoperiod effect, increasing under both L6 and L18 in comparison with L12 conditions.

Interestingly, the administration of ABX had a different effect on the GSPE microbial-derived metabolites depending on the photoperiod condition. Thus, when rats were treated with ABX, significant higher phenylacetic acid and benzoic acid concentrations were observed under L6 conditions. Furthermore, the 3', 4'-dihydroxyphenil propionic acid, 4'-hydroxyphenylpropionic acid and dihydroxyphenilvalerolactona-isomero metabolites were only detected under L12 and L18 conditions, showing that L6 conditions had lower microbial-derived metabolites. In addition, 4'-hydroxyl-3'-methoxycinnamic acid was only detected under L12 conditions (**Figure 3e**; **Table 3**).

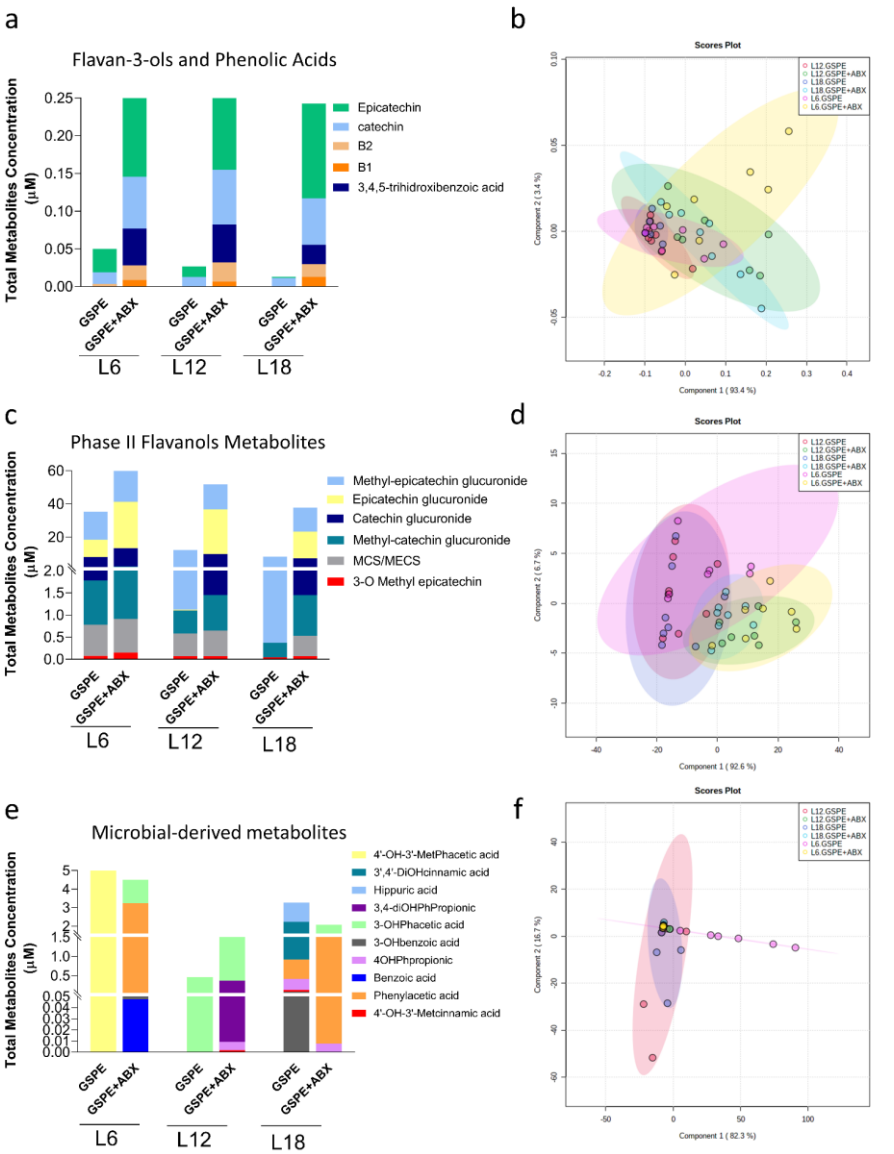

Figure 3. Serum phenolic metabolites quantified 3 h after the last dose of GSPE administered for 4 weeks to CAF-fed rats housed under different photoperiod. *(**a-b**) Flavan-3-ols and phenolic acids; (**c-d**) Phase II metabolites; and (**d-e**) microbial-derived metabolites. Data are visualized by stacked bar plots showing the median of the different metabolites (a,c,e) and by principal component analysis (PCA) 2D plot (b,d,f); (n=7-8). MCS/MECS: methyl-catechin sulphate/methyl-epicatechin sulphate; 4'-OH-3'-metPhacetic acid: 4'-Hydroxy-3'-methoxyphenylacetic acid; 3',4'-DiOHcinnamic acid: 3',4'-Dihydroxycinnamic acid; 3,4-diOHPhPropanoic: 3,4-Dihydroxyphenil propionic acid; 3-OHPhacetic acid: 3'-Hydroxyphenylacetic acid; 3-OHbenzoic acid: 3-hydroxybenzoic acid; 4OHPhpropionic: 4-Hydroxyphenylpropionic acid; 4'-OH-3'-Metcinnamic acid: 3',4'-Dihydroxycinnamic acid; L6: short photoperiod (6h light/18h dark); L12: standard photoperiod (12h light/12h dark); L18: long photoperiod (18h light/6h dark). GSPE: grape seed proanthocyanidin extract; ABX: antibiotic cocktail*

RESULTS

Table 3. GSPE metabolites according to the photoperiod conditions and antibiotic treatment analyzed by HPLC-ESI-MS/MS.

	GSPE metabolites (µM) Median(Q1-Q3)[1]				GSPE metabolites in rats treated with ABX (µM) Median(Q1-Q3)[1]						
	L6	**L12**	**L18**	***P* Ph[2]**	**L6**	**L12**	**L18**	***P* Ph[2]**	***P* L6[3]**	***P* L12[3]**	***P* L18[3]**
Σ Flavan-3-ols and Phenolic Acids	0.19(0.01-0.31)***a***	0.031(0.018-0.05)***ab***	0.029(0-0.069)***b***	0.05	0.25(0.20-0.54)	0.28(0.13-0.49)*	0.26(0.12-0.38)*	0.72	0.11	0.00	0.00
Catechin	0.02(0-0.08)	0.01(0.003-0.03)	0.01(0-0.03)	0.81	0.07(0.01-0.12)	0.07(0.02-0.10)*	0.06(0.03-0.09)*	0.96	0.16	0.02	0.00
Epicatechin	0.03(0-0.12)	0.01(0.002-0.04)	0.001(0-0.03)	0.35	0.12(0.09-0.26)*	0.12(0.08-0.26)*	0.13(0.05-0.20)*	0.92	0.04	0.01	0.00
Procyanidin dimer B1	$4.56x10^{-4}$(0-0.01)	n.d.	n.d.	0.44	0.01(0-0.03)*	0.01(0.002-0.02)*	0.01(0.01-0.03)*	0.75	0.05	0.00	0.00
Procyanidin dimer B2	0.003(0-0.01)	5.56E-04(0-8.30E-04)	n.d.	0.11	0.02(0.002-0.04)	0.03(0.003-0.06)*	0.02(0.01-0.04)*	0.71	0.12	0.00	0.00
3,4,5-trihydroxybenzoic acid	n.d.	n.d.	n.d.	0.14	0.05(0.02-0.11)*	0.05(0.02-0.06)*	0.03(0.03-0.03)*	0.24	0.00	0.00	0.000
4-hydroxy-3-methoxybenzoic acid	n.d.	n.d.	n.d.	0.12	n.d.	n.d.	n.d.	0.11	1.00	1.00	1.00
Σ Phase II Flavan-3-ols	34.34(13.73-55.96)***a***	14.77(10.68-27.21)***ab***	11.67(6.19-20.78)***b***	0.03	60.09(48.161-75)	52.64(36.12-57.09)*	38.02(34.63-49.09)*	0.67	0.13	0.00	0.00
Catechin glucuronide[a]	6.28(0.17-10.96)	n.d.	n.d.	0.06	11.18(7.69-13.53)***a***	8.35(6.63-10.06)****ab***	5.65(5.29-7.25)****b***	0.03	0.20	0.00	0.01
Epicatechin glucuronide[a]	10.28(0.07-22.62)	n.d.	n.d.	0.07	27.93(23.08-36.69)****a***	26.9(17.63-28.48)****ab***	16.15(15.10-21.59)****b***	0.04	0.02	0.00	0.00
Methyl catechin glucuronide[a]	0.99(0.63-1.34)	0.52(0.06-0.94)	0.33(0.03-0.74)	0.08	1.27(0.76-1.66)	0.81(0.49-1.13)	0.92(0.37-1.54)	0.47	0.49	0.29	0.06
3-o-methyl epicatechin[b]	0.01(0.05-0.14)***a***	0.07(0.04-0.12)***ab***	0.05(0.02-0.05)***b***	0.03	0.16(0.07-0.29)	0.07(0.06-0.12)	0.07(0.05-0.14)*	0.15	0.13	0.64	0.01
Methyl-epicatechin glucuronide [a]	16.95(11.37-20.89)***a***	11.09(7.85-15.21)***ab***	7.73(5.96-14.88)***b***	0.03	18.69(14.45-21.62)	15.05(12.71-18.69)	14.45(12.79-16.63)*	0.18	0.64	0.08	0.05
methyl-catechin sulphate/methyl-epicatechin sulphate [a]	n.q.	n.q.	n.q.	0.14	n.q.	n.q.	n.q.	0.02	0.64	0.20	0.43
Σ Microbial-derived metabolites	54.67(5.46-93.24)	9.83(1.76-39.55)	9.45(2.01-28.10)	0.23	6.24(3.41-11.63)	5.76(0.39-8.61)	5.29(2.46-10.95)	0.62	0.13	0.11	0.89
Phenylacetic Acid[e]	n.d.	n.d.	n.d.	0.45	3.19(0.73-4.81)****a***	n.d. ***b***	1.50(0.76-5.61)***a***	0.01	0.01	0.14	0.22
3',4'-Dihydroxyphenylacetic acid	n.d.	n.d.	n.d.	1.00	n.d.	n.d.	n.d.	0.18	0.06	0.06	1.00
4'-Hydroxy-3'-methoxyphenylacetic acid[c]	47.44(3.87-86.57)***a***	n.d. ***b***	n.d. ***b***	0.01	n.d. *	n.d.	n.d.	0.31	0.01	0.63	0.17
3'-Hydroxyphenylacetic acid	n.d. ***a***	0.465(0.285-1.637)***b***	n.d. ***a***	0.00	1.26(0-2.01)*	1.18(0-2.52)	0.52(0.09-1.33)*	0.71	0.03	0.64	0.01
Hippuric acid	n.d.	n.d.	1.04(0-8.58)	0.13	n.d.	n.d.	n.d.*	1.00	1.00	0.11	0.04

3',4'-Dihydroxycinnamic acid	n.q.	n.q.	1.31(0-4.99)	0.13	n.q.	n.q.	n.q.*	1.00	1.00	0.11	0.03
4'-Hydroxy-3'-methoxycinnamic acid	n.d. ***a***	n.d. ***ab***	0.05(0-0.23)***b***	0.05	n.d.	0.002(0-0.006)	n.d.	0.19	0.36	0.68	0.08
Benzoic acid	n.d.	n.d.	n.d.	0.07	0.047(0-0.13)*	n.d.	n.d.	0.12	0.04	1.00	0.69
3-Hydroxybenzoic acid	n.q.	n.q.	n.q.	0.20	n.q.	n.q.	n.q.	0.59	0.57	0.63	0.19
3,4-Dihydroxyphenil propionic acid	n.d.	n.d.	n.d.	0.17	n.d.	0.37(0-0.42)*	0.03(0-0.42)*	0.23	0.72	0.03	0.01
Phenylpropionic Acid[d]	n.d.	n.d.	n.d.	0.41	n.d.	n.d.	n.d.	1.00	0.17	0.17	1.00
3-hydroxyphenylpropionic acid[d]	n.d.	n.d.	n.d.	0.06	n.d.	n.d.	n.d.	1.00	1.00	0.04	0.32
4-Hydroxyphenylpropionic acid	n.d.	n.d.	0.29(0-0.92)	0.05	n.d.	0.01(0-0.05)*	0.01(0-0.34)	0.09	0.08	0.03	0.38
4-Hydroxyphenylvaleric acid	n.d.	n.d.	n.d.	0.57	n.d.	n.d.	n.d.	1.00	0.02	0.04	0.06
4-Hydroxy-5-(3',4'-dihydroxyphenyl)valeric acid	n.d.	n.d.	n.d.	1.00	n.d.	n.d.	n.d.	1.00	1.00	1.00	1.00
4-Hydroxy-5-(3',4'-dihydroxyphenyl)valeric acid isomero	n.d.	n.d.	n.d.	1.00	n.d.	n.d.	n.d.	1.00	1.00	1.00	1.00
3,4-Dihydroxyphenilvalerolactona	n.d.	n.d.	n.d.	0.12	n.d.	n.d.	n.d.	1.00	0.14	1.00	1.00
3,4-Dihydroxyphenilvalerolactona-isomero	n.d.	n.d.	n.d.	0.69	n.d. ***a***	0.01(0-0.01)***b***	$3.64x10^{-4}$(0-0.006)***ab***	0.04	0.11	0.13	0.79

[1]Data shown as median (first (Q1) and third quartile (Q3)) (n = 7-8).

[2]P-value by Kruskal-Wallis test comparing photoperiods in each group. ab letters indicate significant photoperiods differences analyzed by Kruskal-Wallis test followed by Bonferroni p-values adjustment (p<0.016).

*[3]P-value by U Mann-Whitney test comparing experimental groups (GSPE vs GSPE+ABX) under the different photoperiod. * indicates significant differences between GSPE and GSPE+ABX in each photoperiod (p<0.05).*

[a]Quantified using the calibration curve of catechin; [b]Quantified using the calibration curve of 3,4,5-trihydroxybenzoic acid; [c]Quantified using the calibration curve of 4-hydroxy-3-methoxybenzoic acid; [d]Quantified using the calibration curve of 4-Hydroxyphenylpropionic acid; [e]Quantified using the calibration curve of 3'-Hydroxyphenylacetic acid; n.d. not detected; n.q. not quantified; L6: short photoperiod (6h light/18h dark); L12: standard photoperiod (12h light/12h dark); L18: long photoperiod (18h light/6h dark). GSPE: grape seed proanthocyanidin extract; ABX: antibiotic cocktail.

4. Discussion

Polyphenols consumption has been linked to several beneficial effects on obesity and MetS development [32,33]. However, their bioactivity depend on its bioavailability, including both its metabolism and absorption [13]. Hence, the study of factors affecting bioavailability and metabolism of polyphenols is of high interest. Gut microbiota is a key factor in the metabolism of polyphenols. Because of this, alteration of gut microbiota cause changes in the bioavailability of polyphenols and in turn in their bioactivity. On the other hand, high fat diets, such as cafeteria diet, promote obesity development, alter gut microbiota composition [34,35] and affect the bioavailability of polyphenols [36]. Additionally, seasonal rhythms have been recently established as crucial factors in the modulation of gut microbiota composition [37,38], being obese rats more susceptible to photoperiod changes [23]. Moreover, it was reported that changes in photoperiods affected grape seed polyphenols bioavailability [22]. Therefore, the aim of this study was to evaluate if the serum bioavailability of GSPE metabolites is modulated by gut microbiota in a photoperiod dependent manner in an obesogenic context induced by cafeteria feeding.

To evaluate this, a chronic study in CAF-fed rats daily administered 25 mg/Kg of GSPE, with and without an antibiotic cocktail, and exposed to different photoperiod conditions was performed. F344 rats have shown a higher photoperiod sensitivity compared to other strains [39,40]. The administered dose of GSPE was equivalent to the daily intake of 367 mg for a person of 70 kg [41], which is within the estimated range of polyphenols intake in humans [42–44] and has been demonstrated anti-obesity properties [12,45,46]. The ABX used promote a gut microbiota dysbiosis without affecting other physiological parameters such as body composition, biochemical parameters or glucose tolerance [Manuscript 3].

GSPE-derived metabolites were quantified in serum after 3 h of the last GSPE dose administration. Phase-II metabolites were the most abundant while

microbiota-derived metabolites were detected at lower levels. This was expected since the highest plasma concentration of phase-II metabolites was observed at 2 h after GSPE dosage in kinetic studies, finding a wide variety of Phase-II metabolites at 2 and 4 h after GSPE administration [18]. Regarding microbiota-derived metabolites, it has been shown that they reach their maximum levels after 24 h of GSPE administration in adult rats [18,47]. Hence, in this chronic study we are detecting bacterial-derived GSPE metabolites from the dose administered on the previous day (27 h after administration). Non-metabolized flavan-3-ol and phenolic acids as well as phase II metabolites were increased in rats treated with ABX. It was reported that these metabolites are increased in rats fed a cafeteria diet which promote gut microbiota dysbiosis compared to healthy rats [36]. In this context, gut microbiota alterations were linked to higher absorption of small phenolic compounds and flavanol monomers at the level of the small intestine, which can appear in plasma as free and conjugated monomers [48]. The administration of ABX increased the dysbiosis conditions of these rats, reducing gut microbiota diversity [49]. Thus, these findings suggest that intestinal permeability is altered by the dysfunction of tight junctions within the small intestine due to the ABX administration [50,51], which affects the passive diffusion of flavanols through the enterocytes. In this regard, epicatechin and their glucuronic-derived metabolites are one of the most abundant metabolites shown in the serum of rats treated with ABX. The alteration promoted by ABX administration may increase flavanols absorption in the small intestine, which may explain the reduced microbial derived metabolites detected in serum, since 4-Hydroxyphenylvaleric acid, 4-Hydroxy-5-(3',4'-dihydroxyphenyl)valeric acid, 4-Hydroxy-5-(3',4'-dihydroxyphenyl)valeric acid isomer and 3,4-Dihydroxyphenilvalerolactona were not detected [52].

Interestingly a photoperiod effect was observed in phase-II metabolites, which decreased their concentration in the longest photoperiods (L12 and L18). In this context, rats without ABX housed under L6 conditions, showed higher phase-II

metabolites in comparison with those rats housed under both L12 and L18 conditions, which displayed similar concentrations. Interestingly, rats treated with ABX showed a photoperiod effect, which decreased their concentration as the hours of lights per day increased. It is known that the phase-II enzymes implicated in the metabolism of these flavan-3-ols-derived metabolites, follow a diurnal rhythmicity [53]. Circadian and seasonal rhythms are related and both of them are wide regulated by light/dark cycles. Thus, photoperiods can modulate seasonal rhythms, but also can influence circadian rhythmicity [54]. In this regard, Retinoid-related orphan receptors alpha and gamma (RORα and γ) expressed in liver as a component of the circadian clock, play an important role in the regulation of genes encoding several phase II metabolic enzymes [55,56]. Moreover, it has been recently reported that hepatic UDP-glucuronosyltrasnferases (UGTs) phase II enzymes, which carried out metabolites glucuronidation, show a diurnal rhythmicity regulated by Rev-erbα (a circadian clock component) [57,58]. Both RORα and REV-erbα are linked to regulate many metabolism pathways to ensure that metabolic enzymes are produced at appropriate times (i.e., stimulation of catabolic pathways during the wake period to match fuel demands). Along these lines, metabolism and absorption processes variate according to the time of the day, being most optimal and reaching the highest levels of intermediate metabolites during the active phase of the organism [59,60]. In this context, our results showed lower concentration of phase II metabolites under L18 conditions, in which rats have a longer resting phase. Thus, bioavailability and metabolism of these phenolic compounds could be influenced by diurnal rhythmicity of phase II enzymes, being more active in the dark phase, in which rats are in their active phase. In concordance, Iglesias-Carres *et al.* also showed that the bioavailability of grapes seed was higher in rats exposed to L6 conditions compared to rats under L18 conditions [22]. In fact, grapes may present a higher bioavailability under L6 conditions due to the fact that they are normally consumed in winter season. This could be linked with a major bioactivity according to the Xenohormesis

theory [61,62]. This theory, stablished that the heterotrophs organism (i.e. humans) are able to sense singling stress-induced molecules from other species (i.e. plants). Hence, heterotrophs take these phytochemicals cues (polyphenols) from other species through the diet, to get information on the environmental status, adjusting their metabolism in anticipation of adverse conditions to increase their chances of survival [63]. Thus, the consumption of grapes out of their natural conditions season, would provide chemical cues that do not correspond to the current environmental situation to the consuming organism, and thus would result in non-efficient metabolic processes [62].

Regarding microbial-derived metabolites, although their concentrations in serum were low, results showed interesting photoperiod effects. Interestingly, these effects were significantly less prominent when treating with ABX. These findings reinforce the important role of gut microbiota in phenolic compounds metabolites bioavailability and suggest that these bacteria are involved in the photoperiod-mediated changes observed in PAs bioavailability, which may impact in their bioactivity. Indeed, in our previous work we observed that the GSPE affected gut microbiota composition differently depending on the photoperiod conditions, as well as if the rats were or not treated with ABX [Manuscript 3]. Thus, rats administered with GSPE without ABX, showed higher levels of *Butyrivibrio and Coprococcus* and lower levels of *Parabacteroides* under L6. Rats housed under L12 presented higher abundance of *Lactobacillales and Lactococcus* and rats housed under L18 showed higher abundance of *Bifidobacterium* and *Kleibsella*. On the other hand, rats administered with GSPE and ABX, showed a strong photoperiod effect on gut microbiota composition, especially under L18. In this context, rats housed under L6 showed lower levels of *Lactobacillus* and *Bacteroides*. Rats under L12 showed a decreased of *Coprococcus*, *Ruminococcus* and *Prevotella*, and an increase of *Bacteroides*, and *Bilophila* relative abundance genera, while rats under L18 conditions, showed higher relative abundance of *Parabacteroides*, *Bifidobacterium*, *Bilophila* and *Blautia* genera. Along these lines, these changes on the gut microbiota

composition influenced by the different photoperiod conditions, may explain the differences on the bioavailability of GSPE. For instance, *Butirivibrio* genera has been linked to lactone fission reaction and the strains of *Bifidobacterium lactis*, *Lactobacillus gasseri* and *Ruminococcus productus*, have been associated with hydrolysis reaction by esterases enzymes [64]. Thus, these changes in the abundance relative of certain gut bacteria promoted by GSPE and photoperiod could be related to the differences metabolites observed. However, further investigations are needed to stablish an association between these bacteria and the metabolites derived from GSPE metabolism.

Therefore, this study shows that photoperiod-mediated changes in the bioavailability of phenolic compounds is significantly influenced by gut microbiota in obese rats. Thus, these results contribute to a better understanding of polyphenols metabolism and bioavailability and its application in the chronotherapy field.

Author Contributions

Conceptualization: V.A.-G., I.E.-M, A.A.-A. and C.T.-F.; Formal analysis: V.A.-G. and I.E.-M.; Data curation: V.A.-G and I.E-M.; Investigation: V.A.-G., I.E.-M., M.M., B.M., M.S., A.A.-A. and C.T.-F.; Methodology: V.A.-G., A.A.-A. and C.T.-F.; Funding acquisition: M.M., B.M., M.S., A.A.-A. and C.T-F.; Project administration: M.M., B.M., M.S., A.A.-A. and C.T-F.; Resources: M.M., B.M., M.S., A.A.-A. and C.T-F.; Software: V.A-G and I.E.-M; Visualization: V.A.-G. and I.E-M; Supervision: A.A.-A. and C.T-F; Validation: V.A.-G., A.A.-A. and C.T.-F.; Writing original draft: V.A.-G.; Writing review & editing: A.A.-A. and C.T.-F.

Conflict of interest

There are no conflicts to declare.

Acknowledgements

This work was supported by MCIN/AEI/10.13039/501100011033/ FEDER "Una manera de hacer Europa" (AGL2016-77105-R) and "2021/22 Development of a prototype for the establishment of a dysbiosis (alteration) in the intestinal microbiota", co-financed by Diputació de Tarragona (2021PGR-DIPTA-URV09). V.A.-G. was supported by the Martí i Franquès Doctoral Fellowships Programme, Universitat Rovira i Virgili (PMF-PIPF-35); I.E.-M. was supported by the Youth Employment Initiative from the European Social Fund, Ministry of Science, The State Research Agency and Universitat Rovira i Virgili (PEJ2018-002778-A); A.A-A were supported by the Serra Húnter Programme, Government of Catalonia; C.T.-F. was supported by Beatriu de Pinós Postdoctoral Programme of the Government of Catalonia's Secretariat for Universities and Research of the Ministry of Economy and Knowledge. The authors would like to thank Niurka Dariela Llópiz and Rosa Pastor for their assistance.

REFERENCES

[1] Bladé C, Aragonès G, Arola-Arnal A, Muguerza B, Bravo FI, Salvadó MJ, et al. Proanthocyanidins in health and disease. BioFactors 2016;42:5–12. https://doi.org/10.1002/BIOF.1249.

[2] Tsang C, Auger C, Mullen W, Bornet A, Rouanet J-M, Crozier A, et al. The absorption, metabolism and excretion of flavan-3-ols and procyanidins following the ingestion of a grape seed extract by rats. Br J Nutr 2005;94:170–81. https://doi.org/10.1079/BJN20051480.

[3] Mannino G, Chinigò G, Serio G, Genova T, Gentile C, Munaron L, et al. Proanthocyanidins and Where to Find Them: A Meta-Analytic Approach to Investigate Their Chemistry, Biosynthesis, Distribution, and Effect on Human Health. Antioxidants 2021, Vol 10, Page 1229 2021;10:1229. https://doi.org/10.3390/ANTIOX10081229.

[4] Montagut G, Bladé C, Blay M, Fernández-Larrea J, Pujadas G, Salvadó MJ, et al. Effects of a grapeseed procyanidin extract (GSPE) on insulin resistance. J Nutr Biochem 2010;21:961–7. https://doi.org/10.1016/J.JNUTBIO.2009.08.001.

[5] Mas-Capdevila A, Iglesias-Carres L, Arola-Arnal A, Suárez M, Bravo FI, Muguerza B. Changes in arterial blood pressure caused by long-term administration of grape seed proanthocyanidins in rats with established hypertension. Food Funct 2020;11:8735–42. https://doi.org/10.1039/D0FO00981D.

[6] Pons Z, Margalef M, Bravo FI, Arola-Arnal A, Begoña Muguerza ·. Acute administration of single oral dose of grape seed polyphenols restores blood pressure in a rat model of metabolic syndrome: role of nitric oxide and prostacyclin. Eur J Nutr 2016;55:749–58. https://doi.org/10.1007/s00394-015-0895-0.

[7] Pons Z, Margalef M, Bravo FI, Arola-Arnal A, Muguerza B. Chronic administration of grape-seed polyphenols attenuates the development of hypertension and improves other cardiometabolic risk factors associated with the metabolic syndrome in cafeteria diet-fed rats. Br J Nutr 2017;117:200–8. https://doi.org/10.1017/S0007114516004426.

[8] Puiggròs F, Sala E, Vaque M, Ardevol A, Blay M, Fernández-Larrea J, et al. In vivo, in vitro, and in silico studies of Cu/Zn-superoxide dismutase regulation by molecules in grape seed procyanidin extract. J Agric Food Chem 2009;57:3934–42. https://doi.org/10.1021/JF8034868.

[9] Pajuelo D, Quesada H, Díaz S, Fernández-Iglesias A, Arola-Arnal A, Bladé C, et al. Chronic dietary supplementation of proanthocyanidins corrects the mitochondrial dysfunction of brown adipose tissue caused by diet-induced obesity in Wistar rats. Br J Nutr 2012;107:170–8. https://doi.org/10.1017/S0007114511002728.

[10] Bladé C, Arola L, Salvadó MJ. Hypolipidemic effects of proanthocyanidins and their underlying biochemical and molecular mechanisms. Mol Nutr Food Res 2010;54:37–59. https://doi.org/10.1002/MNFR.200900476.

[11] Quesada H, Del Bas JM, Pajuelo D, Díaz S, Fernandez-Larrea J, Pinent M, et al. Grape seed proanthocyanidins correct dyslipidemia associated with a high-fat diet in rats and repress genes controlling lipogenesis and VLDL assembling in liver. Int J Obes (Lond) 2009;33:1007–12. https://doi.org/10.1038/IJO.2009.136.

[12] Baiges I, Palmfeldt J, Bladé C, Gregersen N, Arola L. Lipogenesis Is Decreased by Grape Seed Proanthocyanidins According to Liver Proteomics of Rats Fed a High Fat Diet. Mol Cell Proteomics 2010;9:1499. https://doi.org/10.1074/MCP.M000055-MCP201.

[13] Del Rio D, Rodriguez-Mateos A, Spencer JPE, Tognolini M, Borges G, Crozier A. Dietary (Poly)phenolics in Human Health: Structures, Bioavailability, and Evidence of Protective Effects Against Chronic Diseases. Antioxid Redox Signal 2013;18:1818. https://doi.org/10.1089/ARS.2012.4581.

[14] Monagas M, Urpi-Sarda M, Sánchez-Patán F, Llorach R, Garrido I, Gómez-Cordovés C, et al. Insights into the metabolism and microbial biotransformation of dietary flavan-3-ols and the bioactivity of their metabolites. Food Funct 2010;1:233–53. https://doi.org/10.1039/C0FO00132E.

[15] Serra A, Maclà A, Romero MP, Reguant J, Ortega N, Motilva MJ. Metabolic pathways of the colonic metabolism of flavonoids (flavonols, flavones and flavanones) and phenolic acids. Food Chem 2012;130:383–93. https://doi.org/10.1016/J.FOODCHEM.2011.07.055.

[16] Sánchez-Patán F, Cueva C, Monagas M, Walton GE, Gibson GR, Martín-Álvarez PJ, et al. Gut microbial catabolism of grape seed flavan-3-ols by human faecal microbiota. Targetted analysis of precursor compounds, intermediate metabolites and end-products. Food Chem 2012;131:337–47. https://doi.org/10.1016/J.FOODCHEM.2011.08.011.

[17] Margalef M, Pons Z, Iglesias-Carres L, Bravo FI, Muguerza B, Arola-Arnal A. Lack of tissue accumulation of grape seed flavanols after daily long-term administration in healthy and cafeteria-diet obese rats. J Agric Food Chem 2015;63:9996–10003. https://doi.org/10.1021/ACS.JAFC.5B03856.

[18] Margalef M, Iglesias-Carres L, Pons Z, Bravo FI, Muguerza B, Arola-Arnal A. Age related differences in the plasma kinetics of flavanols in rats. J Nutr Biochem 2016;29:90–6. https://doi.org/10.1016/J.JNUTBIO.2015.11.007.

[19] Frolinger T, Sims S, Smith C, Wang J, Cheng H, Faith J, et al. The gut microbiota composition affects dietary polyphenols-mediated cognitive resilience in mice by modulating the bioavailability of phenolic acids. Sci Reports 2019 91 2019;9:1–10. https://doi.org/10.1038/s41598-019-39994-6.

[20] Cardona F, Andrés-Lacueva C, Tulipani S, Tinahones FJ, Queipo-Ortuño MI. Benefits of polyphenols on gut microbiota and implications in human health. J Nutr Biochem 2013;24:1415–22. https://doi.org/10.1016/j.jnutbio.2013.05.001.

[21] Ibars M, Aragonès G, Ardid-Ruiz A, Gibert-Ramos A, Arola-Arnal A, Suárez M, et al. Seasonal consumption of polyphenol-rich fruits affects the hypothalamic leptin signaling system in a photoperiod-dependent mode. Sci Rep 2018;8. https://doi.org/10.1038/S41598-018-31855-Y.

[22] Iglesias-Carres L, Mas-Capdevila A, Bravo FI, Arola L, Muguerza B, Arola-Arnal A. Exposure of Fischer 344 rats to distinct photoperiods influences the bioavailability of red grape polyphenols. J Photochem Photobiol B Biol 2019;199:111623. https://doi.org/10.1016/j.jphotobiol.2019.111623.

[23] Arreaza-Gil V, Escobar-Martínez I, Suárez M, Bravo F, Muguerza B, Arola-Arnal A, et al. Gut Seasons: Photoperiod Effects on Fecal Microbiota in Healthy and Cafeteria-Induced Obese Fisher 344 Rats. Nutrients 2022;14:722. https://doi.org/10.3390/NU14030722.

[24] Shor EK, Brown SP, Freeman DA. A novel role for the pineal gland: Regulating seasonal shifts in the gut microbiota of Siberian hamsters. J Pineal Res 2020;69:e12696. https://doi.org/10.1111/jpi.12696.

[25] Ren CC, Sylvia KE, Munley KM, Deyoe JE, Henderson SG, Vu MP, et al. Photoperiod modulates the gut microbiome and aggressive behavior in Siberian hamsters. J Exp Biol 2020;223. https://doi.org/10.1242/jeb.212548.

[26] Fan C, Zhang L, Jia S, Tang X, Fu H, Li W, et al. Seasonal variations in the composition and functional profiles of gut microbiota reflect dietary changes in plateau pikas. Integr Zool 2022. https://doi.org/10.1111/1749-4877.12630.

[27] Koliada A, Moseiko V, Romanenko M, Piven L, Lushchak O, Kryzhanovska N, et al. Seasonal variation in gut microbiota composition: Cross-sectional evidence

from Ukrainian population. BMC Microbiol 2020;20:1–9. https://doi.org/10.1186/S12866-020-01786-8/TABLES/3.

[28] Oyola MG, Johnson RC, Bauman BM, Frey KG, Russell AL, Cho-Clark M, et al. Gut microbiota and metabolic marker alteration following dietary isoflavone-photoperiod interaction. Endocrinol Diabetes Metab 2021;4:e00190. https://doi.org/10.1002/edm2.190.

[29] Rodríguez RM, Cortés-Espinar AJ, Soliz-Rueda JR, Feillet-Coudray C, Casas F, Colom-Pellicer M, et al. Time-of-Day Circadian Modulation of Grape-Seed Procyanidin Extract (GSPE) in Hepatic Mitochondrial Dynamics in Cafeteria-Diet-Induced Obese Rats. Nutrients 2022;14. https://doi.org/10.3390/NU14040774.

[30] Margalef M, Pons Z, Muguerza B, Arola-Arnal A. A rapid method to determine colonic microbial metabolites derived from grape flavanols in rat plasma by liquid chromatography-tandem mass spectrometry. J Agric Food Chem 2014;62:7698–706. https://doi.org/10.1021/JF5019752.

[31] Pang Z, Chong J, Zhou G, De Lima Morais DA, Chang L, Barrette M, et al. MetaboAnalyst 5.0: narrowing the gap between raw spectra and functional insights. Nucleic Acids Res 2021;49:W388–96. https://doi.org/10.1093/NAR/GKAB382.

[32] Ohishi T, Fukutomi R, Shoji Y, Goto S, Isemura M. The Beneficial Effects of Principal Polyphenols from Green Tea, Coffee, Wine, and Curry on Obesity. Mol 2021, Vol 26, Page 453 2021;26:453. https://doi.org/10.3390/MOLECULES26020453.

[33] Wang S, Moustaid-Moussa N, Chen L, Mo H, Shastri A, Su R, et al. Novel insights of dietary polyphenols and obesity. J Nutr Biochem 2014;25:1–18. https://doi.org/10.1016/J.JNUTBIO.2013.09.001.

[34] Espín JC, González-Sarrías A, Tomás-Barberán FA. The gut microbiota: A key factor in the therapeutic effects of (poly)phenols. Biochem Pharmacol 2017;139:82–93. https://doi.org/10.1016/J.BCP.2017.04.033.

[35] Gual-Grau A, Guirro M, Mayneris-Perxachs J, Arola L, Boqué N. Impact of different hypercaloric diets on obesity features in rats: a metagenomics and metabolomics integrative approach. J Nutr Biochem 2019;71:122–31. https://doi.org/10.1016/j.jnutbio.2019.06.005.

[36] Margalef M, Pons Z, Iglesias-Carres L, Bravo FI, Muguerza B, Arola-Arnal A. Flavanol plasma bioavailability is affected by metabolic syndrome in rats. Food Chem 2017;231:287–94. https://doi.org/10.1016/J.FOODCHEM.2017.03.141.

[37] Bailey MT, Walton JC, Dowd SE, Weil ZM, Nelson RJ. Photoperiod modulates gut bacteria composition in male Siberian hamsters (Phodopus sungorus). Brain Behav Immun 2010;24:577–84. https://doi.org/10.1016/J.BBI.2009.12.010.

[38] Shor EK, Brown SP, Freeman DA. Bacteria and Bellicosity: Photoperiodic Shifts in Gut Microbiota Drive Seasonal Aggressive Behavior in Male Siberian Hamsters. J Biol Rhythms 2022;37:296–309. https://doi.org/10.1177/07487304221092105.

[39] Heideman PD, John Sylvester C. Reproductive Photoresponsiveness in Unmanipulated Male Fischer 344 Laboratory Rats1. Biol Reprod 1997;57:134–8. https://doi.org/10.1095/biolreprod57.1.134.

[40] Tavolaro FM, Thomson LM, Ross AW, Morgan PJ, Helfer G. Photoperiodic Effects on Seasonal Physiology, Reproductive Status and Hypothalamic Gene Expression in Young Male F344 Rats. J Neuroendocrinol 2015;27:79–87. https://doi.org/10.1111/jne.12241.

[41] Reagan-Shaw S, Nihal M, Ahmad N. Dose translation from animal to human studies revisited. FASEB J 2008;22:659–61. https://doi.org/10.1096/FJ.07-9574LSF.

[42] Saura-Calixto F, Serrano J, Goñi I. Intake and bioaccessibility of total polyphenols in a whole diet. Food Chem 2007;101:492–501. https://doi.org/10.1016/J.FOODCHEM.2006.02.006.

[43] Wang Y, Chung SJ, Song WO, Chun OK. Estimation of Daily Proanthocyanidin Intake and Major Food Sources in the U.S. Diet. J Nutr 2011;141:447–52. https://doi.org/10.3945/JN.110.133900.

[44] Zamora-Ros R, Andres-Lacueva C, Lamuela-Raventós RM, Berenguer T, Jakszyn P, Barricarte A, et al. Estimation of Dietary Sources and Flavonoid Intake in a Spanish Adult Population (EPIC-Spain). J Am Diet Assoc 2010;110:390–8. https://doi.org/10.1016/J.JADA.2009.11.024.

[45] Salvadó MJ, Casanova E, Fernández-Iglesias A, Arola L, Bladé C. Roles of proanthocyanidin rich extracts in obesity. Food Funct 2015;6:1053. https://doi.org/10.1039/c4fo01035c.

[46] Caimari A, Mariné-Casadó R, Boqué N, Crescenti A, Arola L, Maria Del Bas J. Maternal intake of grape seed procyanidins during lactation induces insulin resistance and an adiponectin resistance-like phenotype in rat offspring OPEN n.d. https://doi.org/10.1038/s41598-017-12597-9.

[47] Margalef M, Pons Z, Bravo FI, Muguerza B, Arola-Arnal A. Plasma kinetics and microbial biotransformation of grape seed flavanols in rats. J Funct Foods 2015;Complete:478–88. https://doi.org/10.1016/J.JFF.2014.12.007.

[48] Manach C, Scalbert A, Morand C, Rémésy C, Jiménez L. Polyphenols: food sources and bioavailability 1,2. vol. 79. 2004.

[49] Lange K, Buerger M, Stallmach A, Bruns T. Effects of Antibiotics on Gut Microbiota. Dig Dis 2016;34:260–8. https://doi.org/10.1159/000443360.

[50] Feng Y, Huang Y, Wang Y, Wang P, Song H, Wang F. Antibiotics induced intestinal tight junction barrier dysfunction is associated with microbiota dysbiosis, activated NLRP3 inflammasome and autophagy. PLoS One 2019;14. https://doi.org/10.1371/JOURNAL.PONE.0218384.

[51] Wlodarska M, Finlay BB. Host immune response to antibiotic perturbation of the microbiota. Mucosal Immunol 2010 32 2009;3:100–3. https://doi.org/10.1038/mi.2009.135.

[52] Borges G, Ottaviani JI, van der Hooft JJJ, Schroeter H, Crozier A. Absorption, metabolism, distribution and excretion of (−)-epicatechin: A review of recent findings. Mol Aspects Med 2018;61:18–30. https://doi.org/10.1016/J.MAM.2017.11.002.

[53] Tsurusaki T, Sakakibara H, Aoshima Y, Yamazaki S, Sakono M, Shimoi K. Diurnal rhythmicity in biological processes involved in bioavailability of functional food factors. J Clin Biochem Nutr 2013;52:208–14. https://doi.org/10.3164/JCBN.12-127.

[54] Wood SH, Hindle MM, Mizoro Y, Cheng Y, Saer BRC, Miedzinska K, et al. Circadian clock mechanism driving mammalian photoperiodism. Nat Commun 2020 111 2020;11:1–15. https://doi.org/10.1038/s41467-020-18061-z.

[55] Wada T, Kang HS, Jetten AM, Xie W. The emerging role of nuclear receptor RORalpha and its crosstalk with LXR in xeno- and endobiotic gene regulation. Exp Biol Med (Maywood) 2008;233:1191–201. https://doi.org/10.3181/0802-MR-50.

[56] Hong SK, Angers M, Ju YB, Wu X, Gimble JM, Wada T, et al. Gene expression profiling reveals a regulatory role for ROR alpha and ROR gamma in phase I and phase II metabolism. Physiol Genomics 2007;31:281–94. https://doi.org/10.1152/PHYSIOLGENOMICS.00098.2007.

[57] Xu H, Chen M, Yu F, Zhang T, Wu B. Circadian Clock Component Rev-erb α Regulates Diurnal Rhythm of UDP-Glucuronosyltransferase 1a9 and Drug Glucuronidation in Mice. Drug Metab Dispos 2020;48:681–9. https://doi.org/10.1124/DMD.120.000030.

[58] Zhang T, Guo L, Yu F, Chen M, Wu B. The nuclear receptor Rev-erbα participates in circadian regulation of Ugt2b enzymes in mice. Biochem Pharmacol 2019;161:89–97. https://doi.org/10.1016/J.BCP.2019.01.010.

[59] Reinke H, Asher G. Crosstalk between metabolism and circadian clocks n.d. https://doi.org/10.1038/s41580-018-0096-9.

[60] Arola-Arnal A, Cruz-Carrión Á, Torres-Fuentes C, Ávila-Román J, Aragonès G, Mulero M, et al. Chrononutrition and polyphenols: Roles and diseases. Nutrients 2019;11:1–18. https://doi.org/10.3390/nu11112602.

[61] Hooper PL, Hooper PL, Tytell M, Vígh L. Xenohormesis: health benefits from an eon of plant stress response evolution. Cell Stress Chaperones 2010;15:761. https://doi.org/10.1007/S12192-010-0206-X.

[62] Howitz KT, Sinclair DA. Xenohormesis: Sensing the Chemical Cues of Other Species. Cell 2008;133:387–91. https://doi.org/10.1016/J.CELL.2008.04.019.

[63] Baur JA, Sinclair DA. What is Xenohormesis? Am J Pharmacol Toxicol 2008;3:149–56. https://doi.org/10.3844/AJPTSP.2008.152.159.

[64] Selma M V., Espín JC, Tomás-Barberán FA. Interaction between phenolics and gut microbiota: Role in human health. J Agric Food Chem 2009;57:6485–501. https://doi.org/10.1021/JF902107D/ASSET/IMAGES/LARGE/JF-2009-02107D_0003.JPEG.

SUPPLEMENTARY MATERIAL

Table S1. HPLC-ESI-MS/MS method quality parameters for the studied phenolic compounds in GSPE.

Compound	RT (min)	Calibration curve (µM)	Determination coefficient (R2)	Working linearity range (µM)	LOD (nM)	LOQ (nM)	MDL[a] (nM)	MQL[a] (nM)
Catechin	4.8	Y = 0.145x	0.991	0.079-19.809	6.24	20.80	2.50	8.32
Procyanidin B2	4.9	Y = 0.056x	0.997	0.026-6.482	0.77	2.56	0.31	1.02
3,4,5-trihydroxybenzoic acid	2.7	Y = 1.951x	0.998	0.165-20.574	7.74	25.78	3.09	10.31
4-hydroxy-3-methoxybenzoic acid	3.8	Y = 0.095x	0.997	0.131-16.354	146.68	488.95	58.67	195.58
3-(4'-hydroxyphenyl)propanoic acid	5.6	Y = 0.104x	0.996	0.110-13.723	11.70	39.01	4.68	15.60
3'-hydroxyphenylacetic acid	2.5	Y = 0.020x	0.975	0.164-20.539	140.19	467.31	56.08	186.92
3’,4’-Dihydroxycinnamic acid	4.2	Y = 0.041x	0.995	0.111-13.877	186.36	621.18	74.54	248.47
3-hydroxybenzoic acid	4.9	Y = 1.838x	0.998	0.289-36.200	88.87	296.24	35.55	118.50
Benzoic acid	6.3	Y = 0.439x	0.986	0.180-22.519	13.95	46.50	5.58	18.60
Hippuric acid	4.2	Y = 0.911x	0.998	0.151-18.837	14.71	49.01	5.88	19.61
4’-hydroxy-3’-methoxycinnamic acid	6.5	Y = 0.765x	0.997	0.113-14.162	5.34	17.80	2.14	7.12

[a]MDL (method detection limits) and MQL (method quantification limits) in nmol/L of fresh sample, calculated for the analysis of 250 µL of serum sample.
RT: retention behaviour; LOD: limit of detection; LOQ: limit of quantification;

RESULTS

CHAPTER 3

To elucidate the photoperiod influence on serum oxylipins levels in healthy and obese rats, as well as the impact of PAs and gut microbiota on this lipid metabolites

RESULTS

Manuscript 5

Objective: To investigate the role of gut microbiota on OXLs metabolism in healthy and CAF-diet induced obese Wistar rats.

Impact of gut microbiota on plasma oxylipins profile under healthy and obesogenic conditions

Ávila-Román J, **Arreaza-Gil V**, Cortés-Espinar AJ, Soliz-Rueda JR, Mulero M, Muguerza B, Arola-Arnal A, Arola L, Torres-Fuentes C.

Universitat Rovira i Virgili, Department de Biochemistry and Biotechnology, Nutrigenomics Research Group, Tarragona, 43007, Spain

*Corresponding author

Published in *Clinical Nutrition.* 2021 Apr, 40(4):1475-1486. DOI: 10.1016/j.clnu.2021.02.035. Impact Factor (2021): 7.643. SI Journal Citation Reports © Ranking 13/90 (Q1) in Nutrition & Dietetics.

RESULTS

Clinical Nutrition 40 (2021) 1475–1486

Contents lists available at ScienceDirect

Clinical Nutrition

journal homepage: http://www.elsevier.com/locate/clnu

Original article

Impact of gut microbiota on plasma oxylipins profile under healthy and obesogenic conditions

Javier Ávila-Román**, Verónica Arreaza-Gil, Antonio J. Cortés-Espinar, Jorge R. Soliz-Rueda, Miquel Mulero, Begoña Muguerza, Anna Arola-Arnal, Lluís Arola, Cristina Torres-Fuentes*

Universitat Rovira i Virgili, Departament de Bioquimica i Biotecnologia, Nutrigenomics Research Group, 43007, Tarragona, Spain

ARTICLE INFO

Article history:
Received 8 October 2020
Accepted 17 February 2021

Keywords:
Gut microbiota
Oxylipins
Lipid mediators
Obesity
Inflammation
Cafeteria diet

SUMMARY

Background & aims: Oxylipins (OXLs) are bioactive lipid metabolites derived from polyunsaturated fatty acids (PUFAs) which act as signaling molecules and are involved in inflammatory processes such as those that occur in obesity. On the other hand, gut microbiota plays an essential role in regulating inflammatory responses. However, little is known about the potential impact of gut bacteria on OXLs metabolism. Thus, the objective of this study was to investigate the effect of gut microbiota dysbiosis on plasma oxylipins profile in healthy and diet-induced obese animals.

Methods: Eight-week-old male Wistar rats were fed with either a standard or cafeteria diet (CAF) for 5 weeks and administered an antibiotic cocktail (ABX) in the drinking water (Ampicillin: 1 g/ml, Vancomycin: 0.5 g/ml, Imipenem: 0.25 g/ml) for the last 2 weeks in order to induce gut microbiota dysbiosis. Metabolomics analysis of OXLs in plasma was performed by HPLC–MS analysis. No antibiotic treated animals were included as controls.

Results: Plasma OXLs profile was significantly altered due to both CAF feeding and ABX administration. ABX effect was more pronounced under obesogenic conditions. Several significant correlations between different bacteria taxa and these lipid mediators were observed. Among these, the positive correlation of Proteobacteria with LTB4, a proinflammatory OXL involved in obesity-related disorders, was especially remarkable.

Conclusions: Gut microbiota plays a key role in regulating these lipid metabolites and, therefore, affecting oxylipins-mediated inflammatory processes. These results are the first evidence to our knowledge of gut microbiota impact on OXLs metabolism. Moreover, this can set the basis for developing new obesity markers based on OXLs and gut microbiota profiles.

1. Introduction

Oxylipins (OXLs) are bioactive lipid mediators, mainly generated by the oxidation of PUFAs by lipoxygenases (LOXs), which can lead to the activation of inflammatory response as well as to the resolution and prevention of acute [1] and chronic inflammatory processes [2,3] respectively. The initial phase of inflammation is characterized by the production of arachidonic acid (ARA)-derived lipid mediators also called eicosanoids, which have been shown to be involved in several physiological and pathological processes [4]. These ARA-derived OXLs can be both proinflammatory, such as prostaglandins, leukotrienes and thromboxanes, and anti-inflammatory such as lipoxins. When a certain level of proinflammatory OXLs is reached, lipoxins are synthetized from ARA by the lipoxigenase-15 (LOX-15), cyclooxygenase 2 and cytochrome P450, mediating the resolution of inflammation [5]. Moreover, different anti-inflammatory OXLs can be synthetized from dietary eicosapentanoic acid (EPA) and docosahexaenoic acid (DHA) [6]. The resolution of inflammatory response involves both the decrease of proinflammatory mediators (anti-inflammatory

* Corresponding author.
** Corresponding author.
E-mail addresses: franciscojavier.avila@urv.cat (J. Ávila-Román), veronica.arreaza@urv.cat (V. Arreaza-Gil), antoniojesus.cortes@urv.cat (A.J. Cortés-Espinar), jorgericardo.soliz@urv.cat (J.R. Soliz-Rueda), miquel.mulero@urv.cat (M. Mulero), begona.muguerza@urv.cat (B. Muguerza), anna.arola@urv.cat (A. Arola-Arnal), lluis.arola@urv.cat (L. Arola), cristina.torres@urv.cat (C. Torres-Fuentes).

https://doi.org/10.1016/j.clnu.2021.02.035
0261-5614/

activity) and the removal of immune cells from the inflamed site (pro-resolving activity) [7–9]. In this pro-resolving environment, OXLs are subsequently transformed giving rise to a great variety of oxylipin metabolites such as lipoxins, resolvins, protectins and maresins. These lipid mediators have pivotal biological functions promoting the resolution of inflammatory processes and homeostasis [10]. In autoimmune diseases, low-grade inflammatory diseases, or recurrent inflammatory diseases, the inflammation is maintained over time. This non-resolving inflammatory environment leads to chronic inflammation, which is linked to the pathogenesis and progression of several prevalent disorders such as inflammatory bowel disease, arthritis or Alzheimer's disease among others [11–13] and can worsen obesity-associated conditions.

Obesity is of particular interest as it is a multifactorial disease with a major negative impact on human health that has reached epidemic proportions worldwide [14,15]. Obesity and obesity-related chronic diseases, such as type 2 diabetes, hypertension, cardiovascular disease and certain types of cancer, are linked to low-grade chronic inflammation [16,17]. This inflammation is influenced by the activation of the innate immune system in tissues involved in metabolic processes such as adipose tissue, liver, pancreas and muscle [18]. This inflammatory response leads to increased production and release of proinflammatory cytokines such as interleukin (IL)-6, tumor necrosis factor alpha (TNF-α), monocyte chemoattractant protein-1 (MCP-1), and resistin [19–21]. Evidence suggests that the excess of nutrients consumption and obesity are associated with elevated levels of free fatty acids, which can induce both insulin resistance in peripheral tissues and activation of innate immunity [21,22]. In this regard, the current Western pattern diet consumed in modern societies, characterized by high fat and carbohydrates contents, significantly contributes to the development of obesity and obesity-mediated inflammation due to its high energy density [17].

On the other hand, the gut microbiota has been shown to play a crucial role in the pathophysiology of both obesity and related metabolic disorders as well as in inflammatory responses, and is becoming increasingly recognized as a key regulator of host physiology and metabolism [14,23,24]. These microorganisms protect from pathogen infection, produce bioactive metabolites with anti-inflammatory function, such as short chain fatty acids (SCFAs), and shape the development of the immune system [25]. Gut microbiota dysbiosis can lead to dysregulation of the functions listed above triggering inflammatory processes [26]. Thus, gut bacteria may contribute to proinflammatory signaling via toll-like receptors (TLRs) and Nod-like receptors (NLRs) activation, which recognize several broadly conserved microbial components allowing the innate immune system to sense a wide variety of microorganisms. Moreover, under metabolic syndrome conditions, the loss of epithelial barrier leads to increased translocation of bacterial products such as lipopolysaccharide (LPS), which binds toTLR4 leading to the release of cytokines that promote insulin resistance and low-grade inflammation [27]. Moreover, gut bacteria are involved in PUFAs metabolism [28]. Thus, supplementation with 10-hydroxy-cis-12-octadecenoic acid, an initial linoleic acid-related gut-microbial metabolite, attenuated high-fat diet (HFD)-induced obesity in mice by improving metabolic condition via free fatty acid receptors. This illustrates the interplay between gut microbiota and host energy metabolism via the metabolites of dietary omega-6-FAs and sheds light on the prevention and treatment of metabolic disorders by targeting gut microbial metabolites. However, little is known about the link between gut microbiota and PUFA-derived OXLs metabolites and its implication in the pathophysiology of obesity.

In this study we investigated how alterations in gut microbiota composition induced by a broad-spectrum activity antibiotic cocktail administration may impact on the plasmatic oxylipins profile in Wistar rats under healthy and obesogenic conditions induced by a cafeteria diet (CAF). This diet is a hypercaloric diet, highly palatable, that induces hyperphagia and obesity and has widely been used in the literature. Thus, CAF-fed rats are a robust animal model for simulating diet-induced human obesity associated with muscle, adipose tissue and liver inflammation that leads to the development of metabolic syndrome, including hypertriglyceridemia, hyperglycemia, hypertension and insulin resistance [29,30]. Our findings show, for the first time to our knowledge, that gut microbiota dysbiosis significantly alter plasmatic OXLs levels in healthy and obesity conditions induced by CAF, suggesting a key role for gut bacteria in the metabolism of these inflammatory lipid mediators.

2. Materials and methods

2.1. Animal procedures

Twenty-four 8-weeks-old male Wistar rats (Charles River Laboratories, Barcelona, Spain) were housed by pairs under standard laboratory conditions (temperature 22 °C, 12 h light/dark cycle) with *ad libitum* access to food and drinking water. After one week of acclimatization period, rats were weighted and randomly divided into four groups ($n = 6$) depending on the treatments administered for 5 weeks: (1) a standard chow diet (STD) (kcal/100 g: 72.4% carbohydrate, 8.4% lipid, and 19.3% protein; Safe-A04c, Germany), (2) a STD and an antibiotics cocktail (ABX) administered in drinking water for the last two weeks (weeks 3–5), (3) a CAF composed of highly palatable and energy-dense human foods (kcal/100 g: 58.2% carbohydrate, 31.1% lipid, and 10.7% protein) and (4) a CAF and an ABX administered in drinking water for the last two weeks (weeks 3–5) (Fig. 1). As mentioned above, CAF is a widely used model for diet-induced obesity in rats and allows for the development of metabolic syndrome. Each component of the diet was freshly prepared every day accordingly to previous studies [30–32]. The ABX consisted of 1 g/l ampicillin, 0.5 g/l vancomycin and 0.25 g/l imipenem (Discovery fine chemicals, UK) and was freshly prepared every day. This mixture of antibiotics has a broad-spectrum activity, acting against Gram-positive and Gram-negative bacteria, and is known to have an antimicrobial effect in the rat intestinal microbiome [33]. CAF diet included the following (grams per rat): biscuits with pâté and cheese (14–15 g), bacon (5–7 g), *ensaimada* (pastry) (6–8 g), carrot (6–8 g), standard chow (10–12 g) and milk containing 22% sucrose (w/v). Body weight and food intake were recorded weekly during the whole experimental procedure. At the end of the study both blood and fecal samples were collected for microbiota and oxylipins analysis, respectively. Blood samples were collected from the saphenous vein using capillary action blood collection EDTA-tubes and plasma samples were obtained by centrifugation (5000 *g*, 5 min, 4 °C). Fecal samples were freshly collected and immediately frozen in liquid nitrogen. All the samples were stored at −80 °C until further analyses.

The Animal Ethics Committee of the University Rovira i Virgili (Tarragona, Spain) and the Generalitat de Catalunya approved all the procedures (Code 9495) and in accordance with the EU Directive 2010/63/EU for animal experiments.

2.2. Metabolomics analysis

A volume of 100 μL of plasma was mixed with 100 μL of internal standard prepared in methanol and incubated for 30 min at −20 °C after adding 750 μL of methanol. Then, the samples were centrifugated and supernatants were diluted with 6.5 mL of 0.1% formic acid aqueous solution. Thereupon, a cleanup was applied using

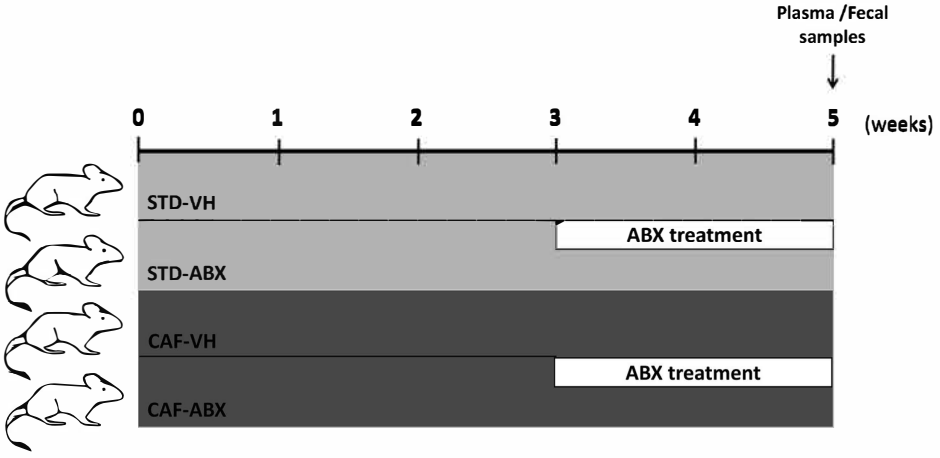

Fig. 1. Experimental model. Rats were randomly divided into four groups ($n = 6$) depending on the treatments administered for 5 weeks: (1) rats fed a standard chow diet and vehicle (STD-VH), (2) rats fed a standard chow diet and antibiotics cocktail (ABX) administered in drinking water for the last two weeks (weeks 3–5) (STD-ABX), (3) rats fed a cafeteria diet and vehicle (CAF-VH) and (4) rats fed a CAF and an ABX administered in drinking water for the last two weeks (weeks 3–5) (CAF-ABX). Plasma and fecal samples were collected at week 5.

OASIS HLB eluting with 600 μL of acetonitrile:methanol (9:1 v/v) twice. The elute was evaporated to dryness in nitrogen and reconstituted in 100 μL of Milli-Q water:methanol (1:1 v/v). All extraction processes were carried out in a dark room.

Plasma OXLs levels were analyzed by liquid chromatography tandem mass spectrometry (LC-MS/MS) using an UHPLC 1290 Series coupled to a QqQ/MS 6490 series instrument (Agilent Technologies, Santa Clara, California, USA). Separation of oxylipins was carried out onto an analytical column Eclipse XDB C18 1.8 um, 2.1 × 10 mm from Agilent Technologies. The chromatographic separation was performed using an acetonitrile:methanol (85:15, v/v) gradient in 0.01% acetic acid aqueous solution (90% acetonitrile–methanol for 4 min, 65% acetonitrile-methanol from 4 to 6 min, 60% acetonitrile–methanol from 6 to 8 min, 58% acetonitrile–methanol from 8 to 10 min, 50% acetonitrile–methanol from 10 to 16 min, 35% acetonitrile–methanol from 16 to 19 min, 25% acetonitrile–methanol from 19 to 21 min, 15% acetonitrile–methanol from 21 to 22, 5% acetonitrile–methanol from 22 to 25 min and finally back to 90% acetonitrile–methanol from 25 to 30 min for column equilibration). The flow rate was 0.4 mL/min, the column temperature was 45 °C and the injection volume was 10 μL at 4 °C. The electrospray source ionization for MS detection was in negative mode, and the capillary voltage was set to 2500 V. The gas source and desolvation temperatures were set at 150 °C and 300 °C, respectively.

2.3. Fecal microbiota analysis

Fecal DNA was isolated using a QiAamp Fast DNA Stool mini kit (Qiagen Inc., Hilden, Germany) and kept at −20 °C until further analysis. Isolated DNA was quantified using a NanoDrop ND2000 spectrophotometer (Thermo Fisher Scientific, Massachusetts, USA) and used for 16S ribosomal RNA sequencing by Ion S5 system (Life Technologies, California, USA) according to the manufacturer's instructions [34]. Briefly, the primer pairs 341F-532R (5′-CCTACGGGRSGCAGCAG-3′; 5′-ATTACCGCGGCTGCT-3′) and 15F-806R (5′-GTGCCAGCMGCCGCGGTAA-3′; 5′-GGACTACHVGGGTWTCTAAT-3′), were used to PCR-amplified the 16S rRNA variable regions V3 and V4 respectively and libraries prepared as previously described [34]. Specific Ion Torrent compatible adapters were ligated onto the 5′ of each primer. Moreover, a barcode sequence of ten bases was also added to allow for sequencing multiple samples simultaneously. Final barcoded amplicons were visualized using 2% agarose gel electrophoresis and further DNA band purification was performed with NucleoSpin (Macherey-Nagel, Berlin, Germany). The Agilent 2100 Bioanalyzer (Agilent Technologies, CA, USA) and the associated Agilent DNA 7500 Reagent kit (Agilent Technologies) were used to determine the quality, length, and concentration of the libraries needed for the sequencing procedure. Once individual libraries were created, they were diluted to 30 pM and pooled. The Ion 520 & Ion 530 Kit-Chef (Life Technologies, California, USA) was employed for template preparation and sequencing according to the manufacturer's instructions. Prepared samples were loaded on a 530 chip (Ion 530TM Chip Kit – 4 Reactions) and sequenced using the Ion S5 system (Life Technologies, California, USA). After sequencing, the reads were filtered by PGM software to remove low-quality and polyclonal sequences, producing a total of 6.615.201 reads. Filtered sequences were subsequently analyzed by QIIME and GreenGenes database. An OTU (operational taxonomic unit) table in BIOM format, which represents the taxa abundance profiles, was obtained and used in the subsequent analysis. The analysis included OTUs clustering, alpha-diversity analysis, and beta-diversity analysis.

2.4. Statistical analysis

Data were plotted using Graphpad Prism 8.0 software (Graphpad software Inc, San Diego, CA, USA) showing mean ± standard error of mean (SEM) of each group for body weight gain graph. Statistical analysis was performed using Statgraphics Centurion 18 (The Plains, VA, USA). For the body weight gain and glucose tolerance test data, normality as well as homogeneity of variance were tested by Shapiro–Wilk test and Levene test respectively, and differences between groups were assessed by one-way ANOVA with repeated measures followed by LSD post hoc test at each individual time point. Principal component analysis (PCA) and Heat map involving plasma OXLs levels and fecal microbiota relative abundance data were analyzed and plotted using MetaboAnalyst v.4.0 (McGuill University, Montreal, Canada) and MicrobiomeAnalyst [35] respectively. Comparisons between groups were performed by Kruskal–Wallis test followed by Dunn's multiple comparison and Bonferroni adjustment of p values. When considering only two groups data were analyzed by Mann–Whitney U test. For the gut

microbiota analysis, the data were filtered to remove those features with very low counts across samples were excluded, establishing 2 as the minimum count with a prevalence in samples of 10%, meaning that a feature could not be maintained unless there were 2 count in 10% of the samples. The number of features remaining after the data filtering step was 7779. Alpha diversity was calculated through Chao1 index, and the mean alpha diversity for each treatment were compared using Kruskal–Wallis test. The β-diversity was measured calculating the Bray–Curtis distances and permutational multivariate analysis of variance (PERMANOVA) was performed to assess the dissimilarity of fecal microbiota composition. The correlation analysis between fecal microbiota and oxylipins composition based on the Spearman's rank correlation method was carried out using Python script (developed by authors). Data and rho indexes were plotted using Seaborn (v.0.10.1), Pandas (v.1.0.3) and Matplotlib (v.3.2.1) libraries. The regression analysis was based on the Lowess method (Locally weighted linear regression) for non-parametric data. The script was developed using PyCharm software (v.2018.2.4, JetBrains s.r.o., Prague, Czech Republic) and Python version 3.7.7. Multiple hypothesis correction for p values was performed using the Benjamini–Hochberg method of False Discovery Rate (FDR) control. Statistical significances are subsequently depicted as follows: *indicating $p \leq 0.05$, **indicating $p \leq 0.01$ or ***indicating $p \leq 0.001$. The statistical test used for individual analysis is provided in the figure legends.

3. Results

3.1. Fecal microbiota is altered by cafeteria diet and antibiotics treatment

To elucidate the role of gut microbiota on OXLs metabolism, the plasma profile of these metabolites was analyzed under dysbiosis conditions induced by antibiotic cocktail administration in both healthy and obesogenic contexts.

Firstly, rats were fed a CAF for 5 weeks to induce obesity. Significant higher body weight gain and corresponding area under curve (AUC) were observed in CAF groups compared to STD groups, independently of ABX administration (Fig. S1a and b). Moreover, an oral glucose tolerance test (OGTT) was carried out in the last week of the experiment. CAF-fed rats showed significant higher blood glucose levels after 15 min of glucose administration and then decreased reaching similar levels to those observed in STD-fed rats (Fig. S1c). Interestingly, ABX administration led to a slower glucose levels decrease in CAF-fed rats showing significant increased blood glucose levels up to 60 min after glucose administration (Fig. S1c). Moreover, ABX administration significantly decreased the AUC derived from the OGTT in STD-fed rats (Fig. S1d). These findings collectively confirmed that the administration of this high-fat high-sugar diet for 5 weeks was enough to induce both obesity and glucose intolerance, and that gut microbiota dysbiosis induced by ABX administration altered glucose tolerance response in these animals.

ABX treatment significantly reduced gut microbiota diversity in both STD- and CAF-fed rats, as revealed by Chao1 alpha-diversity index, while CAF feeding did not significantly affect this diversity (Fig. 2a).

Moreover, overall changes in gut microbiota communities were analyzed by assessing microbial beta-diversity using a Principal Coordinate Analysis (PCoA) based on Bray Curtis dissimilarity metrics (Fig. 2b). ABX- and vehicle-treated animals showed a separation through the first principal coordinate (PC1), which explained 45.8% of the overall variation. Moreover, CAF-fed rats clustered separately from STD-fed rats along the PC2 axis, explaining 16.9% of the overall variation. Therefore, ABX treatment exerted a stronger effect on microbiota composition than CAF feeding.

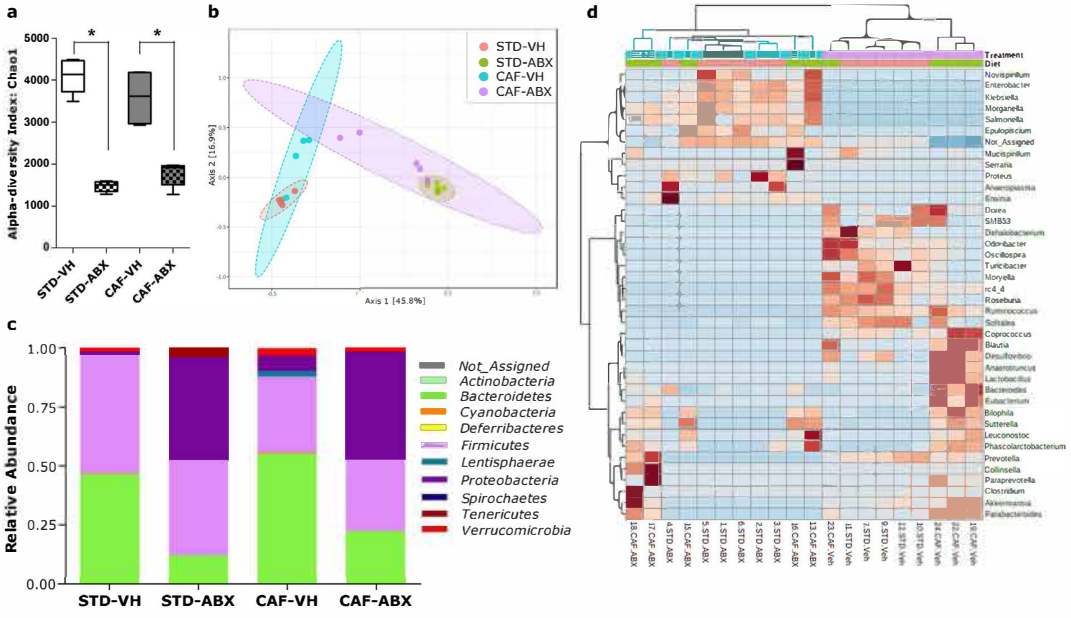

Fig. 2. Fecal microbiota is altered by antibiotics cocktail (ABX) treatment and cafeteria diet (CAF) administration. (**a**) Alpha diversity calculated by Chao1-index. * indicates significant antibiotic cocktail (ABX) effect analyzed by Kruskal–Wallis followed by Bonferroni correction for multiple comparisons ($p < 0.05$); (**b**) β-diversity calculated by Bray–Curtis distances and visualized by a principal coordinates analysis (PCoA) 2D plot (PERMANOVA test ($p < 0.001$)); (**c**) Stacked bar plots showing the average relative abundance of each taxa at phylum level; (**d**) Heat map showing hierarchical clustering of the most abundant genus taxa. STD-VH (standard diet-fed rats); STD-ABX (standard diet-fed and ABX-treated rats); CAF-VH (cafeteria diet-fed rats); CAF-ABX (cafeteria diet-fed and ABX-treated rats).

A significant effect of ABX treatment on phyla relative abundance was also observed in both STD- and CAF-fed rats (Fig. 2c; Table S1). Thus, ABX administration led to both a significant increase in Proteobacteria and a decrease in Bacteroidetes in both STD- and CAF-fed rats. Moreover, ABX did also significantly decrease Actinobacteria, Deferribacteraceae and Verrucomicrobia in STD-fed rats, and Spirochaetes in CAF-fed rats. In addition, CAF feeding also led to changes at phyla level including an increase in Proteobacteria, Lentisphaerae and Tenericutes in vehicle-treated rats only. However, Firmicutes and Bacteroidetes were not significantly altered by diet and, although a decrease in Firmicutes-to-Bacteroidetes ratio was observed, this did not result in significant changes.

When looking at genera level, a hierarchical clustering of bacterial genera was observed by ABX treatment but not by CAF feeding (Fig. 2d, Table S1). Indeed, ABX treatment significantly altered several bacterial genera in both STD- and CAF-fed rats. Although no overall diet clustering effect was observed at genera level, CAF feeding significantly increased the relative abundance of several genera when considering only vehicle-treated rats.

3.2. Oxylipins profile is modified due to cafeteria diet and antibiotic treatment

Overall CAF and ABX treatments effects on plasma OXLs profile were analyzed using a principal component analysis (PCA) (Fig. 3a). As expected, samples clustered based on the type of diet. Interestingly, ABX only showed an effect in CAF-fed rats while STD-fed rats clustered together independently of ABX treatment. Heat map analysis also revealed diet as the main factor affecting plasma OXLs profile and a stronger effect of ABX treatment in CAF-fed rats compared to STD-fed rats (Fig. 3b). Interestingly, although ABX treatment did not change the overall OXLs profile in STD-fed rats, the heat map analysis did show specific changes in some of them such as an increase in EPA, 4-HDHA and 8-HEPE as well as a decrease in 12, 13-DiHODE, Resolvin E2/E3, 910-EpODE, PGF2a, PGJ2, ARA, 9-oxoODE, 15R-Lipoxin A4/L and 18-HEPE, among others. Statistical analysis between the different treatment groups found 35 metabolites whose concentration was significantly decreased due to CAF feeding. However, ABX treatment did not show any significant effect other than increased 4-HDHA levels in STD-fed rats (Table 1). Moreover, when considering only STD-fed

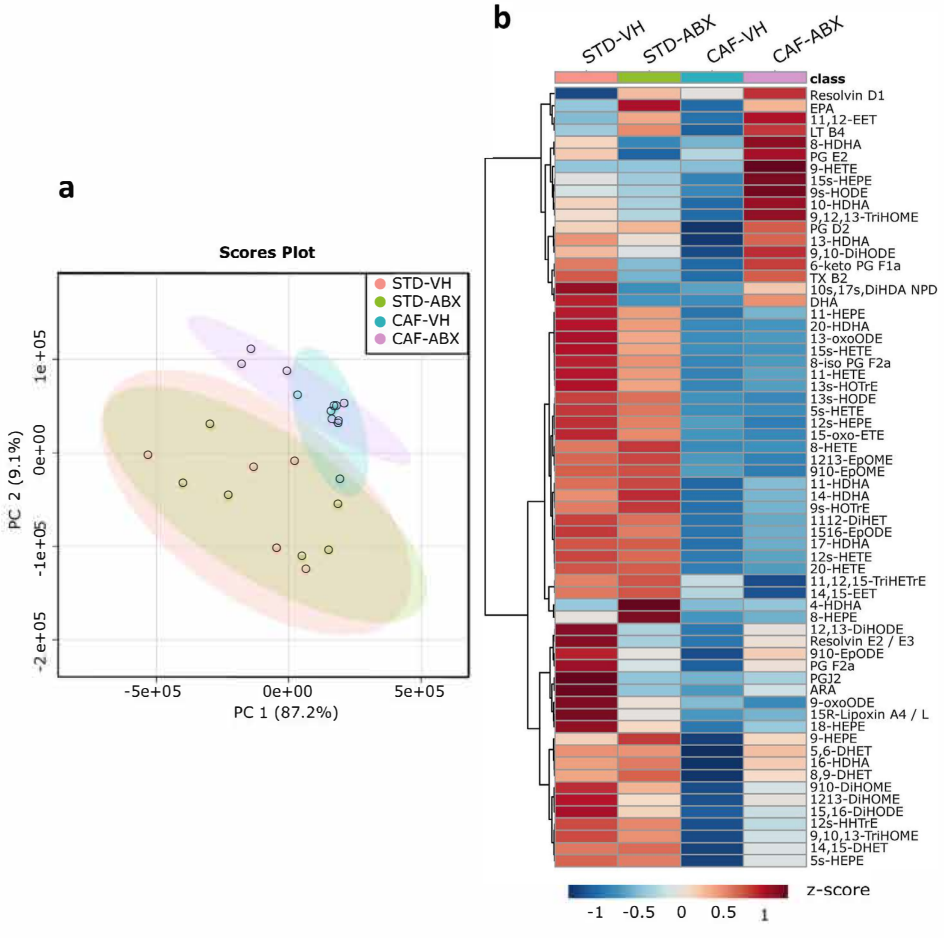

Fig. 3. Cafeteria diet (CAF) feeding and antibiotic cocktail administration led to changes in plasma oxylipins (OXLs) profile. (**a**) Relative OXL composition throughout Principal Component Analysis (PCA) of plasma samples of each group ($n = 5–6$). (**b**) Abundance of plasmatic OXL per experimental group ($n = 5–6$). STD-VH (standard diet-fed rats); STD-ABX (standard diet-fed and ABX-treated rats); CAF-VH (cafeteria diet-fed rats); CAF-ABX (cafeteria diet-fed and ABX-treated rats).

rats, in addition to the increase in 4-HDHA levels, significant increased 8-HEPE and decreased 15(R)-Lipoxin A4/A5 levels were observed in rats treated with ABX. On the other hand, when considering only CAF-fed rats, a significant increase in proinflammatory OXLs (11(12)-DiHET, 9-HETE, LT B4 and PG D2), as well as in anti-inflammatory OXLs (11-HEPE, 15(*S*)-HEPE, 10-HDHA and 13-HDHA) were observed in ABX-treated rats (Table 1).

3.3. Correlation between fecal microbiota and oxylipin composition

In order to further investigate the influence of gut microbiota on OXLs, we investigated the association between plasma OXLs levels and the relative abundance of different bacterial taxonomic groups using the Spearman's rank-order correlation coefficient (rho). To this aim, we selected only those OXLs and bacteria taxa that were significant altered by either CAF feeding or ABX administration. First, we established correlations between those OXLs and fecal microbiota at phylum level. Two main clusters were observed: a first cluster involving Firmicutes and Tenericutes phyla resulting in positive correlations with most of the OXLs, and a second cluster involving the rest of the phyla and resulting mostly in negative correlations with the majority of OXLs (Fig. 4a). In the first cluster, Tenericutes presented the highest number of strong or moderate positive significant correlations (rho > 0.5, Benjamini-Hochberg-FDR adjusted *p* value (FDR) < 0.05) with 13(*S*)-HODE, 12(13)-EpOME, 8-HETE, 15(*S*)-HETE, 15-oxo-ETE, 11-HETE, 20-HDHA, 5(*S*)-HETE, 9, (10)-EpOME, 8-iso PG F2a and 12(S)-HEPE (see Excel supplementary file for rho, *p*-value and FDR details). Among the second cluster, Lentisphaerae showed the highest number of strong or moderate negative significant correlations (rho < −0.5, FDR < 0.05), with 16-HDHA, 4-HDHA, 8-HEPE, PGD2, 13-HDHA, 14,15-DHET, 9,10,13-TriHOME, 11(12)-DiHET, 5,6-DHET, 20-HETE, 17-HDHA, 18-HEPE, LT B4 and 8-iso PGF2a (see Excel supplementary file for rho, *p*-value and FDR details). Bacteroidetes, one of the most abundant phyla, presented strong or moderated negative significant correlation (rho < −0.5 and FDR < 0.05) with 16-HDHA, LT B4, 8-HEPE and PG D2 (Fig. S2). A remarkable phylum on this cluster was Proteobacteria, which showed a strong positive significant correlation with LTB4 (rho = 0.693, FDR = 0.003) throughout the regression analysis based on Lowess method (Fig. 4b). Further, 4-HDHA, which was one of the most affected by CAF feeding and ABX administration, showed significant negative correlation (rho < −0.5 and FDR < 0.05) with Verrucomicrobia, Actinobacteria, Lentisphaerae and Deferribacteres (Fig. S3).

Table 1
Plasma oxylipins levels (pM) in standard (STD)- and cafeteria (CAF)-fed rats treated with vehicle (VH) or an antibiotic cocktail (ABX).

Oxylipins	STD-VH ($n = 5$)	STD-ABX ($n = 6$)	CAF-VH ($n = 6$)	CAF-ABX ($n = 6$)	*P*-value[b]
	Median (IQR)[a]	Median (IQR)[a]	Median (IQR)[a]	Median (IQR)[a]	
11(12)-DiHET	1661.328 (2481.107)	2296.983 (2017.148)	294.622 (39.417)**	660.850 (426.466)$	0.001
11-HEPE	1872.769 (2627.593)	1833.696 (2814.373)	204.662 (167.795)**	534.526 (750.543)$	0.005
11-HETE	1250.555 (835.022)	1031.219 (619.790)	211.392 (147.614)**	309.462 (334.725)	0.001
12(S)-HEPE	26032.015 (10087.113)	25427.630 (2876.542)	16198.007 (5732.323)*	14133.039 (5748.145)**	0.001
12(S)-HETE	28475.604 (46362.692)	34149.279 (53087.197)	3136.320 (5360.185)*	7101.068 (13314.490)	0.014
13(S)-HODE	3001.244 (1268.442)	2578.309 (1457.377)	430.743 (394.688)*	370.671 (257.892)*	0.001
13(S)-HOTrE	116149.483 (47566.768)	77012.056 (33452.778)	17372.566 (16705.742)**	26027.303 (19786.494)	0.001
13-HDHA	2903.827 (2336.121)	2888.441 (1227.410)	939.750 (846.127)*	2569.495 (2552.049)$	0.022
13-oxoODE	3409.196 (2699.442)	2581.990 (2401.890)	673.179 (703.098)*	874.794 (468.636)	0.004
14,15-DHET	19887.447 (7317.751)	18870.004 (9424.917)	7936.933 (2895.549)*	13345.837 (9884.030)	0.006
15(16)-EpODE	7090.270 (9360.003)	7720.084 (12104.890)	800.617 (657.243)**	1858.605 (3187.772)	0.005
15(R)-Lipoxin A4/A5	41085.385 (31264.763)	20452.980 (9789.600)$	8376.811 (7442.714)***	11410.731 (6685.493)	0.000
15(S)-HETE	6105.271 (2844.963)	4334.876 (2137.168)	641.062 (302.835)**	641.736 (559.584)	0.001
15,16-DiHODE	21834.899 (12962.440)	19566.222 (13094.552)	10538.166 (5580.299)*	14385.504 (12769.142)	0.033
15-oxo-ETE	1140.083 (621.224)	1117.735 (517.926)	263.048 (199.126)*	179.738 (157.443)*	0.001
16-HDHA	706.739 (416.855)	868.403 (432.046)	456.349 (176.794)*	701.705 (560.134)	0.021
17-HDHA	1640.338 (1435.356)	1759.262 (1829.995)	392.480 (213.871)*	759.386 (533.688)	0.004
18-HEPE	2259.847 (2467.270)	1380.655 (920.761)	275.811 (403.476)**	503.614 (1019.271)	0.003
20-HDHA	1039.531 (723.020)	818.587 (341.198)	182.281 (82.493)**	214.435 (215.961)*	0.001
20-HETE	1159.873 (567.339)	1257.256 (619.087)	312.673 (102.115)*	391.056 (481.532)*	0.003
5(S)-HETE	5228.429 (2613.529)	4429.005 (2005.372)	801.928 (864.557)**	759.953 (703.549)*	0.001
5,6-DHET	4074.785 (2043.074)	4111.513 (1743.315)	2138.077 (1022.006)*	3563.027 (3010.726)	0.018
8,9-DHET	413.134 (56.597)	402.772 (149.835)	222.518 (70.389)*	342.914 (331.134)	0.013
8-HETE	944.334 (484.475)	937.591 (733.541)	146.088 (54.901)*	125.512 (145.044)**	0.001
8-iso PG F2a	967.042 (796.685)	654.503 (332.533)	123.343 (120.371)**	159.190 (187.765)	0.001
9(10)-EpODE	11066.711 (9853.434)	9368.940 (3869.267)	1555.549 (8472.890)*	8460.025 (11840.393)	0.048
9,10,13-TriHOME	29459.970 (15567.949)	27155.737 (17584.558)	8983.110 (7341.700)*	15334.936 (19536.854)	0.015
PG D2	19571.772 (10361.085)	20808.024 (10588.786)	8849.061 (2427.149)*	17225.502 (19429.022)$	0.009
11,12,15-TriHETrE	5834.522 (3037.580)	5453.101 (3008.983)	4068.687 (3492.481)	3248.543 (1267.808)*	0.029
12(13)-EpOME	174438.699 (71101.345)	170527.002 (68000.594)	35278.717 (26083.618)	29497.559 (12961.138)**	0.001
14,15-EET	10753.041 (3955.561)	9786.236 (3429.102)	7993.635 (6182.779)	6542.202 (1540.205)*	0.018
8-HEPE	349.973 (141.130)	492.613 (316.706)$	262.575 (103.446)	306.150 (64.980)*	0.002
9(10)-EpOME	37363.885 (13854.464)	31401.418 (10580.993)	12067.085 (12172.395)	10955.152 (5886.456)**	0.001
9-oxoODE	1463.233 (1397.373)	728.186 (260.434)	406.493 (248.825)	319.122 (231.936)*	0.013
4-HDHA	3320.832 (1571.543)	6241.716 (4052.207)#$	3365.791 (1256.646)	3884.618 (2741.782)	0.018
10-HDHA	21.102 (20.023)	12.141 (12.356)	3.987 (5.724)	10.161 (69.078)$	0.037
15(S)-HEPE	271.334 (323.040)	211.027 (203.592)	157.825 (166.257)	335.025 (368.186)$	0.111
9-HETE	2359.320 (1605.371)	2751.398 (1371.556)	2181.102 (667.472)	3545.175 (72324.902)$	0.064
LT B4	97.835 (180.721)	191.328 (95.090)	75.717 (118.565)	174.530 (137.621)$	0.081

* and # indicate CAF feeding and ABX effects respectively by Dunn's multiple comparison test followed by Bonferroni *p* values adjustment: $p < 0.0125$, $^{**}p < 0.0025$, $^{***}p < 0.00025$; $\#p < 0.0125$; $ indicates ABX effects when comparing by Mann Whitney test. $ $P < 0.05$.
[a] Data shown as Median ± Interquartile Range (IQR) in pM units.
[b] *p*-value by Kruskal–Wallis test.

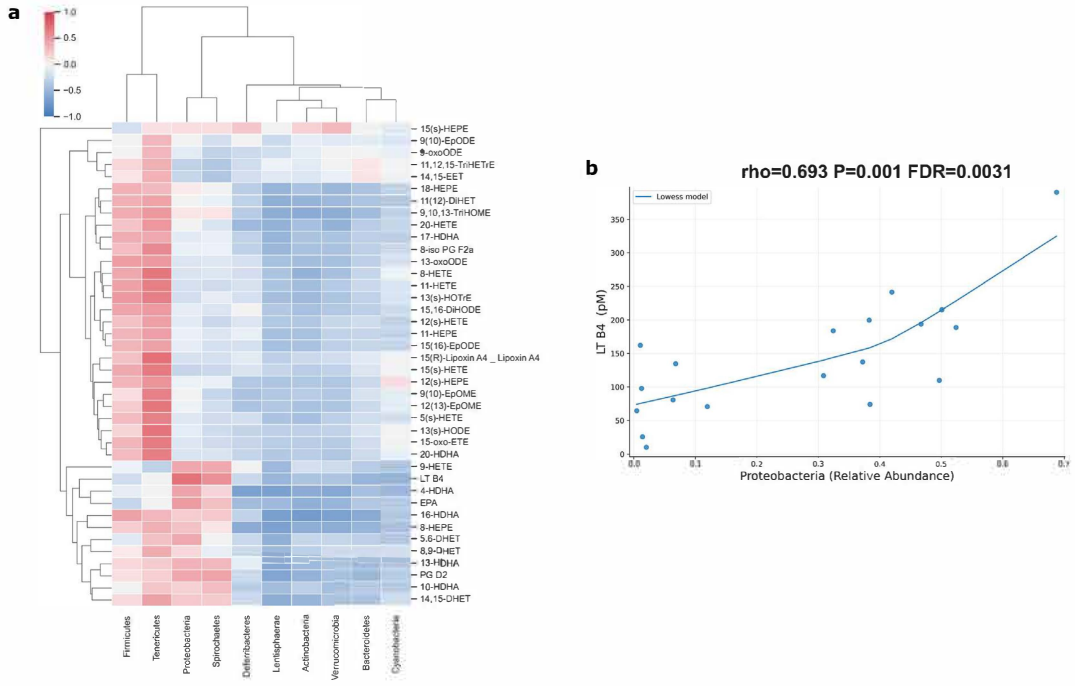

Fig. 4. Correlation analysis between fecal microbiota at phylum level and plasma oxylipin (OXL) composition evaluated by Spearman's rank correlation coefficient (rho). (**a**) Heat map showing the hierarchical clustering of the degree of correlation between phylum and OXL. Positive correlation coefficients are in red and negative correlation coefficients are in blue. The color intensity represents the degree of correlation. (**b**) Locally weighted linear regression (Lowess model) analysis between LT B4 concentration and relative abundance of Proteobacteria showing positive correlation. (For interpretation of the references to color in this figure legend, the reader is referred to the Web version of this article.)

Since the assessment of these OXLs at a phyla level revealed widespread differences, we further investigated these associations at other taxonomical levels. Two clusters were observed when looking at family level. The first cluster is characterized by bacteria families belonging mostly to Firmicutes and Bacteroidetes phyla showing negative correlations (rho < −0.5, $p < 0.05$) with most of the OXLs included in this analysis (Fig. 5). These correlations were mostly moderate, with the exception of *Leuconostocaceae*, which showed a high number of moderate to strong significant negative correlations (rho < −0.6, FDR < 0.004) (see Excel supplementary file for details). The second cluster is characterized by bacteria families showing positive correlations (rho > 0.5, $p < 0.05$) with most of the OXLs. Although a high number of families in this cluster are from the Firmicutes and Bacteroidetes phyla, it is worth mentioning that, in contrast with the first cluster mentioned above, in this group appeared a significant number of families from the Proteobacteria phylum. Unfortunately, most of these correlations in this second cluster did not pass the multiple test corrections (FDR < 0.5) (see Excel supplementary file for details).

Regarding genus level, a first remarkable cluster involving bacteria belonging to the Proteobacteria, Tenericutes and Firmicutes phyla was identified (Fig. 6). This cluster was characterized by strong positive correlations (rho > 0.5, $p < 0.05$) with LTB4, 4-HDHA, EPA, 9-HETE, 8-HEPE, 10-HDHA, 14,15-DHET, 5,6-DHET, 16-HDHA, 13-HDHA and PGD2. From all these correlations, 14 passed the FDR correction (see Excel supplementary file for details). The second cluster was characterized by bacteria genera belonging to Actinobacteria, Bacteroidetes, Deferribacteres, Lentisphaerae, Firmicutes and Verrucomicrobia phyla showing negative correlations (rho < −0.5, $p < 0.05$) with the same group of OXLs. From all these correlations, 79 passed the FDR correction (see Excel supplementary file for details).

In addition to these taxonomical levels, we also looked at class (Fig. S4) and order levels (Fig. S5). Again, two clusters were observed at these levels, a first one characterized by bacteria showing negative correlations (rho < −0.5, $p < 0.05$) and a second cluster characterized by bacteria showing positive correlations (rho > 0.5, $p < 0.05$). However, only two correlations with 4-HDHA passed the FDR correction: strong negative correlations with both the Lentisphaeria class (rho = −0.8312, FDR = 0.0006) and the Victivallales order (rho = −0.831, FDR = 0.0002) (see Excel supplementary file for details).

4. Discussion

OXLs are PUFAs-derived bioactive metabolites and include prostaglandins, thromboxanes, mono-, di-, and tri-hydroxy fatty acids (FAs), epoxy FAs, lipoxins, eoxins, hepoxilins, resolvins, protectins, and maresins [36]. They are involved in different physiological processes including inflammation, immune actions, pain, apoptosis, blood clotting, cell proliferation, blood vessel permeability, blood pressure regulation and tissue repair [37]. Among these, it is worth highlighting their role as potent modulators of inflammatory processes since they can act as activators as well as pro-resolving mediators of inflammation through their binding to both peroxisome proliferator-activated receptors (PPARs) and G protein-coupled receptors (GPCRs) [38–40]. Indeed, they are emerging as potential new biomarkers of chronic low-grade inflammation [41]. In general, OXLs derived from ω3-PUFAs exert anti-inflammatory effects while those derived from ω6-PUFAs are more proinflammatory, which is in accordance with overall

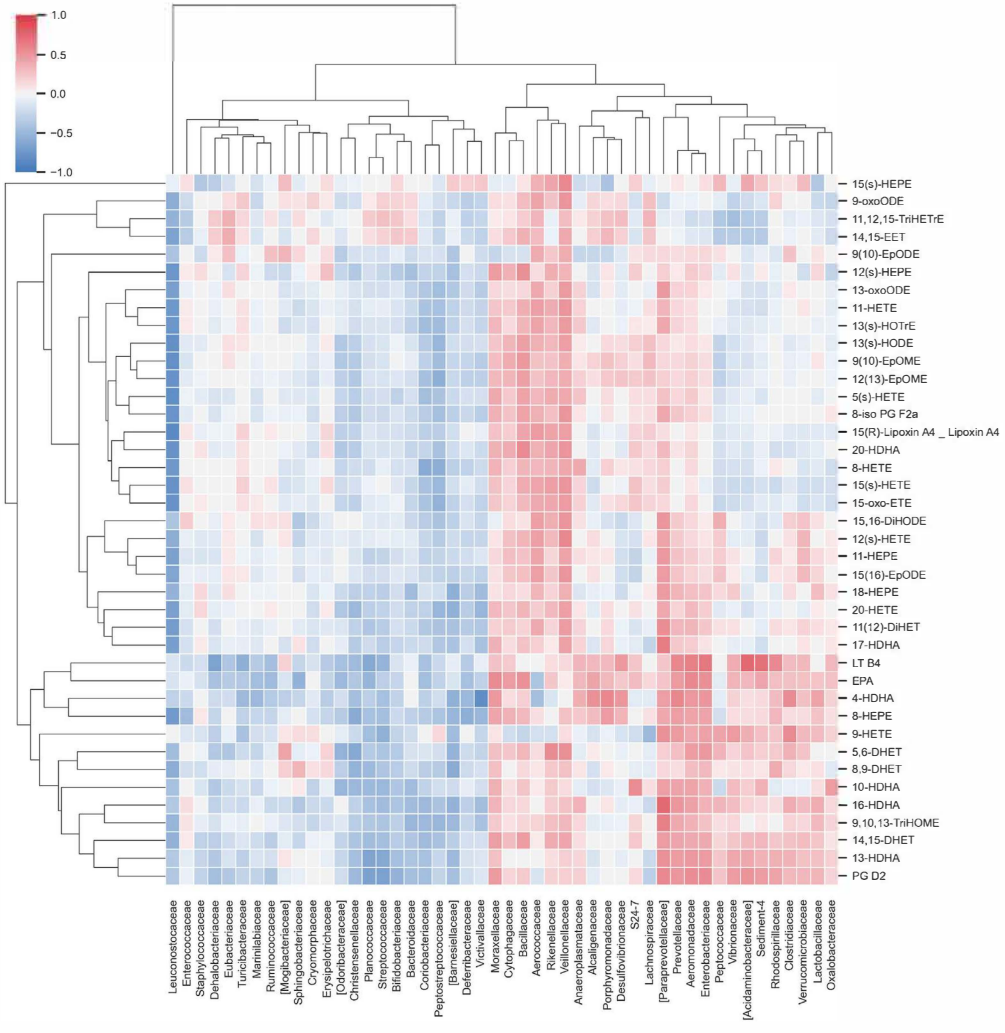

Fig. 5. Correlation analysis between fecal microbiota at family level and plasma oxylipins (OXL) evaluated by Spearman's rank correlation coefficient (rho). Heat map showing the hierarchical clustering of the degree of correlation between bacteria family and OXLs. Positive correlation coefficients are in red and negative correlation coefficients are in blue. The color intensity represents the degree of correlation. (For interpretation of the references to color in this figure legend, the reader is referred to the Web version of this article.)

beneficial and detrimental effects of ω3 and ω6-PUFAs respectively [42]. On the other hand, gut microbiota has been proven to be involved in PUFAs metabolic pathways, but its effects on these metabolites remains poorly understood [28,43]. In the present study, we found that gut microbiota dysbiosis altered plasma OXLs profile, suggesting that intestinal bacteria may indeed influence their metabolism and, ultimately, host inflammatory response and other physiological functions.

In healthy rats, gut microbiota dysbiosis caused by ABX administration did not change the overall plasma OXLs profile, suggesting that intestinal bacteria do not significantly contribute to the metabolism of these bioactive lipid mediators under healthy conditions. However, some specific changes were observed, including a significant increase in 4-HDHA and 8-HEPE, which are related to anti-inflammatory effects, and a significant decrease in 15(R)-Lipoxin A4/A5 levels, which are related to pro-resolving effects. These changes in OXLs may be in response to the known inflammation mediated by the ABX treatment due to both the translocation of gut microbiota [44] and to the long-term disturbances of microbiota composition [45,46]. Indeed, the ABX administration led to a significant increase in the relative abundance of Proteobacteria, which has been extensively linked to inflammation. Thus, bacteria from this phylum are able to utilize inflammatory by-products for their survival and, therefore, during chronic inflammation there is an increase in their relative abundance due to their advantage over other intestinal bacteria that lack this metabolic capacity [47]. Moreover, ABX administration led to significant decreased Bacteroidetes relative abundance, which has also been associated to inflammation [48]. This bacterial taxon, together with Firmicutes, is one of the dominant phyla in healthy vertebrate hosts and play a variety of roles, including the generation of metabolites and immune system maturation [49,50]. Moreover, ABX administration did also significantly affected other less abundant phyla such as Actinobacteria, linked to gut barrier impairment and proinflammatory cytokines [51], Deferribacteraceae, which involves harmful bacteria and has been associated to

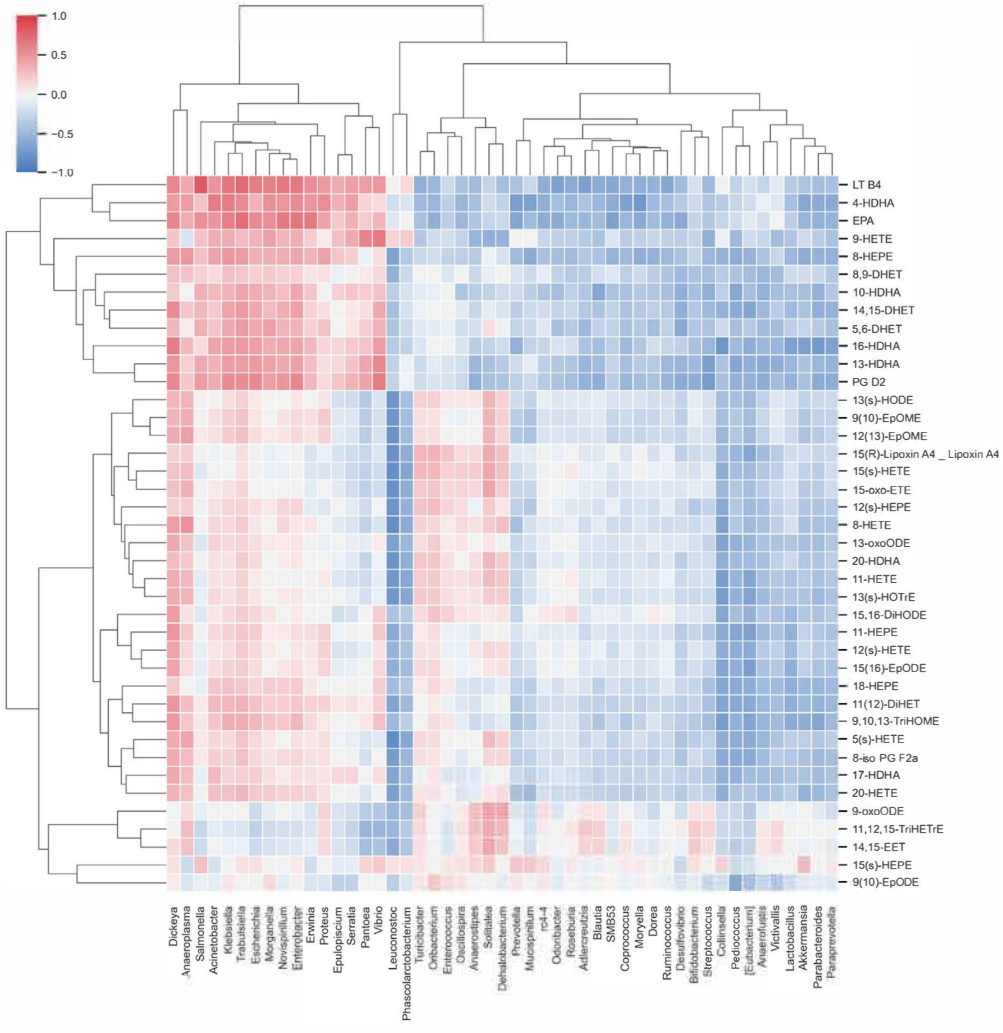

Fig. 6. Correlation analysis between fecal microbiota at genus level and plasma oxylipins (OXL) evaluated by Spearman's rank correlation coefficient (rho). Heat map showing the hierarchical clustering of the degree of correlation between bacteria genus and OXLs. Positive correlation coefficients are in red and negative correlation coefficients are in blue. The color intensity represents the degree of correlation. (For interpretation of the references to color in this figure legend, the reader is referred to the Web version of this article.)

inflammatory diseases such as colitis [52], and Verrucomicrobia, also related to increased inflammation as their abundance bloomed in a mouse model of mucositis [53]. Therefore, ABX treatment leads to changes in gut bacteria that affect inflammatory responses which may ultimately impact on OXLs metabolism.

On the other hand, obesity and obesity-related disorders are linked to low-grade chronic inflammation [54] and gut microbiota dysbiosis [23]. Therefore, the establishment of obesogenic conditions by CAF administration allowed us for a better understanding of the potential role that gut bacteria may have on OXLs metabolism under pathologic conditions associated to chronic low-grade inflammation. Indeed, CAF feeding has been shown to effectively induce obesity, diabetes and other disorders associated to the metabolic syndrome, increasing inflammatory markers and significantly altering gut microbiota composition [29–31]. Moreover, CAF includes food regularly consumed by humans, leading to a more robust model for human obesity in comparison with others high fat and/or high sugar diets traditionally used [29]. We observed a completely different overall plasma OXLs profile in CAF-fed rats compared to STD-fed rats. These differences may be explained by the different nutritional composition of these diets. Indeed, OXLs profile is determined not only by the relative abundance of the enzymes that are involved in their synthesis and metabolization but also by the availability of PUFAs precursors, which is mainly influenced by the composition of dietary fatty acids [36,55–57]. Hence, CAF is enriched in lipid content, including higher levels of PUFAs, in comparison with STD [58]. In addition, the effect of CAF feeding on the OXLs profile may be related to the increased inflammation caused as a result of the chronic administration of this type of high fat high sugar diet and to the obesity development [29]. Interestingly, besides the high lipid content and the increased inflammation, CAF feeding led to an overall reduction in plasma OXLs levels, involving both pro- and anti-inflammatory metabolites. However, this is consistent with other diet induce obesity (DIO) study that show decreased plasma OXLs levels in HFD-fed animals [59]. Moreover, CAF feeding induced changes in

gut microbiota composition that may ultimately impact on the OXLs profile. Thus, CAF-fed rats showed an increased abundance in proinflammatory bacteria such as the above mentioned Proteobacteria as well as Lentisphaerae, which has been linked to patients with inflammation [60], and Tenericutes, which has been shown to positively correlate with proinflammatory cytokines such as IL-6, TNF-α or IL-17A [61]. Among these, it is worth mentioning the increased relative abundance in Proteobacteria, which is consistent with others studies using CAF [30,31] and has been reported to be highly associated to dysbiosis during metabolic disorders [62]. In fact, the mono-association of germ-free mice with *Enterobacter cloacae*, a strain belonging to this phylum, induced obesity and insulin resistance when mice were fed a HFD, which was not observed in control HFD-fed germ-free mice, supporting the relation between metabolic disorders and the expansion of Proteobacteria [63]. Hence, this also supports the potential link of Proteobacteria relative abundance with metabolic disorders associated to chronic low-grade inflammation and corroborates that plasma OXLs profile changes are associated with changes in the abundance of this bacteria taxa. Moreover, the ABX administration did change the overall gut microbiota composition in CAF-fed rats, having a higher impact than that produced by the diet. Indeed, rats administered with ABX showed similar overall gut bacteria composition independently of the diet. This is in agreement with previous studies which reported that the effects of oral antibiotics on gut bacteria composition and function were greater than those mediated by HFD administration [64]. Interestingly, the plasma OXLs profile in CAF-fed rats treated with ABX showed a significant increase in both pro- and anti-inflammatory plasma OXLs metabolites compared to non-ABX treated CAF-fed rats, indicating that gut microbiota may play a key role in the metabolism of these lipid metabolites under obesity conditions. As observed in STD-fed rats, the main change induced by the ABX treatment at phylum level was an increase in Proteobacteria and a decrease in Bacteroidetes relative abundance. Therefore, this corroborates the potential relationship between these bacterial taxa and the OXLs metabolism. The proportion between these two phyla may be a good marker for gut microbiota dysbiosis as ABX administration induced an increase in the Proteobacteria-to-Bacteroidetes ratio, reaching significance in STD-fed rats. Moreover, increase in this ratio has been associated to HFD administration, supporting its relation with gut microbiota alterations [65]. Indeed, decrease in this ratio has been linked to decrease in both LPS production and NF-κB activation in the colon of HFD-fed mice, ameliorating inflammation [66]. When analyzing gut bacteria relative abundance correlation with OXLs levels, there were several associations observed. Among these, it is worth highlighting those that correlated with Proteobacteria and Bacteroidetes, as they were the main phyla changed by the ABX treatment. Regarding Bacteroidetes, they showed negative correlations with most of the plasma OXLs, being significant for 16-HDHA, 8-HEPE, LT B4 and PG D2. Regarding 16-HDHA and 8-HEPE are derived from the ω3-PUFAs DHA and EPA respectively, which have been linked to anti-inflammatory effects. LT B4 and PG D2 are derived from ARA, ω6-PUFA linked to proinflammatory effects. Regarding Proteobacteria, both negative and positive correlations were observed. Among these, the significant positive correlation with LT B4 was especially remarkable. This oxylipin is a chemoattractant for neutrophils that has been demonstrated to initiate pathological inflammation in various tissues as well as to have a key role in the progression of chronic diseases related to inflammation such as infectious diseases, allergy, autoimmune diseases, and metabolic disease [67].

These findings are consistent with the essential role that gut bacteria play in lipid metabolism and absorption. Thus, germ-free animals are resistant to develop DIO and metabolize fat with specifically impaired lipid digestion and absorption [68,69]. Hence, gut microbes regulate gut epithelial processes involved in lipid digestion and assimilation which are crucial for host adaptation to dietary lipid changes [69]. Moreover, gut microbiota has been shown to produce PUFA-derived metabolites, including conjugated linoleic (CLA) and conjugated linolenic acids (CLnA) [43,70]. In addition, it was recently shown that gut microbiota confers host resistance to obesity by metabolizing dietary PUFAs [28]. Hence, it seems evident that OXL metabolites derived by dietary PUFAs such as LA, ALA and ARA, may be influenced by gut bacteria.

On the other hand, the correlations observed may contribute to elucidate specific profiles of OXLs-gut microbiota interactions in an obesity context, which may be useful as novel biomarkers for metabolic profiling. Indeed, OXLs and gut microbiota are emerging as new candidates to define new hallmarks of particular physiological conditions [71,72].

Finally, it is important to mention that ABX treatment also altered glucose tolerance response in both healthy and obese rats, indicating that the above discussed changes in gut microbiota and OXLs plasma profile mediated by the antibiotics intake may be linked to metabolic alterations such as glucose intolerance. Further studies are needed in order to elucidate the mechanisms involved and the effects in different tissues.

5. Conclusions

In conclusion, we have observed a clear association between gut bacteria changes and plasma OXLs profile under healthy and obesogenic conditions induced by CAF feeding in rats. These findings support a potential link between gut microbiota and the metabolism of these lipid mediators, which may be linked to the key role that gut microbiota has in inflammatory response. Moreover, this can set the basis for developing new obesity markers based on OXLs and gut microbiota profiles. Further studies are needed to elucidate the specific mechanisms involved.

Author contributions

Conceptualization: J.A.R., L.A. and C.T.F; Methodology: J.A.R, V.A.G., AJ.C.E., JR.S.R. and C.T.F. Investigation: J.A.R., M.M., B.M., A.A.A., L.A. and C.T.F. Validation: J.A.R., L.A. and C.T.F. Writing the original draft: J.A.R, V.A.G., AJ.C.E., JR.S.R. and C.T.F. Writing, review, and editing: J.A.R. and C.T.F. Funding acquisition: B.M. and L.A.

Funding

This study was funded by the Ministerio de Economía, Industria y Competitividad (AGL2016-77105-R) and the European Union through the operative program ERDF of Catalonia (PECT-NUTRI-SALT, 2014-2020). JAR is Martí i Franquès Postdoctoral Fellow supported by Universitat Rovira i Virgili (URV). VAG and AJCE are Predoctoral Fellow supported by URV. JSR is supported by the Ministerio de Ciencia, Innovación y Universidades (MICINN) and the European Social Fund (ESF). M.M and A.A.A. are Serra Húnter Fellows. CTF is Beatriu de Pinós Postdoctoral Fellow supported by Secretaria d'Universitats i Recerca del Departament d'Empresa i Coneixement de la Generalitat de Catalunya.

Conflicts of interest

The authors declare no conflict of interest.

Acknowledgments

In memory of Prof. Cinta Bladé. We thank to Niurka Dariela LLópiz and Rosa Pastor for technical support.

Appendix A. Supplementary data

Supplementary data to this article can be found online at https://doi.org/10.1016/j.clnu.2021.02.035.

References

[1] Colas RA, Shinohara M, Dalli J, Chiang N, Serhan CN. Identification and signature profiles for pro-resolving and inflammatory lipid mediators in human tissue. Am J Physiol Cell Physiol 2014;307.
[2] Hsiao HM, Thatcher TH, Colas RA, Serhan CN, Phipps RP, Sime PJ. Resolvin D1 reduces emphysema and chronic inflammation. Am J Pathol 2015;185:3189–201.
[3] Sok MCP, Tria MC, Olingy CE, San Emeterio CL, Botchwey EA. Aspirin-Triggered Resolvin D1-modified materials promote the accumulation of pro-regenerative immune cell subsets and enhance vascular remodeling. Acta Biomater 2017;53:109–22.
[4] Yui K, Imataka G, Nakamura H, Ohara N, Naito Y. Eicosanoids derived from arachidonic acid and their family prostaglandins and cyclooxygenase in psychiatric disorders. Curr Neuropharmacol 2015;13:776–85.
[5] Serhan CN, Levy BD, Clish CB, Gronert K, Chiang N. Lipoxins, aspirin-triggered 15-epi-lipoxin stable analogs and their receptors in anti-inflammation: a window for therapeutic opportunity. Ernst Schering Res Found Workshop 2000:143–85.
[6] López-Vicario C, Rius B, Alcaraz-Quiles J, García-Alonso V, Lopategi A, Titos E, et al. Pro-resolving mediators produced from EPA and DHA: overview of the pathways involved and their mechanisms in metabolic syndrome and related liver diseases. Eur J Pharmacol 2016;785:133–43.
[7] Serhan CN, Brain SD, Buckley CD, Gilroy DW, Haslett C, O'Neill LAJ, et al. Resolution of inflammation: state of the art, definitions and terms. FASEB J 2007;21:325–32.
[8] Serhan CN, Chiang N. Endogenous pro-resolving and anti-inflammatory lipid mediators: a new pharmacologic genus. Br J Pharmacol 2008;153:S200.
[9] Freire MO, Van Dyke TE. Natural resolution of inflammation. Periodontol 2000 2013;(63):149–64.
[10] Levy BD, Clish CB, Schmidt B, Gronert K, Serhan CN. Lipid mediator class switching during acute inflammation: signals in resolution. Nat Immunol 2001;2:612–9.
[11] Gewirtz AT, Neish AS, Madara JL. Mechanisms of active intestinal inflammation and potential down-regulation via lipoxins. Adv Exp Med Biol 2002;507:229–36.
[12] Chan MM-Y, Moore AR. Resolution of inflammation in murine autoimmune arthritis is disrupted by cyclooxygenase-2 inhibition and restored by prostaglandin E2-mediated lipoxin A4 production. J Immunol 2010;184:6418–26.
[13] Kantarci A, Aytan N, Palaska I, Stephens D, Crabtree L, Benincasa C, et al. Combined administration of resolvin E1 and lipoxin A4 resolves inflammation in a murine model of Alzheimer's disease. Exp Neurol 2018;300:111–20.
[14] Muscogiuri G, Cantone E, Cassarano S, Tuccinardi D, Barrea L, Savastano S, et al. Gut microbiota: a new path to treat obesity. Int J Obes Suppl 2019;9:10–9.
[15] WHO. Obesity and overweight. 2016.
[16] Gadde KM, Martin CK, Berthoud HR, Heymsfield SB. Obesity: pathophysiology and management. J Am Coll Cardiol 2018;71:69–84.
[17] Rogero MM, Calder PC. Obesity, inflammation, toll-like receptor 4 and fatty acids. Nutrients 2018;10:1–19.
[18] Barden A, Shinde S, Tsai IJ, Croft KD, Beilin LJ, Puddey IB, et al. Effect of weight loss on neutrophil resolvins in the metabolic syndrome. Prostaglandins Leukot Essent Fatty Acids 2019;148:25–9.
[19] Weisberg SP, Mccann D, Desai M, Rosenbaum M, Leibel RL, Ferrante Jr AW. Obesity is associated with macrophage accumulation in adipose tissue. J Clin Invest 2003;112:1796–808.
[20] Xu Haiyan, Barnes Glenn T, Yang Qing, Tan Guo, Yang Daseng, Chou Chieh J, et al. Chronic inflammation in fat plays a crucial role in the development of obesity-related insulin resistance. J Clin Invest 2003;112:1821–30.
[21] Rodríguez-Hernández H, Simental-Mendía LE, Rodríguez-Ramírez G, Reyes-Romero MA. Obesity and inflammation: epidemiology, risk factors, and markers of inflammation. Int J Endocrinol 2013;2013:678159.
[22] Gregor MF, Hotamisligil GS. Inflammatory mechanisms in obesity. Annu Rev Immunol 2011;29:415–45.
[23] Torres-Fuentes C, Schellekens H, Dinan TG, Cryan JF. The microbiota–gut–-brain axis in obesity. Lancet Gastroenterol Hepatol 2017;2:747–56.
[24] Kamada N, Seo SU, Chen GY, Núñez G. Role of the gut microbiota in immunity and inflammatory disease. Nat Rev Immunol 2013;13:321–35.
[25] Clemente JC, Manasson J, Scher JU. The role of the gut microbiome in systemic inflammatory disease. BMJ 2018;360(j5145).
[26] Chassaing B, Gewirtz AT. Gut microbiota, low-grade inflammation, and metabolic syndrome. Toxicol Pathol 2014;42:49–53.
[27] Cani PD, Amar J, Iglesias MA, Poggi M, Knauf C, Bastelica D, et al. Metabolic endotoxemia initiates obesity and insulin resistance. Diabetes 2007;56:1761–72.
[28] Miyamoto J, Igarashi M, Watanabe K, Karaki S-I, Mukouyama H, Kishino S, et al. Gut microbiota confers host resistance to obesity by metabolizing dietary polyunsaturated fatty acids. Nat Commun 2019;10:1–5.
[29] Sampey BP, Vanhoose AM, Winfield HM, Freemerman AJ, Muehlbauer MJ, Fueger PT, et al. Cafeteria diet is a robust model of human metabolic syndrome with liver and adipose inflammation: comparison to high-fat diet. Obesity 2011;19:1109–17.
[30] Del Bas JM, Guirro M, Boqué N, Cereto A, Ras R, Crescenti A, et al. Alterations in gut microbiota associated with a cafeteria diet and the physiological consequences in the host. Int J Obes 2018;42:746–54.
[31] Gual-Grau A, Guirro M, Mayneris-Perxachs J, Arola L, Boqué N. Impact of different hypercaloric diets on obesity features in rats: a metagenomics and metabolomics integrative approach. J Nutr Biochem 2019;71:122–31.
[32] Caimari A, del Bas JM, Boqué N, Crescenti A, Puiggròs F, Chenoll E, et al. Heat-killed Bifidobacterium animalis subsp. Lactis CECT 8145 increases lean mass and ameliorates metabolic syndrome in cafeteria-fed obese rats. J Funct Foods 2017;38:251–63.
[33] Manichanh C, Reeder J, Gibert P, Varela E, Llopis M, Antolin M, et al. Reshaping the gut microbiome with bacterial transplantation and antibiotic intake. Genome Res 2010;20:1411–9.
[34] Guirro M, Costa A, Gual-Grau A, Mayneris-Perxachs J, Torrell H, Herrero P, et al. Multi-omics approach to elucidate the gut microbiota activity: metaproteomics and metagenomics connection. Electrophoresis 2018;39:1692–701.
[35] Chong J, Liu P, Zhou G, Xia J. Using MicrobiomeAnalyst for comprehensive statistical, functional, and meta-analysis of microbiome data. Nat Protoc 2020;15:799–821.
[36] Gabbs M, Leng S, Devassy JG, Monirujjaman M, Aukema HM. Advances in our understanding of oxylipins derived from dietary PUFAs. Adv Nutr 2015;6:513–40.
[37] Chiang N, Serhan CN. Specialized pro-resolving mediator network: an update on production and actions. Essays Biochem 2020;64:443–62.
[38] Rajamani A, Borkowski K, Akre S, Fernandez A, Newman JW, Simon SI, et al. Oxylipins in triglyceride-rich lipoproteins of dyslipidemic subjects promote endothelial inflammation following a high fat meal. Sci Rep 2019;9:1–17.
[39] Colson C, Ghandour RA, Dufies O, Rekima S, Loubat A, Munro P, et al. Diet supplementation in ω3 polyunsaturated fatty acid favors an anti-inflammatory basal environment in mouse adipose tissue. Nutrients 2019;11.
[40] Liakh I, Pakiet A, Sledzinski T, Mika A. Methods of the analysis of oxylipins in biological samples. Molecules 2020;25:349.
[41] van den Brink W, van Bilsen J, Salic K, Hoevenaars FPM, Verschuren L, Kleemann R, et al. Current and future nutritional strategies to modulate inflammatory dynamics in metabolic disorders. Front Nutr 2019;6:129.
[42] Shearer GC, Walker RE. An overview of the biologic effects of omega-6 oxylipins in humans. Prostaglandins Leukot Essent Fatty Acids 2018;137:26–38.
[43] Druart C, Bindels LB, Schmaltz R, Neyrinck AM, Cani PD, Walter J, et al. Ability of the gut microbiota to produce PUFA-derived bacterial metabolites: proof of concept in germ-free versus conventionalized mice. Mol Nutr Food Res 2015;59:1603–13.
[44] Knoop KA, McDonald KG, Kulkarni DH, Newberry RD. Antibiotics promote inflammation through the translocation of native commensal colonic bacteria. Gut 2016;65:1100–9.
[45] Ianiro G, Tilg H, Gasbarrini A. Antibiotics as deep modulators of gut microbiota: between good and evil. Gut 2016;65:1906–15.
[46] Jakobsson HE, Jernberg C, Andersson AF, Sjölund-Karlsson M, Jansson JK, Engstrand L. Short-term antibiotic treatment has differing long- term impacts on the human throat and gut microbiome. PLoS One 2010;5.
[47] Winter SE, Bäumler AJ. Dysbiosis in the inflamed intestine: chance favors the prepared microbe. Gut Microbes 2014;5:71–3.
[48] Zhou Yingting, Zhi Fachao. Lower level of Bacteroides in the gut microbiota is associated with inflammatory bowel disease: a meta-analysis. Biomed Res Int 2016;2016(5828959).
[49] Huttenhower C, Gevers D, Knight R, Al E. Structure, function and diversity of the healthy human microbiome. Nature 2012;486:207–14.
[50] Weldon L, Abolins S, Lenzi L, Bourne C, Riley EM, Viney M. The gut microbiota of wild mice. PLoS One 2015;10:e0134643.
[51] Kim SJ, Kim SE, Kim AR, Kang S, Park MY, Sung MK. Dietary fat intake and age modulate the composition of the gut microbiota and colonic inflammation in C57BL/6J mice. BMC Microbiol 2019;19.
[52] Sorini C, Cosorich I, Conte M, Lo, De Giorgi L, Facciotti F, Lucianò R, et al. Loss of gut barrier integrity triggers activation of islet-reactive T cells and autoimmune diabetes. Proc Natl Acad Sci U S A 2019;116:15140–9.
[53] Li HL, Lu L, Wang XS, Qin LY, Wang P, Qiu SP, et al. Alteration of gut microbiota and inflammatory cytokine/chemokine profiles in 5-fluorouracil induced intestinal mucositis. Front Cell Infect Microbiol 2017;7.
[54] Hotamisligil GS. Inflammation, metaflammation and immunometabolic disorders. Nature 2017;542:177–85.
[55] Caligiuri SPB, Love K, Winter T, Gauthier J, Taylor CG, Blydt-Hansen T, et al. Dietary linoleic acid and α-linolenic acid differentially affect renal oxylipins and phospholipid fatty acids in diet-induced obese rats. J Nutr 2013;143:1421–31.

[56] Ramsden CE, Ringel A, Feldstein AE, Taha AY, MacIntosh BA, Hibbeln JR, et al. Lowering dietary linoleic acid reduces bioactive oxidized linoleic acid metabolites in humans. Prostaglandins Leukot Essent Fatty Acids 2012;87:135–41.
[57] Caligiuri SPB, Parikh M, Stamenkovic A, Pierce GN, Aukema HM. Dietary modulation of oxylipins in cardiovascular disease and aging. Am J Physiol Heart Circ Physiol 2017;313:903–18.
[58] Néia VBMJC, Ambrosio-Albuquerque EP, Figueiredo IL, Boeing JS, Da Silva TC, Lewandowski V, et al. Impact of cafeteria diet on the composition of fatty acids in zebrafish (Danio rerio) fillets. J Braz Chem Soc 2018;29:1183–8.
[59] Deol P, Fahrmann J, Yang J, Evans JR, Rizo A, Grapov D, et al. Omega-6 and omega-3 oxylipins are implicated in soybean oil-induced obesity in mice. Sci Rep 2017;7:1–13.
[60] Fan HN, Zhu P, Lu YM, Guo JH, Zhang J, Qu GQ, et al. Mild changes in the mucosal microbiome during terminal ileum inflammation. Microb Pathog 2020;142:104104.
[61] Li K, Zhang L, Xue J, Yang X, Dong X, Sha L, et al. Dietary inulin alleviates diverse stages of type 2 diabetes mellitus: via anti-inflammation and modulating gut microbiota in db/db mice. Food Funct 2019;10:1915–27.
[62] Shin NR, Whon TW, Bae JW. Proteobacteria: microbial signature of dysbiosis in gut microbiota. Trends Biotechnol 2015;33:496–503.
[63] Fei N, Zhao L. An opportunistic pathogen isolated from the gut of an obese human causes obesity in germfree mice. ISME J 2013;7:880–4.
[64] Miller AW, Orr T, Dearing D, Monga M. Loss of function dysbiosis associated with antibiotics and high fat, high sugar diet. ISME J 2019;13:1379–90.
[65] Jeong MY, Jang HM, Kim DH. High-fat diet causes psychiatric disorders in mice by increasing Proteobacteria population. Neurosci Lett 2019;698:51–7.
[66] Lim SM, Kim DH. Bifidobacterium adolescentis IM38 ameliorates high-fat diet–induced colitis in mice by inhibiting NF-κB activation and lipopolysaccharide production by gut microbiota. Nutr Res 2017;41:86–96.
[67] He R, Chen Y, Cai Q. The role of the LTB4-BLT1 axis in health and disease. Pharmacol Res 2020;158:104857.
[68] Turnbaugh PJ, Ley RE, Mahowald MA, Magrini V, Mardis ER, Gordon JI. An obesity-associated gut microbiome with increased capacity for energy harvest. Nature 2006;444:1027–31.
[69] Martinez-Guryn K, Hubert N, Frazier K, Urlass S, Musch MW, Ojeda P, et al. Small intestine microbiota regulate host digestive and absorptive adaptive responses to dietary lipids. Cell Host Microbe 2018;23:458–69. e5.
[70] Druart C, Neyrinck AM, Vlaeminck B, Fievez V, Cani PD, Delzenne NM. Role of the lower and upper intestine in the production and absorption of gut microbiota-derived PUFA metabolites. PLoS One 2014;9:e87560.
[71] Dieckmann S, Maurer S, Fromme T, Colson C, Richard D. Fatty acid metabolite profiling reveals oxylipins as markers of brown but not brite adipose tissue. Front Endocrinol (Lausanne) 2020;11.
[72] Barengolts E, Green SJ, Chlipala GE, Layden BT, Eisenberg Y, Priyadarshini M, et al. Predictors of obesity among gut microbiota biomarkers in African American men with and without diabetes. Microorganisms 2019;7.

SUPPLEMENTARY MATERIAL

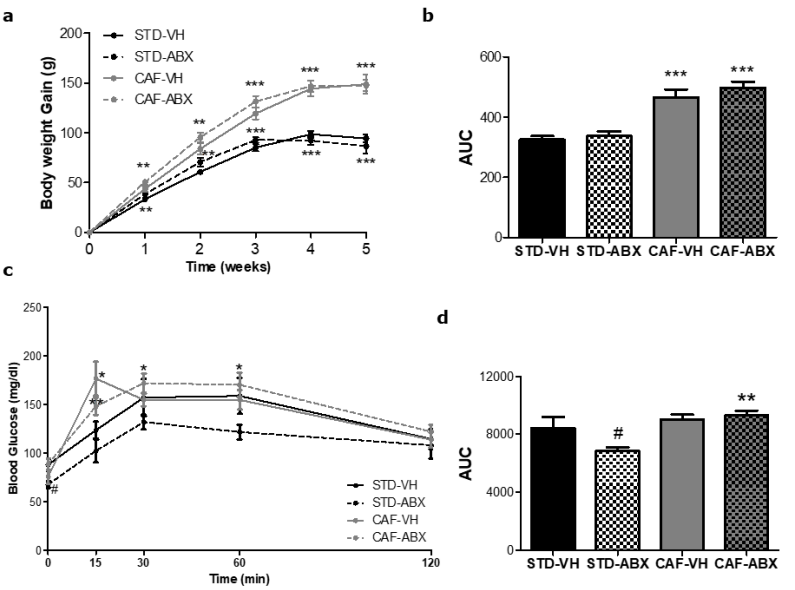

Figure S1. Cafeteria diet and antibiotic effects on body weight gain and oral glucose tolerance test (OGTT). (***a***) *Body weight gain progression of experimental groups;* (***b***) *Area under the curve (AUC) of body weight gain;* (***c***) *Blood glucose levels during the oral glucose tolerance test;* (***d***) *OGTT area under the curve; * and # indicates diet and ABX effect respectively. Data are plotted as the mean ± SEM (n=6 per group). a and c: ANOVA-repeated measures followed by LSD post hoc test; b and d: 2-way ANOVA followed by LSD post hoc test; ***p< 0.001, **p< 0.01, *p<0.05; #p<0.05.*

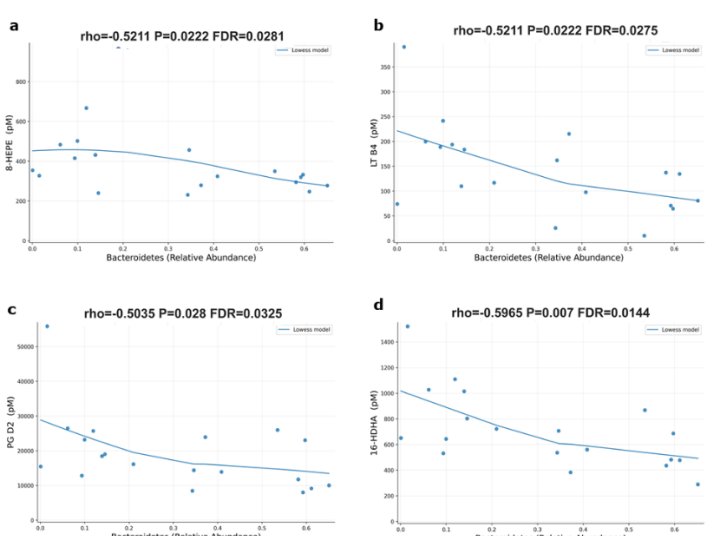

Figure S2. *Locally weighted linear regression (Lowess model) analysis between 8-HEPE (**a**), LT B4 (**b**), PG D2 (**c**) and 16-HDHA (**d**) and relative abundance of Bacteroidetes showing negative correlation.*

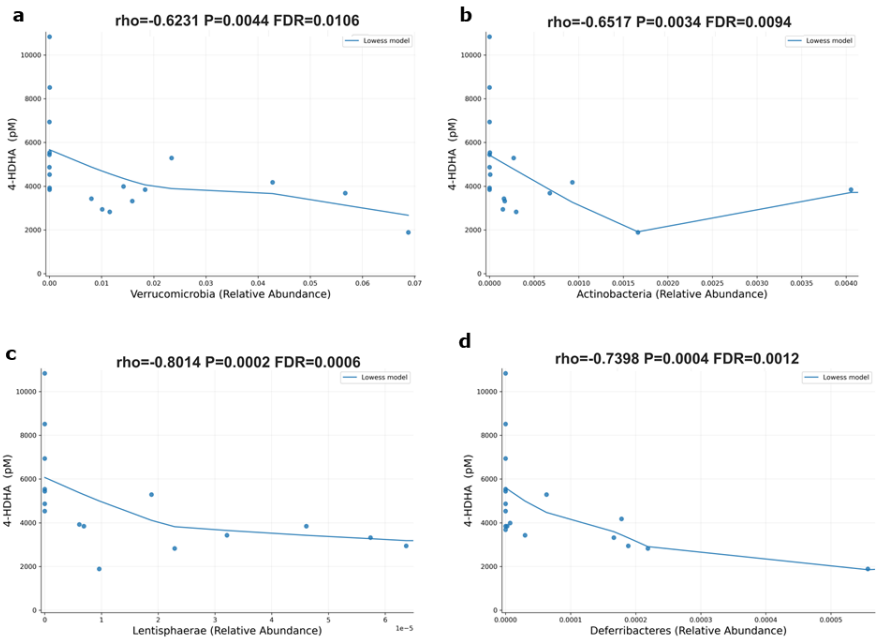

Figure S3. *Locally weighted linear regression (Lowess model) analysis between the relative abundance of Verrucomicrobia (**a**), Actinobacteria (**b**), Lentisphaerae (**c**), Cyanobacteria (**d**) and 4-HDHA levels showing negative correlation.*

Table S1. Significant Diet and ABX effects on microbial relative abundance at different taxonomic levels.

	STD-VH (n=5)	STD-ABX (n=6)	CAF-VH (n=4)	CAF-ABX (n=5)	
TAXA LEVEL	**MEDIAN (IQR)[1]**	**MEDIAN (IQR)[1]**	**MEDIAN (IQR)[1]**	**MEDIAN (IQR)[1]**	**P-VALUE[2]**
• **PHYLUM**					
Lentisphaerae	2.73E-05 (2.42E-05)	0 (1.72E-06)#	0.02 (0.05)*	6.09E-06 (2.79E-05)#	0.002
Proteobacteria	0.01 (9.68E-03)	0.04 (0.14)#	0.06 (0.08)*	0.38 (0.25)#	0.002
Cyanobacteria	1.69E-03 (4.28E-03)	8.40E-06 (1.99E-05)#	1.38E-03 (1.90E-03)	0 (1.26E-05)#	0.002
Bacteroidetes	4.89E-01 (0.19)	1.09E-01 (0.07)#	0.60 (0.23)	0.15 (0.47)#	0.011
Actinobacteria	1.65E-04 (1.30E-04)	0 (8.22E-07)#	8.01E-04 (0.01)	6.26E-06 (2.86E-03)	0.015
Verrucomicrobia	0.01 (0.01)	1.19E-05 (2.77E-05)#	0.03 (0.04)	3.05E-05 (0.04)	0.016
Spirochaetes	0 (0)	1.72E-06 (5.36E-06)	0 (0)	7.37E-06 (4.80E-04)#	0.025
Deferribacteres	1.15E-04 (4.65E-04)	0 (0)#	9.25E-05 (1.84E-04)	2.31E-06 (1.26E-03)	0.026
Tenericutes	1.15E-03 (2.17E-03)	2.86E-05 (0.12)	6.48E-05 (1.03E-03)*	0 (1.36E-04)	0.05
Firmicutes	0.48 (0.19)	3.75E-01 (0.09)	0.25 (0.36)	0.29 (0.53)	0.250
• **CLASS**					
4C0d-2	1.17E-03 (4.28E-03)	0 (0)#	1.37E-03 (1.89E-03)	0 (9.60E-06)#	0.001
Lentisphaeria	2.28E-05 (2.41E-05)	0 (1.72E-06)#	0.02 (0.05)	6.09E-06 (2.79E-05)#	0.002
Gammaproteobacteria	5.08E-04 (7.04E-03)	0.44 (0.01)#	8.53E-04 (1.20E-03)	0.34 (0.23)#	0.003
Erysipelotrichi	7.53E-05 (1.07E-04)	0 (3.31E-06)	1.01E-03 (1.55E-03)	0 (0)#	0.006
RF3	1.98E-04 (1.01E-03)	0 (0)#	1.62E-05(1.17E-04)	0 (0)	0.008
Bacteroidia	0.44 (0.02)	0.11(0.07)#	0.60 (0.24)	0.15 (0.45)#	0.011
Coriobacteriia	1.69E-04 (1.27E-04)	0 (8.23E-07)#	7.94E-04 (0.01)	6.26E-06 (2.86E-03)	0.015
Verrucomicrobiae	0.01 (0.01)	1.19E-05 (2.77E-05)#	0.03 (0.04)	3.05E-05 (0.04)	0.016
Actinobacteria	0 (2.54E-06)	0 (0)	7.86E-06 (2.88E-05)	0 (0)#	0.019
Leptospirae	0 (0)	1.72E-06 (5.37E-06)	0 (0)	7.37E-06 (4.80E-04)#	0.025
Deferribacteres	1.66E-04 (4.65E-04)	0 (0)#	9.25E-05 (0.01)	2.13E-06 (1.26E-03)	0.026
• **ORDER**					
YS2	1.17E-03 (4.28E-03)	0 (0)#	1.37E-03 (1.89E-03)	0 (9.59E-06)#	0.001
Turicibacterales	3.30E-04 (6.26E-04)	0 (0)#	5.304 (1.34E-04)	0 (0)	0.001
Aeromonadales	0 (1.23E-06)	8.72E-06 (1.47E-05)#	0 (0)	4.61E-06 (8.38E-06)#	0.001
Victivallales	2.29E-05 (2.41E-05)	0 (1.72E-06)#	0.02 (0.05)	6.09E-06 (2.79E-05)#	0.002

Pseudomonadales	0 (1.09E-05)	5.90E-05 (4.96E-05)#	0 (1.91E-06)	1.38E-05 (3.30E-05)	0.002
Enterobacteriales	5.08E-04 (7.03E-03)	0.44 (0.13)#	8.53E-04 (1.20E-03)	0.34 (0.23)#	0.003
Vibrionales	0 (1.23E-06)	1.07E-05 (1.82E-05)	0 (0)	2.21E-05 (8.19E-06)#	0.003
Rhodospirillales	0 (0)	8.65E-05 (1.71E-04)#	0 (1.70E-06)	1.25E-05 (1.37E-04)	0.004
Erysipelotrichales	7.53E-05 (1.07E-04)	0 (3.31E-06)	1.01E-03(1.55E-03)	0 (2.62E-04)#	0.006
ML615J-28	1.98E-04 (1.01E-03)	0 (0)#	1.62E-05 (1.17E-04)	0 (0)	0.008
Anaeroplasmatales	0 (0)	2.85E-05 (0.11)#	0 (1.91E-06)	0 (3.05E-06)	0.011
RF39	1.34E-04 (2.41E-03)	0 (0)#	4.86E-05 (9.07E-04)	0 (1.33E-04)	0.014
Verrucomicrobiales	0.01 (0.01)	1.18E-05 (2.77E-05)#	0.03 (0.04)	3.05E-05 (0.043)	0.016
Bifidobacteriales	0 (0)	0 (0)	7.85E-06 (2.88E-05)	0 (0)#	0.019
SHA-98	3.56E-05 (7.59E-05)	0 (0)#	5.59E-05 (1.29E-04)	0 (0)	0.021
Leptospirales	0 (0)	1.72E-06 (5.36E-06)	0 (0)	7.37E-06 (4.80E-04)#	0.025
Deferribacterales	1.66E-04 (4.65E-04)	0 (0)#	9.25E-05 (1.84E-04)	2.31E-06 (1.3E-03)	0.026
• **FAMILY**					
Leuconostocaceae	0 (0)	0 (0)	4.88E-04 (8.31E-04)*	2.86E-04 (1.50E-03)	0.001
Streptococcaceae	1.43E-05 (9.35E-06)	0 (0)	3.72E-05 (7.16E-05)	0 (0)#	0.001
Christensenellaceae	2.37E-04 (2.16E-04)	0 (0)#	7.46E-05 (3.00E-04)	0 (1.52E-06)#	0.001
Turicibacteraceae	3.30E-04 (6.26E-04)	0 (0)#	5.32E-05 (1.34E-04)	0 (0)	0.001
Dehalobacteriaceae	3.08E-04 (5.04E-04)	0 (1.33E-06)#	8.03E-06 (3.84E-04)	0 (0)#	0.001
Aeromonadaceae	0 (1.24E-06)	8.72E-06 (1.47E-05)#	0 (0)	4.61E-06 (8.38E-06)	0.001
Peptococcaceae	3.67E-03 (2.55E-03)	0 (4.47E-06)#	1.63E-03 (2.46E-03)	1.52E-05 (3.34E-03)	0.001
Victivallaceae	2.29E-05 (2.41E-05)	0 (1.72E-06)#	0.02 (0.05)	6.09E-06 (2.79E-05)#	0.002
Odoribacteraceae	1.56E-03 (3.35E-03)	0 (9.42E-07)#	1.28E-03 (6.40E-03)	0 (4.61E-06)#	0.002
Peptostreptococcaceae	3.61E-03 (3.89E-03)	0 (3.42E-06)#	1.53E-03 (3.19E-03)	6.26E-06 (1.58E-05)	0.002
Lachnospiraceae	0.06 (0.05)	1.03E-04 (7.75E-05)#	0.07 (0.03)	3.49E-04 (3.54E-04)#	0.002
Moraxellaceae	0 (1.09E-05)	5.90E-05 (4.96E-05)#	0 (1.91E-06)	1.38E-05 (3.30E-05)	0.002
Paraprevotellaceae	0.09 (0.07)	1.05E-05 (1.21E-05)#	0.04 (0.03)	9.70E-05 (0.09)	0.002
Ruminococcaceae	0.14 (0.94)	1.50E-04 (2.59E-04)#	0.07 (0.21)	1.85E-04 (4.99E-03)	0.002
S24-7	0.09 (0.11)	8.87E-05 (1.10E-04)#	0.11 (0.04)	1.22E-04 (3.32E-04)#	0.002
Enterobacteriaceae	5.08E-04 (7.03E-03)	0.44 (0.14)#	8.53E-04 (1.20E-03)	0.34 (0.23)#	0.003
Vibrionaceae	0 (1.24E-06)	1.07E-05 (1.83E-05)	0 (0)	2.21E-05 (8.19E-06)#	0.003
Planococcaceae	5.74E-06 (2.59E-05)	0 (0)#	1.36E-05 (3.08E-05)	0 (1.56E-06)#	0.003
Clostridiaceae	3.36E-03 (3.53E-03)	3.08E-05 (5.80E-05)#	2.05E-03 (4.17E-03)	1.56E-05 (1.51E-05)#	0.004
Acidaminobacteraceae	0 (0)	1.33E-05 (2.45E-05)#	0 (0)	9.60E-06 (3.40E-05)#	0.004

Rhodospirillaceae	0 (0)	8.65E-05 (1.71E-04)#	0 (1.70E-06)	1.25E-05 (1.37E-04)	0.004
Erysipelotrichaceae	7.54E-05 (1.07E-04)	0 (3.31E-06)	1.01E-03 (1.55E-03)	0 (2.62E-04)#	0.006
Barnesiellaceae	3.21E-03 (5.14E-03)	0 (8.60E-07)#	0.02 (0.02)	3.05E-06 (0.03)	0.009
Anaeroplasmataceae	0 (0)	2.85E-05 (0.12)#	0 (1.91E-06)	0 (3.05E-06)	0.011
Lactobacillaceae	2.64E-04 (4.64E-04)	2.34E-05 (1.51E-04)	0.03 (0.03)	1.52E-05 (3.34E-03)#	0.012
Verrucomicrobiaceae	0.01 (0.01)	1.19E-05 (2.77E-05)#	0.03 (0.04)	3.05E-05 (0.04)	0.016
Prevotellaceae	0.04 (9.71E-03)	1.78E-05 (1.61E-05)	3.30E-02 (4.98E-02)	4.65E-05 (0.15)#	0.018
Bifidobacteriaceae	0 (2.54E-06)	0 (0)#	7.86E-06 (2.88E-05)	0 (0)	0.019
Enterococcaceae	1.60E-05 (1.58E-05)	0 (2.84E-06)#	3.82E-06 (2.79E-05)	0 (3.37E-06)	0.023
Sediment-4	0 (0)	1.72E-06 (5.37E-06)	0 (0)	7.37E-06 (4.80E-04)#	0.025
Deferribacteraceae	1.66E-04 (4.65E-04)	0 (0)#	9.25E-05 (1.84E-04)	2.31E-06 (1.26E-03)	0.026
Mogibacteriaceae	2.08E-04 (1.16E-03)	1.44E-04 (1.73E-04)	2.82E-04 (1.03E-04)	7.73E-05 (1.38E-04)	0.033
Oxalobacteraceae	0 (0)	0 (2.60E-05)	0 (0)	1.83E-05 (3.02E-05)#	0.035
Eubacteriaceae	0 (2.51E-06)	0 (2.66E-06)	1.83E-05 (4.64E-05)	0 (0)#	0.046
• **GENUS**					
Leuconostoc	0 (0)	0 (0)	4.88E-04 (8.31E-04)*	2.86E-04 (1.50E-03)	0.001
Ruminococcus	5.26E-03 (3.05E-03)	0 (4.47E-06)#	8.42E-03 (4.55E-03)	2.19E-05 (5.78E-05)#	0.001
Streptococcus	1.43E-05 (9.35E-06)	0 (0)	3.72E-05 (7.16E-05)	0 (0)#	0.001
Adlercreutzia	9.64E-05 (5.96E-05)	0 (0)#	1.93E-04 (3.32E-04)	0 (3.13E-06)#	0.001
Roseburia	1.76E-03 (1.84E-03)	0 (0)#	3.69E-04 (9.72E-04)	3.68E-06 (1.08E-05)	0.001
Trabulsiella	0 (0)	3.78E-05 (1.45E-05)#	0 (0)	2.08E-05 (4.14E-05)	0.001
Turicibacter	3.30E-04 (6.26E-04)	0 (0)#	5.32E-05 (1.34E-04)	0 (0)	0.001
Moryella	3.75E-04 (5.48E-04)	0 (0)#	8.19E-05 (7.10E-04)	2.31E-06 (3.12E-06)	0.001
Acinetobacter	0 (0)	4.00E-05 (4.77E-05)#	0 (0)	1.38E-05 (3.30E-05)	0.001
Anaerotruncus	6.28E-06 (1.06E-04)	0 (0)	1.47E-04 (1.96E-04)	0 (0)#	0.001
Erwinia	0 (1.24E-06)	2.89E-03 (6.16E-03)#	6.21E-05 (2.10E-04)	3.11E-03 (2.62E-03)	0.001
Dorea	2.21E-04 (7.15E-04)	0 (9.42E-07)#	7.20E-04 (1.35E-03)	2.31E-06 (7.94E-06)#	0.001
Blautia	3.41E-04 (6.46E-04)	1.31E-05 (2.72E-05)	2.01E-02 (5.69E-03)	3.05E-06 (1.99E-05)#	0.001
Salmonella	0 (0)	1.05E-04 (5.14E-05)#	0 (0)	1.15E-04 (3.93E-05)#	0.001
SMB53	2.77E-03 (2.98E-03)	0 (1.33E-06)#	1.60E-03 (3.51E-03)	9.14E-06 (1.24E-05)	0.002
Klebsiella	0 (2.51E-05)	0.02 (8.72E-03)#	6.31E-06 (1.51E-05)	8.13E-03 (0.02)	0.002
rc4_4	3.58E-03 (2.47E-03)	0 (3.41E-06)#	1.63E-03 (2.43E-03)	7.37E-06 (1.43E-05)	0.002
Odoribacter	1.56E-03 (3.35E-03)	0 (9.24E-07)#	1.28E-03 (6.40E-03)	0 (4.61E-06)	0.002
Prevotella	0.09 (0.07)	8.75E-06 (1.11E-05)#	0.04 (0.02)	9.70E-05 (0.09)	0.002

Morganella	0 (1.24E-06)	1.35E-04 (8.16E-05)#	1.27E-06 (3.16E-06)	1.27E-04 (1.08E-04)	0.002
Oribacterium	7.63E-05 (1.85E-04)	0 (0)#	2.31E-06 (1.45E-05)	0 (0)	0.002
Escherichia	0 (1.24E-06)	8.06E-05 (1.82E-04)#	0 (1.91E-06)	5.79E-05 (6.39E-05)#	0.002
Serratia	0 (2.81E-06)	2.57E-04 (2.80E-04)#	2.31E-06 (7.95E-06)	4.06E-04 (8.50E-03)#	0.002
Enterobacter	0 (2.13E-05)	7.66E-03 (4.74E-03)#	2.84E-06 (5.36E-06)	3.41E-03 (6.37E-03)	0.002
Oscillospira	0.07 (0.06)	8.74E-05 (2.59E-04)#	0.03 (0.15)	6.63E-05 (1.13E-04)#	0.002
Coprococcus	7.51E-03 (4.36E-03)	3.57E-06 (1.69E-05)#	0.02 (0.02)	1.83E-05 (2.93E-04)#	0.002
Anaerostipes	2.64E-04 (3.28E-04)	0 (0)#	4.00E-06 (6.26E-06)	0 (0)#	0.002
Pediococcus	0 (0)	0 (0)	8.07E-06 (1.49E-05)*	0 (0)#	0.004
Anaerofustis	0 (0)	0 (0)	9.16E-06 (7.61E-06)*	0 (0)#	0.004
Novispirillum	0 (0)	8.65E-05 (1.71E-04)#	0 (1.70E-06)	1.25E-05 (1.37E-04)	0.004
Pantoea	0 (1.24E-06)	5.47E-06 (1.36E-05)	0 (0)	1.60E-05 (4.29E-05)#	0.005
Desulfovibrio	6.08E-05 (3.69E-03)	1.88E-06 (9.05E-06)	6.38E-03 (2.91E-03)	0 (9.30E-06)#	0.006
Dysgonomonas	2.54E-06 (3.34E-06)	0 (0)#	1.22E-05 (1.72E-05)	0 (0)#	0.007
Vibrio	0 (1.24E-06)	1.07E-05 (1.69E-05)	0 (0)	1.60E-05 (5.92E-06)#	0.008
Proteus	2.20E-05 (5.10E-05)	1.83E-03 (2.44E-03)#	5.95E-05 (5.29E-05)	2.47E-04 (5.17E-04)	0.008
Paraprevotella	2.03E-04 (2.67E-04)	0 (3.52E-06)	2.15E-03 (6.78E-03)	0 (0.01)#	0.009
Phascolarctobacterium	3.14E-06 (3.25E-03)	1.58E-05 (0.01)	0.03 (0.03)*	0.02 (0.03)	0.010
Anaeroplasma	0 (0)	2.85E-05 (0.12)#	0 (1.91E-06)	0 (3.05E-06)	0.011
Lactobacillus	2.64E-04 (4.64E-04)	3.24E-05 (1.51E-04)	0.03 (0.03)	1.52E-05 (3.34E-03)#	0.012
Dehalobacterium	3.00E-04 (4.89E-04)	0 (1.33E-06)#	5.71E-06 (1.80E-04)	0 (1.33E-06)	0.014
Victivallis	0 (0)	0 (8.60E-07)	2.14E-05 (5.71E-05)*	0 (8.60E-07)#	0.015
Parabacteroides	0.01 (0.01)	3.15E-05 (3.94E-05)	0.07 (0.05)	1.52E-05 (0.06)#	0.015
Akkermansia	0.01 (0.01)	1.19E-05 (2.77E-05)#	0.03 (0.04)	3.05E-05 (0.04)	0.016
Epulopiscium	0 (1.60E-06)	3.65E-05 (7.76E-05)#	0 (0)	3.23E-05 (1.60E-04)#	0.016
Solitalea	1.27E-03 (9.05E-04)	1.06E-04 (1.26E-04)	4.52E-04 (1.06E-03)	3.13E-06 (6.01E-05)#	0.017
Eubacterium	0 (1.60E-06)	0 (3.31E-06)	8.88E-04 (1.60E-03)*	0 (2.60E-04)#	0.017
Bifidobacterium	0 (2.54E-06)	0 (0)	7.86E-06 (2.88E-05)	0 (0)#	0.019
Dickeya	0 (0)	4.34E-06 (8.34E-06)#	0 (0)	0 (9.46E-06)	0.023
Enterococcus	1.60E-05 (1.58E-05)	0 (2.84E-06)#	3.82E-06 (2.79E-05)	0 (3.37E-06)	0.023
Mucispirillum	1.66E-04 (4.65E-04)	0 (0)#	9.25E-05 (1.84E-04)	2.31E-06 (1.26E-03)	0.026
Collinsella	0 (0)	0 (0)	4.72E-05 (1.51E-04)*	0 (2.22E-03)	0.045

*Data are plotted as Median (IQR, Interquartile Range)[1]. P-value by Kruskal-Wallis test[2] (p<0.05); * and # indicate CAF feeding and ABX effects respectively, by Kruskal-Wallis test followed by Bonferroni P values adjustment to compare in pairs (p<0.0125).*

Manuscript 6

Objective: To investigate the effects of seasonal rhythms on OXLs metabolites in healthy and CAF-diet induced obese F344 rats, and the impact of PAs and gut microbiota

Photoperiod conditions modulate serum oxylipins levels in healthy and obese rats: impact of proanthocyanidins and gut microbiota

Arreaza-Gil V[1], Ávila-Román J[1,2], Escobar-Martínez I[1], Muguerza B[1], Suarez M[1], Arola-Arnal A[1]*, Torres-Fuentes C[1].

[1]Universitat Rovira i Virgili, Departament de Bioquímica i Biotecnologia, Nutrigenomics Research Group, 43007 Tarragona, Spain.

[2]Present address: Universidad de Sevilla, Department of Pharmacology, Faculty of Pharmacy, Molecular and Apply Pharmacology group (FARMOLAP), 41012 Sevilla, Spain.

*Corresponding author

Summited to *Journal of Photochemistry & Photobiology, B: Biology.*

ABSTRACT

Seasonal rhythms are emerging as a key factor influencing gut microbiota and bioactive compounds functionality as well as several physiological processes such as inflammation. In this regard, their impact on the modulation of oxylipins (OXLs), which are lipid mediators of inflammatory processes, has not been investigated yet. Hence, we aimed to investigate the effects of seasonal rhythms on OXLs metabolites in healthy and obesogenic conditions. Moreover, we evaluated the impact of proanthocyanidins and gut microbiota, as these have been shown to modulate OXLs metabolism and inflammation and to be affected by seasonal rhythms. To this purpose, Fischer 344 rats were housed under three different photoperiod conditions (L6: 6 h of light, L12: 12 h of light or L18:18 h of light) and fed a cafeteria diet (CAF) for 9 weeks. During the last 4 weeks, rats were daily administered with an antibiotic cocktail (ABX), an oral dose of a grape seed proanthocyanidin extract (GSPE) (25 mg/kg-bw) or with their combination. Vehicle and standard chow diet-fed rats were included as controls. CAF feeding and ABX treatment affected OXLs differently depending on the photoperiod condition. Although GSPE did not show any effect on the overall OXLs profile, it significantly altered prostaglandin E2 levels, an important anti-inflammatory OXL, only under L6 and mitigated ABX-mediated effects only under L18. In conclusion, seasonal rhythms affect OXLs levels, and their effects were influenced by gut microbiota. This is the first time that the effects of seasonal rhythms on OXLs metabolites have been demonstrated.

***Keywords**:* biological rhythms, cafeteria diet, GSPE, obesity, resolvins.

RESULTS

1. Introduction

Biological rhythms have been shown to affect several metabolic and physiologic processes [1,2]. Thus, many of these processes follow circadian oscillations whose disruption has been linked to an increased risk of suffering obesity and other related pathologies [3]. Indeed, it has been demonstrated that seasonal rhythms can influence the risk of obesity development [4]. In this context, it was reported that obese children gained more weight in summer compared to winter [5]. Furthermore, studies carried out in animals exposed to different photoperiods, which mimics the differences in day length associated to seasonal rhythms, displayed higher body weight (BW) gain and white adipose tissue accumulation under longer photoperiod conditions (summer) [4,6]. Seasonal rhythms have also been shown to modulate different immune system responses. Thus, photoperiod-mediated changes in immune response were observed in hamsters and associated with changes in thyroid hormone levels [7]. Moreover, healthy individuals showed seasonal different responses in circulatory cytokines levels after endotoxin (lipopolysaccharides, LPS) administration, being anti-inflammatory cytokine production lower in summer compared to winter [8]. In addition to cytokines, there are also other important mediators of inflammatory processes such as oxylipins (OXLs), but their interaction with seasonal rhythms has not been investigated yet.

OXLs are potent bioactive lipid metabolites that are involved in the activation and resolution of the inflammatory response [9]. These metabolites are produced as a result of the oxygenation of dietary polyunsaturated fatty acids (PUFAs) by cyclooxygenase (COX), lipoxygenase (LOX) and cythochrome P450 (CYP) enzymes [10]. Most oxylipins are generated in the initial phase of inflammation from arachidonic acid (ARA, 20:4n-6) [11]. ARA-derived OXLs can be both proinflammatory, such as prostaglandins, leukotrienes and thromboxanes, or anti-inflammatory, such as lipoxins [12]. Moreover, OXLs can also be synthetized from both dietary eicosapentanoic acid (EPA, 20:5 n-3) and

docosahexaenoic acid (DHA, 22:6 n-3), generating mostly anti-inflammatory oxylipins such as resolvins, protectins and maresins [13,14]. In addition, OXLs can be produced by other fatty acids such as from linoleic acid (LA), constituting more than one-half of oxylipins present in tissues [11]. Thus, LA can be converted to di-homo-GLA (DGLA, 20:3, n-6), which can be transformed to arachidonic acid. Hence, OXLs play a key role in the maintenance of inflammatory homeostasis, being of significant relevance in several disorders associated to chronic inflammation such as obesity [15]. In fact, altered OXLs profile has been linked to obesity in both animals and human subjects, suggesting that these metabolites can be used as obesity biomarkers and as a target for the prevention of this disorder [16–18]. This is important as obesity and obesity-related disorders prevalence continues increasing worldwide affecting more than two billion of people, and being a major predisposing factor to several comorbidities such as Type 2 diabetes, hypertension, nonalcoholic fatty liver disease, cardiovascular diseases, and several types of cancer [19–21]. Therefore, OXLs are emerging as potential biomarkers for these diseases and understanding the factors affecting their metabolism is of increasing interest in the last years.

Regarding factors affecting OXLs, gut microbiota has been demonstrated to influence these metabolites via metabolism of PUFAs which, as mentioned above, are OXLs precursors [22]. In fact, a clear association between these bacteria and plasma OXLs profile has been recently reported [18,22]. Moreover, bioactive compounds such as polyphenols have shown to affect oxylipins biosynthesis in human neutrophils [23]. In addition, dietary supplementation with polyphenol rich juice led to changes in urine oxylipins profile in elite triathletes [24], and blueberry consumption mitigated oxylipins generation during the recovery phase after physical exercise in humans [25]. Interestingly, biological rhythms have been shown to affect both gut microbiota [26] and polyphenols bioactivities [27,28].

Taking all together, this study aimed to investigate the influence of different photoperiods, which mimic seasonal rhythms, on OXLs serum profile in healthy and obese rats, and to evaluate their impact in the effects of gut microbiota and proanthocyanidins consumption on these lipid inflammatory mediators. In particular, we evaluated their effects on prostaglandins 6-keto PGF1α and PGE2, resolvin RvD2, lipoxin 15-epi LXA4, and the leukotriene LTB4. 6-keto PGF1α is a marker of prostacyclin (PGI2) biosynthesis, which has been described as anti-inflammatory or immunosuppressive [29], while PGE2 has been described as proinflammatory [30]. RvD2 is involved in the resolution of inflammatory processes and has been demonstrated to prevent different inflammatory conditions, including allergic reactions, chronic low-grade inflammation of adipose tissue and atherosclerosis [31]. 15-epi LXA4 has also been reported to exert anti-inflammatory effects in different tissues [32,33]. LTB4 is a potent proinflammatory lipid mediator that has also been shown to promote insulin resistance in obese mice [34]. Finally, we investigated the effects on linoleic acid, which can also act as OXLs precursor as well as on oleic acid, a non-essential monosaturated fatty acid that has been shown to impact PUFAs content in peripheral tissues such as liver and adipose tissue, influencing the levels of bioactive oxylipins [35].

2. Material and methods

2.1. *Experimental* design

13 weeks-old male Fischer 344 rats (Javier Laboratories, France) were pair-housed at standard conditions (22ºC, 65% relative humidity and 12:12 hour light/dark cycle) with ad libitum access to water and standard chow diet for one week. After this acclimation period, rats were weighted and randomized distributed into three different light-dark cycles (photoperiods) for 9 weeks to mimic seasonal day lengths: short photoperiod [L6, 6 h light/18 h darkness], standard photoperiod [L12, 12 h light/12 h darkness], or long photoperiod [L18, 18 h light/6 h darkness]. Rats were fed with standard chow diet (STD) (72%

carbohydrate, 8% lipid, and 19% protein; Safe-A04c, Germany) or with cafeteria diet (CAF) composed of highly palatable and energy-dense human foods (58% CH, 31% lipid, and 11% protein) for 9 weeks. CAF diet was freshly prepared every day and included the following (grams per rat and per day): biscuits with pâté and cheese (15-17 g), bacon (7-10 g), ensaimada (pastry) (10-15 g), carrot (11-12 g), standard chow (20-25 g) and milk containing 22% sucrose (w/v).

During the last 4 weeks (weeks 6-9), rats were further randomly assigned to five groups (n=8) depending on the experimental treatment (Figure 1): 1) rats fed a standard diet and receiving vehicle (VH, condensed milk diluted with water in 1:5 proportion), 2) rats fed a cafeteria diet and receiving VH, 3) rats fed a cafeteria diet and administered a daily oral dose of a grape seed proanthocyanin extract (GSPE) (25mg/kg BW dissolved in VH), 4) rats fed a cafeteria diet and receiving an antibiotic cocktail (ABX) in drinking water, and 5) rats fed a cafeteria diet and receiving both a daily oral dose of GSPE and ABX in drinking water. The antibiotic cocktail (0.5 g/l ampicillin, 0.250 g/l vancomycin and 0.125 g/l imipenem; Discovery fine chemicals, UK) was freshly prepared every day and the animals were given free access to it. VH and GSPE dose was administered one hour after the light was turned on by allowing rats to drink it from the tip of a syringe. The 25mg/kg GSPE dose can be translated from animals to human, corresponding to an intake of approximately 370 mg of GSPE per day for a 70 kg human [36,37].

BW was recorded weekly. Animals were sacrificed by decapitation following last treatment dose and 3 hours of fasting. The blood was collected from the neck, in non-heparinized tubes, incubated for 1 h at room temperature and immediately centrifuged at 1200 g for 15 min to collect the serum. The Animal Ethics Committee of the University Rovira i Virgili (Tarragona, Spain) and the Generalitat de Catalunya approved all the procedures (number reference 9495) and in accordance with the EU Directive 2010/63/EU for animal experiments.

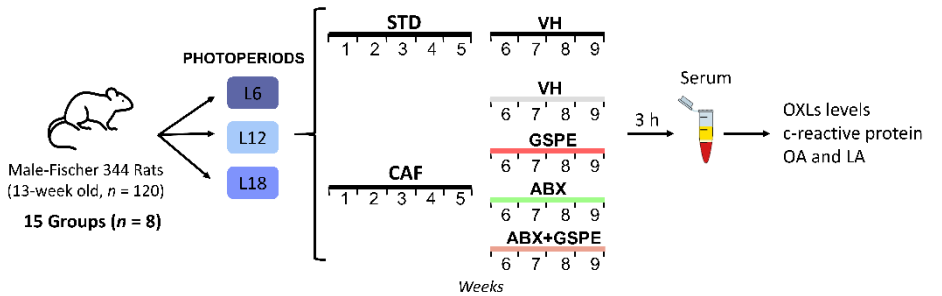

Figure 1. Experimental design. *13-week-old male Fischer 344 rats were pair-housed under three different photoperiods (6, 12 or 18 h of light per day) and fed with STD or CAF for 9 weeks. During the last 4 weeks, animals were daily administered with either an oral dose of GSPE (grape seed proanthocyanidin extract) (25mg/kg) dissolved in a solution of water and condensed milk (5:1, VH), or a combination of GSPE and an antibiotic cocktail (ABX) in drinking water (ampicillin: 0.5g/l, vancomycin: 0.25 g/l, imipenem: 0.125 g/l). Vehicle and ABX-treated animals were included as controls. L6: 6h light/18h darkness; L12: 12h light/12h darkness; L18: 18h light/6h darkness; STD: standard chow diet; CAF: cafeteria diet; VH: vehicle; OXLs: oxylipins; OA: oleic acid; LA: linoleic acid.*

2.2. Grape seed proanthocyanidins extract

GSPE was provided by Les Dérives Résiniques et Terpéniques (Dax, France). According to the manufacturer this phenolic-rich extract is mainly composed by monomers of flavan-3-ols (15.98%), dimers (13.05%), trimers (12.22%), tetramers (9.97%) and oligomers (5–13 units; 23.77%) of proanthocyanindin [36].

2.3. C-reactive protein analysis

C-reactive protein levels were analyzed in serum samples using a rat C-reactive ELISA kit (Elabscience, United States), according to the manufacturers' instructions.

2.4. Oxylipins serum analysis

6-keto Prostaglandin F1α (6-keto PGF1α), 15-epi Lipoxin A4 (15-epi LXA4), Leukotriene B4 (LTB4), Prostaglandin E2 (PGE2) and Resolvin D2 (RvD2) were analyzed in serum samples using Cayman Chemical's AchE kits (Ann Arbor, MI, USA) according to the manufacturers' instructions.

2.5. Fatty acids serum analysis

Linoleic acid (LA; 18:2n-6) and Oleic acid (OA; 18:1n-9) were analyzed from 100 µl of serum samples by gas chromatography-quadrupole time-of-flight (CG-qTOF). Serum sample were deproteiniezed by the addition of 400 µl of methanol:water (8:2) containing internal standard mixture. The samples were vortexed and incubated at 4ºC for 10 min. Then it was centrifuged at 4ºC for 10 min at 15,000 rpm and supernatant was evapored to dryness before compound derivatization (methoximation and silylation). The derivatized compounds were analyzed by GC-qTOF (model 7200 of Agilent, USA). The chromatographic separation was based on Fiehn Method, using a J&W Scientific HP5-MS (30 m x 0.25 mm i.d., 0.25 µm film capillary column) and helium as carrier gas using an oven program from 60 to 325ºC. Ionization was done by electronic impact, with electron energy of 70 eV and operating in full Scan mode.

Identification of LA and OA were performed using commercial standards and by matching their Electronic Impact mass spectrum and retention time to metabolomic Fiehn library (from Agilent). After putative identification of these fatty acids, LA and OA were semi-quantified in terms of internal standard response ratio.

2.6. Statistical analysis

Data are shown as mean ± SEM and were plotted using Graphpad Prism 8.0 software (Graphapad software Inc, San Diego, CA, USA). Statistical analyses were carried out using SPSS software (IBS SPSS statistics 25, Chicago, IL, USA). Normality and homogeneity of variance were evaluated by Shapiro-Wilk and Levene's test respectively. BW gain, serum parameters and oxylipins were analyzed using two-way analysis of variance (ANOVA) to evaluate diet and photoperiod effect (Photoperiod x Diet) followed by LSD post hot test and using three-way ANOVA to evaluate ABX, GSPE and Photoperiod effect followed by LSD post hot test. Statistical significances are subsequently depicted as follows:

*indicating diet effect $p < 0.05$, #indicating ABX effect $p < 0.05$, $indicating GSPE effect $p < 0.05$ and *ab* letters indicating photoperiod effect $p < 0.05$.

Principal component analysis (PCA) involving serum OXLs levels data were analyzed and plotted using MetaboAnalyst v.5.0 [37]. Missing values were replaced by the half of the minimum positive values in the data, assuming that most missing values are caused by low abundance metabolites.

Pearson's rank-order correlation analysis between oxylipins levels and OA and LA were carry out using Python script as previously described [18]. The script was developed using PyCharm software (v.2018.2.4, JetBrains s.r.o., Prague, Czech Republic) and Python version 3.7.7.

3. Results

3.1. CAF feeding affected OXLs levels differently depending on the photoperiod condition.

CAF feeding led to significant higher BW gain and increased levels of inflammation as measured by C-reactive protein serum levels compared to STD-fed rats, indicating successful development of obesity and related inflammatory status with this experimental model independently of the photoperiod condition. Moreover, photoperiod effects were observed for body weight gain in CAF-fed rats, being highest under L18 conditions, while no photoperiod effects were observed in STD-fed rats (**Figure S1**).

Interestingly, changes in OXLs levels between STD- and CAF-fed rats were different depending on the photoperiod conditions (**Figure 2**). Thus, resolving D2 was significant increased in CAF-fed rats under L6 while it was decreased under L12, and no changes were observed under L18 compared to STD-fed rats (**Figure 2a**). Although it was not significant, PGE2 was decreased in CAF-fed rats only when housed under L6 conditions (**Figure 2b**). Furthermore, LTB4 was increased in CAF-fed rats compared to STD-fed rats only under L12 conditions while no changes were observed under L6 or L18 (**Figure 2c**). Moreover, 6-keto-

PG1Fα was increased in CAF-fed rats under L18 while no changes were observed in L6 or L12 conditions (**Figure 2d**). Finally, 15-Epi-LXA4 was decreased in CAF-fed rats under L18 conditions while no changes were observed in L6 or L12 (**Figure 2e**).

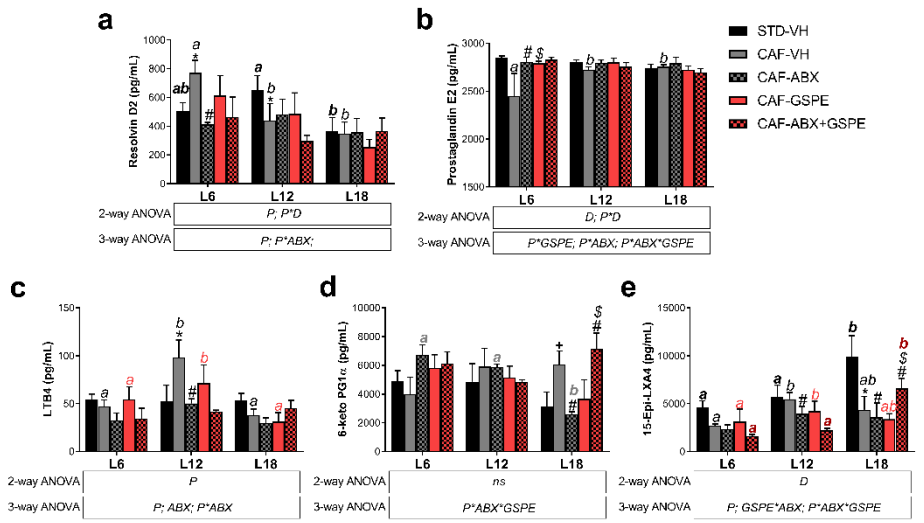

Figure 2. Diet, GSPE and Photoperiod effect on OXLs levels. *(a) 6-keto Prostaglandin F1α, (b) Leukotriene B4, (c) Prostaglandin E2, and (d) 15-Epi Lipoxin A4 levels; (e) Resolvin D2 levels. * indicates significant diet effect between STD-VH and CAF-VH rats by 2-way ANOVA (factors: diet (D) and photoperiod (P)) followed by LSD post hoc test (p<0.01); #, $ and ab indicate significant ABX, GSPE and Photoperiod effect respectively analyzed by 3-way ANOVA followed by LSD post hoc test (p<0.05); + indicates significant differences between STD- and CAF-fed rats analyzed by student's T-test. Data are plotted as the mean ± SEM (n=5). L6: 6h light/18h darkness; L12: 12h light/12h darkness; L18: 18h light/6h darkness; STD: standard diet; CAF: cafeteria diet; VH: vehicle; GSPE: grape seed proanthocyanidin extract; ABX: antibiotic cocktail.*

In addition, the impact of CAF feeding on OXLs levels of rats housed under the different photoperiod conditions was also analyzed using principal component analysis (PCA). PCA showed a higher effect of CAF feeding under long photoperiod conditions (PC1=89.3%) compared to both short (PCA1=67.8%) or standard (PCA1=65.1%) photoperiod conditions (**Figure 3a-c**). Furthermore, OXLs serum levels clustered differently in STD-fed rats housed under L18 conditions compared to STD-fed rats housed under both L6 and L12 conditions (**Figure 3d**). However, this photoperiod effect was different in CAF-fed rats, which showed a higher separation under L6 (**Figure 3e**).

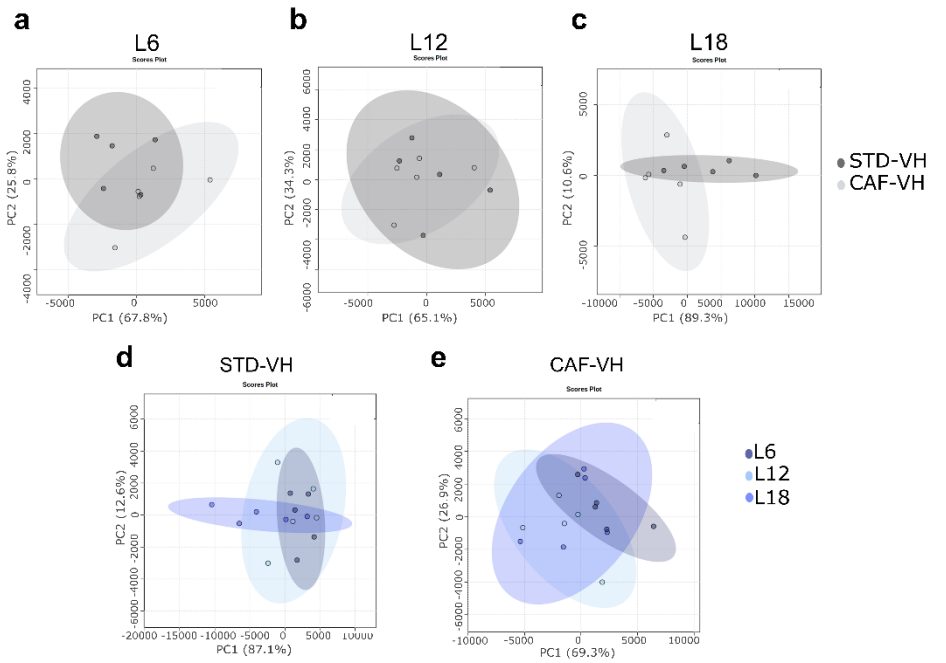

Figure 3. CAF feeding effect on oxylipins profile was different according to the photoperiod exposure. *(**a** to **c**): Diet effect in (a): L6; (b): L12; and (c): L18 conditions throughout Principal Component Analysis (PCA). (**d** to **e**): Photoperiod effect on (d): STD-VH rats; and (e): CAF-VH rats plotted as PCA. (n=5). L6: 6h light/18h darkness; L12: 12h light/12h darkness; L18: 18h light/6h darkness; STD: standard diet; CAF: cafeteria diet; VH: vehicle.*

3.2. Photoperiod effects on OXLs serum levels in CAF-fed rats is influenced by gut microbiota.

ABX treatment did not affect BW gain or C-reactive protein serum levels (**Figure S1**). Interestingly, ABX treatment altered OXLs serum levels differently depending on the photoperiod conditions. Thus, ABX significantly decreased RvD2 and increased PGE2 in rats housed under L6 conditions. Furthermore, in rats housed under L12 conditions, ABX significantly decreased LTB4 and 15-Epi-LXA4 levels. Finally, ABX-treated rats housed under L18 conditions showed a significant decrease in 6-keto PG1Fα and in 15-Epi-LXA4 levels (**Figure 2**). Thus, except by the increase of PGE2 levels by ABX, an overall decreased levels of OXLs were found by ABX depending on photoperiod conditions, being these

levels similar to those observed in STD-fed rats, except in 15-Epi-LXA4 under L18 conditions (**Figure 2a-e**).

In addition, PCA showed a separation between OXLs serum levels of CAF-fed rats and CAF-ABX-treated rats in each photoperiod conditions. ABX-treated rats also showed a different profile compared to STD-fed rats. It is worth highlighting that the ABX effect was higher under L18 condition compared to both L6 and L12 conditions suggesting a stronger effect of long photoperiod (**Figure 4a-c**). Furthermore, when comparing photoperiod effects in CAF-ABX-treated rats, OXLs serum levels were more different in rats housed under L18 conditions compared to those housed under both L6 and L12 (**Figure 4d**).

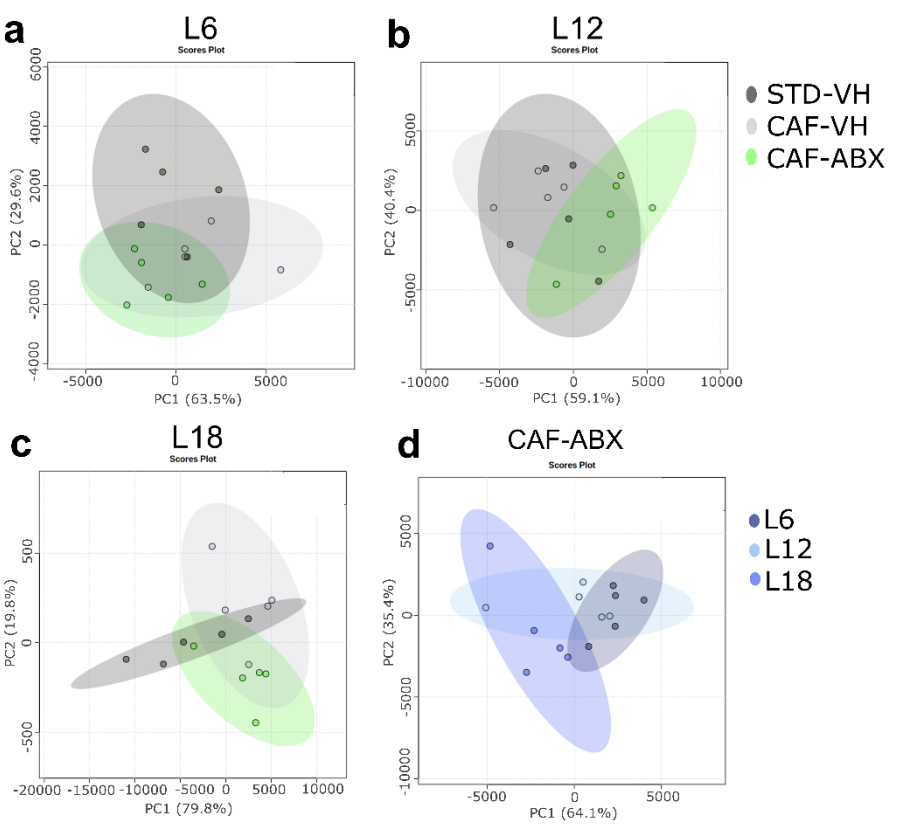

Figure 4. ABX effect on oxylipins profile was different depending on the photoperiod conditions. *(**a** to **c**): ABX effect in (a): L6; (b): L12; and (c): L18 conditions throughout Principal Component Analysis (PCA); (**d**): Photoperiod effect on CAF-ABX-treated rats. (n=5). L6: 6h light/18h darkness; L12: 12h light/12h darkness; L18: 18h light/6h darkness; STD: standard diet; CAF: cafeteria diet; VH: vehicle; ABX: antibiotic cocktail.*

3.3. GSPE significantly altered prostaglandin E2 serum levels in CAF-fed rats in a photoperiod dependent manner.

GSPE decreased BW gain only under L18 condition. However, C-protein serum levels was not affected by GSPE administration (**Figure S1**). Regarding OXLs, GSPE only showed effect on PGE2 serum levels in CAF-fed rats under L6 conditions (**Figure 2**). PCA did not show any GSPE effect on the OXLs levels of CAF-fed rats in any photoperiod condition (**Figure 5a-c**). Furthermore, when comparing GSPE-treated CAF-fed rats under different photoperiod conditions, any specific cluster was observed (**Figure 5d**).

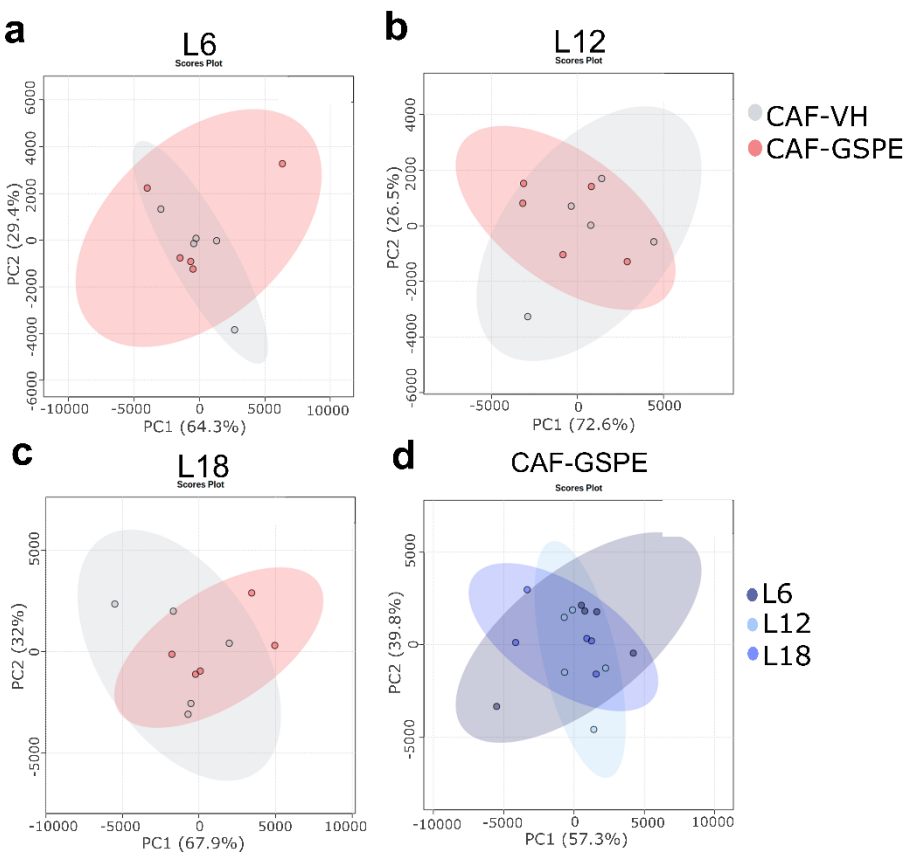

Figure 5. GSPE did not affect oxylipins profile under any photoperiod condition. *(**a** to **c**): GSPE effect in (a): L6; (b): L12; and (c): L18 conditions throughout Principal Component Analysis (PCA); (**d**): Photoperiod effect on GSPE-treated rats. (n=5). L6: 6h light/18h darkness; L12: 12h light/12h darkness; L18: 18h light/6h darkness; CAF: cafeteria diet; VH: vehicle; GSPE: grape seed proanthocyanidin extract.*

3.4. GSPE mitigated ABX-mediated changes in serum OXLs levels in CAF-fed rats in a photoperiod dependent manner.

Although GSPE did not affect C-reactive serum protein levels in CAF-fed rats treated with ABX (Figure S1), it significantly increased 15-Epi LXA4 and 6-keto PG1α levels under L18 conditions, mitigating ABX-mediated changes observed for this OXLs metabolites. Furthermore, an interaction effect of photoperiod, ABX and GSPE on these OXLs levels was observed (ANOVA: Ph*ABX*GSPE, $p<0.05$). However, the combination of ABX+GSPE in CAF-fed rats did not show any effect on OXL levels under either L6 or L12 conditions (**Figure 2**).

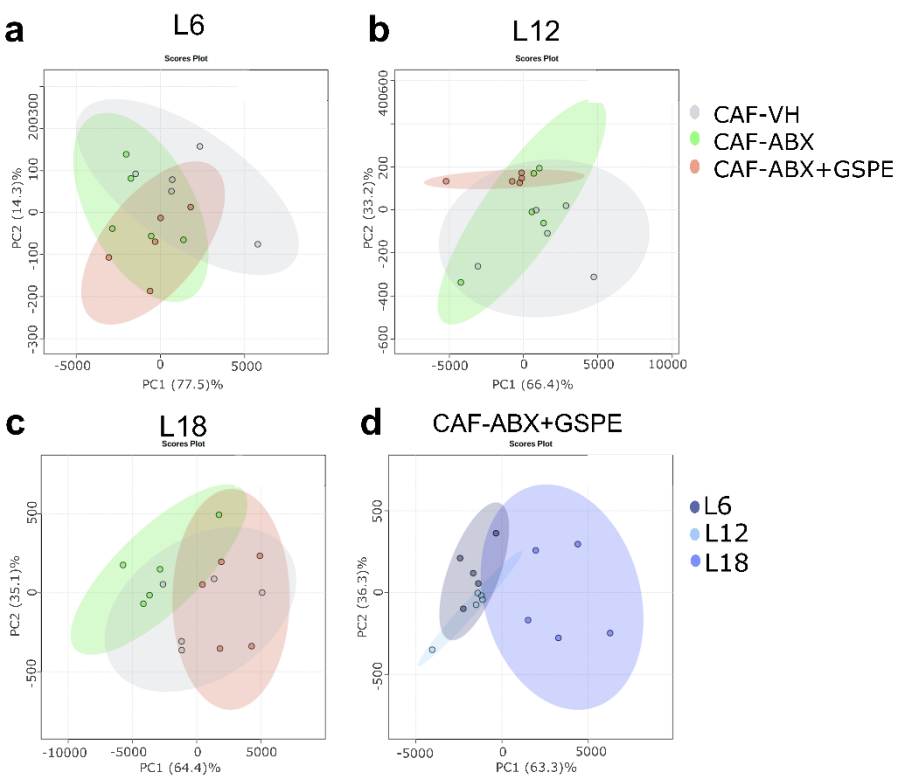

Figure 6. GSPE mitigated ABX-mediated effect on OXLs profile only under L18 conditions. *(**a** to **c**): ABX+GSPE effect in CAF-fed rats in (a): L6; (b): L12; and (c): L18 conditions throughout Principal Component Analysis (PCA); (**d**): Photoperiod effect on CAF-ABX+GSPE rats. (n=5). L6: 6h light/18h darkness; L12: 12h light/12h darkness; L18: 18h light/6h darkness; CAF: cafeteria diet; VH: vehicle; GSPE: grape seed proanthocyanidin extract; ABX: antibiotic cocktail.*

In addition, overall ABX+GSPE effects on OXLs levels in CAF-fed rat were analyzed using PCA. Thus, CAF-ABX+GSPE group showed different effects depending on the photoperiod exposure. CAF-ABX+GSPE-treated rats showed a more different profile of OXLs compared to CAF-ABX-treated rats only under L12 and L18 conditions, whereas no changes were observed in rats under L6 (**Figure 6a-c**). Moreover, CAF-ABX+GSPE rats showed OXLs levels similar to CAF-fed rats only under L18 conditions, suggesting that GSPE treatment may mitigate the effects of ABX on OXLs profile under this photoperiod conditions (**Figure 6a-c**). Interestingly, overall OXLs profile of CAF-ABX+GSPE rats was different depending on photoperiod conditions, especially in rats exposed to L18 (**Figure 6d**).

3.5. Linoleic acid and Oleic acid were affected by diet and GSPE differently depending on photoperiod conditions.

We also investigated the effects of GSPE, diet and ABX in LA and OA, OXLs precursors. We found that CAF feeding affected LA and OA serum levels depending on the photoperiod conditions (P*D $p<0.05$) (**Figure 7**). Thus, CAF-fed rats showed significant higher levels of LA under both L6 ($p<0.05$) and L12 ($p<0.05$) compared to STD-fed rats. However, CAF-fed rats under L18 did not show any diet effect, showing the same levels of these fatty acids than STD-fed rats ($p>0.05$) (**Figure 7a-b**). In contrast, OA levels were significantly higher in CAF-fed rats compared to STD-fed rats independently of the photoperiod conditions ($p<0.05$) (**Figure 7b**). In this context, OA levels showed an interesting photoperiod effect, being their levels under L18 lower in comparison with L12 conditions ($p<0.05$) (**Figure 7b**).

GSPE effect was different depending on photoperiod conditions. Thus, GSPE significantly decreased OA and LA levels compared to CAF-VH rats under both L6 ($p<0.05$) and L12 ($p<0.05$) (**Figure 7a-b**), while the levels of these fatty acids were significantly increased under L18 conditions by GSPE compared to CAF-VH rats ($p<0.05$) (**Figure 7a-b**). Accordingly, GSPE-treated rats showed an

interesting photoperiod effect, being LA and OA levels significantly higher under L18 compared to both L6 ($p<0.05$) and L12 ($p<0.05$) (**Figure 7a-b**).

Additionally, when CAF-fed rats were treated with the combination of ABX and GSPE, LA levels were significantly decreased compared to ABX-treated rats only under L6 (**Figure 7a**) ($p<0.05$). This GSPE effect in ABX-treated rats was not significant in OA, although a tendency to decrease was observed ($p=0.1$) **(Figure 7b)**. In contrast, ABX administration did not affect to LA and OA levels compared to CAF-VH rats, and it did not show any photoperiod effect either.

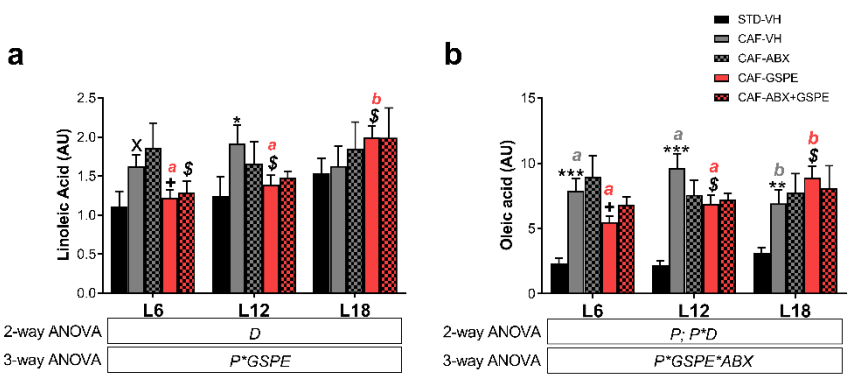

Figure 7. Diet, GSPE and Photoperiod effect on linoleic acid and oleic acid levels. *(**a**) Linoleic acid levels; (**b**) Oleic acids levels; * indicates significant diet effect between STD-VH and CAF-VH rats by 2-way ANOVA (factors: diet and photoperiod (P)) followed by LSD post hoc test (Xp=0.086; *p<0.05; **p<0.01; ***p<0.001); $ and ab indicate significant GSPE and Photoperiod effect respectively analyzed by 3-way ANOVA (factors: ABX, photoperiod and GSPE) and followed by LSD post hoc test (p<0.05). + indicates significant GSPE effect between CAF-VH and CAF-GSPE rats by t-test (p<0.05). Data are plotted as the mean ± SEM (n=7-8). L6: 6h light/18h darkness; L12: 12h light/12h darkness; L18: 18h light/6h darkness; STD: standard diet; CAF: cafeteria diet; VH: vehicle; GSPE: grape seed proanthocyanidin extract; ABX: antibiotic cocktail.*

3.6. Correlations between Oleic and Linoleic acid with oxylipins levels.

Oxylipins levels were positively correlated with OA and LA. Thus, 6-keto PG1Fα levels showed a significant positive correlation with the oleic acid ($r=0.441$ $p=5x10^{-4}$) (**Figure 8a**), while 15-Epi-LXA4 levels showed a significant positive correlation with the linoleic acid ($r=0.5$ $p=5.52x10^{-5}$) (**Figure 8b**).

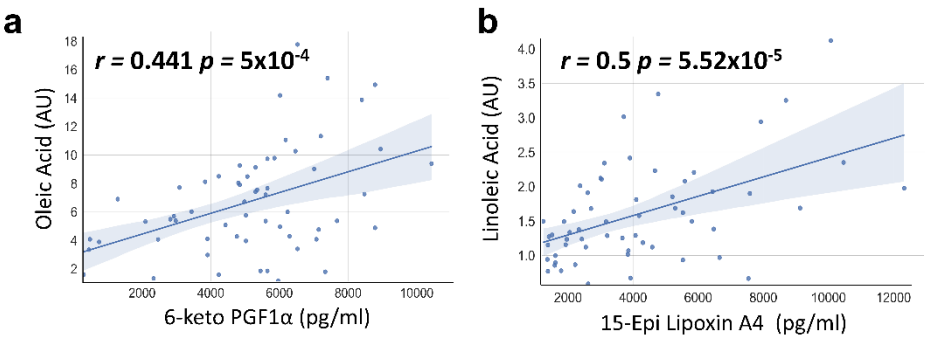

Figure 8. Correlations analyzed by Pearson's rank correlation coefficient (r). *Simple linear regression analysis of the significant observed correlation between: (**a**); 6-keto PGF1α and Oleic Acid levels and (**b**) 15-Epi-Lipoxin A4 and Linoleic Acid levels (**d**). (n=7-8). AU: arbitrary units.*

4. Discussion

OXLs are PUFAs-derived metabolites involved in several physiological processes including inflammation, immune actions, pain, apoptosis, blood clotting, cell proliferation, blood pressure regulation and tissue repair [11,38]. Among these, it is worth highlighting their role as potent modulators of inflammatory processes since they can act as activators and pro-resolving mediators of inflammation. For this reason, they are emerging as potential new biomarkers of chronic low-grade inflammation [39]. This fact is of great relevance in obesity and obesity-related disorders, which have been linked to a chronic state of a low-grade inflammation and associated with a high negative impact on the human health. Therefore, understanding the factors affecting OXLs metabolism is crucial to reduce the incident of these pathologies.

In this study we demonstrate, for the first time to our knowledge, that seasonal rhythms significantly impact OXLs metabolites in healthy and obese rats. These photoperiod-mediated changes in OXLs levels may be due to alterations in OXLs precursors metabolism. Hence, changes in photoperiod has been shown to partially disrupt clock genes signaling, impairing lipid metabolism [40,41]. Indeed, PUFAs from buccal mucosa samples have showed seasonal oscillations [42], suggesting that OXLs levels may also change depending on the season of

the year. Moreover, photoperiod conditions have been reported to impact immune-endocrine interactions altering inflammatory processes, which may suggest that it may also alter inflammatory mediators such as OXLs [43].

Interestingly, photoperiods effects were more prominent in the case of obese rats. The more pronounced photoperiod effects in CAF-fed rats could be explained by a higher influence of these rhythms when altered metabolic conditions due to homeostasis disruption. Indeed, other parameters such as body weight gain were not affected by photoperiod conditions in STD-fed rats while it significantly changed in CAF-fed rats [26]. Moreover, CAF-fed rats showed significant increased levels of C-reactive serum protein compared to STD-fed rats, indicating increased inflammation status. Moreover, significant differences were observed when comparing healthy and obese rats, which is in accordance with previous studies and could be explained by the different nutritional composition of the diets [18]. Thus, dietary intake of different PUFAs can modulate oxylipins profile levels in the circulation and in different tissues [44,45]. Therefore, the differences in OXLs levels can be due to the higher lipid content in CAF, including PUFAs, compared to STD. Interestingly, as mentioned before, these changes in OXLs levels between STD- and CAF-fed rats were different depending on the photoperiod conditions. Thus, for example 6-keto-PG1Fα, which has been related to anti-inflammatory effects, was increased in CAF-fed rats under L18 while no changes were observed in L6 or L12 conditions. 6-keto-PG1Fα acts as vasodilator, regulating vasomotor tone, reducing platelet aggregation, and inhibiting the recruitment and activity of inflammatory cells [46]. Moreover, it has been reported to act as a modulator of adipogenesis [47]. This photoperiod effect in this OXL is therefore in accordance with the increased body weight and fat mass observed in these rats under L18 conditions [26] and with other studies where low levels of 6-keto-PG1Fα have been associated with reductions in both BW gain and epidydimal fat mass in high-fat diet-fed mice [48]. Finally, 15-Epi-LXA4 was decreased in CAF-fed rats under L18 conditions while no changes were observed in L6 or L12. 15-Epi-LXA4 is a lipid mediator

derived from arachidonic acid, which has a strong anti-inflammatory and pro-resolution properties [49], being linked to attenuated obesity-induced adipose inflammation and decreased insulin resistance [50,51]. Hence, the decreased levels of this OXL in CAF-fed rats under long photoperiod conditions is also in agreement with the increased obesity development observed in these animals [26].

Photoperiods effects in these OXLs levels could also be associated with changes in gut microbiota composition induced by photoperiods. Hence, it has been stablished that gut microbiota is involved in dietary PUFAs metabolism and that it significantly affect OXLs profile in both healthy and obese rats [18,22]. Moreover, gut microbiota composition can be influenced by photoperiod conditions [52–54]. In fact, it has recently been shown that CAF-fed rats housed under long photoperiod conditions have a significant different microbiota compared to those housed under either standard or short photoperiods, showing increased *Proteobacteria* and *Bacteroidete*s levels, which have been linked with high inflammatory response [26,55]. Thus, the interaction between gut microbiota and photoperiod may also play a role in the differences in oxylipins levels observed under the different photoperiods conditions. In this study, ABX treatment altered OXLs serum levels differently depending on the photoperiod conditions. Indeed, OXLs levels in ABX-treated rats were decreased and more similar to STD-fed rats than CAF-VH-fed rats independently of photoperiod condition, suggesting that gut microbiota play a key role in the metabolism of these lipid metabolites under obesity conditions, which is in accordance with a previous study [18]. In addition, ABX effect was higher under L18 condition compared to both L6 and L12 conditions suggesting a stronger effect of long photoperiod. Therefore, these results suggested that gut microbiota and photoperiod play an important role modulating the serum OXLs levels.

On the other hand, bioactive dietary compounds such as polyphenols have also been reported to influence OXLs metabolites. Thus, resveratrol affected

oxylipins biosynthesis in human neutrophils [23]. The dietary supplementation with polyphenol rich juice led to changes in urine oxylipins profile in elite triathletes [25], and blueberry consumption mitigated oxylipins generation during the recovery phase after physical exercise in humans [25]. Regarding proanthocyanidins, they are the most abundant polyphenols in human diet and have shown to exert several health effects in obesity and associated pathologies, including anti-inflammatory properties. Currently, several studies have shown the impact of polyphenols on oxylipins metabolism [23–25] and its role in obesity. In this study, GSPE effect was found only in PGE2 under L6 conditions, where it restored the levels of PGE2 observed in CAF-VH rats to the levels found in STD-fed rats. Interestingly, when rats were treated with the combination of ABX and GSPE, we found that GSPE mitigated ABX-mediated changes in serum OXLs levels in CAF-fed rats in a photoperiod dependent manner, showing a strong effect under L18 conditions.

Finally, we investigated the effects of photoperiods in the levels of LA, precursor of OXLs metabolites, as well as in the levels of OA, is a non-essential fatty acid which modulate PUFAs content in peripheral tissues such as liver and adipose tissue, influencing the levels of bioactive oxylipins [35]. Overall, these fatty acids were increased in CAF-fed rats, probably due to their increased levels in this diet compared to STD [56]. In the case of LA, no photoperiod effects were observed other than increased levels in GSPE-CAF rats housed under L18 conditions. OA levels were lower in obese rats while they were higher in GSPE-CAF rats housed under L18 conditions. Hence, L18 conditions seem to be the most influencing photoperiod for these fatty acids. It is worth highlighting that, as mentioned above, this photoperiod was also where more pronounced changes in gut microbiota were observed together with increased body weight and fat accumulation [26]. Moreover, 6-keto-PG1Fα and 15-Epi-LXA4 were positively correlated with OA and LA, respectively. The positive correlation of OA on 6-keto-PG1Fα levels is in accordance with a previous study where OA

treatment increased 6-keto-PG1Fα levels in vascular smooths muscle cells *in vitro* [57].

Therefore, three main preliminary findings were found in the present study. Firstly, photoperiod conditions affected OXLs levels in both healthy and obesogenic conditions. Secondly, gut microbiota influenced the changes of OXLs levels modulated by photoperiods. Finally, GSPE did not affect most of the studied OXLs but mitigated the effects of gut microbiota dysbiosis on these metabolites in a photoperiod dependent manner. Although, further investigation with a higher number of OXLs metabolites is needed to better understand these interactions and the role of these factors on OXLs metabolism, photoperiods seem to be a key factor that must be take into account when OXLs are studied as potential obesity biomarkers.

Author statement

All authors have contributed to the work, participated in the writing of the manuscript, and read and approved the submitted version. All authors declare that the article is the original work and the original material contained in the manuscript has not received prior publication and is not under consideration for publication elsewhere.

Author contributions

Conceptualization: V.A.-G., J.A-R., A.A-A. and C.T-F.; Methodology: V.A-G., J.A-R., A.A-A. and C.T-F; Data analysis: V.A-G. and I.E-M.; Investigation: V.A-G., J.A-R., I.E-M., B.M., M.S., A.A-A., and C.T-F.; Supervision: A.A-A and C.T-F.; Validation: V.A-G., J.A-R., A.A-A and C.T-F. Writing the original draft: V.A-G. Writing, review, and editing: J.A-R., A.A-A and C.T-F. Funding acquisition: B.M., M.S., A.A-A. and C.T-F.

Funding

This work was supported by MCIN/AEI/10.13039/501100011033/ FEDER "Una manera de hacer Europa" (AGL2016-77105-R) and "2021/22 Development of a prototype for the establishment of a dysbiosis (alteration) in the intestinal microbiota", co-financed by Diputació de Tarragona (2021PGR-DIPTA-URV09). V.A.-G. was supported by the Martí i Franquès Doctoral Fellowships Programme, Universitat Rovira i Virgili (PMF-PIPF-35); I.E.-M. was supported by the Youth Employment Initiative from the European Social Fund, Ministry of Science, The State Research Agency and Universitat Rovira i Virgili (PEJ2018-002778-A); C.T.-F. was supported by Beatriu de Pinós Postdoctoral Programme of the Government of Catalonia's Secretariat for Universities and Research of the Ministry of Economy and Knowledge.

Declaration of interest

The authors declare no conflict of interest.

Acknowledgments

The authors would like to thank Niurka Dariela Llópiz and Rosa Pastor for their assistance and technical support.

References

[1] Rácz B, Dušková M, Stárka L, Hainer V, Kunešová M. Links between the circadian rhythm, obesity and the microbiome. Physiol Res 2018;67:S409–20. https://doi.org/10.33549/physiolres.934020.

[2] Onishi KG, Maneval AC, Cable EC, Tuohy MC, Scasny AJ, Sterina E, et al. Circadian and circannual timescales interact to generate seasonal changes in immune function. Brain Behav Immun 2020;83:33–43. https://doi.org/10.1016/j.bbi.2019.07.024.

[3] Touitou Y, Reinberg A, Touitou D. Association between light at night, melatonin secretion, sleep deprivation, and the internal clock: Health impacts and mechanisms of circadian disruption. Life Sci 2017;173:94–106. https://doi.org/10.1016/J.LFS.2017.02.008.

[4] Mariné-Casadó R, Domenech-Coca C, del Bas JM, Bladé C, Arola L, Caimari A. The exposure to different photoperiods strongly modulates the glucose and

lipid metabolisms of normoweight fischer 344 rats. Front Physiol 2018;9:1–17. https://doi.org/10.3389/fphys.2018.00416.

[5] Kobayashi M, Kobayashi M. The relationship between obesity and seasonal variation in body weight among elementary school children in Tokyo. Econ Hum Biol 2006;4:253–61. https://doi.org/10.1016/J.EHB.2005.08.002.

[6] Liu XY, Yang DB, Xu YC, Gronning MOL, Zhang F, Wang DH, et al. Photoperiod induced obesity in the Brandt's vole (Lasiopodomys brandtii): a model of "healthy obesity"? Dis Model Mech 2016;9:1357–66. https://doi.org/10.1242/DMM.026070.

[7] Stevenson TJ, Prendergast BJ. plasticity 2016:76–88. https://doi.org/10.1016/j.yfrne.2014.10.002.Photoperiodic.

[8] Myrianthefs P, Karatzas S, Venetsanou K, Grouzi E, Evagelopoulou P, Boutzouka E, et al. Seasonal variation in whole blood cytokine production after LPS stimulation in normal individuals. Cytokine 2003;24:286–92. https://doi.org/10.1016/J.CYTO.2003.08.005.

[9] Colas RA, Shinohara M, Dalli J, Chiang N, Serhan CN. Identification and signature profiles for pro-resolving and inflammatory lipid mediators in human tissue. Am J Physiol - Cell Physiol 2014;307:C39. https://doi.org/10.1152/AJPCELL.00024.2014.

[10] Hajeyah AA, Griffiths WJ, Wang Y, Finch AJ, O'Donnell VB. The Biosynthesis of Enzymatically Oxidized Lipids. Front Endocrinol (Lausanne) 2020;11. https://doi.org/10.3389/FENDO.2020.591819.

[11] Melissa Gabbs, Leng S, Devassy JG, Monirujjaman M, Aukema HM. Advances in Our Understanding of Oxylipins Derived from Dietary PUFAs. Adv Nutr 2015;6:513–40. https://doi.org/10.3945/AN.114.007732.

[12] Liakh I, Janczy A, Pakiet A, Korczynska J, Proczko-Stepaniak M, Kaska L, et al. One-anastomosis gastric bypass modulates the serum levels of pro- and anti-inflammatory oxylipins, which may contribute to the resolution of inflammation. Int J Obes 2021 462 2021;46:408–16. https://doi.org/10.1038/s41366-021-01013-y.

[13] Hasturk H, Schulte F, Martins M, Sherzai H, Floros C, Cugini MA, et al. Safety and Preliminary Efficacy of a Novel Host-Modulatory Therapy for Reducing Gingival Inflammation. Front Immunol 2021;12. https://doi.org/10.3389/FIMMU.2021.704163.

[14] Fishbein A, Hammock BD, Serhan CN, Panigrahy D. Carcinogenesis: Failure of resolution of inflammation? Pharmacol Ther 2021;218:107670. https://doi.org/10.1016/J.PHARMTHERA.2020.107670.

[15] Barden A, Shinde S, Tsai IJ, Croft KD, Beilin LJ, Puddey IB, et al. Effect of weight loss on neutrophil resolvins in the metabolic syndrome. Prostaglandins Leukot Essent Fatty Acids 2019;148:25–9. https://doi.org/10.1016/J.PLEFA.2019.07.001.

[16] Möller K, Ostermann AI, Rund K, Thoms S, Blume C, Stahl F, et al. Influence of

weight reduction on blood levels of C-reactive protein, tumor necrosis factor-α, interleukin-6, and oxylipins in obese subjects. Prostaglandins, Leukot Essent Fat Acids 2016;106:39–49. https://doi.org/10.1016/J.PLEFA.2015.12.001.

[17] Tans R, Bande R, van Rooij A, Molloy BJ, Stienstra R, Tack CJ, et al. Evaluation of cyclooxygenase oxylipins as potential biomarker for obesity-associated adipose tissue inflammation and type 2 diabetes using targeted multiple reaction monitoring mass spectrometry. Prostaglandins, Leukot Essent Fat Acids 2020;160:102157. https://doi.org/10.1016/J.PLEFA.2020.102157.

[18] Ávila-Román J, Arreaza-Gil V, Cortés-Espinar AJ, Soliz-Rueda JR, Mulero M, Muguerza B, et al. Impact of gut microbiota on plasma oxylipins profile under healthy and obesogenic conditions. Clin Nutr 2021;40:1475–86. https://doi.org/10.1016/j.clnu.2021.02.035.

[19] Blüher M. Obesity: global epidemiology and pathogenesis. Nat Rev Endocrinol 2019;15:288–98. https://doi.org/10.1038/S41574-019-0176-8.

[20] Gadde KM, Martin CK, Berthoud HR, Heymsfield SB. Obesity: Pathophysiology and Management. J Am Coll Cardiol 2018;71:69–84. https://doi.org/10.1016/J.JACC.2017.11.011.

[21] Gjermeni E, Kirstein AS, Kolbig F, Kirchhof M, Bundalian L, Katzmann JL, et al. Obesity-An Update on the Basic Pathophysiology and Review of Recent Therapeutic Advances. Biomolecules 2021;11. https://doi.org/10.3390/BIOM11101426.

[22] Miyamoto J, Igarashi M, Watanabe K, Karaki S ichiro, Mukouyama H, Kishino S, et al. Gut microbiota confers host resistance to obesity by metabolizing dietary polyunsaturated fatty acids. Nat Commun 2019;10. https://doi.org/10.1038/S41467-019-11978-0.

[23] Hartung NM, Fischer J, Ostermann AI, Willenberg I, Rund KM, Schebb NH, et al. Impact of food polyphenols on oxylipin biosynthesis in human neutrophils. Biochim Biophys Acta Mol Cell Biol Lipids 2019;1864:1536–44. https://doi.org/10.1016/J.BBALIP.2019.05.002.

[24] García-Flores LA, Medina S, Gómez C, Wheelock CE, Cejuela R, Martínez-Sanz JM, et al. Aronia – citrus juice (polyphenol-rich juice) intake and elite triathlon training: a lipidomic approach using representative oxylipins in urine. Food Funct 2018;9:463–75. https://doi.org/10.1039/C7FO01409K.

[25] Nieman DC, Gillitt ND, Chen GY, Zhang Q, Sha W, Kay CD, et al. Blueberry and/or Banana Consumption Mitigate Arachidonic, Cytochrome P450 Oxylipin Generation During Recovery From 75-Km Cycling: A Randomized Trial. Front Nutr 2020;7:121. https://doi.org/10.3389/FNUT.2020.00121/BIBTEX.

[26] Arreaza-Gil V, Escobar-Martínez I, Suárez M, Bravo F, Muguerza B, Arola-Arnal A, et al. Gut Seasons: Photoperiod Effects on Fecal Microbiota in Healthy and Cafeteria-Induced Obese Fisher 344 Rats. Nutrients 2022;14:722. https://doi.org/10.3390/NU14030722.

[27] Iglesias-Carres L, Mas-Capdevila A, Bravo FI, Arola L, Muguerza B, Arola-Arnal A. Exposure of Fischer 344 rats to distinct photoperiods influences the

bioavailability of red grape polyphenols. J Photochem Photobiol B Biol 2019;199:111623. https://doi.org/10.1016/J.JPHOTOBIOL.2019.111623.

[28] Arola-Arnal A, Cruz-Carrión Á, Torres-Fuentes C, Ávila-Román J, Aragonès G, Mulero M, et al. Chrononutrition and polyphenols: Roles and diseases. Nutrients 2019;11:1–18. https://doi.org/10.3390/nu11112602.

[29] Dorris SL, Peebles RS. PGI 2 as a regulator of inflammatory diseases. Mediators Inflamm 2012;2012. https://doi.org/10.1155/2012/926968.

[30] Tsuge K, Inazumi T, Shimamoto A, Sugimoto Y. Molecular mechanisms underlying prostaglandin E2-exacerbated inflammation and immune diseases. Int Immunol 2019;31:597–606. https://doi.org/10.1093/INTIMM/DXZ021.

[31] Pirault J, Bäck M. Lipoxin and resolvin receptors transducing the resolution of inflammation in cardiovascular disease. Front Pharmacol 2018;9:1273. https://doi.org/10.3389/FPHAR.2018.01273/BIBTEX.

[32] Sekheri M, Kebir D El, Edner N, Filep JG. 15-Epi-LXA4 and 17-epi-RvD1 restore TLR9-mediated impaired neutrophil phagocytosis and accelerate resolution of lung inflammation. Proc Natl Acad Sci U S A 2020;117:7971–80. https://doi.org/10.1073/PNAS.1920193117/SUPPL_FILE/PNAS.1920193117.SAPP.PDF.

[33] Kieran NE, Maderna P, Godson C. Lipoxins: Potential anti-inflammatory, proresolution, and antifibrotic mediators in renal disease. Kidney Int 2004;65:1145–54. https://doi.org/10.1111/j.1523-1755.2004.00487.x.

[34] Li P, Oh DY, Bandyopadhyay G, Lagakos WS, Talukdar S, Osborn O, et al. LTB4 promotes insulin resistance in obese mice by acting on macrophages, hepatocytes and myocytes. Nat Med 2015 213 2015;21:239–47. https://doi.org/10.1038/nm.3800.

[35] Picklo MJ, Idso J, Seeger DR, Aukema HM, Murphy EJ. Comparative effects of high oleic acid vs high mixed saturated fatty acid obesogenic diets upon PUFA metabolism in mice. Prostaglandins, Leukot Essent Fat Acids 2017;119:25–37. https://doi.org/10.1016/J.PLEFA.2017.03.001.

[36] Margalef M, Pons Z, Iglesias-Carres L, Arola L, Muguerza B, Arola-Arnal A. Gender-related similarities and differences in the body distribution of grape seed flavanols in rats. Mol Nutr Food Res 2016;60:760–72. https://doi.org/10.1002/MNFR.201500717.

[37] Pang Z, Chong J, Zhou G, De Lima Morais DA, Chang L, Barrette M, et al. MetaboAnalyst 5.0: narrowing the gap between raw spectra and functional insights. Nucleic Acids Res 2021;49:W388–96. https://doi.org/10.1093/NAR/GKAB382.

[38] Chiang N, Serha CN. Specialized Pro-Resolving Mediator Network: An Update on Production and Actions. Essays Biochem 2020;64:443. https://doi.org/10.1042/EBC20200018.

[39] van den Brink W, van Bilsen J, Salic K, Hoevenaars FPM, Verschuren L, Kleemann R, et al. Current and Future Nutritional Strategies to Modulate Inflammatory

Dynamics in Metabolic Disorders. Front Nutr 2019;6:129. https://doi.org/10.3389/FNUT.2019.00129/BIBTEX.

[40] Xie X, Zhao B, Huang L, Shen Q, Ma L, Chen Y, et al. Effects of altered photoperiod on circadian clock and lipid metabolism in rats. Chronobiol Int 2017;34:1094–104. https://doi.org/10.1080/07420528.2017.1341906.

[41] Mariné-Casadó R, Domenech-Coca C, del Bas JM, Bladé C, Arola L, Caimari A. Intake of an Obesogenic Cafeteria Diet Affects Body Weight, Feeding Behavior, and Glucose and Lipid Metabolism in a Photoperiod-Dependent Manner in F344 Rats. Front Physiol 2018;9:1–16. https://doi.org/10.3389/fphys.2018.01639.

[42] Ruf T, Arnold W. Daily and seasonal rhythms in human mucosa phospholipid fatty acid composition. J Biol Rhythms 2015;30:331–41. https://doi.org/10.1177/0748730415588190.

[43] Król K, Tomaszewska-Zaremba D, Herman AP. Photoperiod-dependent effect of inflammation on nocturnal gene expression of proinflammatory cytokines and their receptors in pars tuberalis of ewe. J Anim Feed Sci 2016;25:3–11. https://doi.org/10.22358/JAFS/65581/2016.

[44] Penner AL, Waytt V, Winter T, Leng S, Duhamel TA, Aukema HM. Oxylipin profiles and levels vary by skeletal muscle type, dietary fat and sex in young rats. Appl Physiol Nutr Metab 2021;46:1378–88. https://doi.org/10.1139/APNM-2021-0161/SUPPL_FILE/APNM-2021-0161SUPPLA.DOCX.

[45] Ferdouse A, Leng S, Winter T, Aukema HM. Dietary n-6 and n-3 PUFA alter the free oxylipin profile differently in male and female rat hearts. Br J Nutr 2019;122:252–61. https://doi.org/10.1017/S0007114519001211.

[46] Aljada A. Endothelium, Inflammation, and Diabetes. Https://HomeLiebertpubCom/Met 2004;1:3–21. https://doi.org/10.1089/154041903321648225.

[47] Rahman MS. Prostacyclin: A major prostaglandin in the regulation of adipose tissue development. J Cell Physiol 2019;234:3254–62. https://doi.org/10.1002/JCP.26932.

[48] Sasaki Y, Kuwata H, Akatsu M, Yamakawa Y, Ochiai T, Yoda E, et al. Involvement of prostacyclin synthase in high-fat-diet-induced obesity. Prostaglandins Other Lipid Mediat 2021;153:106523. https://doi.org/10.1016/J.PROSTAGLANDINS.2020.106523.

[49] Gutierrez AD, Sathyanarayana P, Konduru S, Ye Y, Birnbaum Y, Bajaj M. The effect of pioglitazone treatment on 15-epi-lipoxin A4 levels in patients with type 2 diabetes. Atherosclerosis 2012;223:204–8. https://doi.org/10.1016/J.ATHEROSCLEROSIS.2012.04.016.

[50] Wang Q, Jin F, Zhang J, Li Z, Yu D. Lipoxin A4 promotes adipogenic differentiation and browning of mouse embryonic fibroblasts. Vitr Cell Dev Biol - Anim 2021 5710 2021;57:953–61. https://doi.org/10.1007/S11626-021-00617-Y.

[51] Börgeson E, Johnson AMF, Lee YS, Till A, Syed GH, Ali-Shah ST, et al. Lipoxin A4 Attenuates Obesity-Induced Adipose Inflammation and Associated Liver and Kidney Disease. Cell Metab 2015;22:125–37. https://doi.org/10.1016/J.CMET.2015.05.003.

[52] Fan C, Zhang L, Jia S, Tang X, Fu H, Li W, et al. Seasonal variations in the composition and functional profiles of gut microbiota reflect dietary changes in plateau pikas. Integr Zool 2022. https://doi.org/10.1111/1749-4877.12630.

[53] Jiang F, Gao H, Qin W, Song P, Wang H, Zhang J, et al. Marked Seasonal Variation in Structure and Function of Gut Microbiota in Forest and Alpine Musk Deer. Front Microbiol 2021;12:2460. https://doi.org/10.3389/FMICB.2021.699797/BIBTEX.

[54] Maurice CF, Cl Knowles S, Ladau J, Pollard KS, Fenton A, Pedersen AB, et al. Marked seasonal variation in the wild mouse gut microbiota. ISME J 2015;9:2423–34. https://doi.org/10.1038/ismej.2015.53.

[55] Yan Y, Zhou X, Guo K, Zhou F, Yang H. Chlorogenic Acid Protects Against Indomethacin-Induced Inflammation and Mucosa Damage by Decreasing Bacteroides-Derived LPS. Front Immunol 2020;11. https://doi.org/10.3389/FIMMU.2020.01125.

[56] Néia VBMJC, Ambrosio-Albuquerque EP, Figueiredo IL, Boeing JS, Da Silva TC, Lewandowski V, et al. Impact of Cafeteria Diet on the Composition of Fatty Acids in Zebrafish (Danio rerio) Fillets. Artic J Braz Chem Soc 2018;29:1183–8. https://doi.org/10.21577/0103-5053.20170213.

[57] Haastrup A, Gadegbeku CA, Zhang D, Mukhin Y V., Greene EL, Jaffa AA, et al. Lipids stimulate the production of 6-keto-prostaglandin f(1alpha) in human dorsal hand veins. Hypertens (Dallas, Tex 1979) 2001;38:858–63. https://doi.org/10.1161/HY1001.092615.

SUPPLEMENTARY MATERIAL

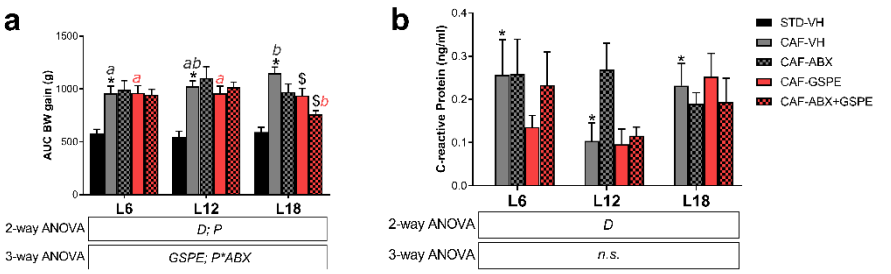

Figure S1. Effects of photoperiods and treatments on body weight gain and C-reactive protein*. (A): Area under the curve (AUC) of body weight (BW) gain; (B): c-reactive protein levels. Bar of the graph in STD-VH rats is not shown due to the levels were zero. * indicates significant diet effect between STD-VH and CAF-VH rats by 2-way ANOVA (factors: diet and photoperiod (P)) followed by LSD post hoc test; $ and ab indicate significant GSPE and Photoperiod effect respectively analyzed by 3-way ANOVA (factors: ABX, photoperiod and GSPE) and followed by LSD post hoc test (p<0.05). Data are plotted as the mean ± SEM (n = 7-8). L6: 6h light/18h darkness; L12: 12h light/12h darkness; L18: 18h light/6h darkness; STD: standard diet; CAF: cafeteria diet; VH: vehicle; GSPE: grape seed proanthocyanidin extract; ABX: antibiotic cocktail.*

GENERAL DISCUSSION

All organism are exposed to predictable environmental changes of food availability, climatic variability and light/darkness cycles variations across the year [1]. However, numerous evidences indicate that changes in day length (photoperiod) provide the primary environmental cue [2]. Accordingly, animals are capable of registering changes in photoperiods and translating them into a neuronal and hormonal response, adjusting the physiological and metabolic processes of the organisms for an optimal function and efficiency to the specific time of the day (circadian rhythms) or season of the year (seasonal rhythms) [3,4]. Adaptation to these environmental variations is therefore essential for survival. Some examples of seasonal physiological adaptations include annual cycles of growth, metabolism, thermogenesis, weight management, hibernation and sexual behavior among others [1]. In this context, F344 rats, which are established as a good model for the study of seasonal rhythms due to their photoperiod-sensitive response [5–7], have shown reduced body mass, food intake and testicle size in response to short photoperiod [8]. In addition, studies carry out by our group demonstrated an interesting photoperiod effects in F344 rats. Thus, normoweight rats exposure to different photoperiods displayed metabolic changes, suggesting that glucose- and lipid-related pathologies such as obesity and MetS could be influence by light variations [9]. Furthermore, F344 rats fed an obesogenic cafeteria diet showed altered BW gain, feeding behavior, and glucose an lipid metabolism in a photoperiod-dependent manner [10]. Additionally, seasonal rhythms haven been related to other many diseases development such as cardiovascular disorders [11], Alzheimer's disease and related dementias [12],MetS development [13] and inflammatory diseases [14]. Therefore, seasonal rhythms are recognized as a critical factor to maintain the properly physiological and metabolic functions of the organism [15–17].

Remarkably, gut microbiota has been reported as a factor modulated by seasonal rhythms. Regarding this, changes in gut microbiota composition by seasonal rhythms have been reported in healthy animals [18–22] and humans

[23]. Thus, gut microbial composition differs in winter and summer in order to contribute to a better environmental adaptation [24]. This interaction between gut microbiota and seasonal rhythms may be altered by different factors, which are able to alter the microbial composition, affecting host homeostasis [25,26]. For instance, obesogenic diets such as high fat diet or cafeteria diet modified gut microbiota composition, promoting obesity development [27–29], which could also be influenced by seasonal rhythms. Additionally, gut microbiota plays an important role in the metabolism of bioactive compounds such as polyphenols, which are receiving great attention due to their beneficial health effects. Therefore, the variations of the gut microbial composition throughout the year could alter the functionality of these bioactive compounds.

Therefore, **the first aim of the current thesis was to evaluate the relationship between seasonal rhythms and gut microbiota in healthy and obese rats** [**Chapter 1**]. **To this goal, firstly we investigate the effects of photoperiods, which mimics seasonal changes, on fecal microbiota composition and its impact on BW gain and fat parameters** [**Manuscript 1**]. Obesity was induced by cafeteria diet which consists in high palatable foods that leads to high caloric intake with poor nutritional value contributing to the development of different disorders such as insulin resistance, metabolic disruption and alterations of gut microbiota composition [29–31]. Moreover, the fact that CAF includes food regularly consumed by humans makes it a more robust model for human obesity in comparison with other high fat and/or high sugar diets traditionally used [32]. Thus, CAF-fed rats showed higher BW gain, lower glucose tolerance, higher fat accumulation and a higher intake compared to STD-fed rats. Moreover, different photoperiod conditions were used to simulate seasonal rhythms. The short photoperiod conditions emulated winter hours of light (L6, 6 hour of light), standard photoperiod conditions emulated spring and autumn hours of light (L12, 12 hour of light) and long photoperiod conditions simulated summer hours of light (L18, 18 hour of light). These photoperiods have been widely used, becoming a precise model to study seasonal rhythms effects on

metabolic and physiologic processes [6,9,33–35]. Hence, photoperiod conditions significantly affected BW gain and fat content which were higher under L18 and lower when exposed to L16 conditions. Remarkably, these effects were not due to changes in either food intake or activity. These results can be explained by the fact that mammals adapt their organism to changes in their environment via detection of the light/dark cycles duration [36]. This adaptation makes possible to optimize the pattern of energy obtaining and storage, being more efficient during the reproductive part of the year, which usually happens under long photoperiods, while in unproductive season, short photoperiods and energy exploitation is scarce [37,38].

Interestingly, L18 conditions led to marked changes in gut microbiota composition. Hence, the overall fecal microbiota profile in both STD and CAF-fed rats were significantly different when rats were housed under L18 conditions, which correlated with increased BW and fat content in obese rats. Indeed, CAF-fed rats showed a trend towards increased the abundance of *Bacteroidetes* and decreased levels of *Firmicutes* when they were housed under L18 conditions. In addition, *Oscillospira* and *Ruminoccoccus*, which belong to the *Firmicutes* phyla and have been shown to be decreased in obese subjects [39,40], were decreased in these conditions and correlated negatively with BW gain and fat depots. These genera are known to produce butyrate, which has been demonstrated to exert beneficial effects against obesity by increasing energy expenditure and lipid oxidation [41]. In contrast, *Bacteroides* genera, belonging to *Bacteroidetes* phyla and prominent among obese individuals, was increased in this group and correlated positively with body composition. Hence, seasonal rhythms influence gut microbiota impacting obesity development, being CAF-fed rats more sensitive to photoperiod changes than STD-fed rats.

The next goal was to elucidate if these changes in gut microbiota may influence the effects of seasonal rhythms at hormonal and molecular levels [**Manuscript 2**]. In particular, the impact of different photoperiods

on corticosterone levels, as well as on circadian and seasonal clocks were investigated. Corticosterone plays an important role in obesity development [42–44]. Indeed, higher levels of circulatory corticosterone hormone have been associated with higher risk for obesity development [45,46], promoting hyperglycaemia and insulin resistance and affecting key metabolic organs such as pancreas, liver, muscle and adipose tissue [47–49]. In addition, is one of the main hormones involved in gut microbiota-mediated effects [50,51]. Moreover, it has been shown to be modulated by seasonal rhythms through the HPA [52,53] and is also involved in the regulation of clock genes [54]. However, little is known about the influence of gut microbiota in corticosterone seasonal oscillations and seasonal clock genes expression. In this study, although it was not significant, a trend towards increased corticosterone levels was observed in CAF-fed rats compared to STD-fed rats under L6 and L12 but not under L18 conditions, indicating that photoperiod conditions influence corticosterone levels in obese rats. Interestingly, as mentioned above, L18 led to the greatest changes in gut microbiota, suggesting a role for these bacteria in this photoperiod effect on corticosterone levels in obese rats. Moreover, expression of corticosterone receptor in colon tissue was affected in a photoperiod-dependent manner in CAF-fed rats. Thus, increased levels of GR expression were observed in CAF-fed rats compared to STD-fed rats when housed under L12 and L18 conditions but not under L6. These photoperiod effects on GR expression in CAF-fed rats were not observed in the pituitary gland. This could be due to the fact that CAF feeding can decrease intestinal barrier integrity promoting inflammation and increasing GR expression in colon [55,56]. Moreover, gut microbiota dysbiosis induced by CAF feeding can also contribute to this increased inflammation and GR expression. Thus, CAF-fed rats showed significantly higher levels of *Proteobacteria*, which has been linked to high grade of inflammation and risk of metabolic disorders [57].

Additionally, to further evaluate the role of gut microbiota in these effects, CAF-fed rats were treated with an ABX. Interestingly, corticosterone serum levels were significantly influenced by photoperiod conditions in ABX-treated CAF-fed rats, being decreased in L18 conditions. Moreover, a photoperiod effect in GR pituitary expression was observed only in ABX-treated rats housed under L12 conditions. These changes suggest a marked influence of gut microbiota in the effects of seasonal rhythms on corticosterone signaling. Moreover, the effects of ABX treatment on molecular circadian and seasonal clocks were investigated. Clock genes are found in the SCN and in peripheral tissues and orchestrate circadian oscillations of several metabolic and physiological processes [58]. In addition, the seasonal clock is located in the pituitary gland where it initiates a cascade of molecular events which translates to seasonal changes of neuroendocrine activity in the hypothalamus [59]. Summer-like photoperiod signals activate *Eya3* gene transcription and suppresses *Chga* gene transcription in the pituitary gland, which expression would indicate winter-like state [59,60]. A clear photoperiod effect was observed for *Eya3* gene expression as expected [9,61,62]. Interestingly, depletion of gut microbiota by ABX treatment led to decreased levels of this gene only under L12 conditions. Moreover, ABX administration to CAF-fed rats led to decreased *Chga* expression, another important seasonal clock gene, being significant only under L18 conditions. However, *Chga* has been reported to be activated under short photoperiod conditions [59,63] and here this was not observed. Therefore, this needs to be further investigated in order to elucidate the role of *Chga* in this system and the potential role of gut microbiota in its regulation. Additionally, a photoperiod effect was found on circadian clock gene expression. However, no differences were found by ABX treatment, which is in contrast to other studies that have reported disruption of clock genes such as *Bmal1*, *Cry1*, *Per1*, and *Per2*, in intestine and liver in germ-free and antibiotic-induced mice [54,64]. However, these studies were not done in obese animals, and this may explain the differences observed for the effect of ABX. Hence, both

CAF feeding and ABX treatment led to gut microbiota dysbiosis and it may be that in both cases the effects on clock genes expression are similar. Indeed, some clock genes such as *Bmal1* showed an altered expression in the pituitary and colon tissue in CAF-fed rats compared to STD-fed rats. This effect was also dependent of photoperiods, reinforcing their influence on clock gene expression in peripheral tissues under obesogenic conditions.

These results suggest a relationship between the gut microbiota and photoperiods, which influence body composition and other parameters such as corticosterone, as well as seasonal clocks in obesity.

PAs are among the flavonoids more consummated in the human diet [65], and they have become of great relevance due to their beneficial health effects. In particular, GSPE has shown several beneficial metabolic properties [66,67]. Thus, GSPE has been extensively studied by our group, showing a potential role in the prevention of obesity development. Hence, GSPE improved insulin resistance [68], hypertension [69–71] oxidative stress [72], mitochondrial dysfunctionality [73] and lipid metabolism [74–76]. These beneficial effects could be attributed to gut microbiota since it is believed that approximately 90-95% of polyphenols reach the colon, where they are metabolized by the intestinal bacteria [77–79]. Interestingly, bioavailability of polyphenols from red grapes have been shown to be influenced by seasonal rhythms [80]. Nevertheless, the relationship between seasonal rhythms, gut microbiota and proanthocyanidins, as well as their impact on an obesogenic context, have not been evaluated yet.

Therefore, **the second objective of this thesis was to investigate the influence of the interaction between seasonal rhythms and gut microbiota in the functionality and bioavailability of PAs in obesity [Chapter 2]**. To this goal, we **firstly evaluate if GSPE anti-obesity properties can be modulated by gut microbiota in a photoperiod-dependent manner** [**Manuscript 3**]. CAF-fed rats exposure to different photoperiod conditions were treated with GSPE or with

the combination of GSPE and ABX for 4 weeks. GSPE was orally administered at 25 mg/kg/day, which is equivalent to the daily intake of 367 mg for a person of 70 kg [81], being easy to achieve with a polyphenol-rich diet [82–84]. In fact, the use of low doses of GSPE has shown beneficial effects in obesity disease [68,85]. For instance, administration of 25 mg/kg/day of GSPE to CAF-fed Wistars rats during 3 weeks decreased BW and adipose depots accumulation [73]. Furthermore, the same dose administered for 2 weeks significantly reduced adiposity index in hamster fed with a HFD, although BW gain was not affected [86]. However, GSPE administration at this dose for 30 days did not significant decrease BW or fat depots in diet-induced obese female Wistars rats [68]. In this regard, our results did not show a significant reduction of BW gain or fat depots in obese rats housed under standard conditions (L12 photoperiod) by GSPE treatment. These discrepancies regarding the GSPE effect on BW gain and fat depots may result from the use of animals of different age, sex, and strains, as well as from the duration of the treatment. Nevertheless, GSPE treatment significantly decreased the BW gain in CAF-fed rats housed under L18 conditions. This interesting effect observed in L18 were associated with the changes in fecal microbiota composition. Hence, GSPE altered gut microbiota composition differently depending on the photoperiod conditions. Thus, GSPE increased levels of *Bifidobacterium* and *Coprobacillus* and decreased *Kleibsella* genera only under L18. These bacteria genera levels are linked to lower BW gain and non-obese phenotypes [87,88]. In contrast, decreased *Parabacteroides* under L6 and *Lactobacillus, Lactococcus* and *Ruminococcus* under L12. Strains belonging to *Parabacteroides* genera such as *P. goldsteinii* and *P. distasonis* have been described as important bacteria with anti-obesity effects [89,90]. Furthermore, strains of *Lactobacillus, Lactococcus* and *Ruminococcus* genera, belonging to Firmicutes phyla, have been associated with lower BW gain. Thus, *Lactobacillus* strains are able to alleviate obesity in HFD-fed mice via reducing fat accumulation and regulating the content of leptin and adiponectin [91]. *Lactococcus* administration have shown to reduce BW gain and lipid

accumulation and to regulate leptin and adipokine secretion in HFD-fed mice [92]. Moreover *Ruminococcu*s genera has been shown to decrease in obese subjects and is known as potential butyrate producer, which exert beneficial effects against obesity by increasing lipid oxidation [39,93]. Therefore, these changes in gut microbiota composition by GSPE depending on photoperiod may help to explain the difference of BW gain in GSPE-treated rats under L18 compared to both L6 and L12 conditions.

In addition, GSPE administration influenced the above mentioned photoperiod effect observed in fecal microbiota composition in CAF-fed rats. Thus, GSPE-treated rats showed similar beta- and alpha-diversity independently of photoperiod conditions. Moreover, GSPE affected the most abundant genera, which were associated with higher BW gain and fat depots accumulation under L18. Therefore, GSPE affected BW gain and gut microbiota composition in a photoperiod-dependent manner, suggesting a relationship between GSPE, gut microbiota and photoperiod conditions. In this regard, the effect of GSPE on BW gain observed in L18 conditions was potentiated in ABX-treated rats, showing also significant decreased fat depots accumulation only under L18. Moreover, GSPE+ABX-treated rats showed a significant L18 effect on fecal microbiota composition similar to that observed in CAF-fed rats. Indeed, ABX+GSPE treatment led to significant photoperiod effect on *Firmicutes* and *Actinobacteria* phyla, increasing both of them under L18. These high levels of *Firmicutes* under L18 promoted an increase in F/B ratio, which could be associated to lower body mass in these rats. In fact, other studies using cafeteria diet also reported this decrease in F/B ratio due to the differences in the type of fat present in this diet, mainly lard and milk-derived fat, in comparison with other high fat diets [28,94]. In addition, the increase of *Actinobacteria* in L18 led to significant higher levels of *Bifidobacterium* genera in this photoperiod. These bacteria metabolize dietary compounds and ferment non-digestible dietary foods resulting in

the formation of SCFAs, exerting anti-obesity effects [95–100]. Therefore, we suggest that the strongest effect of GSPE in decreasing BW gain in ABX-treated rats housed under L18 conditions may be mediated by these changes in gut microbiota observed in these photoperiod conditions.

Therefore, the differences in GSPE-mediated anti-obesity effects observed under L18 could be due to changes in the bioavailability of GSPE mediated by the more pronounced changes in gut microbiota observed in these conditions [101]. Thus, gut microbiota plays an important role in PAs metabolism as these bacteria are able to extensively breakdown polyphenols into low-molecular-weight metabolites that can be absorbed into the circulatory system and exert several health benefits [102]. Hence, **the next goal was to evaluate if the bioavailability of PAs from GSPE in these rats is influenced by the interaction between photoperiod and gut microbiota [Manuscript 4].** A strong photoperiod effect was observed in phase-II flavan-3-ols metabolites, which decreased their concentration as the hours of lights per day increased. This effect was observed in CAF-fed rats independently of ABX treatment, although the metabolites affected were different. It is know that phase II enzymes, involved in the metabolism of flavan-3-ols-derived metabolites, follow a diurnal rhythmicity regulated by Retinoid-related orphan receptors alpha and gamma (RORα and γ) and Rev-erbα (two component of the circadian clock) expressed in liver [103–107]. Both RORα and REV-erbα are involved in the regulation of many metabolic pathways ensuring that metabolic enzymes are produced at appropriate times (i.e., stimulation of catabolic pathways during the wake period to match fuel demands). Hence, metabolism and absorption processes variate according to the time of the day, being most optimal and reaching the highest levels of intermediate metabolites during the active phase of the organism [108,109]. In this context, our results showed lower concentration of phase II metabolites under L18 conditions, which match with longer resting phase in rats. According to these results, Iglesias-Carres *et al.* also showed that the bioavailability of phenolic compounds from red grapes was higher in rats

exposed to L6 conditions compared to rats under L18 conditions [80]. Grapes may present a higher bioavailability under L6 conditions due to the fact that they are normally consumed in winter season. This could be linked with a major bioactivity according to the Xenohormesis theory [110,111]. This theory, stablished that the heterotrophs organism (i.e. humans) are able to sense singling stress-induced molecules from other species (i.e. plants). Hence, heterotrophs take these phytochemicals cues (polyphenols) from other species through the diet, to get information on the environmental status, adjusting their metabolism in anticipation of adverse conditions to increase their chances of survival [112]. Thus, the consumption of grapes out of their natural conditions season, would provide chemical cues that do not correspond to the current environmental situation to the consuming organism, and thus would result in non-efficient metabolic processes [111].

Regarding microbial-derived metabolites, differences were observed depending on photoperiod conditions and antibiotic treatment. These differences reinforce the important role of gut microbiota in phenolic compounds metabolites and may suggest that these bacteria are involved in the photoperiod-mediated changes in PAs bioavailability. Thus, the changes observed in the gut microbiota composition by GSPE and the different photoperiod conditions, may explain the differences on the bioavailability of GSPE. However, further investigations are needed to stablish an association between these bacteria and the metabolites derived from flavan-3-ols metabolism.

Hence, our results reinforce that photoperiods influence gut microbiota and the functionality of bioactive compounds such as polyphenols in obesity. Therefore, this may have implications in several physiological processes related to obesity and other metabolic disorders such as inflammation [14,113]. In this regard, the impact of these factors on the modulation of oxylipins (OXLs), which are important bioactive PUFA-derived metabolites that mediate inflammatory processes, has not been investigated yet. Therefore, the last aim of this thesis

was to **evaluate if photoperiods influence serum OXLs levels in healthy and obese rats, as well as the impact of PAs and gut microbiota on these lipid metabolites [Chapter 3].** In this context, **we firstly carried out an experiment to study if gut microbiota dysbiosis induced by ABX administration may impact on plasmatic OXLs profile in healthy and CAF-induced obese Wistar rats** [**Manuscript 5**]. Thus, the OXLs profile observed was different in healthy and obese rats. CAF feeding led to an overall reduction in plasma OXLs levels, involving both pro-and anti-inflammatory metabolites, which was correlated with the increase of pro-inflammatory bacteria such as *Proteobacteria* and *Lentisphaerae* [114]. Moreover, the ABX administration changed the overall plasmatic OXLs profile in CAF-fed rats, increasing both pro- and anti-inflammatory OXLs levels. These changes correlated with an increase in the relative abundance of *Proteobacteria* phyla. For instance, *Proteobacteria* phyla was positively correlated with LTB4, which has been demonstrated to have a key role in the progression of chronic diseases related to inflammation such as allergy, autoimmune diseases and metabolic disorders [115] . Therefore, these findings showed that gut microbiota dysbiosis significantly alter plasmatic OXLs levels in healthy and obesity conditions induced by CAF, suggesting a clear link between gut microbiota and the metabolism of these lipid mediators.

Based on this finding, **the effects of seasonal rhythms on OXLs metabolites in healthy and obesogenic conditions, and the impact of PAs and gut microbiota was investigated** [**Manuscript 6**]. Interestingly, photoperiods effects were more prominent in the case of CAF-fed rats, in the same way than body composition mentioned above [Manuscript 1]. Photoperiod conditions affected different OXLs metabolites. Interestingly, 6-keto-PG1Fα was increased in CAF-fed rats under L18 while no changes were observed in L6 or L12 conditions. This photoperiod effect in this OXL is in accordance with the increased body weight and fat mass observed in these rats under L18 conditions [Manuscript 1] as low levels of 6-keto-PG1Fα has been associated with reductions in both BW gain and epididymal fat mass in HFD-fed mice [116]. On the other hand, 15-Epi-LXA4,

which has strong anti-inflammatory and pro-resolution properties [117] linked to attenuate obesity-induced adipose inflammation and decrease insulin resistance [118,119], was decreased in CAF-fed rats under L18 conditions while no changes were observed in L6 or L12. Hence, the decreased levels of this OXL in CAF-fed rats under L18 conditions is also in agreement with the increased obesity development observed in these animals. Moreover, L18 was the photoperiod in which the greatest changes in gut microbiota composition were observed, suggesting that gut microbiota plays an important role in the OXLs metabolism. ABX-treated rats showed decreased OXLs levels and a more similar profile to STD-fed rats compared to CAF-fed rats independently of photoperiods, which are in concordance with our previous results commented above. Furthermore, photoperiod conditions significantly affected OXLs levels in ABX-treated rats housed under L18 conditions, suggesting that gut microbiota, as well as photoperiod are key factors in the modulation of serum OXLs levels. Finally, GSPE effect was found only in PGE2 under L6 conditions, where it restored the levels of this OXL observed in CAF-fed rats to the levels found in STD-fed rats. Additionally, when rats were treated with the combination of GSPE and ABX, we found that GSPE mitigated ABX-mediated changes in serum OXLs levels in CAF-fed rats in a photoperiod-dependent manner, showing a strong effect under L18 conditions. This could be explained by the profound effect of L18 on gut microbiota composition in these rats. Hence, these findings firstly suggest that photoperiod influence in OXLs levels may be modulated by gut microbiota in both healthy and obesogenic conditions. Secondly, gut microbiota affected the changes of OXLs levels influenced by photoperiods. Finally, GSPE did not affected most of the studied OXLs, but it mitigated the effects of gut microbiota dysbiosis on these metabolites in a photoperiod-dependent manner. Therefore, photoperiods seem to be a key factor that influence OXLs metabolism, being necessary more investigation to better understand its interaction with gut microbiota and polyphenols.

Taking all together, the results of the current thesis demonstrated a strong interaction between the seasonal rhythms and gut microbiota. This interaction influences body composition and glucose tolerance. Moreover, photoperiod and gut microbiota interaction may be mediate at least in part by corticosterone and seasonal clock genes modulation. In addition, GSPE functionality in obesity is affected by the interaction between photoperiods and gut microbiota. In this context, the bioavailability of phenolic compound derived from GSPE was affected by gut microbiota in a photoperiod-dependent manner, which can explain the different effects of GSPE showed in the different photoperiod conditions. Finally, the interaction between photoperiod and gut microbiota affects OXLs metabolites which may have an impact in inflammatory response. In addition, OXLs were also influenced by the diet, gut microbiota and GSPE in a photoperiod-dependent manner.

All these findings are of great relevance as obesity and obesity-related disorders prevalence continues increasing worldwide affecting more than two billion of people. Therefore, seasonal rhythms and gut microbiota interaction is a key factor that must be taken into account when investigating new approaches to prevent and/or treat these pathologies.

References

[1] Wood S, Loudon A. Clocks for all seasons: Unwinding the roles and mechanisms of circadian and interval timers in the hypothalamus and pituitary. J Endocrinol 2014;222. https://doi.org/10.1530/JOE-14-0141.

[2] Wood S, Loudon A. The pars tuberalis: The site of the circannual clock in mammals? Gen Comp Endocrinol 2018;258:222–35. https://doi.org/10.1016/j.ygcen.2017.06.029.

[3] Dibner C, Schibler U, Albrecht U. The Mammalian Circadian Timing System: Organization and Coordination of Central and Peripheral Clocks. Http://DxDoiOrg/101146/Annurev-Physiol-021909-135821 2010;72:517–49. https://doi.org/10.1146/ANNUREV-PHYSIOL-021909-135821.

[4] Helm B, Ben-Shlomo R, Sheriff MJ, Hut RA, Foster R, Barnes BM, et al. Annual rhythms that underlie phenology: biological time-keeping meets environmental change. Proc R Soc B Biol Sci 2013;280. https://doi.org/10.1098/RSPB.2013.0016.

[5] Togo Y, Otsuka T, Goto M, Furuse M, Yasuo S. Photoperiod regulates dietary preferences and energy metabolism in young developing Fischer 344 rats but not in same-age Wistar rats. Am J Physiol - Endocrinol Metab 2012;303:777–86. https://doi.org/10.1152/ajpendo.00209.2012.

[6] Heideman PD, John Sylvester C. Reproductive Photoresponsiveness in Unmanipulated Male Fischer 344 Laboratory Rats1. Biol Reprod 1997;57:134–8. https://doi.org/10.1095/biolreprod57.1.134.

[7] Heideman PD, Bierl CK, Sylvester CJ. Photoresponsive Fischer 344 Rats are reproductively inhibited by melatonin and differ in 2-[125I] Iodomelatonin binding from nonphotoresponsive Sprague-Dawley rats. J Neuroendocrinol 2001;13:223–32. https://doi.org/10.1046/J.1365-2826.2001.00617.X.

[8] Shoemaker MB, Heideman P. Reduced body mass, food intake, and testis size in response to short photoperiod in adult F344 rats. BMC Physiol 2002;2:11. https://doi.org/10.1186/1472-6793-2-11.

[9] Mariné-Casadó R, Domenech-Coca C, del Bas JM, Bladé C, Arola L, Caimari A. The exposure to different photoperiods strongly modulates the glucose and lipid metabolisms of normoweight fischer 344 rats. Front Physiol 2018;9:1–17. https://doi.org/10.3389/fphys.2018.00416.

[10] Mariné-Casadó R, Domenech-Coca C, del Bas JM, Bladé C, Arola L, Caimari A. Intake of an Obesogenic Cafeteria Diet Affects Body Weight, Feeding Behavior, and Glucose and Lipid Metabolism in a Photoperiod-Dependent Manner in F344 Rats. Front Physiol 2018;9:1–16. https://doi.org/10.3389/fphys.2018.01639.

[11] Stewart S, Keates AK, Redfern A, McMurray JJV. Seasonal variations in cardiovascular disease. Nat Rev Cardiol 2017;14:654–64. https://doi.org/10.1038/NRCARDIO.2017.76.

[12] Lim ASP. Diurnal and seasonal molecular rhythms in the human brain and their relation to Alzheimer disease. Handb Clin Neurol 2021;179:271–84. https://doi.org/10.1016/B978-0-12-819975-6.00017-0.

[13] Reiter RJ, Tan DX, Korkmaz A, Ma S. Obesity and metabolic syndrome: Association with chronodisruption, sleep deprivation, and melatonin suppression. Ann Med 2012;44:564–77. https://doi.org/10.3109/07853890.2011.586365.

[14] Onishi KG, Maneval AC, Cable EC, Tuohy MC, Scasny AJ, Sterina E, et al. Circadian and circannual timescales interact to generate seasonal changes in immune function. Brain Behav Immun 2020;83:33–43. https://doi.org/10.1016/j.bbi.2019.07.024.

[15] Mariné-Casadó R, Domenech-Coca C, del Bas JM, Bladé C, Arola L, Caimari A. The exposure to different photoperiods strongly modulates the glucose and lipid metabolisms of normoweight fischer 344 rats. Front Physiol 2018;9:416. https://doi.org/10.3389/FPHYS.2018.00416/BIBTEX.

[16] Kurhaluk N, Tkachenko H, Lukash O. Photoperiod-induced alterations in biomarkers of oxidative stress and biochemical pathways in rats of different ages: Focus on individual physiological reactivity. Chronobiol Int 2021;38:1673–

91. https://doi.org/10.1080/07420528.2021.1939364.

[17] Xie X, Zhao B, Huang L, Shen Q, Ma L, Chen Y, et al. Effects of altered photoperiod on circadian clock and lipid metabolism in rats. Chronobiol Int 2017;34:1094–104. https://doi.org/10.1080/07420528.2017.1341906.

[18] Bailey MT, Walton JC, Dowd SE, Weil ZM, Nelson RJ. Photoperiod modulates gut bacteria composition in male Siberian hamsters (Phodopus sungorus). Brain Behav Immun 2010;24:577–84. https://doi.org/10.1016/j.bbi.2009.12.010.

[19] Huang G, Wang L, Li J, Hou R, Wang M, Wang Z, et al. Seasonal shift of the gut microbiome synchronizes host peripheral circadian rhythm for physiological adaptation to a low-fat diet in the giant panda. Cell Rep 2022;38:110203. https://doi.org/10.1016/J.CELREP.2021.110203.

[20] Liu J, Song Y, Lu X, Chen T, Guo W, Fan Z, et al. Seasonal Variation Influences on Intestinal Microbiota in Rats. Curr Microbiol 2018;75:1006–10. https://doi.org/10.1007/S00284-018-1480-6/FIGURES/3.

[21] Munley KM, Deyoe JE, Ren CC, Demas GE. Melatonin mediates seasonal transitions in aggressive behavior and circulating androgen profiles in male Siberian hamsters. Horm Behav 2020;117:104608. https://doi.org/10.1016/j.yhbeh.2019.104608.

[22] Reiter RJ. The pineal and its hormones in the control of reproduction in mammals. Endocr Rev 1980;1:109–31. https://doi.org/10.1210/EDRV-1-2-109.

[23] Davenport ER, Mizrahi-Man O, Michelini K, Barreiro LB, Ober C, Gilad Y. Seasonal variation in human gut microbiome composition. PLoS One 2014;9. https://doi.org/10.1371/journal.pone.0090731.

[24] Liu J, Song Y, Lu X, Chen T, Guo W, Fan Z, et al. Seasonal Variation Influences on Intestinal Microbiota in Rats. Curr Microbiol 2018;75:1006–10. https://doi.org/10.1007/S00284-018-1480-6.

[25] Torres-Fuentes C, Schellekens H, Dinan TG, Cryan JF. The microbiota–gut–brain axis in obesity. Lancet Gastroenterol Hepatol 2017;2:747–56. https://doi.org/10.1016/S2468-1253(17)30147-4.

[26] Rhee SH, Pothoulakis C, Mayer EA. Principles and clinical implications of the brain–gut–enteric microbiota axis. Nat Rev Gastroenterol Hepatol 2009 65 2009;6:306–14. https://doi.org/10.1038/nrgastro.2009.35.

[27] Bibbò S, Ianiro G, Giorgio V, Scaldaferri F, Masucci L, Gasbarrini A, et al. The role of diet on gut microbiota composition. Eur Rev Med Pharmacol Sci 2016;20:4742–9.

[28] Gual-Grau A, Guirro M, Mayneris-Perxachs J, Arola L, Boqué N. Impact of different hypercaloric diets on obesity features in rats: a metagenomics and metabolomics integrative approach. J Nutr Biochem 2019;71:122–31. https://doi.org/10.1016/j.jnutbio.2019.06.005.

[29] Guirro M, Costa A, Gual-Grau A, Herrero P, Torrell H, Canela N, et al. Effects from diet-induced gut microbiota dysbiosis and obesity can be ameliorated by

fecal microbiota transplantation: A multiomics approach. PLoS One 2019;14. https://doi.org/10.1371/journal.pone.0218143.

[30] De Macedo IC, De Freitas JS, Da Silva Torres IL. The influence of palatable diets in reward system activation: A mini review. Adv Pharmacol Sci 2016;2016. https://doi.org/10.1155/2016/7238679.

[31] Gual-Grau A, Guirro M, Mayneris-Perxachs J, Arola L, Boqué N. Impact of different hypercaloric diets on obesity features in rats: a metagenomics and metabolomics integrative approach. J Nutr Biochem 2019;71:122–31. https://doi.org/10.1016/j.jnutbio.2019.06.005.

[32] Sampey BP, Vanhoose AM, Winfield HM, Freemerman AJ, Muehlbauer MJ, Fueger PT, et al. Cafeteria diet is a robust model of human metabolic syndrome with liver and adipose inflammation: comparison to high-fat diet. Obesity (Silver Spring) 2011;19:1109–17. https://doi.org/10.1038/OBY.2011.18.

[33] Tavolaro FM, Thomson LM, Ross AW, Morgan PJ, Helfer G. Photoperiodic Effects on Seasonal Physiology, Reproductive Status and Hypothalamic Gene Expression in Young Male F344 Rats. J Neuroendocrinol 2015;27:79–87. https://doi.org/10.1111/jne.12241.

[34] Ibars M, Aragonès G, Ardid-Ruiz A, Gibert-Ramos A, Arola-Arnal A, Suárez M, et al. Seasonal consumption of polyphenol-rich fruits affects the hypothalamic leptin signaling system in a photoperiod-dependent mode. Sci Rep 2018;8. https://doi.org/10.1038/S41598-018-31855-Y.

[35] Iglesias-Carres L, Mas-Capdevila A, Bravo FI, Arola L, Muguerza B, Arola-Arnal A. Exposure of Fischer 344 rats to distinct photoperiods influences the bioavailability of red grape polyphenols. J Photochem Photobiol B Biol 2019;199:111623. https://doi.org/10.1016/J.JPHOTOBIOL.2019.111623.

[36] Goldman BD. Mammalian photoperiodic system: Formal properties and neuroendocrine mechanisms of photoperiodic time measurement. J Biol Rhythms 2001;16:283–301. https://doi.org/10.1177/074873001129001980.

[37] Varpe Ø. Life history adaptations to seasonality. Integr. Comp. Biol., vol. 57, Oxford University Press; 2017, p. 943–60. https://doi.org/10.1093/icb/icx123.

[38] Hut RA, Beersma DGM. Evolution of time-keeping mechanisms: Early emergence and adaptation to photoperiod. Philos Trans R Soc B Biol Sci 2011;366:2141–54. https://doi.org/10.1098/rstb.2010.0409.

[39] Raman M, Ahmed I, Gillevet PM, Probert CS, Ratcliffe NM, Smith S, et al. Fecal microbiome and volatile organic compound metabolome in obese humans with nonalcoholic fatty liver disease. Clin Gastroenterol Hepatol 2013;11:868-875.e3. https://doi.org/10.1016/j.cgh.2013.02.015.

[40] Zarrinpar A, Chaix A, Yooseph S, Panda S. Diet and feeding pattern affect the diurnal dynamics of the gut microbiome. Cell Metab 2014;20:1006–17. https://doi.org/10.1016/j.cmet.2014.11.008.

[41] Gao Z, Yin J, Zhang J, Ward RE, Martin RJ, Lefevre M, et al. Butyrate Improves Insulin Sensitivity and Increases Energy Expenditure in Mice. Diabetes

2009;58:1509–17. https://doi.org/10.2337/DB08-1637.

[42] Acute Severe Steatohepatitis Related To Prednisolone Therapy : Official journal of the American College of Gastroenterology | ACG n.d. https://journals.lww.com/ajg/Citation/2002/04000/Acute_Severe_Steatohepatitis_Related_To.68.aspx (accessed May 31, 2022).

[43] Dimitriadis G, Leighton B, Parry-Billings M, Sasson S, Young M, Krause U, et al. Effects of glucocorticoid excess on the sensitivity of glucose transport and metabolism to insulin in rat skeletal muscle. Biochem J 1997;321:707–12. https://doi.org/10.1042/BJ3210707.

[44] Samuel VT, Petersen KF, Shulman GI. Lipid-induced insulin resistance: unravelling the mechanism. Lancet 2010;375:2267–77. https://doi.org/10.1016/S0140-6736(10)60408-4.

[45] Gathercole LL, Morgan SA, Bujalska IJ, Hauton D, Stewart PM, Tomlinson JW. Regulation of Lipogenesis by Glucocorticoids and Insulin in Human Adipose Tissue. PLoS One 2011;6:e26223. https://doi.org/10.1371/JOURNAL.PONE.0026223.

[46] Kokkinos A, Lambadiari V, Cooney GJ, Rutter GA, Akalestou E, Genser L. Glucocorticoid Metabolism in Obesity and Following Weight Loss. Front Endocrinol | WwwFrontiersinOrg 2020;11:59. https://doi.org/10.3389/fendo.2020.00059.

[47] Liu Y, Nakagawa Y, Wang Y, Liu L, Du H, Wang W, et al. Reduction of hepatic glucocorticoid receptor and hexose-6-phosphate dehydrogenase expression ameliorates diet-induced obesity and insulin resistance in mice. J Mol Endocrinol 2008;41:53–64. https://doi.org/10.1677/JME-08-0004.

[48] Kotelevtsev Y, Holmes MC, Burchell A, Houston PM, Schmoll D, Jamieson P, et al. 11β-Hydroxysteroid dehydrogenase type 1 knockout mice show attenuated glucocorticoid-inducible responses and resist hyperglycemia on obesity or stress. Proc Natl Acad Sci U S A 1997;94:14924–9. https://doi.org/10.1073/PNAS.94.26.14924/ASSET/CCF71866-A747-427A-B4EB-F90F158C0802/ASSETS/GRAPHIC/PQ2673529004.JPEG.

[49] Alberts P, Nilsson C, Selén G, Engblom LOM, Edling NHM, Norling S, et al. Selective Inhibition of 11β-Hydroxysteroid Dehydrogenase Type 1 Improves Hepatic Insulin Sensitivity in Hyperglycemic Mice Strains. Endocrinology 2003;144:4755–62. https://doi.org/10.1210/EN.2003-0344.

[50] Farzi A, Fröhlich EE, Holzer P. Gut Microbiota and the Neuroendocrine System n.d. https://doi.org/10.1007/s13311-017-0600-5.

[51] Vodička M, Ergang P, Hrnčíř T, Mikulecká A, Kvapilová P, Vagnerová K, et al. Microbiota affects the expression of genes involved in HPA axis regulation and local metabolism of glucocorticoids in chronic psychosocial stress. Brain Behav Immun 2018;73:615–24. https://doi.org/10.1016/J.BBI.2018.07.007.

[52] Otsuka T, Goto M, Kawai M, Togo Y, Sato K, Katoh K, et al. Photoperiod regulates corticosterone rhythms by altered adrenal sensitivity via melatonin-independent mechanisms in fischer 344 rats and C57BL/6J mice. PLoS One

2012;7:1–8. https://doi.org/10.1371/journal.pone.0039090.

[53] Lind CM, Moore IT, Vernasco BJ, Farrell TM. Seasonal testosterone and corticosterone patterns in relation to body condition and reproduction in a subtropical pitviper, Sistrurus miliarius. Gen Comp Endocrinol 2018;267:51–8. https://doi.org/10.1016/j.ygcen.2018.05.027.

[54] Mukherji A, Kobiita A, Ye T, Chambon P. Homeostasis in intestinal epithelium is orchestrated by the circadian clock and microbiota cues transduced by TLRs. Cell 2013;153:812–27. https://doi.org/10.1016/j.cell.2013.04.020.

[55] Ayroldi E, Soma KK, Brunner T, Ahmed A, Schmidt C. Extra-Adrenal Glucocorticoid Synthesis in the Intestinal Mucosa: Between Immune Homeostasis and Immune Escape. Front Immunol | WwwFrontiersinOrg 2019;1:1438. https://doi.org/10.3389/fimmu.2019.01438.

[56] Tang S, Zhang Z, Oakley RH, Li W, He W, Xu X, et al. Intestinal epithelial glucocorticoid receptor promotes chronic inflammation–associated colorectal cancer. JCI Insight 2021;6. https://doi.org/10.1172/JCI.INSIGHT.151815.

[57] Shin NR, Whon TW, Bae JW. Proteobacteria: microbial signature of dysbiosis in gut microbiota. Trends Biotechnol 2015;33:496–503. https://doi.org/10.1016/J.TIBTECH.2015.06.011.

[58] Reppert SM, Weaver DR. Coordination of circadian timing in mammals. Nat 2002 4186901 2002;418:935–41. https://doi.org/10.1038/nature00965.

[59] Wood SH, Christian HC, Miedzinska K, Saer BRC, Johnson M, Paton B, et al. Binary Switching of Calendar Cells in the Pituitary Defines the Phase of the Circannual Cycle in Mammals. Curr Biol 2015;25:2651–62. https://doi.org/10.1016/j.cub.2015.09.014.

[60] Lincoln G. A brief history of circannual time. J Neuroendocrinol 2019;31:1–12. https://doi.org/10.1111/jne.12694.

[61] Kawai H, Inabe J, Ishibashi T, Kudo N, Kawashima Y, Mitsumoto A. Short and long photoperiods differentially exacerbate corticosterone-induced physical and psychological symptoms in mice. Biomed Res 2018;39:47–55. https://doi.org/10.2220/biomedres.39.47.

[62] Sakamoto K. Photoperiod Differentially Affects the Expression of Three mPer Genes in the Mouse Heart. Https://DoiOrg/101076/Brhm331751325 2010;33:75–81. https://doi.org/10.1076/BRHM.33.1.75.1325.

[63] Dardente H, Wyse CA, Birnie MJ, Dupré SM, Loudon ASI, Lincoln GA, et al. A molecular switch for photoperiod responsiveness in mammals. Curr Biol 2010;20:2193–8. https://doi.org/10.1016/J.CUB.2010.10.048/ATTACHMENT/25AEE83E-6383-4714-ABB1-95D107956508/MMC1.PDF.

[64] Leone V, Gibbons SM, Martinez K, Hutchison AL, Edmond Y, Cham CM, et al. on Host Circadian Clock Function and Metabolism. Cell Host Microbe 2016;17:681–9. https://doi.org/10.1016/j.chom.2015.03.006.Effects.

[65] Bladé C, Aragonès G, Arola-Arnal A, Muguerza B, Bravo FI, Salvadó MJ, et al. Proanthocyanidins in health and disease. BioFactors 2016;42:5–12. https://doi.org/10.1002/BIOF.1249.

[66] Mannino G, Chinigò G, Serio G, Genova T, Gentile C, Munaron L, et al. Proanthocyanidins and Where to Find Them: A Meta-Analytic Approach to Investigate Their Chemistry, Biosynthesis, Distribution, and Effect on Human Health. Antioxidants 2021, Vol 10, Page 1229 2021;10:1229. https://doi.org/10.3390/ANTIOX10081229.

[67] Rodríguez-Pérez C, García-Villanova B, Guerra-Hernández E, Verardo V. Grape Seeds Proanthocyanidins: An Overview of In Vivo Bioactivity in Animal Models. Nutrients 2019;11. https://doi.org/10.3390/NU11102435.

[68] Montagut G, Bladé C, Blay M, Fernández-Larrea J, Pujadas G, Salvadó MJ, et al. Effects of a grapeseed procyanidin extract (GSPE) on insulin resistance. J Nutr Biochem 2010;21:961–7. https://doi.org/10.1016/J.JNUTBIO.2009.08.001.

[69] Mas-Capdevila A, Iglesias-Carres L, Arola-Arnal A, Suárez M, Bravo FI, Muguerza B. Changes in arterial blood pressure caused by long-term administration of grape seed proanthocyanidins in rats with established hypertension. Food Funct 2020;11:8735–42. https://doi.org/10.1039/D0FO00981D.

[70] Pons Z, Margalef M, Bravo FI, Arola-Arnal A, Begoña Muguerza ·. Acute administration of single oral dose of grape seed polyphenols restores blood pressure in a rat model of metabolic syndrome: role of nitric oxide and prostacyclin. Eur J Nutr 2016;55:749–58. https://doi.org/10.1007/s00394-015-0895-0.

[71] Pons Z, Margalef M, Bravo FI, Arola-Arnal A, Muguerza B. Chronic administration of grape-seed polyphenols attenuates the development of hypertension and improves other cardiometabolic risk factors associated with the metabolic syndrome in cafeteria diet-fed rats. Br J Nutr 2017;117:200–8. https://doi.org/10.1017/S0007114516004426.

[72] Puiggròs F, Sala E, Vaque M, Ardevol A, Blay M, Fernández-Larrea J, et al. In vivo, in vitro, and in silico studies of Cu/Zn-superoxide dismutase regulation by molecules in grape seed procyanidin extract. J Agric Food Chem 2009;57:3934–42. https://doi.org/10.1021/JF8034868.

[73] Pajuelo D, Quesada H, Díaz S, Fernández-Iglesias A, Arola-Arnal A, Bladé C, et al. Chronic dietary supplementation of proanthocyanidins corrects the mitochondrial dysfunction of brown adipose tissue caused by diet-induced obesity in Wistar rats. Br J Nutr 2012;107:170–8. https://doi.org/10.1017/S0007114511002728.

[74] Bladé C, Arola L, Salvadó MJ. Hypolipidemic effects of proanthocyanidins and their underlying biochemical and molecular mechanisms. Mol Nutr Food Res 2010;54:37–59. https://doi.org/10.1002/MNFR.200900476.

[75] Quesada H, Del Bas JM, Pajuelo D, Díaz S, Fernandez-Larrea J, Pinent M, et al. Grape seed proanthocyanidins correct dyslipidemia associated with a high-fat diet in rats and repress genes controlling lipogenesis and VLDL assembling in

liver. Int J Obes (Lond) 2009;33:1007–12. https://doi.org/10.1038/IJO.2009.136.

[76] Baiges I, Palmfeldt J, Bladé C, Gregersen N, Arola L. Lipogenesis Is Decreased by Grape Seed Proanthocyanidins According to Liver Proteomics of Rats Fed a High Fat Diet. Mol Cell Proteomics 2010;9:1499. https://doi.org/10.1074/MCP.M000055-MCP201.

[77] Gasperotti M, Passamonti S, Tramer F, Masuero D, Guella G, Mattivi F, et al. Fate of microbial metabolites of dietary polyphenols in rats: is the brain their target destination? ACS Chem Neurosci 2015;6:1341–52. https://doi.org/10.1021/ACSCHEMNEURO.5B00051.

[78] Ozdal T, Sela DA, Xiao J, Boyacioglu D, Chen F, Capanoglu E. The Reciprocal Interactions between Polyphenols and Gut Microbiota and Effects on Bioaccessibility. Nutr 2016, Vol 8, Page 78 2016;8:78. https://doi.org/10.3390/NU8020078.

[79] Espín JC, González-Sarrías A, Tomás-Barberán FA. The gut microbiota: A key factor in the therapeutic effects of (poly)phenols. Biochem Pharmacol 2017;139:82–93. https://doi.org/10.1016/J.BCP.2017.04.033.

[80] Iglesias-Carres L, Mas-Capdevila A, Bravo FI, Arola L, Muguerza B, Arola-Arnal A. Exposure of Fischer 344 rats to distinct photoperiods influences the bioavailability of red grape polyphenols. J Photochem Photobiol B Biol 2019;199:111623. https://doi.org/10.1016/j.jphotobiol.2019.111623.

[81] Reagan-Shaw S, Nihal M, Ahmad N. Dose translation from animal to human studies revisited. FASEB J 2008;22:659–61. https://doi.org/10.1096/FJ.07-9574LSF.

[82] Saura-Calixto F, Serrano J, Goñi I. Intake and bioaccessibility of total polyphenols in a whole diet. Food Chem 2007;101:492–501. https://doi.org/10.1016/J.FOODCHEM.2006.02.006.

[83] Wang Y, Chung SJ, Song WO, Chun OK. Estimation of Daily Proanthocyanidin Intake and Major Food Sources in the U.S. Diet. J Nutr 2011;141:447–52. https://doi.org/10.3945/JN.110.133900.

[84] Zamora-Ros R, Andres-Lacueva C, Lamuela-Raventós RM, Berenguer T, Jakszyn P, Barricarte A, et al. Estimation of Dietary Sources and Flavonoid Intake in a Spanish Adult Population (EPIC-Spain). J Am Diet Assoc 2010;110:390–8. https://doi.org/10.1016/J.JADA.2009.11.024.

[85] Salvadó MJ, Casanova E, Fernández-Iglesias A, Arola L, Bladé C. Roles of proanthocyanidin rich extracts in obesity. Food Funct 2015;6:1053. https://doi.org/10.1039/c4fo01035c.

[86] Caimari A, Del Bas JM, Crescenti A, Arola L. Low doses of grape seed procyanidins reduce adiposity and improve the plasma lipid profile in hamsters. Int J Obes 2013 374 2012;37:576–83. https://doi.org/10.1038/ijo.2012.75.

[87] Yin YN, Yu QF, Fu N, Liu XW, Lu FG. Effects of four Bifidobacteria on obesity in high-fat diet induced rats. World J Gastroenterol 2010;16:3394–401.

https://doi.org/10.3748/wjg.v16.i27.3394.

[88] Zeng Q, Li D, He Y, Li Y, Yang Z, Zhao X, et al. Discrepant gut microbiota markers for the classification of obesity-related metabolic abnormalities n.d. https://doi.org/10.1038/s41598-019-49462-w.

[89] Wu TR, Lin CS, Chang CJ, Lin TL, Martel J, Ko YF, et al. Gut commensal Parabacteroides goldsteinii plays a predominant role in the anti-obesity effects of polysaccharides isolated from Hirsutella sinensis. Gut 2019;68:248–62. https://doi.org/10.1136/GUTJNL-2017-315458.

[90] Wang K, Liao M, Zhou N, Bao L, Ma K, Zheng Z, et al. Parabacteroides distasonis Alleviates Obesity and Metabolic Dysfunctions via Production of Succinate and Secondary Bile Acids. Cell Rep 2019;26:222-235.e5. https://doi.org/10.1016/J.CELREP.2018.12.028.

[91] Wang M, Zhang B, Hu J, Nie S, Xiong T, Xie M. Intervention of five strains of Lactobacillus on obesity in mice induced by high-fat diet. J Funct Foods 2020;72:104078. https://doi.org/10.1016/J.JFF.2020.104078.

[92] Zhang Q, Kim JH, Kim Y, Kim W. Lactococcus chungangensis CAU 28 alleviates diet-induced obesity and adipose tissue metabolism in vitro and in mice fed a high-fat diet. J Dairy Sci 2020;103:9803–14. https://doi.org/10.3168/JDS.2020-18681.

[93] Gao Z, Yin J, Zhang J, Ward RE, Martin RJ, Lefevre M, et al. Butyrate improves insulin sensitivity and increases energy expenditure in mice. Diabetes 2009;58:1509–17. https://doi.org/10.2337/db08-1637.

[94] Devkota S, Wang Y, Musch MW, Leone V, Fehlner-Peach H, Nadimpalli A, et al. Dietary-fat-induced taurocholic acid promotes pathobiont expansion and colitis in Il10-/- mice. Nature 2012;487:104–8. https://doi.org/10.1038/nature11225.

[95] Ghouri YA, Richards DM, Rahimi EF, Krill JT, Jelinek KA, DuPont AW. Systematic review of randomized controlled trials of probiotics, prebiotics, and synbiotics in infammatory bowel disease. Clin Exp Gastroenterol 2014;7:473–87. https://doi.org/10.2147/CEG.S27530.

[96] Salvini F, Riva E, Salvatici E, Boehm G, Jelinek J, Banderali G, et al. A specific prebiotic mixture added to starting infant formula has long-lasting bifidogenic effects. J Nutr 2011;141:1335–9. https://doi.org/10.3945/jn.110.136747.

[97] Tojo R, Suárez A, Clemente MG, De Los Reyes-Gavilán CG, Margolles A, Gueimonde M, et al. Intestinal microbiota in health and disease: Role of bifidobacteria in gut homeostasis. World J Gastroenterol 2014;20:15163–76. https://doi.org/10.3748/wjg.v20.i41.15163.

[98] Schellekens H, Torres-Fuentes C, van de Wouw M, Long-Smith CM, Mitchell A, Strain C, et al. Bifidobacterium longum counters the effects of obesity: Partial successful translation from rodent to human. EBioMedicine 2021;63. https://doi.org/10.1016/J.EBIOM.2020.103176.

[99] An HM, Park SY, Lee DK, Kim JR, Cha MK, Lee SW, et al. Antiobesity and lipid-lowering effects of Bifidobacterium spp. in high fat diet-induced obese rats.

Lipids Health Dis 2011;10. https://doi.org/10.1186/1476-511X-10-116.

[100] Cani PD, Neyrinck AM, Fava F, Knauf C, Burcelin RG, Tuohy KM, et al. Selective increases of bifidobacteria in gut microflora improve high-fat-diet-induced diabetes in mice through a mechanism associated with endotoxaemia. Diabetologia 2007;50:2374–83. https://doi.org/10.1007/s00125-007-0791-0.

[101] Liu W, Zhao S, Wang J, Shi J, Sun Y, Wang W, et al. Grape seed proanthocyanidin extract ameliorates inflammation and adiposity by modulating gut microbiota in high-fat diet mice. Mol Nutr Food Res 2017;61:1601082. https://doi.org/10.1002/MNFR.201601082.

[102] Cardona F, Andrés-Lacueva C, Tulipani S, Tinahones FJ, Queipo-Ortuño MI. Benefits of polyphenols on gut microbiota and implications in human health. J Nutr Biochem 2013;24:1415–22. https://doi.org/10.1016/j.jnutbio.2013.05.001.

[103] Tsurusaki T, Sakakibara H, Aoshima Y, Yamazaki S, Sakono M, Shimoi K. Diurnal rhythmicity in biological processes involved in bioavailability of functional food factors. J Clin Biochem Nutr 2013;52:208–14. https://doi.org/10.3164/JCBN.12-127.

[104] Wada T, Kang HS, Jetten AM, Xie W. The emerging role of nuclear receptor RORalpha and its crosstalk with LXR in xeno- and endobiotic gene regulation. Exp Biol Med (Maywood) 2008;233:1191–201. https://doi.org/10.3181/0802-MR-50.

[105] Hong SK, Angers M, Ju YB, Wu X, Gimble JM, Wada T, et al. Gene expression profiling reveals a regulatory role for ROR alpha and ROR gamma in phase I and phase II metabolism. Physiol Genomics 2007;31:281–94. https://doi.org/10.1152/PHYSIOLGENOMICS.00098.2007.

[106] Xu H, Chen M, Yu F, Zhang T, Wu B. Circadian Clock Component Rev-erb α Regulates Diurnal Rhythm of UDP-Glucuronosyltransferase 1a9 and Drug Glucuronidation in Mice. Drug Metab Dispos 2020;48:681–9. https://doi.org/10.1124/DMD.120.000030.

[107] Zhang T, Guo L, Yu F, Chen M, Wu B. The nuclear receptor Rev-erbα participates in circadian regulation of Ugt2b enzymes in mice. Biochem Pharmacol 2019;161:89–97. https://doi.org/10.1016/J.BCP.2019.01.010.

[108] Reinke H, Asher G. Crosstalk between metabolism and circadian clocks n.d. https://doi.org/10.1038/s41580-018-0096-9.

[109] Arola-Arnal A, Cruz-Carrión Á, Torres-Fuentes C, Ávila-Román J, Aragonès G, Mulero M, et al. Chrononutrition and polyphenols: Roles and diseases. Nutrients 2019;11:1–18. https://doi.org/10.3390/nu11112602.

[110] Hooper PL, Hooper PL, Tytell M, Vígh L. Xenohormesis: health benefits from an eon of plant stress response evolution. Cell Stress Chaperones 2010;15:761. https://doi.org/10.1007/S12192-010-0206-X.

[111] Howitz KT, Sinclair DA. Xenohormesis: Sensing the Chemical Cues of Other Species. Cell 2008;133:387–91. https://doi.org/10.1016/J.CELL.2008.04.019.

[112] Baur JA, Sinclair DA. What is Xenohormesis? Am J Pharmacol Toxicol 2008;3:149–56. https://doi.org/10.3844/AJPTSP.2008.152.159.

[113] Myrianthefs P, Karatzas S, Venetsanou K, Grouzi E, Evagelopoulou P, Boutzouka E, et al. Seasonal variation in whole blood cytokine production after LPS stimulation in normal individuals. Cytokine 2003;24:286–92. https://doi.org/10.1016/J.CYTO.2003.08.005.

[114] Fan HN, Zhu P, Lu YM, Guo JH, Zhang J, Qu GQ, et al. Mild changes in the mucosal microbiome during terminal ileum inflammation. Microb Pathog 2020;142:104104. https://doi.org/10.1016/J.MICPATH.2020.104104.

[115] He R, Chen Y, Cai Q. The role of the LTB4-BLT1 axis in health and disease. Pharmacol Res 2020;158:104857. https://doi.org/10.1016/J.PHRS.2020.104857.

[116] Sasaki Y, Kuwata H, Akatsu M, Yamakawa Y, Ochiai T, Yoda E, et al. Involvement of prostacyclin synthase in high-fat-diet-induced obesity. Prostaglandins Other Lipid Mediat 2021;153:106523. https://doi.org/10.1016/J.PROSTAGLANDINS.2020.106523.

[117] Gutierrez AD, Sathyanarayana P, Konduru S, Ye Y, Birnbaum Y, Bajaj M. The effect of pioglitazone treatment on 15-epi-lipoxin A4 levels in patients with type 2 diabetes. Atherosclerosis 2012;223:204–8. https://doi.org/10.1016/J.ATHEROSCLEROSIS.2012.04.016.

[118] Wang Q, Jin F, Zhang J, Li Z, Yu D. Lipoxin A4 promotes adipogenic differentiation and browning of mouse embryonic fibroblasts. Vitr Cell Dev Biol - Anim 2021 5710 2021;57:953–61. https://doi.org/10.1007/S11626-021-00617-Y.

[119] Börgeson E, Johnson AMF, Lee YS, Till A, Syed GH, Ali-Shah ST, et al. Lipoxin A4 Attenuates Obesity-Induced Adipose Inflammation and Associated Liver and Kidney Disease. Cell Metab 2015;22:125–37. https://doi.org/10.1016/J.CMET.2015.05.003.

CONCLUSIONS

The main conclusions drawn from the results of this Doctoral Thesis are presented below:

1. Photoperiods influence gut microbiota composition in healthy and obese rats, being the latest the most affected. These effects are stronger under long photoperiod conditions.
2. Changes in microbiota composition influenced by photoperiods are associated with changes in body weight gain and different fat depots in obese rats.
3. The effects of photoperiod exposure on serum corticosterone hormone levels in obese rats are influenced by gut microbiota.
4. The effects of photoperiod exposure on circadian and seasonal clock genes expression in obese rats are modulated by gut microbiota.
5. Proanthocyanidins affects fecal microbiota composition in a photoperiod-dependent manner in obese rats.
6. Proanthocyanidins decrease body weight gain and fat depots only under long photoperiod conditions, which is associated with changes in gut microbiota in a photoperiod-dependent manner.
7. Gut microbiota dysbiosis alters photoperiod-mediated changes in proanthocyanidins bioavailability.
8. Exposure to long photoperiod conditions lead to a higher variability of gut microbiota-derived proanthocyanidins metabolites, which correlates with greater changes in microbiota composition and higher anti-obesity effects of these phenolic compounds in these conditions.
9. Gut microbiota plays a key role in regulating oxylipins metabolites under healthy and obesogenic conditions.
10. Photoperiod conditions affect oxylipins levels in both healthy and obese rats. These changes are influenced by gut microbiota in a photoperiod-dependent manner.

11. Proanthocyanidins administration mitigates the effects of gut microbiota dysbiosis on oxylipins metabolites levels in a photoperiod-dependent manner.

Therefore, the findings obtained in this thesis demonstrated a strong relationship between photoperiods and gut microbiota in obesity. In this regard, body composition and other physiological parameters such as oxylipins are affected by photoperiod exposure depending on gut microbiota composition. Moreover, proanthocyanidins functionality and bioavailability are influenced by gut microbiota in a photoperiod-dependent manner. This corroborates that seasonal rhythms and their impact on gut microbiota are key factors that must be taken into account when investigating the effects of bioactive compounds such as proanthocyanidins.

Biological rhythms are crucial to adjust the physiological and metabolic processes of the organism to the time of day (circadian rhythms) or year (seasonal rhythms). This synchronization is orchestrated by external signals (*Zeitgeber*), being the light the most important one. In this context, the gut microbiota, which plays an important role to maintaining the homeostasis of the organism, can be modulated by changes in the light length of the day (photoperiod). This fact is of great relevance due to the gut microbiota is involved in the metabolism of bioactive compounds, such as proanthocyanidins (PAs), which are the most abundant polyphenols in western diet. In fact, these compounds have shown beneficial effects on metabolic disorders such as obesity. Therefore, the functionality of these PAs could be influenced by the time of the year or even the day in which they are administered. Hence, this thesis aims to study the relationship between seasonal rhythms, which have been less studied than circadian rhythms, gut microbiota, and their impact on the functionality of PAs in obesity. To do this, we studied the influence of seasonal rhythms on gut microbiota composition and other physiological parameters in healthy and cafeteria-induced obese Fischer 344 rats, and evaluated the effect of PAs administration in different conditions of gut microbiota dysbiosis. The results showed that seasonal rhythms alter the composition of the gut microbiota, which was associated with changes in weight, glucose tolerance, and levels of oxylipins (inflammatory mediators). Likewise, this interaction between seasonal rhythms and the gut microbiota affected the functionality and bioavailability of PAs, which showed a differently effect depending on the photoperiod conditions in which they were administered. Therefore, these results contribute to expand the knowledge in the field of chrononutrition, establishing the importance of taking into account seasonal rhythms and gut microbiota when evaluating the beneficial effects of bioactive compounds.